SUPERCONDUCTIVITY, HIGH-TEMPERATURE SUPERCONDUCTIVITY

AC transport losses in multifilamentary $(Bi,Pb)_2Sr_2Ca_2Cu_3O_x$/Ag tapes

I. A. Rudnev, A. E. Khodot, and A. V. Eremin

*Moscow State Engineering Physics Institute (Technical University), 115409 Moscow, Russia**

I. I. Akimov

*A. Bochvar All-Russia Scientific and Research Institute of Inorganic Materials, 123479 Moscow, Russia***

(Submitted July 27, 1998; revised September 14, 1998)
Fiz. Nizk. Temp. **25**, 141–147 (February 1999)

The results of ac transport losses measurements are presented for multifilamentary HTSC composite Bi-2223/Ag tapes with the number of filaments $N=7$, 19, 37, 61, 91, 127, 169, and 703. The measurements have been made under the self-field conditions as well as in a constant magnetic field applied to the tapes at different angles. The dependence of AC losses on the amplitude and frequency of the alternating transport current have been obtained. It is found that the dependence of the AC losses on the current amplitudes for all the tapes are in accord with the Norris theoretical predictions for an elliptical or strip geometry of the wire. The external magnetic field increases the magnitude of the AC losses. It is concluded that transport AC losses in multifilamentary HTSC composites are ''saturation losses.'' © *1999 American Institute of Physics.* [S1063-777X(99)00202-9]

INTRODUCTION

High-temperature superconductors (HTSC) have found a wide technical application in various electrical-engineering systems in which high densities of electric current are required. Electric energy transmission cables, permanent and ac magnets, as well as transformers are examples of successful application of HTSC materials. Unfortunately, some factors requiring optimization hinder the application of HTSC in real electrical engineering devices. Above all, we are speaking of low mechanical strength and low critical current density. The HTSC response to the applied varying electromagnetic field and ac energy losses in such fields including self-field ac transport losses are equally important.

In many electrical systems, external magnetic fields of various configurations are applied to a superconductor carrying alternating transport current. Consequently, it is important to know the effect of the applied field on transport losses in real HTSC tapes. In spite of intense investigations of transport losses in mono-[1–4] and multifilamentary[5–9] tapes, the effect of external magnetic field has not been studied comprehensively. Experimental data[1–9] can be successfully described by the model of the critical state created for traditional low-temperature superconductors. Self-field losses are described by the expression obtained from the Londons theory for round wires.[10] Solutions for elliptical and rectangular cross sections were obtained by Norris.[11] These models were based on the assumption that the critical current density is independent of magnetic field, and the superconductor is isotropic relative to its electromagnetic properties. The models under consideration were not intended for describing the behavior of transport losses in the magnetic field of heterogeneous multifilamentary composite materials. Nevertheless, the experimental results obtained by Ciszek *et al.*[12] who studied the effect of magnetic field on transport losses in mono- and 37-filamentary composite HTSC were successfully explained on the basis of the Norris equations.

In this communication, we report on the results of analysis of transport losses in multifilamentary $(Bi,Pb)_2Sr_2Ca_2Cu_3O_x$/Ag composite tapes in a (Bi-2223/Ag) silver coating in magnetic fields applied at different angles to the tape plane. We consider a set of eight tapes with the number of filaments varying from 7 to 703. The measurements made by us show that the magnetic field changes transport losses only though a change in the critical current of the superconductor in a magnetic field. Our results, as well as those obtained in Ref. 12, are successfully explained by the Norris model. In addition, we prove that transport losses in composite HTSC are not purely hysteresis losses, but are ''saturation losses'' as in the case of low-temperature superconducting wires. The main difference between these types of losses lies in that ''saturation losses'' decrease upon an increase in the critical current. Hysteresis losses are determined by the area of the magnetization loop of a superconductor and increase with the critical current.

SAMPLES AND EXPERIMENTAL TECHNIQUE

Composite $(Bi,Pb)_2Sr_2Ca_2Cu_3O_x$ tapes with the number of filaments $N=7$, 19, 37, 61, 91, 127, 169, and 703 were prepared by the ''oxide powder in tube'' (OPIT) method which is described in the literature in detail.[13] The characteristic size of the tapes were $0.1-0.2\times3-4\times30$ mm for the HTSC-to-silver ratio $\sim 20:80$.

TABLE I. Values of critical current and normalized losses.

N	I_c, A $T=77$ K, $B=0$	Q, 10^{-6} W/cycle·m $(I=I_c)$	Q/I_c^2 $(I=I_c)$
7	14.8	12.4	0.05
19	13.3	13.1	0.07
37	12.1	11.6	0.08
61	14.1	11.6	0.06
91	13.7	9.8	0.05
127	13.6	9.8	0.05
169	19.0	8.3	0.02
703	18.6	20.0	0.05

We measured the synphase component of the first harmonic of voltage across the sample under investigation as a function of the amplitude of alternating transport current of various frequencies. The voltage for each value of frequency was determined by using a selective amplifier. The inductive component of voltage was compensated by using a transformer loop in the current circuit. The power of total transport losses was defined as the product of the synphase current and voltage. The frequency and amplitude dependences of losses were determined in the range $30\,\text{Hz}<f<150\,\text{Hz}$ for $I<30$ A from the frequency and amplitude, respectively, of the current. The ac frequency was fixed by a sine-wave generator, and the current was amplified by a low-frequency amplifier and a transformer. In order to avoid possible industrial noise, we ensured that the transport ac frequency and its first harmonics were not multiple of 50 Hz.

It was noted in Refs. 9, 14, and 15 that the losses measured in HTSC tapes are determined to a considerable extent by the position of potential contacts on the sample. In order to obtain the ''correct'' value of losses (i.e., the value independent of the position of the contacts), potential leads must have the shape of a loop whose size is 1.5–2 widths of the tape and must be located in the tape plane.[16–18] All the requirements of the ''correct'' arrangement of potential probes were satisfied in our experiments.

We measured critical current by the standard four-probe method according to the criterion 1 μV/cm. The value of the current I_c in zero magnetic field at $T=77$ K varied from 12 to 19 A for different samples (see Table I). The table also contains the value of losses per cycle for $I=I_c$ as well as losses normalized to the square of critical current.

For measurements in an external magnetic field, the samples were placed in a special magnetic system so that the angle α between the direction of the magnetic field and the plane of the sample could be varied from 0 to 360° with a step of 5°. The angle between the directions of the field and current was always 90°. The magnitude of the magnetic field was controlled through the current in the magnetic system. The losses in the magnetic field were measured as a function of the ac amplitude at a frequency $f=33$ Hz for different angles α and several values of the magnetic field. The value of critical current was also measured for each angle α for all values of the magnetic field. All measurements were made at $T=77$ K.

EXPERIMENTAL RESULTS

Self-field AC transport losses

Figure 1 shows the specific loss power W (per unit length of the wire) as a function of the amplitude $\beta=I/I_c$ of transport current normalized to the critical current at zero frequency (i.e., dc critical current) for composite tapes with various number of filaments N. For subcritical currents, i.e., for $\beta<1$, the curves measured at different frequencies are different, while the $W(\beta)$ dependences measured for $\beta\geqslant 1$ coincide. Indeed, for $I>I_c$, the samples are in the normal state in which the loss power is independent of frequency. However, the $W(\beta)$ curves do not coincide for $\beta=1$. This can be due to strongly blurred current transition from the superconducting to the normal state (with an IVC), which makes practical determination of critical current from the fixed voltage threshold rather conditional. Also, the discrepancy in the $W(\beta)$ dependences for $\beta=1$ can be attributed to the difference between intergranular and intragranular critical currents. It can seen from Fig. 1a and 1b that the frequency dependence vanishes at a current amplitude approximately twice as large as the critical current. For such current ampli-

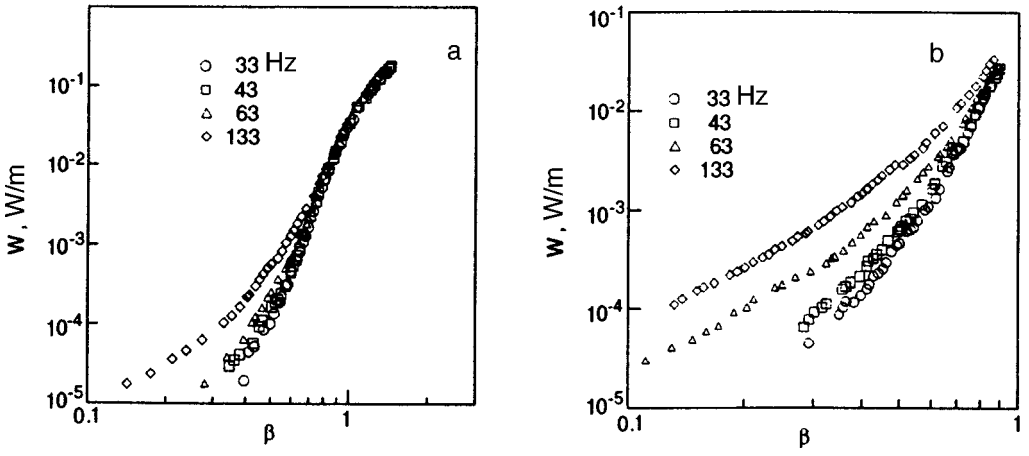

FIG. 1. Specific transport loss power as a function of the normalized amplitude $\beta=I/I_c$ of transport current at different frequencies for composite HTSC with $N=37$ (a) and 169 (b).

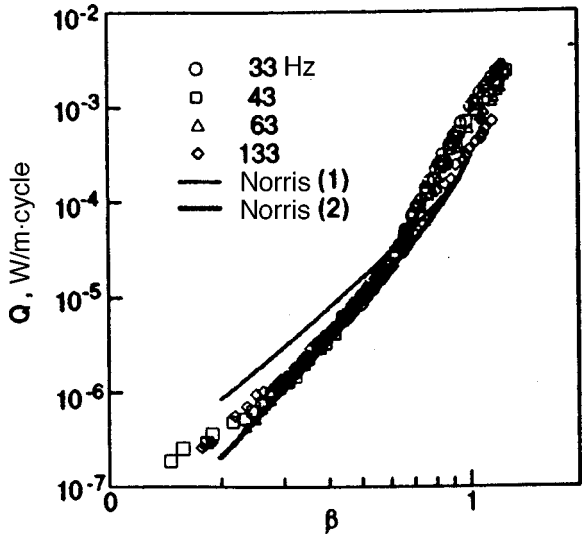

FIG. 2. Dependence of specific transport losses per cycle on $\beta = I/I_c$ at different frequencies.

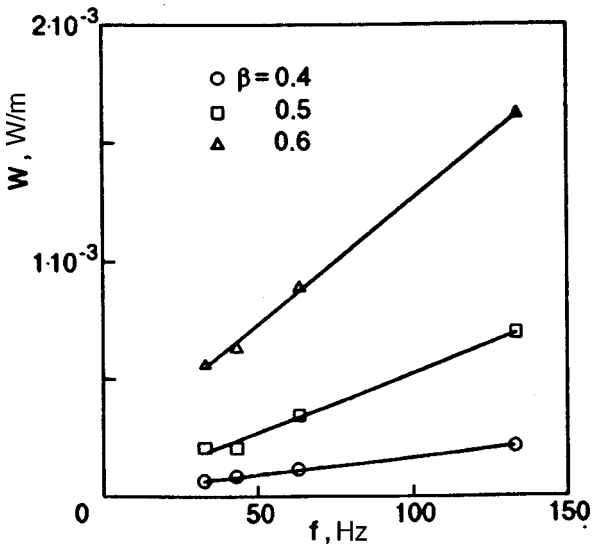

FIG. 3. Frequency dependence of specific transport losses for a composite material with $N = 7$ for various values of β.

tudes, all experimental points approach asymptotically the universal curve $W \propto \beta^2$ characterizing the normal ohmic behavior of the conductor.

Figure 2 shows the dependence of specific energy losses Q per cycle on β at different frequencies for a 127-filamentary sample. All the samples exhibited virtually the same behavior of $Q(\beta)$ described by a power function $Q \propto \beta^n$, where $n = 3-4$ for small β.

Norris[11] proved long ago that the $Q(\beta)$ dependence for $\beta < 1$ for elliptical and rectangular cross sections of the wires can be described by the following equations:

$$Q = \frac{\mu_0 I_c^2}{\pi}\left[(2-\beta)\frac{\beta}{2} + (1-\beta)\ln(1-\beta)\right] \tag{1}$$

and

$$Q = \frac{\mu_0 I_c^2}{\pi}[(1+\beta)\ln(1+\beta) + (1-\beta)\ln(1-\beta) - \beta^2]. \tag{2}$$

For small β, these equations can be reduced to

$$Q \approx \mu_0 I^3/6\pi I_c, \tag{3}$$

and

$$Q \approx \mu_0 I^4/6\pi I_c^2, \tag{4}$$

while for $\beta = 1$ they approach the following equations:

$$Q = 0{,}16\mu_0 I_c^2, \tag{5}$$

and

$$Q = 0{,}12\mu_0 I_c^2. \tag{6}$$

The results of our experiments correspond to both dependences (1) and (2) for different composites. This is probably due to the deviation of the shape of wire cross section from the rectangular and elliptical shape.

Having chosen a constant value of $\beta \neq 1$, we can construct frequency dependences of losses. In this case, it is expedient to use the value of total losses since their frequency dependences are different functions for different sources. It was noted above that ohmic losses are frequency independent. These occur either in a sample in the normal state, or when a current flows through the silver matrix. Hysteresis losses occurring in superconductor materials increase linearly with frequency, while eddy-current losses in the silver matrix are proportional to the square of frequency.

We observed a linear dependence for all samples, which indicates that the losses were of the hysteresis type. Figure 3 shows the frequency dependence of specific transport losses for a composite with $N = 7$.

Effect of external magnetic field

Figure 4 shows the angular dependence of critical current I_c (normalized to I_{c0} for $B = 0$) for different values of applied magnetic field B for a composite with $N = 61$. The angle $\alpha = 90°$ corresponds to a transverse configuration (the

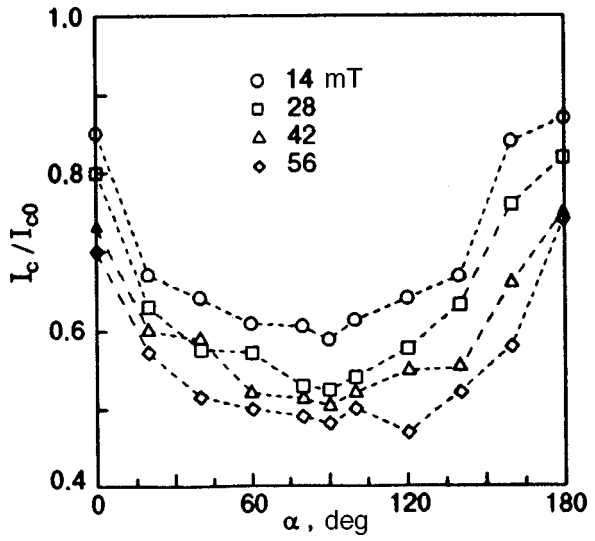

FIG. 4. Angular dependence of the normalized critical current for various values of the external magnetic field for a composite with $N = 61$.

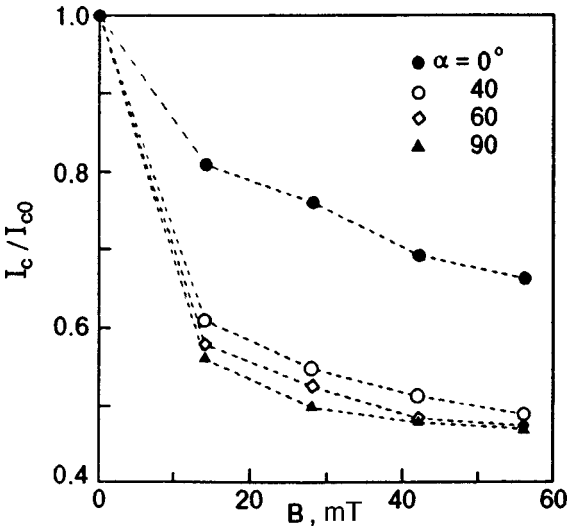

FIG. 5. Dependence of normalized critical current on magnetic field of various orientations.

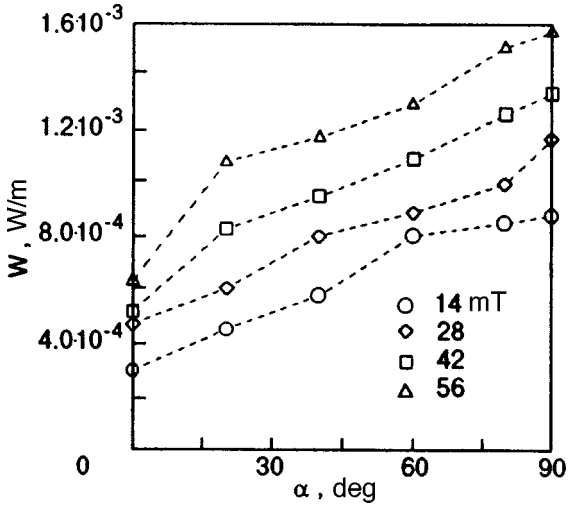

FIG. 7. Angular dependence of transport losses for various values of the external magnetic field for a composite with $N=61$.

field is perpendicular to the tape plane). The dependences of I_c/I_{c0} on the applied magnetic field for $\alpha=0$, 40, 60, and 90° are shown in Fig. 5. In a field applied at right angles to the tape plane, the critical current decreases at a much higher rate than for a parallel configuration.

The effect of external magnetic field on the losses is shown in Fig. 6, where specific current losses are plotted for a composite material with $N=61$ as a function of the current amplitude for different magnetic fields of perpendicular and parallel configurations. The magnetic field increases the magnitude of losses significantly. The angular dependence of transport losses is shown in Fig. 7. Since the magnitude and direction of the magnetic field alter simultaneously the magnitude of critical current as well as the losses, it is interesting to plot the dependence of losses on I_c. An example of such a dependence is shown in Fig. 8 (the critical current is normalized to I_{c0} for $B=0$). It can be seen that experimental results fit to the general dependence, the magnitude of losses increasing upon a decrease in critical current.

DISCUSSION OF EXPERIMENTAL RESULTS

Let us try to find out what type of losses occurs in the composite materials under investigation and estimate possible values of losses. For this purpose, we generalize the experimental results as follows:

(1) the current dependence of transport losses per cycle is $W \propto I^n$, where $n=3-4$;
(2) the frequency dependence of losses is linear;
(3) transport losses decrease with increasing critical current;
(4) the losses increase with the magnetic field.

It follows from these results that, as in the case of traditional low-temperature superconductors, transport losses in composite HTSC are ''saturation losses'' (see, for example, Ref. 17). What are ''saturation losses'' and what is the difference between these and hysteresis losses? It is well known[17] that current flows in a composite superconductor near its surface, occupying larger and larger region as the

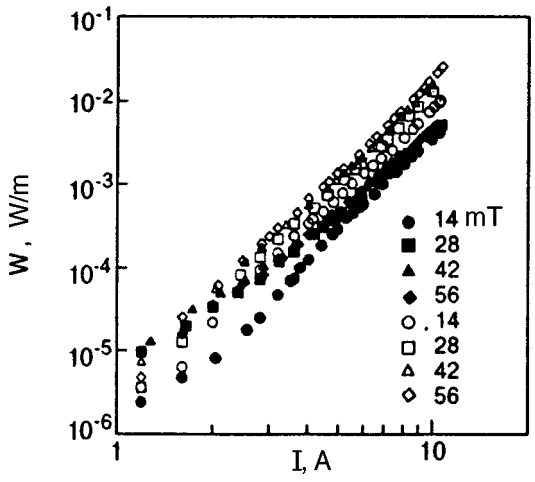

FIG. 6. Specific transport losses as a function of current amplitude for various values of magnetic field. Light an dark symbols correspond to a field perpendicular and parallel to the tape plane respectively.

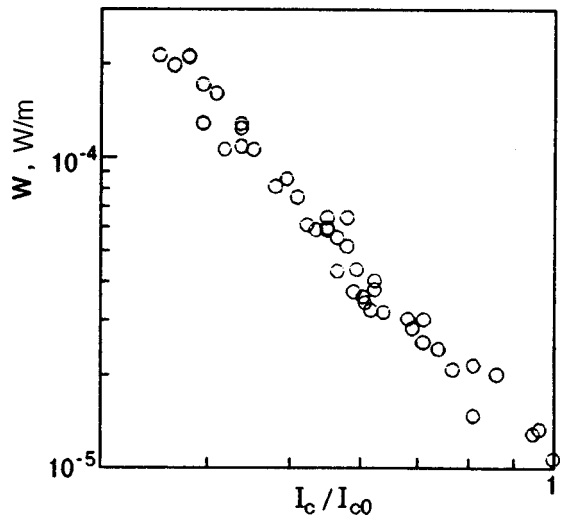

FIG. 8. Dependence of transport losses on the normalized critical current for a composite with $N=19$.

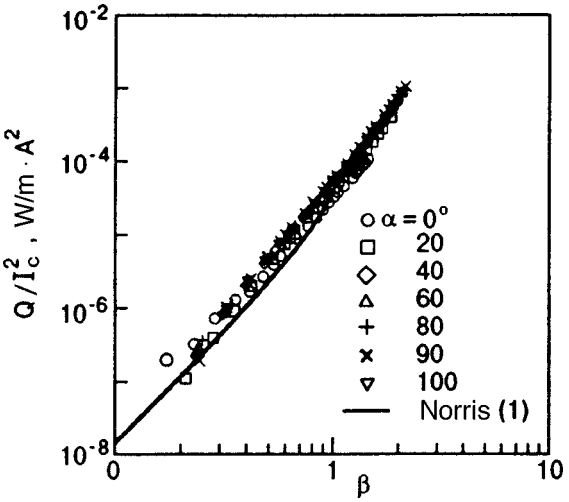

FIG. 9. Dependence of $Q/I_c^2(\beta)$ for a composite with $N=61$ for various orientations of the magnetic field.

transport current becomes stronger. In this region known as the saturation zone (saturation layer or saturation region), the current density is equal to its critical value. Ac power is liberated just in this region and not in the bulk of the superconductor. Saturation losses are of the hysteresis type. However, the volume of the saturation layer for a fixed current amplitude depends on the critical current. The higher the value of I_c, the smaller the volume of the saturation region, and accordingly the smaller than total value of losses. ''Pure'' hysteresis losses exhibit a different behavior. Hysteresis losses increase with the critical current since they are determined by the magnetization loop of the superconductor.

Saturation losses are successfully described by the Norris equations (1) and (2). Among other things, it follows from these equations that Q/I_c^2 is the value losses normalized to I_c^2, which is a general function for a given geometry. Figure 9 shows the experimental dependence of Q/I^2 on β, where losses as well as critical current change under the action of a magnetic field. It can be seen that the results fit into the universal curve as predicted. A similar behavior of losses upon a change in temperature was recently observed by Yang *et al.*[19] in a monofilamentary Ag/Bi-2223 tape. Moreover, the normalization of losses at $I=I_c$ (i.e., when the entire conductor is in the saturated state) to the square of critical current gives close values for the tapes under investigation (see Table I). The Norris equations (5) and (6) for $\beta=1$ can be used to estimate the upper limit of transport losses. It was noted that the calculated values of transport losses can differ from actual values due to ambiguity in the determination of the critical current from the blurred IVC.

CONCLUSION

The results of measurements of ac transport losses in multifilamentary superconducting Bi-2223/Ag tapes in an external magnetic field proved that transport losses are saturation losses differing from ''pure'' hysteresis losses. Saturation losses increase with decreasing critical current, which was observed in experiments. An applied constant magnetic field causes an increase in losses, correlating with the decrease in the critical current in the samples under investigation. The value of transport losses Q/I_c normalized to the square of critical current and plotted as a function of the normalized transport current amplitude fit to the same curve in accordance with the Norris equations.

This research was carried out under the support of the Scientific Council of the State Scientific and Technical Program ''Modern Trends in Physics of Condensed Media,'' subprogram ''Superconductivity,'' project No. 95019.

*E-mail: rudnev@supercon.mephi.ru
**E-mail: postmaster@vniinm402.msk.su

[1] M. N. Pitsakis, T. Haugan, F. C. H. Wong *et al.*, Appl. Phys. Lett. **67**, 4584 (1995).
[2] S. P. Ashworth, Physica C **229**, 355 (1994).
[3] Y. Yang, T. Hughes, C. Beduz *et al.*, Physica C **256**, 378 (1996).
[4] M. Ciszek, B. A. Glowacki, S. P. Ashworth *et al.*, Physica C **260**, 93 (1996).
[5] S. A. Awan, S. Sali, C. M. Friend, and T. P. Beales, IEEE Trans. Appl. Supercond. **7**, 335 (1997).
[6] Y. Fukumoto, H. J. Wiesmann, M. Garber *et al.*, J. Appl. Phys. **78**, 4584 (1995).
[7] K. Kwasnitza and St. Clerc, Physica C **233**, 423 (1994).
[8] A. Oota, T. Fukunaga, M. Matsui *et al.*, Physica C **249**, 157 (1995).
[9] T. Fukunaga, T. Itou, A. Oota *et al.*, IEEE Trans. Appl. Supercond. **7**, 1666 (1997).
[10] H. London, Phys. Lett. **6**, 162 (1963).
[11] W. T. Norris, J. Phys. D **3**, 489 (1970).
[12] M. Ciszek, B. A. Glowacki, A. M. Campbell *et al.*, IEEE Trans. Appl. Supercond. **7**, 314 (1997).
[13] A. D. Niculin, A. K. Shikov, I. I. Akimov *et al.*, IEEE Trans. Appl. Supercond. **7**, 2094 (1997).
[14] T. Fukunaga, S. Maruyama, and A. Oota, *Adv. in Superconductivity VI*, Springer-Verlag, Tokyo (1994), p. 633.
[15] M. Ciszek, A. M. Campbell, and B. A. Glowacki, Physica C **233**, 203 (1994).
[16] A. M. Campbell, IEEE Trans. Appl. Supercond. **5**, 682 (1995).
[17] T. Pe, J. McDonald, and J. R. Clem, *Proceedings of Polish–USA Conference on HTS*, Springer-Verlag (1995).
[18] M. Wilson, *Superconducting Magnets*, Clarendon Press, Oxford (UK) (1983).
[19] Y. Yang, T. Hughes, C. Beduz *et al.*, Physica C **256**, 378 (1996).

Translated by R. S. Wadhwa

Dynamics of vortex lattice in the current state in high-temperature superconductors: Monte Carlo method

M. E. Gracheva, V. A. Kashurnikov, and I. A. Rudnev

*Moscow State Engineering Physics Institute (Technical University), 115409 Moscow, Russia**
(Submitted July 27, 1998)
Fiz. Nizk. Temp. **25**, 148–152 (February 1999)

The current–voltage characteristics (IVC) of real defective high-temperature layered superconductors are calculated by simulating the vortex lattice by means of the Monte Carlo method. The temperature dependence of the defect activation energy is obtained. It is shown that IVC singularities in different temperature ranges are due to the change in the phase conditions of the vortex system and, in particular, the presence of the ''rotating lattice'' phase in a wide temperature range. © *1999 American Institute of Physics.* [S1063-777X(99)00302-3]

INTRODUCTION

In recent years, considerable attention is paid to phase transformations and their dynamics in the vortex lattice of HTSC.[1] Wide application of numerical methods (especially the Monte Carlo method, see the review in Ref. 2) has made it possible to simulate the phase states and phase transitions in various vortex systems and to demonstrate the peculiarities of the vortex lattice melting dynamics in the presence of the pinning centers.[3]

Problems associated with dynamic interaction of the vortex lattice with pinning centers in the presence of transport current and current–voltage characteristics (IVC) are important for practical application of superconducting materials. First computations of IVC by the Monte Carlo method appeared only in 1996.[4–7] Current–voltage characteristics were calculated in the presence of a large number of defects (relative to the number of vortices) with different potential energies.[4] However, defects with different values of activation energy and temperature dependences of IVC have not been studied.

The results on various phase modes of current flow obtained recently from an analysis of IVC of HTSC deserve special attention (see Ref. 7 as well as Refs. 8–10). The modes of pinned vortex glass, plastic flow of vortex liquid, and flowing vortex glass were observed. These phase states of the Abrikosov lattice as well as transitions between them are close to the phase transitions between the states of ''rotating lattice'' and ''vortex liquid'' considered by us recently, but now in the current state.[3]

In this communication, we report on the results of calculations of IVC in model layered superconductors and compare them with the experimental IVC. We shall demonstrate the modification of IVC upon a change in temperature and as a result of an increase in the number of defects. Our aim is also to demonstrate the potentialities of the Monte Carlo method as applied for determining real physical characteristics of HTSC and for analyzing the phase states of the vortex lattice.

MODEL AND COMPUTATIONAL METHOD

Let us consider a two-dimensional vortex lattice simulating a superconducting HTSC layer on a periodic rectangular mesh under the assumption of weak coupling between filaments in a direction perpendicular to the ab plane and in the presence of pinning centers. The discreteness of the spatial mesh is chosen in such a way that its period is much smaller than the period of a perfect triangular vortex lattice.

If we disregard the interaction between vortices and external field, the effective Hamiltonian of such a system has the form[11]

$$H=\frac{1}{2}\sum_{i\neq j}^{N} H(r_i,r_j)n_i n_j+\sum_{i=1}^{N} U_p(r_i)n_i, \tag{1}$$

where

$$H(r_i,r_j)=\frac{\Phi_0^2 d}{2\pi\lambda^2(T)\mu_0}K_0\left(\frac{|r_i-r_j|}{\lambda(T)}\right)$$
$$=U_0(T)K_0\left(\frac{|r_i-r_j|}{\lambda(T)}\right). \tag{2}$$

Here $U_p(r_i)$ is the energy of interaction between a vortex and a defect at the ith lattice site, n_i the occupation numbers of vortices (0 or 1) at the ith site of the spatial mesh with the total number of nodes N, $\Phi_0=hc/2e$ the magnetic flux quantum, K_0 Bessel's function of the imaginary argument, d the superconducting layer thickness, $\lambda(T)=\lambda_0[1-(T/T_c)^{3,3}]^{-1/2}$ the depth of magnetic field penetration into the superconductor, and $\mu_0=4\pi\times10^{-7}$ H/m.

We choose for simulation a real high-temperature superconductor $Bi_2Sr_2CaCu_2O_8$ with the following parameters: $d=2.7$ Å; $\lambda(T=0)=1800$ Å; $T_c=84$ K[9] in the external field $B=0.1$ T. The experimental IVC were obtained for the same parameters.

The calculations were mainly carried out on a spatial mesh with 200×200 cells under periodic boundary conditions with the help of the standard Monte Carlo method by using the Metropolis algorithm. The discreteness of the spatial mesh with 200×200 cells means that if the system contains $N_\nu=150$ vortices, each vortex corresponding to ap-

proximately 260 cells. Such a discreteness is sufficient for constructing a nearly perfect triangular lattice at zero temperature and current.

The actual concentration of vortices corresponding to the given field B was attained by changing the value of the division of a spatial cell so that the period a_ν of the triangular vortex lattice satisfied the relation

$$a_\nu = \left(\frac{2\Phi_0}{\sqrt{3}B} \right)^{1/2}. \tag{3}$$

In order to analyze the behavior of the system with defects, we introduced pinning centers with different concentrations. In this case, the energy of interaction with a pinning center was chosen in the form

$$U_p(T) = -\alpha U_0(T), \tag{4}$$

which corresponds, for example, to $U_p(T=2\,\mathrm{K}) = -3.5\,\mathrm{meV}$ for $\alpha = 0.1$.

The chosen values of the depth of the potential well for a pinning center are close to those observed in actual practice in HTSC.[11,12] Calculations were made for strong pinning, the potential well depth being $U_p(T=2\,\mathrm{K}) = -100\,\mathrm{meV}$. We analyzed various types of (one- and two-dimensional) defects, but main calculations were made for point defects, a defect occupying a single cell of the spatial mesh. This corresponds to the size of a defect $\sim\xi$ (vortex core size of 20 Å) so that only one vortex could be pinned at such a defect. The range of two-dimensional concentrations of defects was from $10^{12}-3\times10^{14}\,\mathrm{m}^{-2}$ (from one to 100 defects corresponded to 150 vortices in the system under investigation).

Dynamic processes were investigated by introducing a transport current in the system. In this case, the Hamiltonian describing the behavior of the entire system was supplemented with the term due to the action of the Lorentz force on each vortex. In the case of elementary motion of a vortex, the term $\delta U = \Phi_0 J \Delta x$ was subtracted from the total energy if the direction of vortex movement coincided with the direction of the Lorentz force exerted to it, and added to it if the vortex moved against the Lorentz force. The transport current was directed along the y-coordinate. In the case of a nonzero current, vortex tubes could move at random over any distance within the size of the system (i.e., the value of Δx was chosen in accordance with the Gibbs distribution). The voltage emerging across the boundaries of the system was calculated from the relation $V = B\nu_{\mathrm{dr}}$, where B is the applied field and $\nu_{\mathrm{dr}} = X_{cm}/\tau$ the drift velocity of a vortex, i.e., the displacement of the center of mass X_{cm} of the vortex tube per unit time τ. The unit of time was conventionally chosen to be equal to an elementary step in the Monte Carlo method, i.e., the indeterminacy is manifested in the arbitrariness of the choice of the voltage scale. This indeterminacy can be eliminated by normalization to an actual IVC.

In order to take into account the boundary conditions correctly, it is necessary that a vortex tube not be able to reach the edge of the system as a result of a single random displacement under the action of the current. This condition in fact determined the maximum possible current for calculations and was verified every time. Figure 1 shows by way of an example a typical distribution of vortex tube displacements relative to the center of mass (actually, the distribution of drift velocities) at $T = 70\,\mathrm{K}$ and $J/J_p = 5$ ($J_p = 5\times10^{10}\,\mathrm{A/m^2}$). Averaging was carried out over all vortex tubes and over 60 000 MC steps. It can be clearly seen that the distribution has the form of an ellipsoid prolate perpendicularly to the direction of the current and that the distribution does not reach the boundaries of the system.

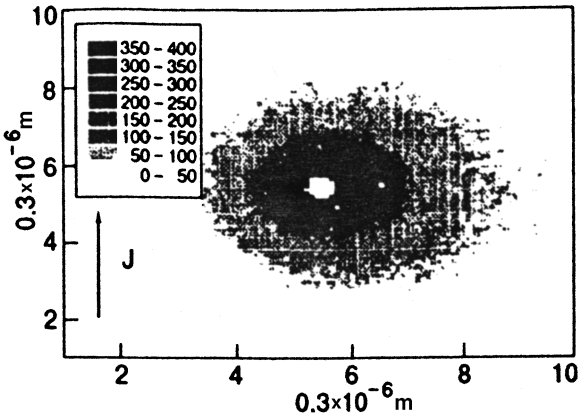

FIG. 1. Drift velocity distribution at $T = 70\,\mathrm{K}$ and $J/J_p = 5$. The intensity is given in terms of the number of vortex jumps over 20 000 MC steps.

DISCUSSION OF THE RESULTS OF CALCULATIONS

We calculated the current–voltage characteristics for systems containing from 1 to 100 defects at temperatures 10, 20, 30, 40 K, etc. (up to 83 K). In the vicinity of the critical temperature, the characteristics were calculated with an interval of 1 K up to the critical region. Typical IVC are presented in Fig. 2 for $T = 20\,\mathrm{K}$ and for various concentrations of defects.

These results were compared with experimental IVC (for small currents) obtained for $Bi_2Sr_2CaCu_2O_x$ films bombarded by high-energy ions.[12] Such a comparison of experimental and theoretical IVC makes it possible to determine the actual scale of electric field strength (i.e., the value of E_p). In our case, for example, $E_p = 5\times10^{-2}\,\mathrm{V/m}$, which indeed corresponds to the actually observed values. Moreover, knowing the magnetic field, we can estimate the vortex relaxation time τ. In our calculations, $\tau \simeq 10^{-12}\,\mathrm{s}$, which is in accord with physical estimates.[1]

There is another coincidence. According to our estimates, the characteristic values of critical currents obtained as a result of calculations differ from actual currents in HTSC approximately by a factor of five. But exactly this numerical factor corresponds to the approximate fraction of superconducting layers (of thickness 2.7 Å) in the entire volume of a unit cell in the compound $Bi_2Sr_2CaCu_2O_x$!

Let us analyze the results of calculations. It can be seen that as the concentration of defects decreases, IVC are ''straightened,'' demonstrating an increasing tendency to a simple ohmic behavior of the system for strong currents. This is also observed as the temperature approaches the critical value (Fig. 3). An analysis of the initial segment of IVC (for small currents) leads to the following result: the current–

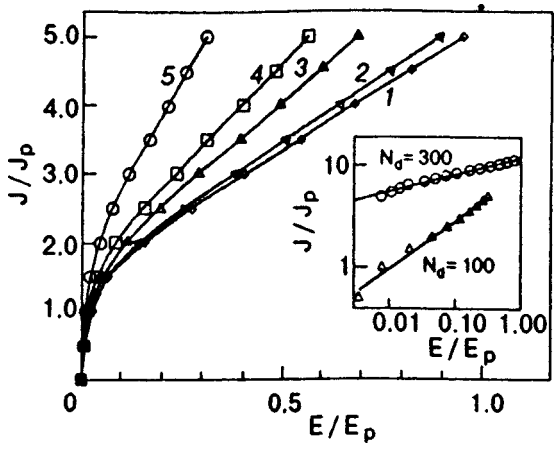

FIG. 2. Typical IVC at $T=20\,\mathrm{K}$ and various numbers of defects N_d: 1 (curve *1*), 10 (curve *2*), 40 (curve *3*), 60 (curve *4*), and 100 (curve *5*). The inset shows IVC for $N_d=100$ and 300 on the log–log scale.

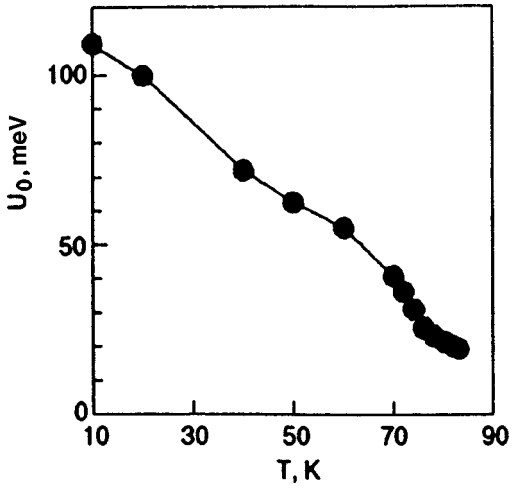

FIG. 4. Temperature dependence of theoretical activation energy.

voltage characteristic on the log–log current and voltage scale is strictly linear (see the inset to Fig. 2), which confirms the existence of magnetic flux creep under these conditions.

Figure 3 shows IVC of the system for a fixed concentration of defects, but at different temperatures. The conditional threshold $J/J_p=0.5$ (chosen as the critical current) can be used to obtain an important physical parameter of point defects from these results, viz., the activation energy U (as a function of temperature) on the basis of the relation

$$U=kT\ln\left(\frac{\partial(E/E_p)}{\partial(J/J_p)}\right)\Bigg|_{E\to 0}. \tag{5}$$

The results of calculations are shown in Fig. 4. These results are in accord with the known experimental dependences.[9]

Concluding the section, we make the following remark. It was proved in our recent publication[3] that the melting of a vortex lattice occurs through an intermediate phase in which lattice deformation and violation of its long-range order away from defects take place, and the triangular lattice splits into islands attached to pinning centers (the rotating lattice phase). This phase can apparently be identified with the observed phase of pinned vortex glass.[7]

Our results of calculation of the motion of a vortex system in the field of defects in the presence of current demonstrate different modes of IVC behavior depending on the phase state of the system. For example, Fig. 3 shows two groups of curves conditionally divided by the temperature boundary $T_{m2}\simeq 70\,\mathrm{K}$ (the temperature of transition from a ''rotating lattice'' to a ''vortex liquid'' according to the terminology adopted in Ref. 3). A visual analysis of the density of vortex distribution shows that a ''rotating lattice'' is observed at $T<T_{m2}$ and a ''vortex glass'' at $T>T_{m2}$. In the ''rotating lattice'' phase, IVC change slowly upon heating, which can be explained by a still strong interaction with pinning centers. On the contrary, at $T>T_{m2}$ we observe a strong influence of temperature (a virtually equidistant increase in voltage upon an increase in temperature by only two degrees) up to the critical region. Thus, the observed difference in the temperature behavior of IVC of a real HTSC can be attributed to different states of the vortex system, which is in accord with the results obtained in Ref. 3.

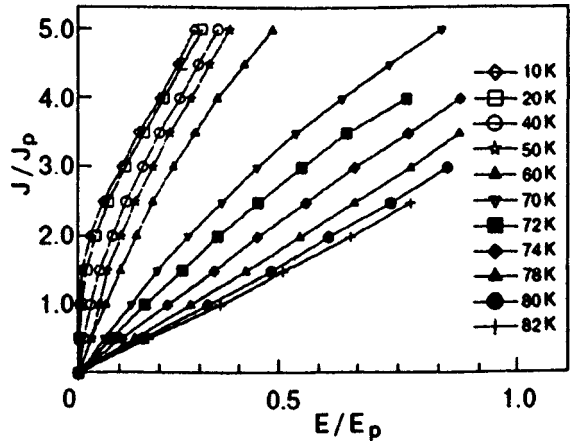

FIG. 3. IVC at various temperatures and $N_d=100$.

CONCLUSION

In this communication, we described the results of simulation of actual current–voltage characteristics of defective layered HTSC. The method used by us makes it possible to obtain real characteristics of defects (like activations energy) as well as information on the dynamics of motion of vortex tubes, i.e., the distribution of their drift velocities, relaxation times, etc. The adaptability of the approach makes it possible to analyze IVC in an arbitrary preset field of defects by simulating technological, radiation, and other defects in high-temperature superconductors.

This research was carried out under the financial support of the States Scientific and Engineering Program ''Contemporary Problems in Physics of Condensed State,'' subprogram ''Superconductivity,'' project Nos. 95019 and 96026.

*E-mail: rudnev@supercon.mephi.ru

[1] G. Blatter, M. V. Feigelman, V. B. Geshkenbein *et al.*, Rev. Mod. Phys. **66**, 1125 (1994).
[2] M. E. Gracheva, M. V. Katargin, V. A. Kashurnikov, and I. A. Rudnev, Fiz. Nizk. Temp. **23**, 1151 (1997) [Low Temp. Phys. **23**, 863 (1997)].
[3] M. E. Gracheva, V. A. Kashurnikov, and I. A. Rudnev, **66**, 269 (1997) [JETP Lett. **66**, 291 (1997)]; M. E. Gracheva, V. A. Kashurnikov, and I. A. Rudnev, Phys. Low-Dimens. Semicond. Struct. **8/9**, 125 (1997).
[4] E. Bonabeau and P. Lederer, Phys. Rev. Lett. **77**, 5122 (1996).
[5] R. Sugano, T. Onogi, and Y. Murayama, Physica C **263**, 17 (1996).
[6] K. Moon, R. T. Scalettar, and G. T. Zimanyi, Phys. Rev. Lett. **77**, 2778 (1996).
[7] S. Ryu, M. Hellerqvist, S. Doniach *et al.*, Phys. Rev. Lett. **77**, 5114 (1996).
[8] A. N. Lykov, C. Attanasio, L. Maritato, and S. L. Prischepa, Supercond. Sci. Technol. **10**, 119 (1997).
[9] B. Khaykovich, M. Konczykowski, E. Zeldov *et al.*, Phys. Rev. B **56**, R517 (1997).
[10] C. Goupil, A. Ruyter, V. Hardy, and Ch. Simons, Physica C **278**, 23 (1997).
[11] V. M. Vinokur, M. V. Feigel'man, V. B. Geshkenbein, and A. I. Larkin, Phys. Rev. Lett. **65**, 259 (1990).
[12] V. F. Elesin, I. A. Esin, I. A. Rudnev *et al.*, Sverkhprovodimost: Fiz., Khim., Tekh. **6**, 807 (1993).

Translated by R. S. Wadhwa

Nonlinear mixed-state longitudinal and transverse resistivities of superconductors with anisotropic pinning—a phenomenological approach

Valerij A. Shklovskij

*National Science Center ''Kharkov Institute of Physics and Technology,'' Institute of Theoretical Physics, 1 Akademicheskaya St., 310108, Kharkov, Ukraine and Kharkov State University, Physical Department, 4 Svobody Sq., 310077, Kharkov, Ukraine**

(Submitted September 24, 1998)
Fiz. Nizk. Temp. **25**, 153–159 (February 1999)

In the presence of anisotropic pinning due to unidirected twins, the nonlinear vortex dynamics is discussed in terms of phenomenologically introduced anisotropic drag and pinning viscosities. A theoretical basis for experimental reconstruction of these viscosities is proposed. A nonlinear Ohm's law is derived. Assuming the anisotropic pinning alone (*a*-pinning model): a) new scaling relations for the anisotropic Hall conductivity are predicted; b) nonlinear guiding effects are discussed; c) specific current and angular behavior of current-voltage characteristics are analyzed. © *1999 American Institute of Physics.* [S1063-777X(99)00402-8]

The influence of twin boundaries (TB's) on the transport properties of high-T_c superconductors is a topic of great current interest.[1–11,16–18] One of the reasons for this interest is that the TB's are naturally occurring planar defects that can easily be formed in a high-T_c $YBa_2Cu_3O_{7-\delta}$ (YBCO) compound.

It is generally recognized that the order parameter is slightly suppressed at TB's.[1] As a result, an isolated TB attracts vortices and pins them.[1] The TB pinning force acting on the vortices directed along the **c**-axis (and the TB) of the crystal is often strongly anisotropic, because it is usually considerably weaker for the motion of vortices along twins than across them.[2]

Recently, the problem of twin influence on the vortex motion in plane geometry has been studied numerically.[3,4] The simulations in[3,4] were performed for the interaction of moving vortices with only one isolated TB. Some interesting dynamic peculiarities of this interaction were elucidated. However, it is worth noting that, in a real transport experiment[2,5–10] we usually probe a certain ''self-averaged'' vortex dynamics, which results from the interaction of vortices with many TB's, distributed with some average density between voltage leads. Obviously, this self-averaging will ''smear'' some subtle details of the vortex interaction with an isolated TB, which were detected in.[3,4]

Several Hall experiments[5–7] were performed on YBCO samples, where TB's were oriented basically in two mutually orthogonal directions. Because the transport response of the crystals was always measured as an integral property, the pinning anisotropy of twins in this case was commonly masked, i.e., the influence of TB's pinning on *ab*-plane transport in the $\mathbf{H}\|\mathbf{c}$ geometry is, on the average, isotropic, as for point pins (neglecting small *ab*-axis anisotropy).

A much different type of situation (anisotropic) occurs if we measure the *ab*-plane transport response of single crystal with unidirected twins.[2,8–10] It is generally believed[11] that the main special feature of this response lies in the possibility of the ''guided'' motion (GM) of vortices along the easiest direction (in the case of TB's—mostly along them). This GM generates a new, specific contribution to the transverse (with respect to the current direction) resistivity of the sample $\rho_\perp^+$, which is even with respect to the magnetic field reversal (in addition to the odd Hall contribution $\rho_\perp^-$, inherent in the isotropic pinning contribution).

Earlier, experimental and certain theoretical aspects of anisotropic pinning and GM of vortices moving in the flux flow regime (for cold-rolled Nb–Ta sheets) have been discussed in detail by Niessen and Weijesenfeld in.[12] Interest in these problems was renewed after detection of TB's in YBCO. Apart from the experimental works,[2,5–10] we should also mention in this connection the recent theoretical paper by Mawatari,[11] where the single-vortex anisotropic pinning dynamics has been discussed within the frame-work of the ''microscopic'' approach based on the Fokker–Planck equation.

Another approach to the anisotropic pinning was first suggested by Sonin and Kholkin in.[13] They proposed the general form of a linear Ohm's law in uniaxially anisotropic media, which was formulated (on the basis of symmetry considerations) in terms of four phenomenologically introduced ''intrinsic'' resistivities.[13] In this approach, besides $\rho_\perp^+$ (and in addition to the usually measured even longitudinal contribution $\rho_\parallel^+$), a new, angle-dependent, odd longitudinal resistivity $\rho_\parallel^-$ also appears, due to a possible anisotropy of the Hall drag coefficient in the twinned sample. The last effect has recently been observed for the first time in a YBCO single crystal with unidirected twins.[9]

Note, however, that there are no reasons to expect the change of the Hall drag coefficient α_i due to point pins, for isotropic pinning.[14,15] This directly implies a simple scaling relation $\rho_\perp^- \sim \alpha_i(\rho_\parallel^+)^2$ between current-dependent, nonlinear resistivities $\rho_\perp^-(j)$ and $\rho_\parallel^+(j)$ for $\rho_\perp^- \ll \rho_\parallel^+$.[14,15]

In order to study possible scaling relations within the frame-work of the phenomenological approach,[13] we have generalized its results to the nonlinear case. In so doing, we follow the phenomenological approach used recently by

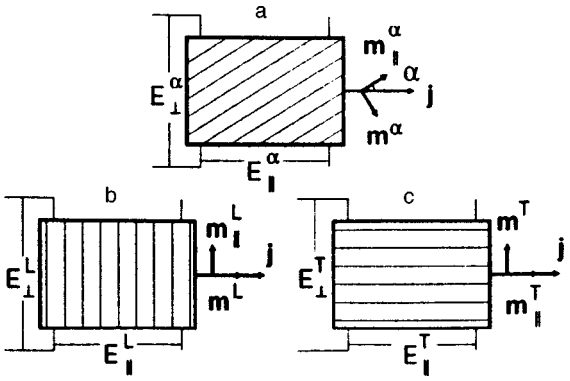

FIG. 1. The schematic sample configuration for three cases with different values of angle α between the current density vector $\mathbf{j}$ and the unit vector $\mathbf{m}_\parallel$ directed along TB's, which are shown by thin parallel lines: general case, $\alpha \neq 0,\ \pi/2$ (a); longitudinal L-geometry, $\mathbf{j} \perp \mathbf{m}_\parallel^L,\ \alpha = \pi/2$ (b); transverse T-geometry, $\mathbf{j} \perp \mathbf{m}_\parallel^T,\ \alpha = 0$ (c); in all cases $E_\perp$ and $E_\parallel$ are transverse and longitudinal (with respect to $\mathbf{j}$-direction) electric-field components, $\mathbf{m} \perp \mathbf{m}_\parallel$.

Vinokur *et al.* in[14] for the case of isotropic pinning. Below we use the method of[14] for considering both the isotropic and anisotropic pinning, and so we can derive the nonlinear Ohm's law, which was postulated earlier for the linear case in.[13] In this way we clarify the origin of the four phenomenological resistivities, earlier introduced in[13], in terms of drag and pinning viscosities, i.e., at a more detailed level. Below we also show that these viscosities can be reconstructed (for purely anisotropic pinning) from current-voltage measurements in two simple special experimental LT-geometries (see Figs. 1.b,c).

The main advantage of this phenomenological approach (for example, in comparison with the microscopic approach in[11]) lies in the possibility of predicting and explaining the most general aspects of self-averaged vortex motion in the presence of TB's anisotropy in simple, physically transparent terms. We can than elucidate the appearance of two new anisotropic contributions to longitudinal and transverse resistivities (odd $\rho_\parallel^-$ and even $\rho_\perp^+$, respectively), the scaling of anisotropic Hall conductivities, the nontrivial angular dependence of current-voltage characteristic's (CVC's) in a nonlinear regime, the peculiarities of nonlinear guiding of the vortices, and some other general results.

a) *Discussion of the model and nonlinear Ohm's law derivation.* To be specific, let us consider the YBCO single crystal with unidirected twins in the geometry, where a homogeneous transport current of density $\mathbf{j}$ flows in the *ab*-plane and external magnetic field $\mathbf{H}$ is directed along the $\mathbf{c}$-axis. We ignore below small *ab*-plane anisotropy of the detwinned crystal; so, all the anisotropic effects under consideration are caused by TB's with the average distance between them $d \gg a_0$, where a_0 is the intervortex distance. In this limit we can suppose that $\varepsilon \equiv a_0/d$ is the relative fraction of vortices trapped by the twins. The TB's presence changes both electronic and pinning properties of the previously isotropic crystal. Let η_i and α_i be isotropic (bulk) vortex drag and Hall drag viscosities, respectively. In addition, we attribute the anisotropy of these viscosities to the vortices being at the TB's. Then for appropriate viscous drag and Magnus forces we have

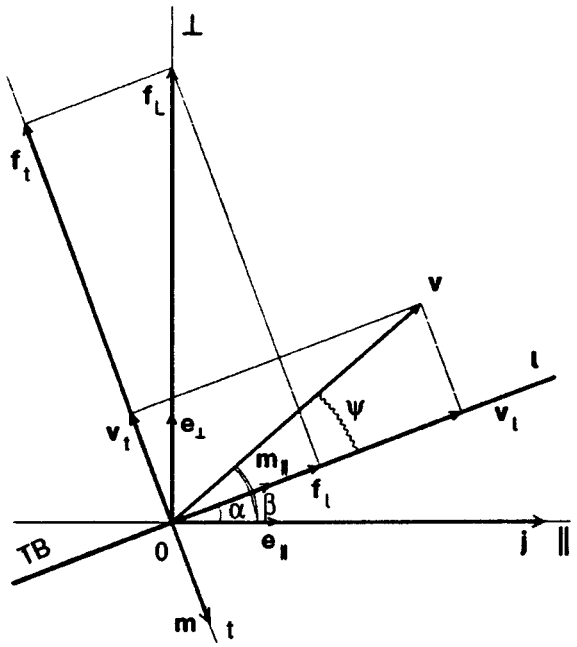

FIG. 2. The *ab*-plane geometry of $\mathbf{v}$ and $\mathbf{f}$ components in two coordinate systems: (l,t) coordinates with unit vectors $\mathbf{m}_\parallel$ (along $\mathbf{j}$) and $\mathbf{m}$; $(\perp,\parallel)$ coordinates with unit vectors $\mathbf{e}_\parallel$ (along $\mathbf{j}$) and $\mathbf{e}_\perp$; $\mathbf{v}$—average vortex velocity, $\mathbf{f}_L$—Lorentz force, $\mathbf{j}$—current density. Angles α, β, ψ—see text.

$$\mathbf{f}_\eta^i = -\eta_i \mathbf{v}, \quad \mathbf{f}_\eta^a = -\eta_i \mathbf{v} - \eta_t \mathbf{v}_t - \eta_l \mathbf{v}_l, \tag{1}$$

$$\begin{aligned} \mathbf{f}_M^i &= -\alpha_i \mathbf{v} \times \mathbf{n}, \\ \mathbf{f}_M^a &= -\alpha_i \mathbf{v} \times \mathbf{n} - \alpha_t \mathbf{v}_t \times \mathbf{n} - \alpha_l \mathbf{v}_l \times \mathbf{n}. \end{aligned} \tag{2}$$

Here $\mathbf{v}_t$ and $\mathbf{v}_l$ are transverse and longitudinal (with respect to TB) average vortex velocities, respectively ($\mathbf{v} = \mathbf{v}_l + \mathbf{v}_t$, see Fig. 2); η_t, η_l and α_t, α_l are the corresponding excess anisotropic viscosities (as compared to isotropic contributions); $\mathbf{n}$ is the unit vector in the magnetic field direction ($\mathbf{n} \equiv \mathbf{H}/H$). As for now, we also consider both bulk (isotropic) and anisotropic (TB's) pinning forces. Also, for the former, we assume, as in,[14] that $\mathbf{f}_p^i = -\gamma_i(v)\mathbf{v}$, where $\gamma_i(v) > 0$ is the nonlinear phenomenological viscosity, which depends only on the magnitude of $v \equiv |\mathbf{v}|$. The anisotropic pinning force $\mathbf{f}_p^a$, which acts on the vortices at TB's, can be written as

$$\mathbf{f}_p^a = -\gamma_i(v)\mathbf{v} - \gamma_t(|\mathbf{v}_t|)\mathbf{v}_t - \gamma_l(|\mathbf{v}_l|)\mathbf{v}_l, \tag{3}$$

where γ_t and γ_l are the average phenomenological transverse and longitudinal vortex pinning viscosities, respectively. Equations (1)–(3) allow us to write the force balance equation for the kth vortex in much the same way as in:[14] Then, on averaging it over disorder, thermal fluctuations, and also vortex twin and bulk positions,[14] we arrive at the following dynamic equation for the average velocity of ''effective'' vortex in the crystal with unidirected TB's

$$\hat{\eta}_i \mathbf{v} + \alpha_i \mathbf{v} \times \mathbf{n} + \varepsilon(\hat{\eta}_t \mathbf{v}_t + \alpha_t \mathbf{v}_t \times \mathbf{n} + \hat{\eta}_l \mathbf{v}_l + \alpha_l \mathbf{v}_l \times \mathbf{n}) = \mathbf{f}_L, \tag{4}$$

$$\hat{\eta}_i \equiv \eta_i + \gamma_i(v), \quad \hat{\eta}_t \equiv \eta_t + \gamma_t(|\mathbf{v}_t|), \quad \hat{\eta}_l \equiv \eta_l + \gamma_l(|\mathbf{v}_l|), \tag{5}$$

where $\mathbf{f}_L=(\Phi_0/c)\mathbf{j}\times\mathbf{n}$ is the Lorenz force (Φ_0 is the flux quantum and c is the velocity of light). Let $\mathbf{m}$ and $\mathbf{m}_\parallel\equiv\mathbf{z}\times\mathbf{m}$ be the unit vectors of (t,l) coordinate system (see Fig. 2), directed perpendicularly and parallel to the TB's, and z be the unit vector along the **z**-axis, which is perpendicular to the sample plane ($\mathbf{n}=n\mathbf{z}$, where $n=\pm1$). Then, taking into account that $\mathbf{v}=(c/H)\mathbf{E}\times\mathbf{n}$, where $\mathbf{E}$ is the in-plane electric field, we can arrive at a nonlinear Ohm's law in the form

$$\mathbf{j}=(c^2/H\Phi_0)\{\hat{\eta}_i\mathbf{E}+\alpha_i\mathbf{E}\times\mathbf{n}+\varepsilon[\hat{\eta}_t\mathbf{E}_l+\alpha_t\mathbf{E}_l\times\mathbf{n}+\hat{\eta}_l\mathbf{E}_t+\alpha_l\mathbf{E}_t\times\mathbf{n}]\}. \tag{6}$$

Here $\mathbf{E}_t=E_t\mathbf{m}$, $\mathbf{E}_l=E_l\mathbf{m}_\parallel$ and $E_t=\mathbf{m}\cdot\mathbf{E}$, $E_l=\mathbf{m}_\parallel\cdot\mathbf{E}$. Because of $E_l=(nH/c)v_t$ and $E_t=-(nH/c)v_l$, viscosities (5), actually, depend on corresponding electric-field components.

Vector Eq. (6) can be represented in the scalar form

$$\begin{cases}\hat{\sigma}_l E_t-\sigma_{Ht}nE_l=j_t\\ \sigma_{Hl}nE_t+\hat{\sigma}_t E_l=j_l\end{cases}, \tag{7}$$

where $j_t\equiv\mathbf{m}\cdot\mathbf{j}$, $j_l\equiv\mathbf{m}_\parallel\cdot\mathbf{j}$, and the quantities

$$\hat{\sigma}_l\equiv(c^2/H\Phi_0)[\hat{\eta}_i(E)+\varepsilon\hat{\eta}_l(|E_t|)]\equiv\sigma_i(E)+\sigma_l(|E_t|), \tag{8a}$$

$$\hat{\sigma}_t\equiv(c^2/H\Phi_0)[\hat{\eta}_i(E)+\varepsilon\hat{\eta}_t(|E_l|)]\equiv\sigma_i(E)+\sigma_t(|E_l|), \tag{8b}$$

$$\sigma_{Ht}\equiv-(\alpha_i+\varepsilon\alpha_t)(c^2/H\Phi_0),\quad \sigma_{Hl}\equiv-(\alpha_i+\varepsilon\alpha_l)(c^2/H\Phi_0) \tag{8c}$$

are the additive functions of the appropriate viscosities and have a physical meaning of the corresponding components of the conductivity tensor (in $t-l$ representation):

$$\hat{\sigma}\equiv\begin{pmatrix}\hat{\sigma}_l & -n\sigma_{Ht}\\ n\sigma_{Hl} & \hat{\sigma}_t\end{pmatrix}. \tag{9}$$

The formal solution of Eqs. (7) as linear equations (but with nonlinear coefficients!) allows one to deduce the nonlinear Ohm's in the $\mathbf{E}(\mathbf{j})$ form (see also[16]):

$$\mathbf{E}=\hat{\rho}_l\mathbf{m}(\mathbf{m}\cdot\mathbf{j})+\hat{\rho}_t\mathbf{m}_\parallel(\mathbf{m}_\parallel\cdot\mathbf{j})+n[\hat{\rho}_{Hl}\mathbf{m}_\parallel(\mathbf{m}\cdot\mathbf{j})-\hat{\rho}_{Ht}\mathbf{m}(\mathbf{m}_\parallel\cdot\mathbf{j})], \tag{10}$$

$$\hat{\rho}_l\equiv\hat{\sigma}/D_\sigma,\quad \hat{\rho}_t\equiv\hat{\sigma}'_l/D_\sigma,\quad \hat{\rho}_{Hl}\equiv-\hat{\sigma}_{Hl}/D_\sigma,\quad \hat{\rho}_{Ht}\equiv-\hat{\sigma}_{Ht}/D_\sigma, \tag{11}$$

where $D_\sigma\equiv\hat{\sigma}_l\hat{\sigma}_t+\sigma_{Hl}\sigma_{Ht}$, and Eqs. (11) give the elements of resistivity tensor $\hat{\rho}$ which is the reciprocal of $\hat{\sigma}$. Although Eq. (10) formally resembles a similar expression for the linear Ohm's law in,[13] its physical meaning is wider, because, generally, the resistivities $\hat{\rho}_l$, $\hat{\rho}_t$, $\hat{\rho}_{Hl}$, $\hat{\rho}_{Ht}$, are the nonlinear functions of **E** [see Eqs. (8)], and this circumstance is denoted by the superscript ''^'' If **E**-dependence of $\hat{\rho}$ is irrelevant, then Eq. (10) is equivalent to the similar equation in[13] (see also[17]).

In experiment, one usually measures the longitudinal $E_\parallel$ and transverse $E_\perp$ (with respect to **j**-direction) components of **E**. In these $(\perp,\parallel)$ coordinates (see Fig. 2) the unit vectors are $\mathbf{e}_\parallel\equiv\mathbf{j}/j$, $\mathbf{e}_\perp\equiv\mathbf{z}\times\mathbf{j}/j$, and $\mathbf{E}=E_\parallel\mathbf{e}_\parallel+E_\perp\mathbf{e}_\perp$. Then there are simple relations between E_t, E_l and $E_\parallel$, $E_\perp$ of the form

$$\begin{cases}E_t=xE_\parallel-yE_\perp\\ E_l=yE_\parallel+xE_\perp\end{cases};\quad \begin{cases}E_\parallel=yE_l+xE_t\\ E_\perp=xE_l-yE_t\end{cases}, \tag{12}$$

where $x\equiv\mathbf{m}\cdot\mathbf{e}_\parallel$ and $y\equiv\mathbf{m}_\parallel\cdot\mathbf{e}_\parallel$. Then, in view of (12), we have

$$E_\parallel=(\hat{\rho}_\parallel^+ + n\hat{\rho}_\parallel^-)j,\quad E_\perp=(\hat{\rho}_\perp^+ + n\hat{\rho}_\perp^-)j; \tag{13}$$

$$\begin{cases}\hat{\rho}_\parallel^+\equiv x^2\hat{\rho}_l+y^2\hat{\rho}_t\\ \hat{\rho}_\perp^+\equiv xy(\hat{\rho}_t-\hat{\rho}_l)\end{cases};\quad \begin{cases}\hat{\rho}_\perp^-\equiv x^2\hat{\rho}_{Hl}+y^2\hat{\rho}_{Ht}\\ \hat{\rho}_\parallel^-\equiv xy(\hat{\rho}_{Hl}-\hat{\rho}_{Ht})\end{cases}. \tag{14}$$

Note that the experimentally measured $\hat{\rho}_{\perp,\parallel}^{\pm}$ values generally depend, as defined by Eqs. (14), on the angle α between $\mathbf{m}_\parallel$ and **j** (see Fig. 2) in two ways. The explicit dependence on α can easily be seen from Eqs. (14), provided that the elements of the tensor $\hat{\rho}$ do not depend on **E**, i.e., if $\hat{\rho}\to\rho$, where ρ is the tensor of the linear Ohm's law. However, in nonlinear regimes there appears an additional nonlinear angular dependence of $\hat{\rho}_{\perp,\parallel}^{\pm}$ through the implicit dependence of $\hat{\rho}$-tensor elements on E_l, E_t fields, which, in their turn, depend on the α value through $j_t=xj$ and $j_l=yj$ by Eqs. (7). Below we pay a special attention to this α-dependence due to its nontriviality.

b) *Scaling and ''reconstruction'' of $\hat{\sigma}$ in the a-pinning model.* Equations (14) show that, in the case of linear Ohm's law, resistivities $\rho_{\parallel,\perp}^{\pm}(\alpha)$ can be found for the sample with an arbitrary α value (see Fig. 1a), if four current-independent intrinsic resistivities ρ_l, ρ_t, ρ_{Hl}, ρ_{Ht} are known. In their turn, they can be measured experimentally (''reconstructed'') in two special (''reduced'') geometries of experiment (see Figs. 1b, 1c), namely, ρ_l, ρ_{Hl}—in the longitudinal L-geometry ($\mathbf{j}\perp$ TB's), and ρ_t, ρ_{Ht}—in the transverse T-geometry ($\mathbf{j}\parallel$TB's). In these reduced LT-geometries the sample with unidirected twins behaves isotropically, because, by virtue of Eqs. (14), the two new resistivity components $\rho_\perp^+$ and $\rho_\parallel^-$, which are specific to anisotropic geometry of general type ($\alpha\neq0,\ \pi/2$), are equal to zero. Below we show that for the case of purely anisotropic pinning [*a*-pinning model, $\gamma_i(v)=0$], the above-mentioned situation can be generalized to the nonlinear regime.

Actually, it can be shown that Eqs. (7) can be written for both L-geometry ($x\equiv x_L=1$, $y\equiv y_L=0$) and T-geometry ($x_T=0$, $y_T=1$) as

$$\begin{cases}\hat{\sigma}_l(E_\parallel^L)E_\parallel^L-\sigma_{Ht}E_\perp^L=j\\ \hat{\sigma}_t(E_\perp^L)E_\perp^L+\sigma_{Hl}E_\parallel^L=0\end{cases},\quad \begin{cases}\hat{\sigma}_l(E_\perp^T)E_\perp^T+\sigma_{Ht}E_\parallel^T=0\\ \hat{\sigma}_t(E_\parallel^T)E_\parallel^T-\sigma_{Hl}E_\perp^T=j\end{cases}. \tag{15}$$

Now we assume that four CVC's, namely $E_\parallel^L(j)$, $E_\perp^L(j)$, $E_\parallel^T(j)$, $E_\perp^T(j)$, are experimentally known. Let also $E_\parallel^L=f_L(E_\perp^L)$ and $E_\parallel^T=f_T(E_\perp^T)$, where the functions $f_L(x)$ and $f_T(x)$ are also known. Then, after some algebra with Eqs. (15) we arrive at

$$\begin{cases}\sigma_{Ht}=-j/[E_\perp^L+f_T(E_\parallel^L)]\\ \sigma_{Hl}=-j/[E_\perp^T+f_L(E_\parallel^T)]\end{cases},\quad \begin{cases}\hat{\sigma}_l(x)=[j_\parallel^L(x)/x]/[1+f_L^{-1}(x)/f_T(x)]\\ \hat{\sigma}_t(x)=[j_\parallel^T(x)/x]/[1+f_T^{-1}(x)/f_L(x)]\end{cases}, \tag{16}$$

where $j_\parallel^L(E_\parallel^L)$, $j_\parallel^T(E_\parallel^T)$ are the functions inverted to the functions $E_\parallel^L(j)$, $E_\parallel^T(j)$, respectively. Equations (16) give the

complete and exact solution of the $\hat{\sigma}$-tensor reconstruction problem in the *a*-pinning model. They allow us to express exactly the longitudinal and transverse CVC's of the sample with arbitrary angle α (see Fig. 1a) in terms of four CVC's experimentally measured in LT-geometries[17] at arbitrary constant values of σ_{Hl}, σ_{Ht}; the expressions for the last are, in fact, the desired scaling relations in the *a*-pinning model. If, as is often the case in experiment,[5,9] the Hall components of the $\hat{\sigma}$-tensor are considerably smaller then the diagonal components, then Eqs. (16) are greatly simplified to

$$\begin{cases} \sigma_{Ht}=-j/f_T[E_\parallel^L(j)] \\ \sigma_{Hl}=-j/f_L[E_\parallel^T(j)] \end{cases}, \quad \begin{cases} \hat{\sigma}_l(x)=j_\parallel^L(x)/x \\ \hat{\sigma}_t(x)=j_\parallel^T(x)/x \end{cases}. \tag{17}$$

Physical realization of pure anisotropic pinning considered here is most probable in the temperature range $T_{\rm dp}^i < T < T_{\rm dp}^\parallel$, where $T_{\rm dp}^i$ and $T_{\rm dp}^\parallel$ are depinning temperatures[1] for the point pins and the longitudinal motion of vortices on TB's, respectively.

c) *Guiding analysis.* Below we present the main results of studying the GM in the *a*-pinning model. For simplicity, we here neglect generally small nondiagonal Hall terms in the $\hat{\sigma}$-tensor (Eq. (13)).

First we consider the linear case, where $\rho_l=\rho_\parallel^{+L}$, $\rho_t=\rho_\parallel^{+T}$, i.e., ρ_l, ρ_t values can be measured in LT-geometries. At arbitrary angle $\alpha\neq 0$, $\pi/2$, the directions of **v** and **f** do not coincide (see Fig. 2), if $\eta_l\neq\eta_t$ (i.e., $\rho_t\neq\rho_l$). Let us define the auxiliary angle ψ as a measure of competition between guided ($-v_l$) and transverse ($-v_t$) motion of vortices across TB's (''slipping,'' in terms of[12]). It follows from Eq. (4) that

$$\tan\psi\equiv v_t/v_l=\tan\alpha_c/\tan\alpha, \tag{18}$$

where $\tan\alpha_c\equiv\rho_t/\rho_l$. In general, $0<\alpha_c<\pi/2$, however, normally[2,8] $\rho_t<\rho_l$ and $\alpha_c<\pi/4$. We also introduce another angle $\beta\equiv\alpha+\psi$ (see Fig. 2), which can be measured experimentally,[12] because

$$\cot\beta\equiv -E_\perp^+/E_\parallel^+=-\rho_\perp^+(\alpha)/\rho_\parallel^+(\alpha). \tag{19}$$

As it follows from (19) and the definition of β,

$$\cot\beta=\tan\alpha(1-\tan\alpha_c)/(\tan^2\alpha+\tan\alpha_c). \tag{20}$$

From Eq. (20) one can deduce that the $\beta(\alpha)$ dependence is always nonmonotonic (see Fig. 3). The extreme value of $\beta_{\rm ext}$ ($\beta_{\max}$ at $\alpha_c>\pi/4$ or $\beta_{\min}$ at $\alpha_c<\pi/4$) is attained at the $\tan\alpha_0=(\tan\alpha_c)^{1/2}$ and $\beta_{\rm ext}=2\alpha_0$. Experimentally, of special interest are the cases where $\cot\beta\gg 1$, i.e., the transverse electric field $E_\perp^+$ is considerably greater than the longitudinal field $E_\parallel^+$ due to the dominant role of the GM. More detailed examination of Eq. (20) shows that the most favorable conditions for that case will be at $\tan\alpha_c\ll 1$ and $\tan\alpha\ll 1$. In fact, there are two limiting cases, were $|E_\perp^+|\gg|E_\parallel^+|$, namely

$$\cot\beta\approx\begin{cases} \dfrac{\tan a}{\tan\alpha_c}\gg 1, \quad \tan^2\alpha\ll\tan\alpha_c\ll\tan\alpha & (21a) \\ \dfrac{t}{\tan\alpha}\gg 1, \qquad \tan\alpha_c\ll\tan^2\alpha & (21b) \end{cases}.$$

The situation is quite real experimentally, because in experiment[8] it was shown that $\tan\alpha_c<10^{-6}$ at $T\approx 87$ K for YBCO (see Fig. 1, curves *1* and *5* in[8]). Note also that the distinction between cases a) and b) in Eq. (21) follows from the fact that the angle β always shows an extreme behavior in the vicinity of angle α_0 (see Fig. 3).

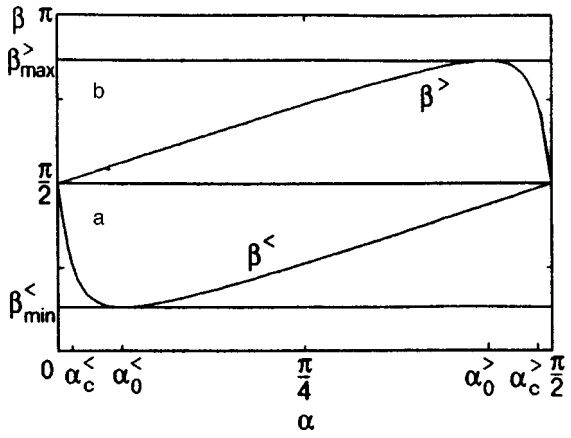

FIG. 3. Schematic nonmonotonic dependence of β on α, where β is the angle between **j** and **v** (see Fig. 2) and α is the angle between **j** and $\mathbf{m}_\parallel$: $\alpha_c=\alpha_c^<$, $\beta=\beta^<$ (a); $\alpha_c=\alpha_c^<$, $\beta=\beta^>$ (b).

The linear result can be generalized to the nonlinear regimes if we replace $\tan\alpha_c$ by $\tan\hat{\alpha}_c\equiv\hat{\rho}_t(|E_l|)/\hat{\rho}_l(|E_t|)$, i.e., we take into account that $\alpha_c\to\hat{\alpha}_c(\alpha,j)$. It can be demonstrated (see Eqs. (8) and (11)) that

$$\tan\hat{\alpha}_c=\rho_T(j_l)/\rho_L(j_t)=\left[\frac{E_\parallel^T(j\cos\alpha)}{E_\parallel^L(j\sin\alpha)}\right]\tan\alpha, \tag{22}$$

where, as previously, $E_\parallel^L(j)=j\rho_L(j)$ and $E_\parallel^T(j)=j\rho_T(j)$ are longitudinal CVC's in LT-geometries, respectively. Because $\hat{\alpha}_c=\hat{\alpha}_c(\alpha,j)$, the nonlinear $\alpha-j$ dynamics of $\cot\hat{\beta}$ may be more complicated than in the linear case. The two limits ($\alpha\to 0$ and $\alpha\to\pi/2$) are of particular interest. For example, if $\alpha\to\pi/2$, then in the creep regime (for the power-law CVC's) we may have $\rho_T(j\cos\alpha)\to\rho_T[j(\pi/2-\alpha)]\ll\rho_T(j)$, whereas $\rho_L(j\sin\alpha)\approx\rho_L(j)$. So, if for LT-geometries at fixed j the values of $\rho_T(j)$ and $\rho_L(j)$ are of the same order, i.e., $\tan\hat{\alpha}_c\lesssim 1$ for $\alpha\approx\pi/4$ (weak guiding), then in the limit $\alpha\to\pi/2$ there should be $\tan\hat{\alpha}_c\ll 1$, i.e., we can expect an essential nonlinear enhancement of the guiding effect. Similar reasoning for $\alpha\to 0$ shows that $\tan\hat{\alpha}_c\gg 1$ is feasible; then it is possible that in the process of α increase from 0 to $\pi/2$ at fixed j the observed voltage $V_\perp^+$ changes its sign, passing over $V_\perp^+=0$ at $\tan\hat{\alpha}_c=1$. Yet, from the experimental viewpoint, it is of greater interest to realize this transition for the given sample ($\alpha=$const) by changing the current; qualitative analysis of these effects for the power-law CVC has been made.[17]

Now we show that both longitudinal $E_\parallel^\alpha(j)$ and transverse $E_\perp^\alpha(j)$ CVC's of the sample with an arbitrary α value in the model under study can be expressed through the longitudinal CVC's in LT-geometries. Actually, in the *a*-pinning model $E_t=E_t(j_t)$ and $E_l=E_l(j_l)$ [see Eqs. (7), where small Hall terms are ignored]. Then it follows from Eqs. (12), if we apply them to the LT-geometries, that $E_t(j_t)=E_\parallel^L(j_t)$ and $E_l(j_l)=E_\parallel^T(j_l)$. The repeated use of Eqs. (12) yields

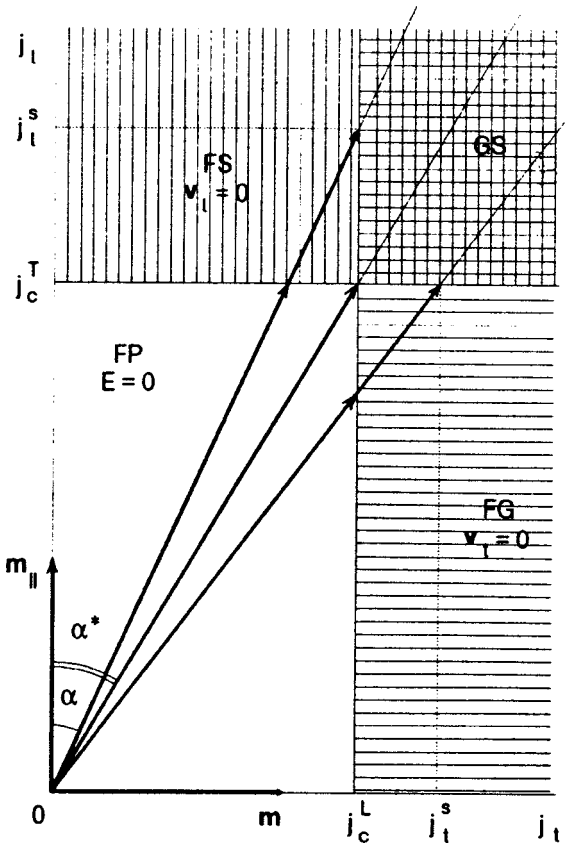

FIG. 4. Schematic diagram of the dynamic states of the vortex system on (j_l, j_t) plane. There are four regions: FP—full pinning, FS—full slipping, FG—full guiding, GS—guiding and slipping. j_c^L and j_c^T—critical current densities in L- and T-geometries, respectively.

$$\begin{cases} E_{\parallel}^{\alpha}(j) = xE_{\parallel}^{L}(xj) + yE_{\parallel}^{T}(yj) \\ E_{\perp}^{\alpha}(j) = xE_{\parallel}^{T}(yj) - yE_{\parallel}^{L}(xj) \end{cases}. \tag{23}$$

Note the nontrivial angular dependence in the arguments of $E_{\parallel}^{L}$ and $E_{\parallel}^{T}$ functions. Equations (23) also show how the peculiarities of CVC's in the ''basic'' LT-geometries are manifested in the $E_{\parallel,\perp}^{\alpha}(j)$ CVC's. First we shall study the α-dependence of critical current densities $j_c(\alpha)$ in terms of the basic critical current densities of our model $j_c^L \equiv j_c(\pi/2)$ and $j_c^T \equiv j_c(0)$ in LT-geometries, respectively. For the analysis we assume the simplest form of CVC's in LT-geometries

$$\begin{aligned} E_{\parallel}^{L}(j) &= \rho_l(j - j_c^L)\,\theta(j - j_c^L); \\ E_{\parallel}^{T}(j) &= \rho_t(j - j_c^T)\,\theta(j - j_c^T), \end{aligned} \tag{24}$$

where $\theta(x) = 1$ for $x > 0$ and $\theta(x) = 0$ for $x < 0$. Using these ''ideal'' CVC's we ignore the creep and, at the same time, we fix the singularities of CVC's in the form of a kink at $j = j_c$. Substitution of Eqs. (24) into Eqs. (23) gives the analytical form of CVC's.

But it is more instructive to analyze these equations on the (j_t, j_l) plane. In Fig. 4 the first quadrant of the plane is divided by straight lines $j_l = j_c^T$ and $j_t = j_c^L$ into four regions. The end of the vector **j** with the coordinates $(j \sin\alpha,\ j \cos\alpha)$ dependent on j, α values, can belong to each of these regions with different physical meaning of dynamic states of the vortex system.

The region of ''full pinning'' (FP in Fig. 4), where $E_{\parallel}^{\alpha}(j) = E_{\perp}^{\alpha}(j) = 0$, is shown by the unshaded rectangle and its diagonal determines the critical angle α^* ($\tan\alpha^* \equiv j_c^L/j_c^T$). Then it is easy to see that

$$j_c(\alpha) \equiv \begin{cases} j_c^{>}(\alpha) = j_c^L/\sin\alpha & \alpha > \alpha^* \\ j_c^{<}(\alpha) = j_c^T/\cos\alpha & \alpha < \alpha^* \end{cases}. \tag{25}$$

In the region of ''full slipping'' (FS in Fig. 4), shaded by vertical lines, $\alpha < \alpha^*$, $j_t(\alpha) < j_c^L$, and the vortices are moving normally to the TB's, i.e., $\mathbf{v}_{FS} = \mathbf{v}_t \| \mathbf{m}$. The ''full guiding'' (FG) region is shaded in Fig. 4 by horizontal lines, it represents the fully GM of vortices with $\mathbf{v}_{FG} = \mathbf{v}_l \| \mathbf{m}_{\parallel}$, because at $\alpha > \alpha^*$ we always have $j_l(\alpha) < j_c^T$. And lastly, the ''slipping and guiding'' (SG) region, shaded by crossed lines, realizes the coexistence of slipping and guiding, where $\mathbf{v} = \mathbf{v}_t + \mathbf{v}_l$ with $\mathbf{v}_t \neq 0$ and $\mathbf{v}_l \neq 0$.

If, for the given sample with fixed $\alpha = \alpha_j$, the transport current is increasing from zero, then, depending on the α, j values it is possible to realize sequentially different variants of intersection by the end of **j**-vector of the boundaries between the neighboring regions (see Fig. 4). For example, if $\alpha > \alpha^*$, then the series of intersections FP→FG→GS exists. Since a new source of dissipation appears, at each of the intersection, the longitudinal CVC of the sample $E_{\parallel}^{\alpha}(j, \alpha)$ acquires a kink (inflection point) at corresponding values of j. In general, there are two such kinks on the CVC (if $\alpha \neq \alpha^*$, 0, $\pi/2$); only in the case $\alpha = \alpha^*$ these two kinks merge into one.

In conclusion, we note, that anisotropic transport effects caused by unidirected twins have only begun to be observed experimentally; until now, all the measurements were taken on YBCO single crystals.[8–10] However, recently fabricated[18] **c**-axis-oriented YBCO thin films with unidirected twins, owing to a more pronounced anisotropy of their resistive properties and attainability of higher current densities without overheating, might appear more suitable for observation of the predicted here nonlinear effects than the crystals.

I am grateful to A. K. Soroka and A. A. Soroka for their help in preparing this paper for publication.

*E-mail: valerij.a.shklovskij@univer.kharkov.ua

[1] G. Blatter, M. V. Feigelman, V. B. Geshkenbein, A. I. Larkin, and V. M. Vinokur, Rev. Mod. Phys. **66**, 1125 (1994).
[2] S. Fleshler, W.-K. Kwok, U. Welp, V. M. Vinokur, M. K. Smith, J. Downey, and G. W. Crabtree, Phys. Rev. B **47**, 14448 (1993).
[3] G. W. Crabtree, G. K. Leaf, H. G. Kaper, V. M. Vinokur, A. E. Koshelev, D. W. Braun, D. M. Levine, W. K. Kwok, and J. A. Fendrich, Physica C **263**, 401 (1996).
[4] J. Groth, C. Reichhardt, C. J. Olson, S. B. Field, and F. Nori, Phys. Rev. Lett. **77**, 3625 (1996).
[5] T. R. Chien, T. W. Jing, N. P. Ong, and Z. Z. Wang, Phys. Rev. Lett. **66**, 3075 (1991).
[6] T. R. Chien, D. A. Brawner, Z. Z. Wang, and N. P. Ong, Phys. Rev. B **43**, 6242 (1991).
[7] A. V. Samoilov, A. Legris, F. Rullier-Albenque, P. Lejay, S. Bouffard, Z. G. Ivanov, and L.-G. Johansson, Phys. Rev. Lett. **74**, 2351 (1995).

[8] A. V. Bondarenko, M. A. Obolenskii, R. V. Vovk, A. A. Prodan, V. A. Shklovskij, A. G. Sivakov, in *Proceedings of the 7th IWCC in Superconductors*, Alpbach, Austria, 1994, H. W. Weber (Ed.), World Scientific, Singapore (1994), p. 177.
[9] A. A. Prodan, V. A. Shklovskij, V. V. Chabanenko, A. V. Bondarenko, M. A. Obolenskii, H. Szymczak, and S. Piechota, Physica C **302**, 271 (1998).
[10] H. Ghamlouch and M. Aubin, Physica C **269**, 163 (1996).
[11] Y. Mawatari, Phys. Rev. B **56**, 3433 (1997).
[12] A. K. Niessen and C. H. Weijsenfeld, J. Appl. Phys. **40**, 384 (1969).
[13] E. B. Sonin and A. L. Kholkin, Fiz. Tverd. Tela **34**, 1147 (1992) [Sov. Phys. Solid State **34**, 610 (1992)].
[14] V. M. Vinokur, V. B. Geshkenbein, M. V. Feigelman, and G. Blatter, Phys. Rev. Lett. **71**, 1242 (1993)].
[15] Wu Liu, T. W. Clinton, and C. J. Lobb, Phys. Rev. B **52**, 7482 (1995).
[16] V. A. Shklovskij, Fiz. Nizk. Temp. **23**, 1134 (1997) [Low Temp. Phys. **23**, 853 (1997)].
[17] V. A. Shklovskij, submitted to Phys. Rev. B.
[18] C. Villard, G. Koren, D. Cohen, E. Polturac, Phys. Rev. Lett. **77**, 3913 (1996).

This article was published in English in the original Russian journal. It was edited by R. T. Beyer.

LOW-TEMPERATURE MAGNETISM

Magnetic helix in MnO_2

O. V. Kovalev

National Science Center ''Kharkov Institute of Physics and Technology,'' 310108 Kharkov, Ukraine
(Submitted September 8, 1998)
Fiz. Nizk. Temp. **25**, 160–167 (February 1999)

The paper pursues the following two goals: to demonstrate the principle of concordance of the basic sets of representations and to investigate possible incommensurate magnetic structures proceeding from the previously developed theory of induced representations. The methods and the results obtained differ essentially from those obtained on the basis of Lifshitz invariants. The effect of exchange energy spectrum smoothing as a result of inclusion of a nonexchange interaction is established The role of dipole interaction in the magnetic helix orientation is elucidated. © *1999 American Institute of Physics.* [S1063-777X(99)00502-2]

Let us illustrate the general results obtained in Ref. 1 by an example in order to elucidate the problems emerging in the method of induced representations applied for describing the energy spectrum and analyze a noncommensurate magnetic structure on the basis of Refs. 1–3 as well as our earlier publications (the list of these works is given in Ref. 3). We proposed a rule for concordance of basic vectors (BV) of irreducible corepresentations (ICR) at symmetric points, obtained and analyzed the coefficients of invariant combinations (IC), elucidated the role of dipole interaction, and introduced the concept of energy spectrum ''smoothing.'' The MnO_2 crystal was chosen, among other things, to compare the method proposed by us with the approach developed by Dzyaloshinskii.[4] The results differ significantly. In Ref. 4, they are based on an error of fundamental nature: the author attributed the existence of an incommensurate structure to the Lifshitz invariant which in fact is equal to zero at the point $\mathbf{k}_s$ characterizing the helix.

In the following analysis, the information and notations from Refs. 1–3 are used.

1. We give information about the crystal and reduce representations to the form required for calculations. The Fedorov group is $G=D_{4h}^{14}=P4_2/mnm$, and Mn atoms occupy in the zeroth cell the positions (1,0) and (2,0) with the coordinates $\mathbf{r}_1=(0,\tau,\tau/2)$ and $\mathbf{r}_2=(\tau,0,3\tau/2)$. We consider vectors (points) $\mathbf{k}_0=0$, $\mathbf{k}_1=(0,0,k)$ and $\mathbf{k}_{19}=b_3/2$ and denote by T, τ, and t the irreducible representations (IR) associated with them and by D, δ, and d the ICR. Since all the vectors listed above contain only Z-components, we omit in the further analysis the X- and Y-components of vectors $\mathbf{k}$ and translations $\boldsymbol{\alpha}$ in elements $g=(\boldsymbol{\alpha}/h)$. The main elements of group G are h_i and $(0,0,\tau/h_j)$, where $i=1,\ldots,4,37,\ldots,40$ and $j=13,\ldots,16,25,\ldots,28$. The local group $G(1,0)=mmm$ of the first position contains elements g_i with $i=1,4,37,40,13,16,25,28$. The $H(\mathbf{k}_1)$ group contains rotations with numbers 1, 14, 4, 15, 26, 37, 27, and 40, and $G(\mathbf{k}_0)=G(\mathbf{k}_{19})=G$. All IR considered below generate ICR of the a type. We speak of an ICR when antiunitary symmetrization of the basic sets is implied (Eq. (19) in Ref. 3).

We use the information on induced representations (IR) presented in Ref. 3. In the exchange approximation, we must use representations induced by unit representations $\Gamma1$ of the group $G(1,0)$. That is, $\Gamma1\rightarrow T^1+T^7$; $\tau^1+\tau^4$; t^3 for $\mathbf{k}_0,\mathbf{k}_1,\mathbf{k}_{19}$, respectively. If we are speaking of all interactions (magnetic spectrum), we must induce all IR of the $G(1,0)$ group according to which the components of the magnetic moment of an atom in the (1,0) position are transformed. For the Z-component, we have $\Gamma7\rightarrow T^3+T^5$, $\tau^2+\tau^3$, t^4. For components in the XY-plane, $\Gamma3\rightarrow T^9$, τ^5, t^1 $\Gamma5\rightarrow T^9$, τ^5, t^2.

Table I is the occurrence table[1] divided into two parts for exchange and magnetic representations (the lines containing only zeros are omitted; numbers of IR are given according to Ref. 3).

In order to avoid misunderstanding, and going slightly ahead, we make the following remark. Not the unit vectors $\mathbf{e}_x$ and $\mathbf{e}_y$, but the unit vectors $\mathbf{e}_1$ and $\mathbf{e}_2$ directed along the rotational axes h_{13} and h_{16} are transformed according to the IR $\Gamma3$ and $\Gamma5$. It appears at first sight that the evolution of the BV during motion from point $\mathbf{k}_0$ to point $\mathbf{k}_{19}$ must occur in two ways: (1) BV of IR $T^9\rightarrow$BV of IR $\tau^5\rightarrow$BV of IR t^1, and (2) BV of IR $T^9\rightarrow$BV of IR $\tau^5\rightarrow$BV of IR t^2. Supplying IR T^9 and τ^5 with the additional superscripts 1 and 2, we should write these evolutions in the form $T^{91}\rightarrow\tau^{51}\rightarrow t^1$; $T^{92}\rightarrow\tau^{52}\rightarrow t^2$, and the problem on evolution of basic sets would be solved unambiguously. However, such arguments (which unfortunately appear sometimes in the literature) are erroneous for the following reason. A mixed second-order IC containing magnetic symmetrized coordinates $m(5i\mathbf{k})$ exists for the BV of two identical IR τ^5 [formula (1) from Ref. 2] on the entire $\mathbf{k}_1$ line (except the single point $\mathbf{k}_{19}$) irrespective of the choice of the basic sets for these two IR τ^5. Actual basic sets on the $\mathbf{k}_1$ line are determined not from symmetry considerations, but through the solution of a secular equation by reducing the quadratic form to the sum of squares. The

TABLE I.

τ	1	7	3	τ	3	5	9	1	2	4
1	1	0	1	2	1	0	0	0	0	1
4	0	1	1	3	0	1	0	0	0	1
				5	0	0	1	1	1	0

mixing of the basic sets of two identical IR starts at the point $\mathbf{k}_0$, proceeds continuously along the $\mathbf{k}_1$ line, and it is only at the point $\mathbf{k}_{19}$ that the basic sets are determined from the requirement on concordance of the basic sets at this point. In any problem on the energy spectrum (electron, phonon, magnetic, or exciton) of this type, calculations are controlled at the concordance points of basic sets, which is especially important in approximate calculations.

We believe that the proposed method can be used by readers for solving other problems also. For this reason, we present the required minimum of tabulated data, the more so that the information given in Ref. 3 should be partially modified. First we transform ICR matrices. We proceed from ICR tables T147, T119, and T159 from Ref. 3 for the points $\mathbf{k}_0$, $\mathbf{k}_1$, and $\mathbf{k}_{19}$. The two-dimensional matrices M in these tables are replaced by the matrices

$$A_n^+ \hat{M}(h) A_n, \quad A_n^+ M(Kg) A_n^* \quad (M = D, \delta, d),$$

where K is the complex conjugation operator. We have two goals. First, we reduce T^9 and τ^5 to the real-valued form (this is not a necessary transformation, but it facilitates computations). Second (which is of primary importance), we obtain the reduced form for limitations $d^3\downarrow$ and $d^4\downarrow$ of ICR $\hat{d}^3$ and $\hat{d}^4$ imposed on the subgroup $G(\mathbf{k}_1)$ in accordance with the recommendations given in Ref. 1. The matrices $\hat{d}^1$ and $\hat{d}^2$ are transformed in order that the limitations of these ICR imposed on $G(\mathbf{k}_1)$ coincide with the ICR matrices $\hat{\delta}^5$. New ICR matrices for generating elements and unitary matrices A ar given in Table II, $\sqrt{2}\gamma_0 = 1$, $\sqrt{2}\gamma_1 = \exp(i\pi/4)$. Table III contains the rules of positions transformation (only the Z-components are indicated). These tables are also required for constructing BV and for determining the relations between constants Φ of the exchange interaction.

We shall calculate the magnetic energy spectrum by using the method developed in Ref. 2. Let us recall its basic concepts. The magnetic density can be written in the following three forms:

$$\mathbf{M}(\mathbf{r}) = \sum \mu(\alpha p \mathbf{a}) \mathbf{e}_\alpha \varphi(p\mathbf{a}) = \sum \mu(\alpha F j i k) \mathbf{e}_\alpha \varphi(F j i \mathbf{k})$$

$$= \sum m(F j i \mathbf{k}) \psi(F j i \mathbf{k}), \tag{1}$$

where $\alpha = x, y, z$; $\mathbf{e}_\alpha$ are magnetic unit vectors, p is the number of a position in the unit cell, and $\varphi(p\mathbf{a})$ the position function localized in the position $(p, \mathbf{a})$. The second sum is the expansion of $\mathbf{M}(\mathbf{r})$ in the ICR basis φ contained in the transposition corepresentation $P = I(\Gamma 1)$. In this case, F is the class of equivalence (the number of ICR in their complete table), j the number of the ICR class F in P, and i the number of the basic vector of the small ICR of the $G(\mathbf{k})$ group. The summation is carried out over all possible values of indices F, j, i whose ranges are determined by the composition of P. In the absence of limitations of any kind, i.e., for an arbitrary vector $\mathbf{M}(\mathbf{r})$, the second and third sums involve all vectors $\mathbf{k}$ from the Brillouin zone. However, in our problem on the incommensurate structure (which will be sometimes referred to simply as a helical structure), only two vectors ($\mathbf{k}$ and $-\mathbf{k}$) appear in the above-mentioned sums. In the third sum, $\mathbf{M}(\mathbf{r})$ is not decomposed into its components, $\psi(F j I \mathbf{k})$ are the BV of the magnetic corepresentation $D_m = P \times V$, the unit vectors $\mathbf{e}_\alpha$ being transformed according to V. The set of indices F, j, i in the third sum is determined by the composition of the corepresentation $D_m = I(\Gamma m)$, where Γm is the corepresentation of the local group $G(1,0)$ according to which the unit vectors $\mathbf{e}_\alpha$ are transformed. In the crystal under investigation, $\Gamma m = \Gamma 3 + \Gamma 5 + \Gamma 7$. In the

TABLE II.

	h_{14}	h_{26}	h_{25}	Kg_{25}	A_n
$\hat{\delta}^5$, T^5	$\begin{pmatrix} 0 & 1 \\ -1 & 0 \end{pmatrix}$	$\begin{pmatrix} 1 & 0 \\ 0 & -1 \end{pmatrix}$	$\begin{pmatrix} 1 & 0 \\ 0 & 1 \end{pmatrix}$	$\begin{pmatrix} 1 & 0 \\ 0 & 1 \end{pmatrix}$	$\gamma_0 \begin{pmatrix} 1 & -i \\ 1 & i \end{pmatrix}$
$\hat{d}^1$	$\begin{pmatrix} 0 & 1 \\ -1 & 0 \end{pmatrix}$	$\begin{pmatrix} 1 & 0 \\ 0 & -1 \end{pmatrix}$	$\begin{pmatrix} 0 & i \\ i & 0 \end{pmatrix}$	$\begin{pmatrix} 1 & 0 \\ 0 & 1 \end{pmatrix}$	$\gamma_1 \begin{pmatrix} 1 & i \\ -1 & i \end{pmatrix}$
$\hat{d}^2$	$\begin{pmatrix} 0 & 1 \\ -1 & 0 \end{pmatrix}$	$\begin{pmatrix} 1 & 0 \\ 0 & -1 \end{pmatrix}$	$\begin{pmatrix} 0 & -i \\ -i & 0 \end{pmatrix}$	$\begin{pmatrix} 1 & 0 \\ 0 & 1 \end{pmatrix}$	$\gamma_1^* \begin{pmatrix} 1 & i \\ 1 & -i \end{pmatrix}$
$\hat{d}^3$	$\begin{pmatrix} 1 & 0 \\ 0 & -1 \end{pmatrix}$	$\begin{pmatrix} 1 & 0 \\ 0 & -1 \end{pmatrix}$	$\begin{pmatrix} 0 & -i \\ -i & 0 \end{pmatrix}$	$\begin{pmatrix} -i & 0 \\ 0 & -i \end{pmatrix}$	$\begin{pmatrix} 1 & 0 \\ 0 & -i \end{pmatrix}$
$\hat{d}^4$	$\begin{pmatrix} 1 & 0 \\ 0 & -1 \end{pmatrix}$	$\begin{pmatrix} -1 & 0 \\ 0 & 1 \end{pmatrix}$	$\begin{pmatrix} 0 & -i \\ -i & 0 \end{pmatrix}$	$\begin{pmatrix} -i & 0 \\ 0 & -i \end{pmatrix}$	$\begin{pmatrix} -i & 0 \\ 0 & 1 \end{pmatrix}$

TABLE III.

p	$g_{1,4,37,40}$	$g_{14,15,26,27}$	$g_{2,3,38,39}$	$g_{13,16,25,28}$
1	$\mathbf{r}_1$	$\mathbf{r}_2$	$\mathbf{r}_2-\mathbf{a}_3$	$\mathbf{r}_1$
2	$\mathbf{r}_2$	$\mathbf{r}_1+\mathbf{a}_3$	$\mathbf{r}_1-\mathbf{a}_3$	$\mathbf{r}_2-\mathbf{a}_3$

subsequent analysis, the cases $\Gamma mxy=\Gamma 3+\Gamma 5$ and $\Gamma mz=\Gamma 7$ are considered separately. The former case corresponds to the density $\mathbf{M}(\mathbf{r})\perp Z$, while the second corresponds to $\mathbf{M}(\mathbf{r})\parallel Z$.

A transition from one some to another in (1) is carried out through the relations

$$\varphi(p\mathbf{k})=n^{-1}\varepsilon(p)\sum\ \varphi(p\mathbf{a})\exp(i\mathbf{k}\cdot\mathbf{a}),$$

$$\sigma(Fji\mathbf{k})=\sum\ R_3(p/Fji)\varphi(p\mathbf{k}), \tag{2}$$

$$\varphi(\alpha p\mathbf{k})=\mathbf{e}_\alpha\varphi(p\mathbf{k}),$$

$$\psi(Fji\mathbf{k})=\sum\ R_{21}(\alpha p/Fji)\psi(\alpha p\mathbf{k}), \tag{3}$$

$$\varepsilon(p)=\exp i\mathbf{k}\cdot[(\mathbf{r}(p,0)-\boldsymbol{\alpha}_0/2)], \tag{4}$$

where $\boldsymbol{\alpha}_0$ is the translation in an antiunitary element $a_0=Kg_0=K(\boldsymbol{\alpha}_0/h_0)$. Henceforth, we put $g_0=g_{25}$. Owing to the factor ε, the matrices R_3 and R_{21} are analytically independent of the vector $\mathbf{k}$.

The quantities $\mu(\alpha p\mathbf{a})$ can be referred to as local magnetic coordinates, and the quantities $\mu(\alpha Fji\mathbf{k})$ and $m(Fji\mathbf{k})$ can be regarded as symmetrized. If $\mathbf{M}(\mathbf{r})$ contains only the basic vectors ψ with fixed values of F and $\mathbf{K}$, the energy has the form

$$H(F\mathbf{K})=\frac{1}{2}\sum\ \varphi(ji/j'i';\mathbf{k})m(Fji\mathbf{k})^*m(Fj'i'\mathbf{k}), \tag{5}$$

$$\varphi(ji/j'i)=\varphi(j1/j'1)$$

$$=\sum\ D(\alpha p/\alpha' p')R_{21}(\alpha p/j1)^*R_{21}(\alpha' p'/j'1), \tag{6}$$

$$D(\ldots)=\varepsilon(p)^*\varepsilon(p')\sum\ \Phi(\alpha p\mathbf{a}/\alpha' p'0)\exp(-i\mathbf{k}\cdot\mathbf{a}), \tag{7}$$

$$\varphi=\varphi^+,\quad D=D^+,\quad D(-\mathbf{k})=D(\mathbf{k})^*,$$

$$\varphi(ji/j'i')=0\ \text{ for }\ i\neq i'. \tag{8}$$

In the exchange approximation, i.e., for $\alpha=\alpha'$, $\Phi(\alpha p\mathbf{a}/\alpha p'\mathbf{a}')=\varphi(p\mathbf{a}/p'\mathbf{a}')$ we have

$$H_e(F\mathbf{K})=\frac{1}{2}\sum\ \varphi_e(j1/j'1)\sum_{\alpha,i}\ \mu(\alpha Fji\mathbf{k})^*\mu(\alpha Fji\mathbf{k}), \tag{9}$$

$$\varphi_e(\ldots)=\sum\ D_e(p/p')R_3(p/j1)^*R_3(p'/j'1), \tag{10}$$

$$D_e(\ldots)=\varepsilon(p)^*\varepsilon(p')\sum\ \Phi(p\mathbf{a}/p'0)\exp(-i\mathbf{k}\cdot\mathbf{a}). \tag{11}$$

We assume that the magnetic phase transition is associated with a certain single star $\mathbf{K}$ and one equivalence class F. Having determined the values of the second sums in (9) through the minimization of thermodynamic potential, we must refine the result by including nonexchange interactions.

2. Let us consider our specific case. The functions $\varphi(p\mathbf{k})$ are defined as

$$\varphi(1\mathbf{k})=n^{-1}\sum\ \varphi(1\mathbf{a})\exp(i\mathbf{k}\cdot\mathbf{a}),$$

$$\varphi(2\mathbf{k})=n^{-1}\mu\sum\ \varphi(2\mathbf{a})\exp(i\mathbf{k}\cdot\mathbf{a}), \tag{12}$$

where $\varepsilon(1)=1$, $\varepsilon(2)=\mu=\exp(ik\tau)$. The BV $\varphi'(Fji\mathbf{k})$ of the IR τ^1 and τ^4 can be obtained by the formulas

$$\varphi'(111\mathbf{k})\sim\sum\ t^3(g)^*_{11}g\varphi(1\mathbf{k}),$$

$$\varphi'(411\mathbf{k})\sim\sum\ t^3(g)^*_{21}g\varphi(1\mathbf{k}), \tag{13}$$

where $g\in G(\mathbf{k}_{19})$, $F=1$ and 4, $j=i=1$. We use the relation $g\varphi(p\mathbf{a})=\varphi[g(\mathbf{r}_p+\mathbf{a})]$. After antiunitary symmetrization and normalization, we arrive at the BV of ICR δ^1 and δ^4:

$$\sqrt{2}\varphi(111\mathbf{k})=\varphi(2\mathbf{k})+\varphi(1\mathbf{k}),$$
$$\sqrt{2}\varphi(411\mathbf{k})=\varphi(2\mathbf{k})-\varphi(1\mathbf{k}). \tag{14}$$

These relations lead to the following value of the matrix R_3:

$$R_3(p/Fji;\mathbf{k})=\frac{1}{2}\begin{pmatrix}1 & -1\\ 1 & 1\end{pmatrix}.$$

Formulas (13) contained our proposition concerning induces representations. That is, we propose that the BV of IR and ICR be constructed at a nonsymmetric point on the basis of exactly the same rules as those used for constructing the BV of IR and ICR at a symmetric point. In this case, the compatibility relations should be taken into account (see Table I). This leads to concordance of basic sets and to a correct physical pattern. The specific rules (matrices R) can in general be different for neighborhoods of the points $\mathbf{k}_0$ and $\mathbf{k}_{19}$.

Using formulas (17)–(19), we obtain the exchange energy branches from Ref. 2. In our case, $j=j'=1$ and $i=i'=1$ so that the first sum in (17) is reduced to a single term. The second sum over $\alpha=x,y,z$ written in Ref. 2 will be denoted by $c_1c_1^*$ for $F=1$ and $c_4c_4^*$ for $F=4$. Finally, we obtain

$$H_e(1\mathbf{K})=\varphi_1c_1c_1^*,\quad H_e(4\mathbf{K})=\varphi_4c_4c_4^*, \tag{15}$$

$$\varphi_{1,4}=\sum\ \Phi(1\mathbf{a}/10)\cos\mathbf{k}\cdot\mathbf{a}\pm\Phi(2\mathbf{a}/10)\cos\mathbf{k}\cdot(\mathbf{a}+\mathbf{a}_3/2). \tag{16}$$

It should be recalled that $\Phi(p\mathbf{a}/p'0)$ is the magnitude of exchange interaction between atoms in positions $(p,\mathbf{a})$ and $(p',0)$. Here, we use the relations

$$\Phi(p\mathbf{a}/p'\mathbf{a}') = \Phi(p'\mathbf{a}'/p\mathbf{a}),$$

$$\Phi(\mathbf{r}_p + \mathbf{a}/\mathbf{r}_{p'} + \mathbf{a}') = \Phi[g(\mathbf{r}_p + \mathbf{a})/g(\mathbf{r}_{p'} + \mathbf{a}')]. \qquad (17)$$

Let us analyze relations (15) and (16). The functions φ_1 and φ_4 of the vector $\mathbf{k}$ are the branches of the energy spectrum, and hence their dependence on $\mathbf{k}$ can be shown graphically by specifying certain values of the constants Φ.

a. $\varphi_1(\mathbf{k}_{19}) = \varphi_4(\mathbf{k}_{19})$, i.e., two spectral branches intersect at the point $\mathbf{k}_{19}$. This is a visual illustration of compatibility relations. Besides, it can be seen that the value of energy at $\mathbf{k}_{19}$ is determined only by the interaction between atoms in positions $(1,\mathbf{a})$.

b. The star $\mathbf{K}_1$ contains two rays: $\mathbf{k}_1$ and $-\mathbf{k}_1$. It can be verified that the following equalities hold:

$$\psi(111,-\mathbf{k}_{19}) = -\psi(411,\mathbf{k}_{19}),$$

$$\psi(411,-\mathbf{k}_{19}) = -\psi(111,\mathbf{k}_{19}).$$

These equalities clarify the result obtained in Ref. 1: a linear dependence between the BV of complete IR (ICR) in contact is observed at symmetric points.

c. It follows from (15) and (16) that

$$\frac{\partial}{\partial k}\varphi_1(\mathbf{k}_0) = \frac{\partial}{\partial k}\varphi_4(\mathbf{k}_0) = 0,$$

$$\frac{\partial}{\partial k}\varphi_1(\mathbf{k}_{19}) = -\frac{\partial}{\partial k}\varphi_4(\mathbf{k}_{19}) \neq 0. \qquad (18)$$

The two branches have extrema at the point $\mathbf{k}_0$, but there are not extrema at the point $\mathbf{k}_{19}$, i.e., a magnetic structure characterized by the vector $\mathbf{k}_{19}$ cannot exist. This statement and the fact that there is no interaction between atoms in positions $(1,\mathbf{a})$ and $(2,\mathbf{a}')$ in $\varphi_1(\mathbf{k}_{19})$ and $\varphi_4(\mathbf{k}_{19})$ are closely related. This aspect, however, has not been investigated by us.

d. The existence of a helical structure is determined by the values of quantities $\Phi(p\mathbf{a}/p'0)$, and a possible magnetic structure in the exchange approximation is described either by the ICR δ^1, or the ICR δ^4, but not by these two ICR simultaneously. The δ^1 helix degenerates to ferromagnetism for $\mathbf{k}_1 = \mathbf{k}_0$ and will be henceforth referred to as ferromagnetic. Similarly, the δ^4 helix will be referred to as antiferromagnetic since the equality $\mu(1,\mathbf{a}) = -\mu(2,\mathbf{a}')$ holds for $\mathbf{k}_1 = \mathbf{k}_0$.

e. We assume for definiteness that $\varphi_1 < \varphi_4$ in the entire range of the vector $\mathbf{k}_1$ except the point $\mathbf{k}_{19}$. If we take into account a small number of positions in (16), the φ_1 curve may have no minimum for $k > 0$. The absence of a minimum at the point $\mathbf{k}_{19}$ does not indicate at all the existence of a helix. The existence of a helix is a consequence of a comparatively strong interaction of atoms separated by a large distance. In the case of several minima, the absolute minimum corresponds to a helix. In some cases, an absolute minimum exists at a certain point $\mathbf{k}_{s1}$, while a relative minimum is observed at another point $\mathbf{k}_{s2}$ at a certain temperature. At another temperature, however, the situation can be reverse. Accordingly, we can speak of the jumpwise variation of the parameter $\mathbf{k}_s$ of the helix, a first-order phase transition, metastable states, domain helical structure, etc. Naturally, a smooth variation of the helicity parameter can also take place upon the variation of external parameters. It turns out that the situation is determined by the values of Φ almost completely.

It should be noted that, in order to obtain the helicity parameter $\mathbf{k}_s$, we must actually minimize not energy, but thermodynamic potential. This formally means that we must at least minimize the expression containing high-order IC. In the exchange approximation under investigation, we must speak of IC composed of the quantities c_1 (or c_4) written in (4). Constructing IC according to the algorithm adopted here, we obtain the coefficients of IC in the form of a sum over $\mathbf{a}$ of expressions containing cosines (and probably sines) of $\mathbf{k}\cdot\mathbf{a}$ and $\mathbf{k}\cdot(\mathbf{a} + \mathbf{a}_3/2)$. The problem becomes virtually unsolvable. However, the magnetic moments of atoms at temperatures much lower than the magnetic ordering temperature are close to possible limiting values, and we can omit the minimization in c. The role of high-order IC is formally reduced to a renormalization of the quantities Φ in the sum (16), which is more significant for large vectors $\mathbf{a}$. Consequently, an additional tendency towards a change in the vector $\mathbf{k}_s$ appears below the magnetic ordering temperature. This circumstance can probably explain the fact that a helix appears in many crystals below the temperature of phase transition from the paramagnetic to the magnetic state.

f. We can assume in principle that the curves φ_1 and φ_4 intersect. consequences of this effect can be easily found.

3. Let us consider the common magnetic spectrum. The magnetic XY-density on the $\mathbf{k}_1$ line is transformed according to ICR δ^{51} and δ^{52}. Their BV are linear combinations of the functions

$$\varphi(x1) = \mathbf{e}_x\varphi(1,\mathbf{k}), \quad \varphi(x2) = \mathbf{e}_x\varphi(2,\mathbf{k}),$$

$$\varphi(y1) = \mathbf{e}_y\varphi(1,\mathbf{k}), \quad \varphi(y2) = \mathbf{e}_y\varphi(2,\mathbf{k}). \qquad (19)$$

It is expedient to choose the linear combinations at the point $\mathbf{k}_{19}$ and the point $\mathbf{k}_s$ characterizing the helix in different ways.

For the point $\mathbf{k}_{19}$, we require the concordance of basic sets. Let the BV of the ICR δ^{51} be transformed at $\mathbf{k}_{19}$ into the BV of the ICR d^1, while the BV of the ICR δ^{52} be transformed into the BV of the ICR d^2. We proceed as follows.

(1) We apply the operator projecting onto the space of the ICR d^1 to a function from (19) at $\mathbf{k}_1 = \mathbf{k}_{19}$. We use the matrices d^1 from Table II and carry out summation over the basic elements of the group $G(\mathbf{k}_{19})$. The obtained basis vectors are subjected to antiunitary symmetrization and normalization. The BV for the ICR d^2 is determined in a similar way.

(2) The obtained matrix $R_{21}(\alpha p/Fji;\mathbf{k}_{19})$ is applied directly for writing the BV for the ICR δ^{51} and δ^{52}.

It should be noted that since we introduced a factor $\varepsilon(p)$ into formula (2) in Ref. 2, the elements of the matrix R are just numbers and not functions of the vector $\mathbf{k}$. These numbers must satisfy only two requirements: R is a unitary matrix, and the matrix R ensures a transition to the BV of corresponding ICR.

We can write the BV of the ICR δ^{51} and δ^{52} concordant at $\mathbf{k}_{19}$ in the form

$$2\psi(511)_{19}=\varphi(x1)+\varphi(x2)-\varphi(y1)+\varphi(y2),$$

$$2\psi(512)_{19}=\varphi(x1)-\varphi(x2)-\varphi(y1)-\varphi(y2), \quad (20)$$

$$2\psi(521)_{19}=\varphi(x1)+\varphi(x2)+\varphi(y1)-\varphi(y2),$$

$$2\psi(522)_{19}=\varphi(x2)-\varphi(x1)-\varphi(y1)-\varphi(y2). \quad (21)$$

The choice concordant basic sets has an important peculiarity. Since the limiting BV of the ICR δ^{51} and δ^{52} carry out the nonequivalent ICR d^1 and d^2, the coefficient of the mixed IC at the point $\mathbf{k}_{19}$ must vanish. If, however, we take discordant basic sets, this coefficient does not vanish, and we must solve a secular equation in order to obtain spectral branches at the point $\mathbf{k}_{19}$.

We choose the basic sets in the neighborhoods of the points $\mathbf{k}_0$ and $\mathbf{k}_s$ in accordance with the direct products $\tau^{51}=\tau^1\times V^1$ and $\tau^{52}=\tau^4\times V^1$, where V^1 is the representations according to which $\mathbf{e}_x$ and $\mathbf{e}_y$ are transformed:

$$\sqrt{2}\psi(511)=\varphi(x1)+\varphi(x2),$$

$$\sqrt{2}\psi(512)=-\varphi(y1)-\varphi(y2); \quad (22)$$

$$\sqrt{2}\psi(521)=\varphi(y2)-\varphi(y1),$$

$$\sqrt{2}\psi(522)=-\varphi(x2)+\varphi(x1). \quad (23)$$

We ensured that the matrices of ICR have the same form as in Table II.

Naturally, the result of calculation of the energy spectrum does not depend on the choice of the basic sets for the ICR δ^{51} and δ^{52}. Let us find out why the choice of (22) and (23) is preferable in certain cases. We shall consider the general formulas (12)–(15) from Ref. 2. Since the vector $\mathbf{k}$ appears in the factor $\exp(i\mathbf{k}\cdot\mathbf{r})$ in all formulas, a transition from the vector $\mathbf{k}$ to the vector $-\mathbf{k}$ is equivalent to complex conjugation. In the given case, the star contains only the vectors $\mathbf{k}_1$ and $-\mathbf{k}_1$. We write the expression for the energy H_{xy} associated with the XY-density in the form

$$H_{xy}=\varphi_{11}i_{11}+\varphi_{12}i_{12}+\varphi_{21}i_{21}+\varphi_{22}i_{22}, \quad (24)$$

$$\varphi_{jj'}=\varphi(j1/j'1), \quad i_{jj'}=\sum m(ji\mathbf{k})^*m(ji\mathbf{k}). \quad (25)$$

The actual spectral branches correspond to the roots λ_1 and λ_2 of the secular equation appearing when H_{xy} is reduced to the sum of squares. In this way, the basic sets of the ICR δ^{51} and δ^{52} belonging to the roots λ_1 and λ_2 for a given value of $\mathbf{k}_1$ are established. If we choose (22) and (23), the coefficients φ_{12} and φ_{21} contain only nonexchange interactions, while the coefficients φ_{11} and φ_{22} also include exchange interactions. Consequently, for the point $\mathbf{k}_0$ as well as the points $\mathbf{k}_s$ corresponding to the helix we can write

$$|\varphi_{11}-\varphi_{22}|\approx|\varphi_1-\varphi_4|\geqslant|\varphi_{12}|.$$

If we assume for definiteness that $\varphi_{11}<\varphi_{22}$ and $\lambda_1<\lambda_2$, we obtain $\lambda_1\approx\varphi_1$ and $\lambda_2\approx\varphi_4$ at the above-mentioned points. The inclusion of nonexchange energy leads to only a slight shift in the energy levels. The actual basic sets of the ICR δ^{51} and δ^{52} corresponding to the roots λ_1 and λ_2 differ insignificantly from the basic sets (22) and (23).

The above inequality is violated only in the vicinity of the point $\mathbf{k}_{19}$ as well as the points at which the branches φ_1 and φ_4 intersect. In these regions, nonexchange interaction leads to a peculiar effect of energy level ''smoothing'' and to a considerable rearrangement of basic sets of ICR.

Choosing (20) and (21), we have

$$\varphi_{11,22}=\sum [\Phi(x1\mathbf{a}/x10)\mp\Phi(y1\mathbf{a}/x10)]\cos\mathbf{k}\cdot\mathbf{a}, \quad (26)$$

$$\varphi_{12}=\varphi_{21}=\sum \Phi(x2\mathbf{a}/x10)\cos\mathbf{k}\cdot(\mathbf{a}+\mathbf{a}_3/2). \quad (27)$$

If we choose (22) and (23), we can write

$$\varphi'_{11,22}=\sum \Phi(x1\mathbf{a}/x10)\cos\mathbf{k}\cdot\mathbf{a}\pm\Phi(x2\mathbf{a}/x10)\times\cos\mathbf{k}\cdot(\mathbf{a}+\mathbf{a}_3/2), \quad (28)$$

$$\varphi'_{12}=\varphi'_{21}=\sum \Phi(y1\mathbf{a}/x10)\cos\mathbf{k}\cdot\mathbf{a}. \quad (29)$$

We have used the following relations:

$$\Phi(\alpha,\mathbf{r}_p+\mathbf{a}/\alpha',\mathbf{r}_{p'},+\mathbf{a}')=H(h)_{\beta\alpha}H(h)_{\beta'\alpha'}\Phi[\beta,g(\mathbf{r}_p+\mathbf{a})/\beta', g(\mathbf{r}_{p'}+\mathbf{a}')], \quad (30)$$

$$\Phi(\alpha p\mathbf{a}/\alpha' p'\mathbf{a}')=\Phi(\alpha' p'\mathbf{a}'/\alpha p\mathbf{a}), \quad (31)$$

where $H(h)$ is the matrix of rotation of h. Condition (31) is hypothetical.

It follows from expressions (26)–(29) that $\varphi_{12}(\mathbf{k}_1=\mathbf{k}_{19})=0$; $\lambda_1\neq\lambda_2$ for $\mathbf{k}_1=\mathbf{k}_{19}$; φ'_{12} contains only nonexchange interactions.

We can verify that the derivatives of the roots λ_1 and λ_2 with respect to $\mathbf{k}$ vanish not only at the point $\mathbf{k}_0$, but also at the point $\mathbf{k}_{19}$. This is the effect of ''smoothing'' [cf. (18)].

Let us now consider the Z-density. On the line $\mathbf{k}_1$, it can be expanded in the BV of the ICR δ^2 and δ^3. The basis vectors of the latter ICR are given by

$$\varphi(21)\sim\mathbf{e}_z[\varphi(2\mathbf{k})+\varphi(1\mathbf{k})],$$

$$\psi(31)\sim\mathbf{e}_z[\varphi(2\mathbf{k})-\varphi(1\mathbf{k})].$$

The limiting values of these vectors are transformed at the point $\mathbf{k}_0$ according to the ICR D^3 and D^5, respectively, and the Z-density generates two energy levels:

$$H_{2z}=\varphi_{2z}i_2, \quad H_{3z}=\varphi_{3z}i_3, \quad i_2=m(211)^*m(211),$$

$$i_3=m(311)^*m(311). \quad (32)$$

The quantities φ_{2z} and φ_{3z} can be obtained by a formal replacement of exchange constants by magnetic constants in (16). In order to avoid misunderstanding, we note that the constants $\Phi(\alpha p\mathbf{a}/\alpha' p'\mathbf{a}')$ always contain exchange interactions for $\alpha=\alpha'$ and do not contain them for $\alpha\neq\alpha'$. The levels φ_{2z} and φ_{3z} are slightly shifted relative to the levels

φ_1 and φ_4, respectively. The branches φ_{2z} and φ_{3z} can intersect; they come in contact at the point $\mathbf{k}_{19}$ and satisfy inequalities similar to (18).

Formulas (26)–(28) and (32) correspond to the most exact approach but contain the quantities Φ that are in fact unknown. In addition, the division of interactions into exchange and nonexchange interactions cannot be made unambiguously.

4. We can draw a conclusion concerning the orientation of the helix under the assumption that a nonexchange interaction can be mainly reduced to the dipole interaction. For this purpose, we calculate the following four quantities: $\varphi_{dz}(\varphi_1)$, $\varphi_{dx}(\varphi_1)$, $\varphi_{dz}(\varphi_4)$ and $\varphi_{dx}(\varphi_4)$. The first and third quantities can be determined from (16) by substituting the quantity $R^{-5}(R^2-R_z^2)$ for the quantities Φ appearing in this formula, where $\mathbf{R}$ is the vector between positions. The quantities $\varphi_{dx}(\varphi_1)$ and $\varphi_{dx}(\varphi_4)$ can be calculated from (28) by substituting $R^{-5}(R^2-R_x^2)$ for Φ, and $\varphi_{dz}(\varphi_1)$ and $\varphi_{dx}(\varphi_1)$ and $\varphi_{dz}(\varphi_4)$, $\varphi_{dx}(\varphi_4)$ are the corrections to the levels φ_1 and φ_4, respectively. The absolute values of these corrections are immaterial for our problem, and only their signs and relative values for different points on the line $\mathbf{k}_1$ play an important role. The periods of the crystal lattice are $a=4.44$ Å and $a_3=c=2.89$ Å. We took into account 428 positions arranged over a sphere of radius ≈ 14 Å around the position (1,0) (we are not sure, however, that this number is sufficient). We do not describe here the results and only formulate some conclusions.

If $\varphi_4<\varphi_1$, and the helix is due to the minimum of the level φ_4, we have $\varphi_{dx}(\varphi_4)<\varphi_{dz}(\varphi_4)$ almost everywhere. Consequently, the magnetic moments of atoms rotate in the XY plane for any value of $\mathbf{k}_1$. The helix orientation is also the same when $\varphi_1<\varphi_4$ and $k_s\tau>50°$. For $\varphi_1<\varphi_4$ and $k_s\tau<50°$, we have $\varphi_{dx}(\varphi_1)>\varphi_{dz}(\varphi_1)$. In this case, it is difficult to determine the type of the helix. We are probably dealing with a cycloidal elliptical helix, and the rotational axes of magnetic moments lie in the XY plane. In such uncertain cases, we must resort to high-order IC. We shall not consider this problem here.

5. The spectrum ''smoothing'' effect lies in the following. It should be recalled that $\varphi_1(\mathbf{k}_{19})=\varphi_4(\mathbf{k}_{19})$, the derivatives of the levels λ_1 and λ_2 with respect to $\mathbf{k}$ vanish at $\mathbf{k}_{19}$, and $\lambda_1\approx\varphi_1$, $\lambda_2\approx\varphi_4$ away from the point $\mathbf{k}_{19}$. Thus, $\lambda_1\neq\lambda_2$ at the point $\mathbf{k}_{19}$. The upper of the λ curves is displaced upwards near $\mathbf{k}_{19}$ and has a minimum at this point. The other curve is displaced downwards and has a peak at $\mathbf{k}_{19}$ (we mean deviations from the corresponding curves φ_1 and φ_4). It follows from (24) and (27) that at $\mathbf{k}_{19}$ we have

$$|\lambda_1-\lambda_2|=|\varphi_{22}-\varphi_{11}|=\sum \Phi(y1\mathbf{a}/x10)\cos\mathbf{k}_{19}\cdot\mathbf{a}.$$

If the curves φ_1 and φ_4 intersect at a certain point $\mathbf{k}_1'$, a similar ''smoothing'' is observed at this point. The true energy levels λ_1 and λ_2 do not intersect at the point $\mathbf{k}_1'$, but simply converge. This point is a point of zero inclination. It should be noted that we have $\Phi(yp\mathbf{a}/xp'0)=0$ for a dipole interaction in MnO_2. Among other things, this means that the existence of the effect and its intensity are determined by the adopted model.

The ''smoothing'' effect must also be observed for other energy spectra, e.g., in the electron spectrum upon a transition from the zero-spin theory to the theory of an electron with a spin. The effect was noted by other authors in special cases. It is assumed, for example, that in the first approximation the levels belonging to identical ICR intersect. In the next approximation, mixed IC are introduced, and the intersection is eliminated. This effect is attributed to symmetry, namely, it takes place if energy levels belong to nonequivalent ICR in the first approximation and to equivalent ICR in the next approximation.

6. The components $\mu(\alpha p\mathbf{a})$ of atomic magnetic moments are defined by formulas (8) from Ref. 2. The sum (8) contains magnetic symmetrized coordinates $m(Fji\mathbf{k})$ which must be determined in the course of minimization of the energy expansion in IC. The coefficients of IC cannot be calculated, and it is expedient to treat them as parameters. We shall assume that these parameters satisfy the conditions under which an incommensurate structure with the vector $\mathbf{k}_1=\mathbf{k}_s$ is realized. We shall consider the case of a magnetic XY density described by the ICR δ^5 (i.e., either δ^{51} or δ^{52}) and try to gain maximum information on atomic magnetic moments.

In our case, $F=5$, $j=1$ or 2, and $i=1,2$. We put

$$m(5j1,\mathbf{k})=m_{1k}=c\cos\theta\exp(i\nu_1),$$

$$m(5j2;\mathbf{k})=m_{2k}=c\sin\theta\exp(i\nu_2),$$

$$m(5ji,-\mathbf{k})=m_{i-k}=g_{25}m(5ji,\mathbf{k}),\quad c>0. \tag{33}$$

These four coordinates are transformed according to the matrices of the ICR Δ of the group $G+KG$ (we assume that the small ICR δ^5 leads to the complete ICR Δ^5). The invariant combinations of the Nth order can be obtained by applying the operator of projection onto the unit representation of the group to the product $(m_{1k})^{s_1}(m_{1-k})^{s_2}(m_{2k})^{t_1}(m_{2-k})^{t_2}$. The obtained expression is subjected to antiunitary symmetrization according to expression (19) from Ref. 3. This gives

$$I_N=c^N(\cos^{s_1+s_2}\theta\sin^{t_1+t_2}\theta + \cos^{t_1+t_2}\theta\sin^{s_1+s_2}\theta)\cos(s_1-s_2)\nu, \tag{34}$$

where $s_1+s_2+t_1+t_2=N$; $s_1+t_1=s_2+t_2$; $s_i,t_i=0,1,...$; N,s_1+s_2,t_1+t_2 are even positive numbers, and $\nu=\nu_1-\nu_2$. Giving the numbers s_i and t_i possible values, we obtain all IC of the order N.

If the equalities $s_1+s_2=0$ or $t_1+t_2=0$ are satisfied, we can factor out $\sin 2\theta$ to a certain even power in (34) and are left with the sum $\cos^l\theta+\sin^l\theta$ in the parentheses, where l is an even number. If, however, one of the above equalities holds, the parentheses contain the sum $\cos^N\theta+\sin^N\theta$. On the other hand, if L is even, the sum $\cos^L\theta+\sin^L\theta$ is a polynomial in $\sin^2 2\theta$.

It follows from the above considerations that the minimization of energy expansion leads to two series of particular (steady-state) solutions:

$$\theta=\frac{\pi}{4}+\frac{\pi}{2}n_1,\quad \nu=\frac{\pi}{2}n_2\quad\text{and}\quad \theta=\frac{\pi}{2}n_3. \tag{35}$$

Let us determine the type of magnetic density. The summation in formula (8) from Ref. 2 is carried out over the vectors $\mathbf{k}$ and $-\mathbf{k}$. The matrix R_{21} is chosen in accordance with (22) and (23) by using definitions (33). This gives

$$\mu(x1\mathbf{a}) \sim \cos\theta\cos(\mathbf{k}\cdot\mathbf{a}+\nu_1),$$
$$\mu(x2\mathbf{a}) \sim \pm\cos\theta\cos(\mathbf{k}\cdot\mathbf{a}+k\tau+\nu_1),$$
$$\mu(y1\mathbf{a}) \sim \mp\sin\theta\cos(\mathbf{k}\cdot\mathbf{a}+\nu_2),$$
$$\mu(y2\mathbf{a}) \sim -\sin\theta\cos(\mathbf{k}\cdot\mathbf{a}+k\tau+\nu_2), \quad (36)$$

where the upper signs correspond to the ICR Δ^{51} and the lower signs to the ICR Δ^{52}. Steady-state solutions are obtained as a result of substitution of (35) into (36). For $\mathbf{k}=\mathbf{k}_s$, a mixed IC exists, and its coefficient is of the order of the ratio of the nonexchange energy to the exchange energy, i.e., is very small. Nevertheless, the actual magnetic density must be equal to the corresponding superposition of densities described by the ICR Δ^{51} and Δ^{51}.

In addition to steady-state solutions, solutions of a more general type are also possible, for which conditions (35) do not hold, and the values of the quantities θ, ν_1, and ν_2 depend strongly on extrinsic parameters. In our opinion, the corresponding structures can be established experimentally only when they are intermediate between steady-state solutions.

We omit an analysis of the magnetic Z-density as well as the cases when both XY- and Z-densities differ from zero simultaneously.

Incommensurate magnetic structures in MnO_2 were studied phenomenologically in Ref. 5. The method worked out in Ref. 5 is also developed here: the determination of the form of coefficients of IC, spectrum ''smoothing,'' etc. In Ref. 5, it was pointed out (probably, for the first time) that the helix has an elliptic shape and proposed that Lifshitz invariants have almost nothing to do with the possibility of the emergence of a helical structure.

7. The magnetic helical structure in MnO_2 was described by Dzyaloshinskii[4] on the basis of the Lifshitz invariant $I_L=\psi_1\nabla\psi_2-\psi_2\nabla\psi_1$. It was noted above that ψ_1 and ψ_2 are the limiting values of the basis vectors $\psi(1...)$ and $\psi(4...)$ of the ICR δ^1 and δ^4. At the point $\mathbf{k}_s$, we have either $\psi(1...)\neq 0$, $\psi(4...)=0$, or $\psi(1...)=0$, $\psi(4...)\neq 0$. Consequently, although the invariant I_L exists, it has nothing to do with an incommensurate structure. It was explained in items **d** and **e** that the realization of magnetic incommensurate structures and transitions between them are determined by the values of the quantities Φ in formula (16). The method used in Ref. 4 is probably justified in the case when the ICR d at a symmetry point is concordant (compatible) only with a single ICR of the same dimensionality at a nonsymmetric point. If the limitation imposed by an ICR from P at a symmetric point can be decomposed, for example, into two ICR δ and δ' for a nonsymmetric point, it is proposed in Ref. 4 that the BV of the ICR δ and δ' should be determined according to the perturbation theory by expanding them into a series in the difference $\boldsymbol{\varkappa}=\mathbf{k}_0-\mathbf{k}_s$. But, first, it is incorrect to speak of a power series expansion in $\boldsymbol{\varkappa}$ for sums of the type (2). Second, such an expansion requires also the fulfillment of the inequality $|\boldsymbol{\varkappa}|\ll|\mathbf{b}|$. This inequality does not hold for experimentally established helical structures (in fact, these structures are not long-periodic). The branches of the exchange spectrum corresponding to δ and δ' are separated at the point $\mathbf{k}_s$ by an interval of the order of exchange energy. If the ICR δ and δ' are nonequivalent, the mixed IC is of the relativistic nature and can be neglected. If the ICR δ and δ' are equivalent, the mixed IC is of the exchange type and plays an important (sometimes decisive) role in the formation of an incommensurate structure.[6,7]

[1] O. V. Kovalev, Fiz. Nizk. Temp. **25**, 160 (1999) [Low Temp. Phys. **25**, 115 (1999)].
[2] O. V. Kovalev, Fiz. Tverd. Tela (Leningrad) **32**, 2381 (1990) [Sov. Phys. Solid State **32**, 1382 (1990)].
[3] O. V. Kovalev, *Representations of the Crystallographic Space Groups*, Gordon and Breach Science Publ. (1993).
[4] I. E. Dzyaloshinskii, Zh. Eksp. Teor. Fiz. **46**, 1420 (1964) [Sov. Phys. JETP **19**, 960 (1964)].
[5] O. V. Kovalev, Fiz. Tverd. Tela (Leningrad) **7**, 103 (1965) [Sov. Phys. Solid State **7**, 77 (1965)].
[6] O. V. Kovalev, Fiz. Tverd. Tela (Leningrad) **36**, 2074 (1994) [Phys. Solid State **36**, 1132 (1994)].
[7] O. V. Kovalev, Fiz. Tverd. Tela (Leningrad) **37**, 3382 (1995) [Phys. Solid State **37**, 1859 (1995)].

Translated by R. S. Wadhwa

ELECTRONIC PROPERTIES OF METALS AND ALLOYS

Quantum size effect and interlayer electron tunneling in metal-semiconductor superlattices

N. Ya. Fogel' and A. A. Slutskin

*Department of Applied Physics, Chalmers University of Technology an Göteborg University, S 41296, Göteborg, Sweden and B. Verkin Institute for Low Temperature Physics and Engineering, 47 Lenin Ave., 310164 Kharkov, Ukraine**

H. A. Kovtun

B. Verkin Institute for Low Temperature Physics and Engineering, 47 Lenin Ave., 310164 Kharkov, Ukraine

R. I. Shekhter

Department of Applied Physics, Chalmers University of Technology and Göteborg University, S 41296, Göteborg, Sweden

(Submitted July 31, 1998; revised August 14, 1998)
Fiz. Nizk. Temp. **25**, 168–171 (February 1999)

A new type of quantum size effect in metal-semiconductor superlattices is predicted. Giant oscillations of the transverse tunnel conductivity arise if size quantization of the electron spectrum in the metal layers takes place. This effect is due to the fact that the probability of metal electron tunneling through a semiconductor layer depends sharply on the electron incidence angle. The oscillations have been found to exist even in disordered systems, provided the electrons in metal layers undergo low-angle scattering on imperfections. © *1999 American Institute of Physics.* [S1063-777X(99)00602-7]

Recently new unusual oscillation effects have been discovered[1–4] on metal-semiconductor Mo/Si superlattices (SL) with a constant thickness of Si layers, d_s, and a variable thickness of the metal ones, d_m. SL in-plane resistivity, ρ_l, as well as superconducting characteristics (the transition temperature, T_c, the transverse critical magnetic field derivative, $dH_{c\perp}/dT|_{T_c}$, and the coupling strength) reveal oscillating periodic dependence on d_m. All oscillations are well pronounced, and in the case of the coupling strength they reach a giant amplitude. Of even greater importance is the fact that the oscillation effects are inherent only to *multi*layers. Three layer samples, Si/Mo/Si, have not revealed any oscillations.[3] This fact alone suggests that the oscillations cannot be explained in simple terms of the conventional quantum size effect,[5] though their period in d_m does not conflict with a value predicted by the size-quantization theory for metal single films.

In this note we would like to discuss an anisotropic tunneling through SL semiconductor layers as a possible explanation of the above unusual size effects. To demonstrate the possibility of such effects we shall consider here the transverse SL conductivity which originates from the interlayer tunneling of electrons.

The idea is based on the fact that the probability of the tunneling of metal electrons through a semiconducting interlayer, W, differs from zero only for those with a practically normal incidence on an interface metal-semiconductor. Owing to this sharp dependence of W on the incidence angle of a tunneling electron, θ, the probability W experiences sharp outbursts as quantized electron energies in the metal pass through the Fermi level with a d_m variation. This effect reminds in some sense so-called giant resonance oscillations of the ultrasonic absorption in metals[6] with the essential difference that instead of a small electron group singled out by the resonance condition there is one determined by the sharpness of the function $W(\theta)$ mentioned. It is this group that participates in the tunnel current. It is obvious that such an effect can lead to the giant oscillations of the tunnel current.

At first sight, the effect described seems to be irrelevant to the experiments mentioned above because of a rather strong disorder in metal layers. Nevertheless we shall show that, for the small group of electrons we are interested in, the size quantization results in an enhancement of their lifetime in $d_m/a \gg 1$ times (a is the interatomic distance in metal). As will be shown, such an enhancement is sufficient to provide giant oscillations of the tunnel current.

To show this we consider a periodic one-dimensional system comprised of the alternating quantum wells (conducting layers) and the tunnel barriers (semiconductor layers). For simplicity we shall assume further that the electron dispersion law is quadratic and isotropic.

As follows from general quantum mechanics considerations, W as a function of the in-plane momentum modulus, $p_\parallel$, and the electron energy, E (which is considered to be

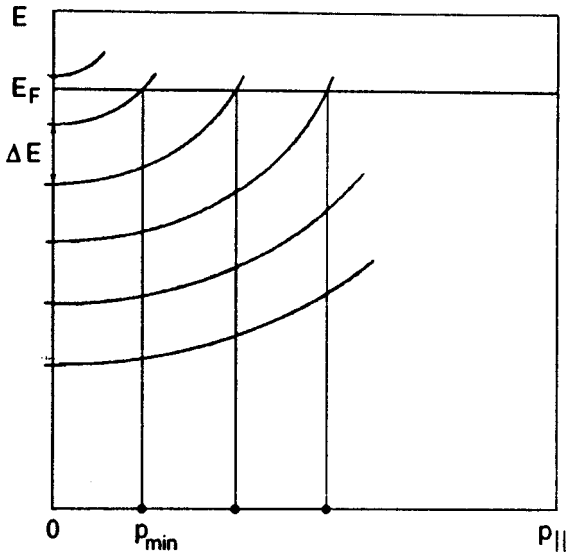

FIG. 1. The size-quantization spectrum in a metal layer. The bold dots on the $p_\parallel$-axis are p_n (quantized values of $p_\parallel$ at $E=E_F$).

close to the Fermi energy, E_F) can be represented in the form

$$W=A\exp\left\{-\frac{2d_s\sqrt{(\delta p)^2+2m_s(E-E_F)+p_\parallel^2}}{\hbar}\right\}, \tag{1}$$

where d_s is the thickness of semiconductor layers,

$$\delta p=\sqrt{2m_s\Delta}, \tag{2}$$

Δ is a phenomenological parameter which is of order of the typical energy of the effective tunnel barrier, the constant $m_s\sim m_0$ (m_0 is the free electron mass); the form of the preexponential factor A is irrelevant to further consideration. The Δ value cannot exceed one-half the semiconductor gap, E_g, which is, in turn, much less than E_F. In the case of amorphous semiconductors, which is realized in SL Mo/Si, there are strong reasons to expect that energy parameter Δ is even much less than E_g. It is just the smallness of Δ that causes the sharp dependence of W on the angle θ or, what is the same, on $p_\parallel$. Formula (1) shows that the probability $W(p_\parallel)$ reaches its maximum at the normal incidence ($p_\parallel=0$) of an electron on the metal-semiconductor interface, abating to exponentially small values within an interval of order of $\delta p\ll p_F=\sqrt{2mE_F}$ (m is the mass of an electron in the metal). Such a behavior of $W(p_\parallel)$ is a main point of our consideration.

Another important scale in momentum space results from the size quantization in the metal layers. In the isotropic case under consideration the size-quantization electron spectrum in a metal layer (in the limit $W=0$) is a set of terms

$$E_n^0(p_\parallel)=[(\hbar\pi n/d_m)^2+p_\parallel^2]/2m, \tag{3}$$

where n is the term number.

It is clear (see Fig. 1) that at zero temperature only quantized $p_\parallel$ values (we denote them by p_n) which are the roots of the equation

$$E_n^0(p_\parallel)=E_F \tag{4}$$

make a contribution to SL kinetic characteristics. At finite but rather small W the situation is not changed essentially because the broadening of size-quantization levels, $\delta E\sim\sqrt{W}\Delta E$, which is produced by the electron tunneling is small as compared with the typical distance

$$\Delta E\sim\hbar v_F/d_m \tag{5}$$

between nearest terms (v_F is the Fermi velocity). Therefore, permitted $p_\parallel$ values are localized within narrow momentum intervals that are isolated one from another (their lengths are $\propto\sqrt{W}$) centered at p_n.

As follows from (1), only those $p_\parallel$ values make the main contribution to a tunnel current, I, that meet condition $p_\parallel\leqslant\delta p$. Taking also into account condition (4), one finds that I depends crucially on the ratio between δp and the smallest of the quantized p_n values

$$p_{\min}=\left(\left\{\frac{d_mp_F}{\hbar}\right\}\frac{\pi\hbar}{d_m}p_F\right)^{1/2}. \tag{6}$$

Here {...} means the fractional part of a number. If $p_{\min}\gg\delta p$ the tunnel current is negligibly small, while at $p_{\min}\lesssim\delta p$ it essentially increases, reaching a maximum at $p_{\min}=0$. One can easily see from (6) that the monotonic change in the metal layer thickness d_m results in oscillations of $p_{\min}$ between the value $p_{\min}=0$ and its maximum value

$$\Delta p=\left(\frac{2\pi\hbar}{d_m}p_F\right)^{1/2}-p_F\left(\frac{a}{d_m}\right)^{1/2}. \tag{7}$$

As is seen from the figure, these oscillations arise because the monotonic change in d_m produces successive passage of size-quantization terms (3) through the Fermi level. Such an oscillatory behavior of $p_{\min}$ results in giant oscillations of the transverse current if the following condition takes place:

$$\Delta p\gtrsim\delta p \tag{8a}$$

or, in terms of d_m:

$$d_m\lesssim a(m/m_s)E_F/\Delta. \tag{8b}$$

In the opposite case, $\Delta p\ll\delta p$, the amplitude of I oscillations is bound to be exponentially small in the parameter $\delta p/\Delta p$. The criterion (8) of existence of the giant oscillations is not a rigid restriction. Though the parameter Δp is much less than p_F, it considerably exceeds the typical distance, $\hbar/d_m$, between quantized values p_n [see (4)]. Therefore, the requirement (8) can be fulfilled at $d_m\gg a$. Certainly, the criterion (8) is not the only one determining appearance of the giant oscillations. Along with it, the common conditions of quantum-size-effect existence must be fulfilled:

$$\hbar/\tau\lesssim\Delta E\sim\hbar v_F/d_m, \tag{9}$$

$$T\lesssim\Delta E. \tag{10}$$

Here τ is the time of electron life in a quantized state, T is the temperature. The latter condition is weaker than the previous one, and we can assume, for simplicity, that $T=0$.

At sufficiently large τ (this statement will be specified below) the tunnel current may be calculated directly in terms of the multilayer electron spectrum. The latter is a set of minibands

$$E(n,p_\parallel,\mathscr{P})=E_n^0(p_\parallel)+\delta E(p_\parallel,\mathscr{P}) \tag{11a}$$

which are size-quantization terms (3) broadened due to finiteness of tunneling probability. This broadening is determined by the small correction

$$\delta E=\frac{2\hbar v_{F\perp}(p_\parallel)}{d_m}\sqrt{W}\cos(\mathscr{P}d/\hbar), \tag{11b}$$

where $\mathscr{P}$ is a new quantum number (quasimomentum) enumerating the stationary states in minibands, $v_{F\perp}=\sqrt{2mE_F-p_\parallel^2}/m$ is the modulus of the transverse velocity of Fermi electron with a given $p_\parallel$, $d=d_s+d_m$. Taking into account that the average transverse velocity in a miniband stationary state, $v_\perp=\partial E(n,p_\parallel,\mathscr{P})/\partial\mathscr{P}$, has the form

$$v_\perp=2(d/d_m)v_{F\perp}\sqrt{W}\sin(\mathscr{P}d/\hbar), \tag{12}$$

after some calculations carried out in the relaxation time approach we obtain the transverse conductivity, $\sigma_\perp$, in the form

$$\sigma_\perp=\frac{me^2\tau d}{2\pi\hbar^2 d_m^2 m_s^2}[p_{\min}^2(d_m)+(\delta p)^2]\times\exp\left\{-\frac{2d_s}{\hbar}\sqrt{p_{\min}^2(d_m)+(\delta p)^2}\right\}. \tag{13}$$

This formula describes the limiting case $\Delta p\gg\delta p$. Here we have specified the expression for the preexponential A in (1), assuming for definiteness that the semiconductor layer may be considered as a square-topped barrier. As one can see from the expressions (13) and (6), the oscillatory dependence $\sigma_\perp$ on d_m is a periodic succession of sharp spikes whose height is of order of the transverse conductivity itself. They arise when d_m lies within rather narrow ranges determined by the relations

$$\left\{\frac{d_m p_F}{\hbar}\right\}\sim(\delta p/\Delta p)^2\ll 1.$$

Just at these d_m values electrons with $p_\parallel=p_{\min}$ tunnel between adjacent metal layers. Outside these ranges the tunneling is weak. The formula (13) also shows that the amplitude of $\sigma_\perp$ oscillations is

$$\sim(\hbar/d_m p_F)^2\exp\left\{-\frac{2d_s}{\hbar}\delta p\right\}\sigma_0.$$

Here σ_0 is the conductivity of the metal.

The expression (13) holds true only when the collision broadening $\hbar/\tau$ is much less than the typical miniband width $\delta E\sim\sqrt{W}\Delta E$. It is a very rigid restriction. The situation

$$\delta E\ll\hbar/\tau\lesssim\Delta E$$

seems to be much more realistic. In such a case the electron scattering completely destroys quantum coherent interference in the multilayer system as a whole, but it does not markedly affect the size quantization in individual metal layers. One can show that in this intermediate situation the formula (13) holds true with an accuracy of corrections $\sim W^{3/2}$. In such a case $\tau=\hbar/\Gamma$, where Γ is the imaginary part of the mass operator of the one-electron Green function in metal for normal incident electrons.

In the limiting case

$$\hbar/\tau\gg\Delta E \tag{14}$$

collisional broadening destroys not only the minibands but also the terms of size quantization in separate metal layer. It is clear that under such conditions the considered oscillation effects are absent.

As has been mentioned above, the present work was stimulated by the experimental observations [1–4] of the oscillations of kinetic and superconducting parameters on Mo/Si SLs. These investigations have been carried out on rather disordered Mo/Si multilayers with mean free path of electrons which is less than d_m.[7,8] At first sight the observation of the oscillatory behavior is impossible under these conditions. Here we shall show that in a case of soft (low-angle) scattering on the imperfections the lifetime of the size-quantized electron states for the electron group which is responsible for the tunneling ($p_\parallel\leqslant p_{\min}$) can significantly exceed the typical τ in a metal layer. Such a situation arises when the typical scale of a space inhomogenity in Mo layers, L, is more than a (in the experiment cited L was $\sim 10a$ for all d_m values). Actually, from the general expression for the inverse lifetime, $\tau^{-1}(n,p_\parallel)$, of an electron in a given size-quantization state, $|n,p_\parallel\rangle$, we obtain

$$\tau^{-1}(n,p_\parallel)\propto\sum_{n',p_\parallel'}\overline{|\langle n,p_\parallel|V|n',p_\parallel'\rangle|^2}\,\delta(E_n^0(p_\parallel)-E_{n'}^0(p_\parallel')). \tag{15}$$

Here $V=V(\mathbf{r})$ is a random potential in the metal layer, r is the electron radius vector, the line over the matrix element means the averaging over the random realization of $V(\mathbf{r})$. In virtue of the fact that the matrix element in (15) is not small only for momenta transferred $\leqslant\hbar/L$, only transitions with $|p_n-p_{n'}|\leqslant\hbar/L$ should be taken into account. As is clear from our preceding reasoning, the distance between the least p_n and its nearest neighbor is $\sim\Delta p$. This value can exceed $\hbar/L$ despite the fact that $L\ll d_m$. For this reason $\tau(n,p_\parallel)$ for the electrons participating in the tunnel transport turns out to be $d_m/a\gg 1$ times more than the typical τ value. That is why the giant oscillations can indeed arise in rather disordered multilayers.

In summary, we have considered a new quantum oscillation effect arising in metal/semiconductor multilayers due to combination of size quantization in thin metal layers and selective tunneling of electrons through the semiconductor interlayers. It is shown that giant oscillations of $\sigma_\perp$ appear, which result from sharp W dependence on an incidence angle of electron, so that only the electrons belonging to the small group with the least of quantized $p_\parallel$ values contribute to the tunnel current. Another remarkable feature of the quantum oscillations described is that the disorder is not so destructive

for the above effect as it is for the conventional quantum size effects. The next step is to show how this phenomenon affects the in-plane transport and superconducting properties in the experimental situation.

*E-mail: slutskin@theor.kharkov.ua

[1] E. I. Buchstab, V. Yu. Kashirin, N. Ya. Fogel, V. G. Cherkasova, V. V. Kondratenko, A. I. Fedorenko, and S. A. Yulin, Fiz., Nizk. Temp. **19**, 704 (1993) [Low Temp. Phys. **19**, 506 (1993)].
[2] V. Yu. Kashirin, N. Ya. Fogel, V. G. Cherkasova, E. I. Buchstab, and S. A. Yulin, Physica B **194-196**, 2381 (1994).
[3] N. Ya. Fogel, O. A. Koretskaya, A. S. Pokhila, V. G. Cherkasova, E. I. Buchstab, and S. A. Yulin, Fiz. Nizk. Temp. **22**, 359 (1996) [Low Temp. Phys. **22**, 277 (1996)].
[4] N. Ya. Fogel, O. G. Turutanov, A. S. Sidorenko, and E. I. Buchstab, Phys. Rev. B **56**, 2372 (1997).
[5] Yu. F. Komnik, *Physics of Metal Films*, Atomizdat, Moscow (1978).
[6] V. L. Gurevich, V. G. Skobov, and Yu. A. Firsov, Zh. Éksp. Teor. Fiz. **40**, 786 (1961) [Sov. Phys. JETP **13**, 552 (1961)].
[7] E. I. Buchstab, A. V. Butenko, N. Ya. Fogel, and V. G. Cherkasova, Phys. Rev. B **50**, 10063 (1994).
[8] N. Ya. Fogel, E. I. Buchstab, A. S. Pokhila, A. I. Erenburg, and V. Langer, Phys. Rev. B **53**, 71 (1996).

This article was published in English in the original Russian journal. It was edited by R. T. Beyer.

Semiclassical quantization condition for magnetic energy levels of electrons in metals with band-contact lines

G. P. Mikitik and Yu. V. Sharlai

*B. Verkin Institute for Low Temperature Physics and Engineering, National Ukrainian Academy of Sciences, 47 Lenin Ave., 310164 Kharkov, Ukraine**

(Submitted August 31, 1998)
Fiz. Nizk. Temp. **25**, 172–176 (February 1999)

We refine the well-known quantization condition for magnetic energy levels of a semiclassical electron. The refined condition results in the energy shift of the levels when in **k** space the closed electron orbit links to the band-contact line (i.e., surrounds it). This effect is closely analogous to that of Aharonov–Bohm provided the band-contact line plays the role of the infinitely thin ''solenoid'' with the fixed ''magnetic flux.'' The predicted shift must manifest itself in oscillation phenomena. © *1999 American Institute of Physics.*
[S1063-777X(99)00702-1]

It is common knowledge that the degeneracy of electron energy bands in a metal can occur along symmetry axes of its Brillouin zone. In addition, as was shown by Herring,[1] there are lines of an accidental contact between the bands in crystals. The term ''accidental'' means that the degeneracy of electron states is not caused by their symmetry. Such band-contact lines is likely to exist in many metals. This statement is easily understood when one takes into account Herring's result obtained for the case of a crystal with a center of inversion: if there is a point of contact between two energy bands in an axis of symmetry of the Brillouin zone, and the interband matrix element of the velocity operator is nonzero at this point, then a band-contact line has to pass through the point. Most metals have a center of inversion (and only such ones are considered below). Moreover, it is known (see, e.g., Ref. 2) that bands in many metals intersect at points on axes of symmetry. As for the matrix element of the velocity operator, the necessary information on it follows from the irreducible representations of the intersecting bands. Simple analysis of literature data shows that the lines of the accidental contact must exist, for example, in Be, Mg, Zn, Cd, Al and other metals (see Fig. 1a and 1b). Strictly speaking, any degeneracy of bands along a line of the Brillouin zone (excluding spin degeneracy) is lifted by the spin-orbit interaction. However, if this interaction is weak, the bands still approach each other, and the energy gap between them is small near that line in which the contact of the bands would take place if we ignored the interaction. Moreover, the inclusion of the weak spin-orbit coupling leaves the magnetic energy levels practically unchanged.[3] For this reason, to elucidate the heart of the matter, we completely neglect the spin-orbit interaction and spin of an electron in the subsequent discussion.

Semiclassical magnetic energy levels of electrons provide the basis for the analysis of many physical phenomena in metals.[4,5] These levels were studied in a number of papers.[6–17] It was established that a semiclassical electron orbit in the space of wave vectors, **k**, is the intersection of the constant-energy surface, $\varepsilon = \text{const}$, with the plane, $k_z = \text{const}$, where z is the direction of the magnetic field **H**. In the case of closed orbits the quantization condition for magnetic energy levels looks like

$$S(\varepsilon, k_z) = (2\pi|e|H/\hbar c)(n+\gamma), \tag{1}$$

where S is the cross-sectional area of the orbit in **k** space; n is a large integer ($n>0$); γ is a constant ($0 \leqslant \gamma < 1$), and e is the electron charge. In what follows we shall consider only those orbits for which probabilities of intraband and interband magnetic breakdowns are negligible. In other words, the orbit under study does not come close to any other trajectory with the same k_z, and its shape differs noticeably from an intersecting one. In this case, according to Ref. 8 (see also Ref. 18); γ always has the value

$$\gamma = 1/2. \tag{2}$$

It is this value that is commonly used in describing oscillation phenomena in metals[5] (e.g., the de Haas–van Alphen effect, the Shubnikov–de Haas effect, etc.). If a magnetic breakdown occurs, γ essentially depends on ε and k_z[10,11,15] but, as noted above, we shall not consider this situation.

In this paper we show that the equality

$$\gamma = 0 \tag{3}$$

can be valid if the closed electron orbit in **k** space associated with a certain energy band $\varepsilon_0(\mathbf{k})$ surrounds the line of degeneracy of this band with some other one. The above result depends neither on the form of $\varepsilon_0(\mathbf{k})$ in the neighborhood of the orbit nor on the shape and the size of this electron trajectory, and is topological in nature. It is due to the fact that the electron orbit links[19] (see Fig. 1) to the band-contact line which is the line of singularities for the Bloch wave functions. If the linking is absent, Eq. (2) holds. For the above-stated effect to be the case the band-contact line must satisfy the only condition: in its immediate vicinity the energies of the intersecting bands separate linearly in **k** as **k** moves away from the line. This condition is met for any accidental contact between the bands and in the case of degeneracy of the bands along a 3-fold symmetry axis of a crystal.

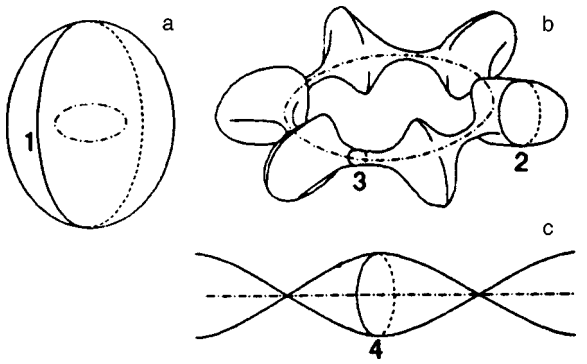

FIG. 1. The schematic sketch of Fermi surfaces for several metals with band-contact lines: the third-band electron ''lens'' of Zn and Cd (a); the second-band hole ''coronet'' (''monster'') of Be and Mg (b); the self-intersecting Fermi surface of graphite (c). The band-contact lines are shown as the dash-dot lines. The semiclassical orbits 3 and 4 link to the band-contact lines while the orbits 1 and 2 do not.

Equation (3) is obtainable from the results of Blount[20,21] and Roth.[14,22] In **k** space the effective one-band Hamiltonian of an electron in a magnetic field can be represented by a power series in **H**.[21,22] Two terms of this series suffice to calculate γ and thus we can use the following Hamiltonian:

$$\hat{H}=\varepsilon_0(\hat{\mathbf{k}})+(e/c)HM_0(\hat{\mathbf{k}}),$$

which must be considered as a symmetrized operator, that is, the components of $\hat{\mathbf{k}}$ always appear symmetrically in it. Here $\hat{\mathbf{k}}=\mathbf{k}-(e/\hbar c)\mathbf{A}(i\nabla_k)$, $\mathbf{A}(\mathbf{r})$ is the vector potential for **H** and the quantity $M_0(\mathbf{k})$ is associated with the diagonal matrix element of the orbital angular momentum of the electron in the band under study (this band is designated by subscript 0). More precisely, M_0 is the periodic part of z-component of the above-mentioned element divided by the electron mass. The quantity M_0 falls into the intraband and interband constituents:

$$M_0(\mathbf{k})=[\mathbf{v}\times\Omega]_z+\hbar\sum_{l\neq 0}\frac{\mathrm{Im}[(v_x)_{0l}(v_y)^*_{0l}]}{\varepsilon_l(\mathbf{k})-\varepsilon_0(\mathbf{k})}, \tag{4}$$

where $(\mathbf{v})_{0l}$ is the interband matrix element of the velocity operator at the point **k**, $\mathbf{v}\equiv(1/\hbar)\nabla_{\mathbf{k}}\varepsilon_0(\mathbf{k})$, and Ω is the periodic part of the coordinate operator:

$$\Omega(\mathbf{k})=i\int d\mathbf{r}u^*_{\mathbf{k}0}(\mathbf{r})\nabla_{\mathbf{k}}u_{\mathbf{k}0}(\mathbf{r}).$$

Here the integration is carried out over a unit cell, and $u_{\mathbf{k}l}(\mathbf{r})$ denotes the periodic factor in the Bloch wave function of the band l:

$$\Psi_{\mathbf{k}l}(\mathbf{r})=\exp(i\mathbf{k}\cdot\mathbf{r})u_{\mathbf{k}l}(\mathbf{r}).$$

In the case of interest (the spin-orbit interaction is neglected for a crystal with inversion symmetry) $M_0(\mathbf{k})$ can be made to vanish at any point **k** of the Brillouin zone. This well-known statement results from the following considerations. Electron states are invariant under the transformation: $U=KI$, where K and I are the operators of complex conjugation and inversion, respectively. Hence, one can take the phases of Bloch factors in such a way as to fulfil the relation

$$Uu_{\mathbf{k}l}=u_{\mathbf{k}l} \tag{5}$$

for any l. Under this condition the matrix elements $\mathbf{v}_{0l}(\mathbf{k})$ are real and $\Omega(\mathbf{k})=0$.[20] Thus, Eq. (4) yields $M_0(\mathbf{k})=0$. To consider M_0 in the general situation when $u_{\mathbf{k}l}$ have arbitrary phases and do not satisfy condition (5) let us take the transformation

$$u_{\mathbf{k}l}\to u'_{\mathbf{k}l}=u_{\mathbf{k}l}\exp[i\varphi_l(\mathbf{k})], \tag{6}$$

where $\varphi_l(\mathbf{k})$ are some regular functions of **k**, and $u_{\mathbf{k}l}$ before the transformation obey Eq. (5) in a vicinity of the point concerned. Then

$$\mathbf{v}_{0l}\to\mathbf{v}'_{0l}=\mathbf{v}_{0l}\exp[i(\varphi_l-\varphi_0)], \tag{7}$$

$$\Omega\to\Omega'=\Omega-\nabla_{\mathbf{k}}\varphi_0 \tag{8}$$

and we find from Eq. (4) that the interband part of M_0 is still equal to zero while its intraband component becomes nonvanishing and depends on the phase φ_0.

According to Roth,[14] γ is determined by the formula

$$\gamma-\frac{1}{2}=-\frac{1}{2\pi}\oint_\Gamma\frac{M_0(\mathbf{k})}{v_\perp(\mathbf{k})}\,d\kappa, \tag{9}$$

where Γ is the closed semiclassical orbit in **k** space; $d\kappa$ is the length of an infinitesimal element of Γ: $v_\perp$ is the absolute value of the projection of **v** on the plane of the orbit. Taking into account that the interband part of M_0 is zero, Eq. (9) can be rearranged as follows:

$$\gamma-\frac{1}{2}=-\frac{1}{2\pi}\oint_\Gamma\Omega d\mathbf{k}, \tag{10}$$

where $d\mathbf{k}\equiv d\kappa[\mathbf{i}_z\times\mathbf{v}]/v_\perp$ and $\mathbf{i}_z$ is the unit vector parallel to **H** ($d\mathbf{k}$ is aligned with the tangent to Γ and $|d\mathbf{k}|=d\kappa$). It is evident from Eqs. (8) and (10) that, in contrast to M_0, the measurable quantity γ is invariant under transformation (6).

It is generally believed that Ω (and M_0) can be made to vanish everywhere over the Brillouin zone, and thus $\gamma=1/2$. This is true in the absence of the degeneracy. However, if a line of the contact between the band under study and some other one exists, and the energies of the bands separate linearly in **k** in the vicinity of the line, then, according to Blount,[23] Ω can be made to vanish locally (i.e., in the neighborhood of any point that does not lie in the band-contact line) but this is impossible to attain along the whole length of a closed path P surrounding the line.[24] Moreover, one has

$$\oint_P\Omega d\mathbf{k}=\pm\pi, \tag{11}$$

where the sign in the right-hand side of the equation is determined by a direction of the integration. We emphasize that the integral in Eq. (11) does not depend on the shape and the size of the contour P. This is not surprising, since the equation

$$\nabla_{\mathbf{k}}\times\Omega(\mathbf{k})=0 \tag{12}$$

holds everywhere out of the band-contact line.[25] Finally, one more comment needs to be made. In general, the term $2\pi q$ must be added to the right-hand side of Eq. (11)[23] where q is

some integer. However it can be shown[3] that $q=0$ when the spin-orbit interaction is taken into account. (Besides, nonzero q would modify n and not affect γ).

Now we are able to find γ for any mutual arrangement of the semiclassical electron orbit Γ and the band-contact line. If Γ links to this line (see, e.g., orbits 3 and 4 in Fig. 1) formula (3) follows from Eqs. (10) and (11) (note that the values $\gamma=1$ and $\gamma=0$ are equivalent). If the linking is absent, a surface with boundary Γ necessarily exists which does not intersect the band-contact line[19] (for the surface in the case of orbit 1 (or 2) we can take a part of the constant-energy one shown in Fig. 1). Transforming Eq. (10) into the integral over this surface and taking into account Eq. (12), we arrive at formula (2). Interestingly, Eq. (2) is also obtained when Γ links to an even number of band-contact lines (such a situation takes place, e.g., for any central cross-section of the second-band Fermi surface of Al).

In the cases of Eqs. (2) and (3) the appropriate sets of the magnetic energy levels are shifted relative each other. The origin of this shift is easy to understand. As discussed above, the quantity M_0 can be made to vanish for any nondegenerate electron state with a fixed wave vector **k**. In essence, this is the so-called quenching of orbital angular momenta[26] (but only their periodic parts are quenched in the case of nonlocalized states considered here). Then Eq. (10) must be interpreted as the lack of the quenching for the semiclassical electron moving round the band-contact line. This gives rise to the additional magnetic moment of the electron: $(|e|\hbar/2m^*c)$, where m^* is its cyclotron mass:

$$m^*=\frac{\hbar^2}{2\pi}\left(\frac{\partial S}{\partial \varepsilon}\right)=\frac{\hbar}{2\pi}\oint_\Gamma \frac{d\kappa}{v_\perp}.$$

It is the interaction of this moment with **H** that leads to the above-mentioned shift of the magnetic energy levels.

The obtained result is closely analogous to the Aharonov–Bohm effect.[27] As pointed out by Blount[20], the quantity $\mathbf{\Omega}$ is similar to a vector potential for a magnetic field [see Eqs. (6) and (8)]. Taking Eqs. (11) and (12) into account, we can treat a band-contact line as an infinitely thin ''solenoid'' which carries the fixed flux of the ''field'' $[\nabla_{\mathbf{k}}\times\mathbf{\Omega}]$. With this in mind the above-mentioned analogy becomes apparent. Although the semiclassical electron moving round the band-contact line does not reach the region in which the ''field'' is nonzero, it experiences the ''vector potential'' $\mathbf{\Omega}$ that cannot be made to vanish along the whole length of the orbit. The semiclassical electron state with energy determined by Eq. (1) is the standing wave. If the electron orbit surrounds the band-contact line (i.e., the ''solenoid''), the interference picture corresponding to this wave is shifted as compared to the case when the line is absent. This shift manifests itself as the change in γ.

The above results can be also understood with the concept of Berry's phase.[28] If the Hamiltonian of a quantum system depends on parameters and the parameters undergo adiabatic changes so that they eventually return to their original values, then the wave function of the system can acquire, according to Berry, some constant phase in addition to the familiar dynamical one. This additional phase is completely determined by a closed trajectory P of the system in the parameter space and does not depend on details of the temporal evolution. In addition, it was obtained[28] that the phase is equal to π when the trajectory P surrounds a point of degeneracy of the Hamiltonian. More recently, Zak[29] has argued that Berry's results are applicable to an electron moving in a crystal, with **k** space playing the role of the parameter space, and the above-mentioned phase is described by the integral given in the left-hand side of Eq. (11). Then Eq. (3) may be interpreted as a manifestation of Berry's phase. In this connection we emphasize that measurements of γ in crystals with band-contact lines offer a way of detecting this phase in the physics of metals.[30]

The value γ can be experimentally determined through the investigation of oscillation effects in metals.[5] Since the measurement of γ is easiest to make for semiclassical orbits corresponding to small extremal cross sections of a Fermi surface, we point out that such orbits exist, e.g., in beryllium, magnesium, graphite, and in these metals they link to the band-contact lines (see Fig. 1). In Be and Mg the accidental contact between the second and third bands occurs in the basal plane of the crystals. If **H** lies, e.g., in this plane too, Eq. (3) must be valid for the orbits on the ''necks'' of the second-band hole ''coronet'' (or ''monster''). It should be noted that in Zn and Cd which are akin, in many respects, to Be and Mg the same band-contact line is located in the third-band electron ''lens'' and does not link to the semiclassical orbits (therefore, in this case $\gamma=1/2$). In graphite the degeneracy of two bands takes place along the vertical edge HKH of the Brillouin zone (i.e., along the 3-fold symmetry axis). Thus, Eq. (3) is expected to be true for the extremal orbit surrounding the point K (see orbit 4 in Fig. 1).

In summary, we have shown that in quantization condition (1) γ is equal to zero when the appropriate semiclassical orbit of an electron links to the band-contact line. This value differs essentially from the conventional one $\gamma=1/2$. Thus, measurements of γ can provide a possibility of detecting band-contact lines in metals (beryllium, magnesium and graphite appear to have considerable promise on this point).

*E-mail: mikitik@ilt.kharkov.ua

[1] C. Herring, Phys. Rev. **52**, 365 (1937).
[2] D. A. Papaconstantopoulos, *Handbook of the Band Structure of Elemental Solids*, Plenum, New York (1986).
[3] G. P. Mikitik and Yu. V. Sharlai, Zh. Éksp. Teor. Fiz. **114**, 1375 (1998) [JETP **87**, 747 (1998)].
[4] I. M. Lifshitz, M. Ya. Azbel', and M. I. Kaganov, *Electron Theory of Metals*, Consultant Bureau, New York (1973).
[5] D. Shoenberg, *Magnetic Oscillations in Metals*, Cambridge Univ. Press, Cambridge-Sydney (1984).
[6] L. Onsager, Philos. Mag. **43**, 1006 (1952).
[7] I. M. Lifshitz and A. M. Kosevich, Zh. Éksp. Teor. Fiz. **29**, 730 (1955) [Sov. Phys. JETP **2**, 636 (1956)].
[8] G. E. Zilberman, Zh. Éksp. Teor. Fiz. **32**, 296 (1957) [Sov. Phys. JETP **5**, 208 (1957)].
[9] G. E. Zilberman, Zh. Éksp. Teor. Fiz. **33**, 387 (1957) [Sov. Phys. JETP **6**, 299 (1958)].
[10] G. E. Zilberman, Zh. Éksp. Teor. Fiz. **34**, 748 (1958) [Sov. Phys. JETP **7**, 513 (1958)].
[11] M. Ya. Azbel', Zh. Éksp. Teor. Fiz. **39**, 1276 (1960) [Sov. Phys. JETP **12**, 891 (1961)].

[12] M. Ya. Azbel', Zh. Éksp. Teor. Fiz. **46**, 929 (1964) [Sov. Phys. JETP **19**, 634 (1964)].
[13] L. A. Falkovsky, Zh. Éksp. Teor. Fiz. **49**, 609 (1965) [Sov. Phys. JETP **22**, 423 (1966)].
[14] L. M. Roth, Phys. Rev. **145**, 434 (1966).
[15] A. A. Slutskin, Zh. Éksp. Teor. Fiz. **53**, 767 (1967) [Sov. Phys. JETP **26**, 474 (1968)].
[16] S. S. Nedorezov, Fiz. Nizk. Temp. **2**, 1047 (1976) [Sov. J. Low Temp. Phys. **2**, 513 (1976)].
[17] B. M. Gorbovitsky and V. I. Perel', Zh. Éksp. Teor. Fiz. **85**, 1812 (1983) [Sov. Phys. JETP **58**, 1054 (1983)].
[18] E. M. Lifshitz and L. P. Pitaevskii, *Statistical Physics*, Pergamon, Oxford (1986), vol. 9.
[19] B. A. Dubrovin, S. P. Novikov, and A. T. Fomenko, *Modern Geometry*, Springer-Verlag, NY, 1990.
[20] E. I. Blount, Solid State Phys. Academic Press, New York-London (1962), vol. 13.
[21] E. I. Blount, Phys. Rev. **126**, 1636 (1962).
[22] L. M. Roth, J. Phys. Chem. Solids **23**, 433 (1962).
[23] See pages 327, 328, 361 in Ref. 20.
[24] This result is due to the nonanalytical behavior of $u_{\mathbf{k}0}$ in the band-contact line and can be explained in the following manner. If the point $\mathbf{k}$ moves along P and in the process the phases of $u_{\mathbf{k}0}$ are chosen so that condition (5) be met, then $u_{\mathbf{k}0}$ goes over into $-u_{\mathbf{k}0}$ when $\mathbf{k}$ returns to the starting position $\mathbf{k}_0$. Thus, continuous $u_{\mathbf{k}0}$ cannot satisfy condition (5) along the whole length of P.
[25] Since $\nabla_{\mathbf{k}}\times\mathbf{\Omega}$ is invariant under phase transformations and $\mathbf{\Omega}$ can be made to vanish locally, Eq. (12) is true for any choice of $u_{\mathbf{k}0}$.
[26] R. W. White, *Quantum Theory of Magnetism*, Springer-Verlag, Berlin-New York (1983).
[27] Y. Aharonov and D. Bohm, Phys. Rev. **115**, 485 (1959).
[28] M. V. Berry, Proc. R. Soc. London, Ser. **A392**, 45 (1984).
[29] J. Zak, Phys. Rev. Lett. **62**, 2747 (1989).
[30] As to experimental investigations of Berry phase in molecular physics, optics and resonance phenomena in nuclear quadrupole systems, see, e.g., papers: G. Delacretaz *et al.*, Phys. Rev. Lett. **56**, 2598 (1986); A. Tomita and R. Y. Chiao, Phys. Rev. Lett. **57**, 937 (1986); R. Tycko, Phys. Rev. Lett. **58**, 2281 (1987).

This article was published in English in the original Russian journal. It was edited by R. T. Beyer.

Concordance of the basis vectors of representations at symmetric points of the Brillouin zone

O. V. Kovalev

National Science Center ''Kharkov Institute of Physics and Technology, 310108 Kharkov, Ukraine
(Submitted September 8, 1998)
Fiz. Nizk. Temp. **25**, 177–185 (February 1999)

The behavior of the basis vectors of the complete representation for a nonsymmetric point in the passage to the limit to a symmetric point is studied. The structure of the limiting representation and the fact of the emergence of a linear relation between the basis vectors are established, thus eliminating a number of contradictions. The concept of a limited induced representation is introduced. The formulas for basis vectors formulated by using this concept are transformed upon the passage to the limit into the basis vectors of only one irreducible representation at a symmetric point. The principle that an irreducible representation corresponds to a single energy level is used. Two versions of the basic vectors are considered: Bloch functions (electron spectrum) and infinite sums over translations (magnetic, phonon, and exciton spectra as well as the strong coupling method). The paper is in a certain sense an extension of the well-known publication by L. P. Bouckaert, R. Smoluchowski, and E. Wigner, Phys. Rev., **50**, 58 (1936). [S1063-777X(99)00802-6]

In their fundamental work[1] on the electron energy spectrum of a crystal, Bouckaert *et al.* pointed out a relationship between the solutions of the Schrödinger equation for a certain symmetric point (SP) $\mathbf{k}_{01}$ and solutions for a neighboring nonsymmetric point $\mathbf{k}_1$. The basis vectors (BV) of a small irreducible representation (IR) t^α of the $G(\mathbf{k}_{01})$ group are transformed into the BV of the sum $\Sigma\tau^\beta$ for the IR τ^β of the $G(\mathbf{k}_1)$ group in accordance with the equality $\hat{t}^\alpha\downarrow=\hat{t}^\beta$ for loaded representations. It is assumed that $G(\mathbf{k}_1)$ is a subgroup of the $G(\mathbf{k}_{01})$ group. For $\mathbf{k}_1\neq\mathbf{k}_{01}$, the $G(\mathbf{k}_1)$ group does not change upon a transition $\mathbf{k}_{01}\rightarrow\mathbf{k}_1$ (or $\mathbf{k}_1\rightarrow\mathbf{k}_{01}$). The downward arrow indicates the limitation of the representation from the group to the subgroup. The IR appearing in the equality are known as compatible. Bouckaert *et al.*[1] proceeded from the principles of continuity and conservation of the symmetry properties of BV. Compatibility relations (tables) are widely used in practice.

However, some questions arise in an analysis of the behavior of BV and energy levels. We shall list some of them under the assumption that $G(\mathbf{k}_{01})=G$ is the entire Fedorov group.

(1) The dimensionality of the complete representation ΣT^β is always higher than the dimensionality of the IR T^α since the star of the IR T^β has a large number of rays. What happens to the BV of the IR T^β during the passage to the limit $\mathbf{k}_1\rightarrow\mathbf{k}_{01}$? Which of them vanish (if any)? It is absolutely clear that none of the BV of the representation T^β vanishes at $\mathbf{k}_1=\mathbf{k}_{01}$ unless the BV are subjected to some special conditions. What are these conditions?

(2) If several energy levels E_β belonging to the IR τ^β merge into one level E_α at a SP, the BV of the IR τ^β must possess some specific properties. What are these properties?

(3) A certain IR τ^β can be compatible with two IR T^α and T^δ. Consequently, there must be at least two identical IR τ^β with different basis vectors. What are the properties of these bases?

(4) If the sum $\Sigma\tau^\beta$ contains more than one term, the energy levels E_β for the IR τ^β must converge for $\mathbf{k}_1\rightarrow\mathbf{k}_{01}$. How should the bases of the IR τ^β be chosen for this to occur in actual practice? Is it possible to make such a choice in general?

(5) If BV are constructed from localized functions, the concept of continuity is inapplicable to them. Consequently, an approach that is new in principle is required in this case. How can a physically reasonable pattern be obtained?

In this paper, the author carries out a complete (to the maximum possible extent) analysis of the behavior of matrices and BV of IR near a SP and establishes the rules for constructing BV that ensure the obtaining of a correct physical pattern. These rules should be used in practical calculations of any energy spectra of the crystal. (Naturally, the answers to the above questions are obtained.) In Sec. 1, the obtained results are of general nature in the sense that they are independent of the choice of the BV of an IR. Only the properties of IR matrices are used, and the lemma on the relation between the matrices of complete IR at a SP with those at a neighboring nonsymmetric point is proved. This attaches a new meaning to the concept of compatibility. In Sec. 2, Bloch's functions $\psi=u\exp(i\mathbf{k}\cdot\mathbf{r})$ are considered, and the continuity of u on $\mathbf{k}$ is basically used. In Sec. 3, basic sets of induced representations in the sense of Ref. 2 are analyzed. The fact that BV are constructed from a certain limited number of linearly independent functions is used.

Thus, quite different approaches are used in Secs. 2 and 3, but in both cases the rules of constructing BV ensuring a correct physical pattern are formulated.

It should be noted that we are speaking of two versions of application of the induction procedure. It can be described in general as follows. Let G_1 be a subgroup of a finite or spatial group G; ψ_i are the BV of a certain IR of the subgroup G_1. We apply all the elements of the group G to ψ_i. The obtained linearly independent functions form the basis of the induced representations. In the subsequent analysis, the induction procedure is used, first, for constructing representations of the group $G(\mathbf{k}_{01})$ of the vector $\mathbf{k}_{01}$ (or the entire group G) from small IR $\tau^{\beta}(\mathbf{k}_1)$ of the group $G(\mathbf{k}_1)$. The induced representations in this case are irreducible. Second, in other cases we mean induced representations in the sense of Ref. 2. These induced representations are reducible. It is always clear from the text which induced representations are considered. In addition, the concept of limited induced representations (LIR) will be introduced.

In the subsequent analysis, the notation and terminology from Ref. 2 will be used. Rotations h and elements $g=(\alpha/h)$ are sometimes regarded as operators.

1. In this section, we solve the following formal problem: we carry out the substitution $\mathbf{k}_1 \to \mathbf{k}_{01}$ in the matrices of complete IR of the group G and determine the composition of the obtained representation.

Let us specify the notation more accurately. For definiteness, we assume that all points $\mathbf{k}_1$ form a straight line ($\mathbf{k}_1$ line) passing through the point $\mathbf{k}_{01}$, where $\mathbf{k}_{01}$ is either the center of the Brillouin zone, or a SP on the surface of the zone, $\mathbf{K}_0$, v_0, $H(\mathbf{k}_{01})$, $\tau(\mathbf{k}_{01})$ and $T(\mathbf{K}_0)$ are respectively the star, the number of its rays, the group of rotations in elements of the group $G(\mathbf{k}_{01})$, and the small and complete representations as applied to the SP $\mathbf{k}_{01}$. The notation $\mathbf{K}$, v, $H(\mathbf{k}_1)$, $\tau(\mathbf{k}_1)$ and $T(\mathbf{K})$ has a similar meaning for the point $\mathbf{k}_1$.

Let us proceed to the limit $\mathbf{k}_1 \to \mathbf{k}_{01}$, i.e., replace $\mathbf{k}_1$ by $\mathbf{k}_{01}$ in the matrices of the representations $\tau(\mathbf{k}_1)$ and $T(\mathbf{K})$ and simultaneously replace the vectors of the star $\mathbf{K}$ by the vectors of the star $\mathbf{K}_0$. In this case, not one but several vectors from the star $\mathbf{K}$ become equivalent to the vector $\mathbf{k}_{01}$. Let us suppose that these vectors are $\mathbf{k}_1,\ldots,\mathbf{k}_{\sigma}$. We denote the set of these vectors by $\mathbf{K}_{\sigma}$, and the set of their limiting values $\mathbf{k}_{01},\ldots,\mathbf{k}_{0\sigma}$ by $\mathbf{K}_{0\sigma}$. Obviously, $v=\sigma v_0$.

Let $T^{\beta}(\mathbf{K})$ be a complete IR of the group G. As a result of the above transition, it is transformed into a certain representation $T_0^{\beta}=\lim T^{\beta}(\mathbf{k}_1 \to \mathbf{k}_{01})$, belonging to the star $\mathbf{K}_0$ and is reducible in the general case. The number of occurrences of a certain IR $T^{\alpha}(\mathbf{K}_0)$ in T_0^{β} is given by

$$\mu(T^{\alpha}(\mathbf{K}_0) \to T_0^{\beta}) = \frac{1}{N} \sum \chi_0^{\beta}(g)^* \chi^{\alpha}(g) \equiv \mu, \tag{1}$$

where summation is carried out over the main elements of the group G, and N is the number of these elements.

Let us simplify expression (1). The BV of the representation T_0^{β} associated with vectors from $\mathbf{K}_{0\sigma}$ form a subspace invariant to the group $G(\mathbf{k}_{01})$. These vectors are transformed according to a certain intermediate representation $t^{\beta}(\mathbf{K}_{0\sigma})$ of the group $G(\mathbf{k}_{01})$. This follows from the fact that the vector $h\mathbf{k}_i$ belongs to the set $\mathbf{K}_{\sigma}$ if $\mathbf{k}_i$ belongs to $\mathbf{K}_{\sigma}$, and h is a rotation from $H(\mathbf{k}_{01})$. The following two considerations are important here.

First, $t^{\beta}(\mathbf{K}_{0\sigma})$ can be interpreted as a small representation of the group $G(\mathbf{k}_{01})$ which can be used for constructing the corresponding complete representation of the entire group G according to general rules. The latter representation is equivalent to the representation T_0^{β}. Consequently, we can replace the complete representations of the group G in (1) by the small representations of the group $G(\mathbf{k}_{01})$:

$$\mu = \frac{v_0}{N} \sum \chi[t^{\beta}(\mathbf{K}_{0\sigma}), g]^* \chi[\tau^{\alpha}(\mathbf{k}_{01}), g], \tag{2}$$

where summation is carried out over the main elements of the group $G(\mathbf{k}_{01})$.

Second, the representation $t^{\beta}(\mathbf{K}_{\sigma})$ is equivalent to the representation $t_1^{\beta}(\mathbf{K}_{\sigma})$ which is constructed as follows. We consider the group $G(\mathbf{k}_{01})$ as a certain Fedorov group G_1 and construct its complete representation from the small representation $\tau^{\beta}(\mathbf{k}_1)$ according to the general induction rule. We introduce the vectors $\mathbf{k}_1,\ldots,\mathbf{k}_{\sigma}$. As we proceed to the limit $\mathbf{k}_1 \to \mathbf{k}_{01}$, the IR $t_1^{\beta}(\mathbf{K}_{\sigma})$ is transformed into a certain (generally, reducible) representation $t_1^{\beta}(\mathbf{K}_{0\sigma})$. Since $t^{\beta}(\mathbf{K}_{\sigma})$ and $t_1^{\beta}(\mathbf{K}_{\sigma})$ are equivalent, $t^{\beta}(\mathbf{K}_{0\sigma})$ and $t_1^{\beta}(\mathbf{K}_{0\sigma})$ are also equivalent. Consequently, we have

$$\mu = \frac{v_0}{N} \sum \chi[t_1^{\beta}(\mathbf{K}_{0\sigma}), g]^* \chi[\tau^{\alpha}(\mathbf{k}_{01}), g]. \tag{3}$$

Further, we can assume that the representation $t_1^{\beta}(\mathbf{K}_{0\sigma})$ can be obtained from the IR $\tau^{\beta}(\mathbf{k}_{01}) \equiv \tau^{\beta}(\mathbf{k}_1 \to \mathbf{k}_{01})$, as before, according to the general induction method as a result of extension from the group $G(\mathbf{k}_1)$ to the group $G(\mathbf{k}_{01})$. Since $\tau^{\alpha}(\mathbf{k}_{01})$ is an IR, on the basis of the Frobenius theorem on induced representations we obtain

$$\mu = \frac{v}{N} \sum \chi[\tau^{\beta}(\mathbf{k}_{01}), g]^* \chi[\tau^{\alpha}(\mathbf{k}_{01}), g], \tag{4}$$

where summation is carried out over the main elements of the group $G(\mathbf{k}_1)$. Let us go over to loaded representations:

$$\mu(T^{\alpha}(\mathbf{K}_0) \to T_0^{\beta}) = \frac{v}{N} \sum \chi[\hat{\tau}^{\beta}(h)]^* \chi[\hat{\tau}^{\alpha}(h)]$$
$$= \mu(\hat{\tau}^{\beta} \to \hat{\tau}^{\alpha}\downarrow), \tag{5}$$

where $h \in H(\mathbf{k}_1)$. We ave proved the following

Lemma. The number of occurrences of the complete IR $T^{\alpha}(\mathbf{K}_0)$ in the limiting value T_0^{β} of the complete IR $T^{\beta}(\mathbf{K})$ of the group G is equal to the number of occurrences of the loaded IR $\hat{\tau}^{\beta}$ in the limitation $\hat{\tau}^{\alpha}\downarrow$ of the loaded IR $\hat{\tau}^{\alpha}(\mathbf{k}_{01})$ to the subgroup $H(\mathbf{k}_1)$ of the group $H(\mathbf{k}_{01})$.

Corollary. If the IR τ^{β} is incompatible with the IR τ^{α} at the point $\mathbf{k}_{01}$, the space of the IR T^{α} is orthogonal to the space of he limiting representation T_0^{β}.

The lemma can also be derived by using the formulas for matrices of complete representations from Refs. 2 and 3.

We shall illustrate the lemma and some other results by using as an example the group $G=O_h^7=Fd3m$ with non-

TABLE I.

$\mathbf{k}_1$	$\mathbf{k}_0$, α										$\mathbf{k}_{10}$, α			
β	1	2	3	4	5	6	7	8	9	10	1	2	3	4
1	1	0	0	0	1	0	0	0	0	1	0	0	1	0
2	0	1	0	0	0	1	0	0	1	0	0	0	0	1
3	0	0	1	0	1	0	0	1	0	0	0	0	1	0
4	0	0	0	1	0	1	1	0	0	0	0	0	0	1
5	0	0	0	0	0	0	1	1	1	1	1	1	0	0

symmetric points on the straight line $\mathbf{k}_1=(0,0,k_1)$ and two SP $\mathbf{k}_0=0$, $\mathbf{k}_{10}=(0,0,\pi/\tau)=(\mathbf{b}_1+\mathbf{b}_2)/2$. The first star $\mathbf{K}_0$ has only one ray whose number will be omitted. The second star $\mathbf{K}_{10}$ has three rays.

Let us explain the lemma. We calculate the value of μ for all α and β according to (5). Proceeding to the limits $\mathbf{k}_1\rightarrow\mathbf{k}_0$ and $\mathbf{k}_1\rightarrow\mathbf{k}_{10}$, we take the characters of loaded IR from Tables T119, T205 and T119, T159 respectively in Refs. 2 and 3. The result (the number of occurrences) is given in Table I which will be referred to as the table of occurrences. Table T119 contains five IR whose numbers β are placed in the first column, while Table T205 contains ten IR whose numbers are written under the symbol $\mathbf{k}_0$. The symbol $\mathbf{k}_{10}$ stands for the numbers of IR from table T159. The numbers of occurrences $\mu(T^\alpha\rightarrow T_0^\beta)=\mu(\hat\tau^\beta\rightarrow\hat\tau^\alpha\downarrow)$ are indicated at the intersection of the line β and the column α. For example, the line with the number $\beta=5$ shows that the complete IR $T^5(\mathbf{K})$ is transformed into the sum of IR $T^7+T^8+T^9+T^{10}$ belonging to the star $\mathbf{K}_0$ upon the transition $\mathbf{k}_1\rightarrow\mathbf{k}_0$ and to the sum of IR T^1+T^2 belonging to the star $\mathbf{K}_{10}$ upon the transition $\mathbf{k}_1\rightarrow\mathbf{k}_{10}$.

The table of occurrence and the set of corresponding compatibility tables contain the same information by virtue of the lemma. The information on the compositions of limiting representations is required in an analysis of the energy levels of a crystal, phase transitions, etc. Let us consider only one problem. In Ref. 2, only the compositions of induced representations for a SP are presented. It is recommended that such representations for nonsymmetric points should be determined with the help of compatibility relations, but this recommendation is not substantiated in Ref. 2. The substantiation is contained in the lemma.

2. We shall speak below about the basic sets of representations. The Frobenius (reciprocity) theorem indicates the relation between the matrices of representations, and the composition of the induced representation is determined by using this theorem. It can also be obtained in the course of induction of basic sets, but under the conditions that all the introduced BV are linearly independent. If, however, such an independence is not observed, the induced basis implements not true Frobenius induced representations, but somewhat different representations. Let, for example, H be a certain point group and H_1 its subgroup. We shall induce the unit IR τ^1 of the subgroup H_1. This leads to an automatically reducible rather than unit representation of the group H. We assume, however, that a spherically symmetric function ψ is taken for the BV of the IR τ^1. In this case, the basis of the representation obtained as a result of induction is obviously exhausted by the function ψ. Thus, if the initial BV of the IR of a subgroup are such that the above principle of linear independence is not observed, we obtain (as a result of induction of basic sets) an induced representation and its basis differing from those predicted by the Frobenius classical theory. Such representations will be referred to as limited induced representations (LIR). The composition of a LIR is determined by the symmetry properties of the BV ψ_i of the initial IR of the τ-subgroup. These properties supplement those following from the fact that the BV ψ_i are transformed according to the IR τ.

The motivation of an analysis of LIR can be illustrated by the following example. According to Table I, the IR $T^5(\mathbf{K})$ is transformed as a result of the transition $\mathbf{k}_1\rightarrow\mathbf{k}_0$ into $T_0^5=T^7+T^8+T^9+T^{10}$, while the IT $T^4(\mathbf{K})$ is transformed into $T_0^4=T^4+T^6+T^7$ (we are speaking of the IR T^α from Table T205). In a physical problem (e.g., an analysis of the energy spectrum), the energy levels E correspond to IR. The IR $T^5(\mathbf{K})$ and $T^4(\mathbf{K})$ on the line $\mathbf{k}_1$ correspond to certain energy levels E_5 and E_4. The concordance at the point $\mathbf{k}_0$ can be presented in the form

$$T^4\rightarrow E_4^0,\quad T^6\rightarrow E_6^0,\quad T^7\rightarrow E_7^0,\ldots,T^{10}\rightarrow E_{10}^0.$$

It is clear, however, that one energy level $E(\mathbf{K})$ cannot be transformed into several levels at $\mathbf{k}_0$. The level E_5 must be transformed only into one of the levels E_7^0, E_8^0, E_9^0, or E_{10}^0, while the level E_4 can be transformed only into one of the levels E_4^0, E_6^0, or E_7^0.

We can make the following assumption. On the line $\mathbf{k}_1$, we have four IR with identical matrices $T^5(\mathbf{K})$, but with different basic sets. We denote these IR by $T^{5,7}(\mathbf{K})$, $T^{5,8}(\mathbf{K})$, $T^{5,9}(\mathbf{K})$ and $T^{5,10}(\mathbf{K})$. As we proceed to the limit $\mathbf{k}_1\rightarrow\mathbf{k}_0$, the BV of the IR $T^{5,7}(\mathbf{K})$ are transformed into the BV of the IR $T^7(5)$, where the number 5 in the parentheses indicates that the basis originates from the BV of the IR $T^5(\mathbf{K})$. Similarly, the BV of the IR $T^8(5)$, $T^9(5)$, and $T^{10}(5)$ are formed. The line $\mathbf{k}_1$ also contains three IR with identical matrices $T^4(\mathbf{K})$, but with different basic sets. These are $T^{4,4}(\mathbf{K})$, $T^{4,6}(\mathbf{K})$ and $T^{4,7}(\mathbf{K})$. As we proceed to the limit $\mathbf{k}_1\rightarrow\mathbf{k}_0$, their BV are transformed into the BV of the IR $T^4(4)$, $T^6(4)$, and $T^7(4)$, respectively. On the other hand, $\hat T^7\downarrow=T^7\downarrow=\hat\tau^4(\mathbf{k}_1)+\hat\tau^5(\mathbf{k}_1)$. i.e., the three-dimensional space of the IR T^7 is formed by two BV of the small IR $\tau^5(\mathbf{k}_1)$ and one BV of the small IR $\tau^4(\mathbf{k}_1)$ taken after the transition $\mathbf{k}_1\rightarrow\mathbf{k}_0$. The remaining BV of complete limiting IR T_0^5 and T_0^4 must be linear combinations of the three BV mentioned above. This means that the spaces of the IR $T^7(5)$ and $T^7(4)$

coincide, and the energy levels E_5 and E_4 merge into one level E_7^0 at the point $\mathbf{k}_0$. We shall not consider other possible versions of matching of the basic sets of IR at the points $\mathbf{k}_0$ and $\mathbf{k}_{10}$, which can be derived from Table I and which correspond to a reasonable physical pattern. Let us formulate the following problem: in the general case, find the conditions that should be imposed on the basic sets of representations to obtain a correct physical pattern in all cases.

Let us start from a related problem. Let H be a finite point group and H_1 its subgroup, while T and τ are the IR of the group and the subgroup respectively, the IR τ appearing in the limitation $T\downarrow$ imposed by the IR T on the subgroup H_1. We assume that $T\downarrow$ is taken in the reduced form, and the matrices of the IR τ lie in the left upper part of the matrices $T\downarrow$. Let F be a certain position function of the general form, such that $hF(\mathbf{r})=F(h^{-1}\mathbf{r})$. We introduce the function

$$f_i=\sum T(h)^*_{i1}hF, \tag{6}$$

where $h\in H$. The function f_i belongs to the ith line of the IR T and simultaneously belongs to the ith line of the IR τ. If we apply the induction procedure to it, we obtain exclusively the BV of the IR T (T is a LIR). The function f_i possesses some symmetry properties following from (6), but not just from the fact that f_i belongs to the space of the IR τ.

If we have only the characters of IR at our disposal, we can use [instead of (6)] the formula

$$f=\sum \chi_\tau(h')^*\chi_T(h)^*h'hF, \tag{7}$$

where summation is carried out over $L'\in H_1$ and $h\in H$. The function f belongs to the space of the IR τ. Applying the induction procedure to f, we obtain only the BV of the IR T.

It should be noted that in (6) we can replace the subscript ''1'' by the number of any column of the IR T. In this case, we must specially prove that f_i belongs to the ith line of the IR τ.

In an analysis of BV in the vicinity of a SP in the Brillouin zone, we use formula (6) as a prompt. For brevity, we shall refer to the representations of the group $G(\mathbf{k}_{01})$ as complete representations (using the notation T^α and T^δ instead of t^α and t^δ). These representations are truly complete if $G(\mathbf{k}_{01})=G$. If, however, $G(\mathbf{k}_{01})$ is a nontrivial subgroup of the group G, truly complete representations are constructed from the representations of the group $G(\mathbf{k}_{01})$ by the conventional induction method. In this case, each IR of the group $G(\mathbf{k}_{01})$ generates the corresponding single IR of the group G. Consequently, our simplification does not lead to a loss of generality. We can write the BV $\psi^\alpha_{i\lambda}$ belonging to the ith line of the IR T^α of the group $G(\mathbf{k}_{01})$ in the form

$$\psi^\alpha_{i\lambda}(\mathbf{k}_{01})=u^\alpha_{i\lambda}(\mathbf{k}_{01})\exp i\mathbf{k}_{01}\mathbf{r}$$

$$=\sum T^\alpha(g)^*_{i\lambda}g[u(\mathbf{k}_{01})\exp i\mathbf{k}_{01}\cdot\mathbf{r}], \tag{8}$$

where $u(\mathbf{k}_{01})$ is an arbitrary periodic function (that will be referred to as a generating function). We carry out summation over the main elements of the group $G(\mathbf{k}_{01})$. It follows from (8) that

$$u^\alpha_{i\lambda}(\mathbf{k}_{01})=\sum S(g/\alpha i\lambda)gu(\mathbf{k}_{01}),$$

$$S(g/\alpha i\lambda)=\hat{T}^\alpha(h)^*_{i\lambda}\exp[i\,\mathbf{b}\cdot(\alpha-\mathbf{r})], \tag{9}$$

where $\mathbf{b}=\mathbf{k}_{01}-h\mathbf{k}_{01}$; $g=\boldsymbol{\alpha}/h$, $h\in H(\mathbf{k}_{01})$, and S can be treated as a matrix.

We assume that the limitation imposed by the IR $\hat{T}^\alpha$ on the subgroup $H(\mathbf{k}_1)$ is expanded on the IR and that this expansion contains the IR $\hat{\tau}^\beta$ of dimensionality l (it is known that l can be equal to 1 or 2). We arrange the matrices $\hat{\tau}(h)$ at the left upper corners of the matrices $\hat{T}^\alpha\downarrow(h)$ and propose that the functions

$$\psi^\beta_{i1}(\mathbf{k}_1)=u^\beta_{i\lambda}(\mathbf{k}_1)\exp i\mathbf{k}_1\mathbf{r},$$

$$u^\beta_{i1}(\mathbf{k}_1)=\sum S(g/\alpha i1)gu(\mathbf{k}_1), \tag{10}$$

be taken as the BV of the IR τ^β, where S is the same matrix as in (9). We assume that $u(\mathbf{k}_1)$ is transformed continuously into $u(\mathbf{k}_{01})$.

The proposed functions allow us to satisfy all the requirements following from physical considerations.

a. It is quite obvious that the transition $\mathbf{k}_1\to\mathbf{k}_{01}$ leads to limiting values of the functions (10), which are BV of the IR T^α.

b. In order to prove that the functions (10) are the BV of the IR τ^β (for $i\leqslant l$), we can apply to $\psi^\beta_{i1}(\mathbf{k}_1)$ the element $g'=(\boldsymbol{\alpha}'/h')$ from the group $G(\mathbf{k}_1)$. We must take into account the relations

$$T^\alpha(h')_{ij}=\hat{\tau}^\beta(h')_{ij};\quad i,j\leqslant l;$$

$$g'\exp(i\mathbf{k}_1\cdot\mathbf{r})=\exp[i\mathbf{k}_1\cdot(\mathbf{r}-\boldsymbol{\alpha}')].$$

c. As a rule, a certain IR T^α at a SP is compatible with not one but several IR at a neighboring nonsymmetric point. We assume for definiteness that $\hat{T}^\alpha\downarrow=\hat{\tau}^\beta+\hat{\tau}^\gamma$ (τ^β is a two-dimensional IR and τ^γ a one-dimensional IR). Using relations (10), we determined ψ^β_{11} and ψ^β_{21}. In formulas (10), we put $i=3$ and omit the superscript β for the time being. Let $g'\in G(\mathbf{k}_1)$. Then

$$g'\psi_{31}=\sum \exp\{i[(\mathbf{k}_1-h'\mathbf{b})\cdot(\mathbf{r}-\boldsymbol{\alpha}')$$

$$+\mathbf{b}\cdot\boldsymbol{\alpha}]\}\hat{T}^\alpha(h)_{31}g'gu,$$

where summation is carried out over the main elements of the group $G(\mathbf{k}_{01})$. We go over to the summation over the elements $g''=g'g$ and take into account the fact that $\hat{T}^\alpha(h')_{j3}=0$ for $j=1,2$ and $\hat{T}^\alpha(h')_{33}=\hat{\tau}^\gamma(h')_{11}$. We find that $g'\psi_{31}=\tau^\gamma(g')_{11}\psi_{31}(\mathbf{k}_1)$. Thus, the function ψ_{31} is a BV of the IR τ^γ (and hence can be marked by the superscript γ).

These considerations can easily be extended to any type of the decomposition of $\hat{T}^\alpha\downarrow$ into the IR $\hat{\tau}$. The result is that the BV of the IR T^α are the limiting values of BV of all IR τ which are compatible with T^α.

d. Let us suppose that $\hat{T}^\alpha\downarrow=\Sigma\hat{\tau}^\beta$ and $\hat{T}^\alpha\downarrow$ is decomposed into the IR. We slightly change the notation of the BV of the representation $\Sigma\tau^\beta$, namely, omit the superscript β

and label all BV of the representation $\Sigma\tau^{\beta}$ by a subscript. Thus, $\psi_{i1}(\mathbf{k}_1)$ are the BV of the representation $\Sigma\tau^{\beta}, 1 \leqslant i \leqslant l_{\alpha}$. We transform the limiting values of $\psi_{i1}(\mathbf{k}_{01})$ obtained as a result of transition $\mathbf{k}_1 \to \mathbf{k}_{01}$ according to the IR T^{α}. Let us prove that the limiting values of all the BV of the complete representation ΣT^{β} without any exception are linear combinations of the limiting values of the BV $\psi_{i1}(\mathbf{k}_{01})$.

Let $g'=(\boldsymbol{\alpha}'/h)$ be an element such that $h'\mathbf{k}_1=\mathbf{k}_2$, where $\mathbf{k}_2$ is a vector from the star $\mathbf{K}$. Moreover, g' is a representative of the left co-set of the expansion of the group $G(\mathbf{k}_{01})$ in the subgroup $G(\mathbf{k}_1)$. In this case, according to the rule for constructing complete IR,[2,3] $g'\psi_{i1}(\mathbf{k}_1)=\psi_{i1}(\mathbf{k}_2)$ are the BV of the IR T^{β}. On the other hand, we have

$$g'\psi_{i1}(\mathbf{k}_1)=\sum \exp\{i[(h'\mathbf{k}_1-h'\mathbf{b})\cdot(\mathbf{r}-\boldsymbol{\alpha}')+h\mathbf{k}_{01} \cdot \boldsymbol{\alpha}]\}T^{\alpha}(g)^{*}_{i1}g'gu(\mathbf{k}_1).$$

We introduce $g''=g'g$ and $\boldsymbol{\kappa}=\mathbf{k}_1-\mathbf{k}_{01}$ and transform the exponential. This gives

$$\psi_{i1}(\mathbf{k}_2)=\exp\{i[h'\boldsymbol{\kappa}\cdot(\mathbf{r}-\boldsymbol{\alpha})-\boldsymbol{\kappa}\cdot\mathbf{r}]\}T^{\alpha}(g')_{ji}\psi_{j1}(\mathbf{k}_1), \tag{11}$$

$$\psi_{i1}(\mathbf{k}_{02})=T^{\alpha}(g')_{ji}\psi_{j1}(\mathbf{k}_{01}). \tag{12}$$

Relation (11) indicates that any BV of the complete representation ΣT^{β} is a sort of ''linear'' combination of the BV of the small representation $\Sigma\tau^{\beta}$. Its coefficients depend on the vector $\boldsymbol{\kappa}$. Relation (12) can be obtained from (11) as a result of the transition $\mathbf{k}_1 \to \mathbf{k}_{01}$ $(\boldsymbol{\kappa}\to 0)$. It should be emphasized that relations (11) and (12) hold when condition (10) is satisfied and not at all in the general case. Equality (12) corresponds to physical pattern.

e. Let us suppose that $\hat{T}^{\alpha}\downarrow=\hat{\tau}^{\beta}+\hat{\tau}^{\gamma}$, $l_{\beta}=2$, $l_{\gamma}=1$. We prove that under the condition (10), the energy levels $E_{\beta}(\mathbf{k}_1)$ and $E_{\gamma}(\mathbf{k}_1)$ merge into a single level $E_{\alpha}(\mathbf{k}_{01})$ at the point $\mathbf{k}_{01}$.

Considering the IR τ^{β}, we can write

$$\psi_1(\mathbf{k}_1)=\psi_1(\mathbf{k}_{01})+\boldsymbol{\kappa}\nabla_{\mathbf{k}}\psi_1(\mathbf{k}_{01})+\ldots, \tag{13}$$

$$E_{\beta}(\mathbf{k}_1)=\langle\psi_1(\mathbf{k}_{01}),H\psi_1(\mathbf{k}_{01})\rangle+\boldsymbol{\kappa}\cdot\mathbf{A}+\ldots, \tag{14}$$

where $\mathbf{A}$ is the sum of matrix elements emerging as a result of (13). Replacing β by γ and the subscript 1 by 3 in (13) and (14), we obtain an expression for $E_{\gamma}(\mathbf{k}_1)$. In accordance with (10), the BV $\psi_1(\mathbf{k}_{01})$ and $\psi_3(\mathbf{k}_{01})$ belong to the first and third lines of the IR T^{α}. Consequently, we have

$$E_{\beta}(\mathbf{k}_1)=E_{\alpha}(\mathbf{k}_{01})+\boldsymbol{\kappa}\cdot\mathbf{A}, \quad E_{\gamma}(\mathbf{k}_1)=E_{\alpha}(\mathbf{k}_{10})+\boldsymbol{\kappa}\cdot\mathbf{A}',$$

if we neglect the terms with $\boldsymbol{\kappa}$ to the second and higher powers.

f. We assume that a certain IR τ^{β} is compatible with T^{α} and T^{δ} at $\mathbf{k}_{01}$, T^{α} and T^{δ} being nonequivalent: $\hat{T}^{\alpha}\downarrow=\hat{\tau}^{\beta 1}+\Sigma\hat{\tau}$, $\hat{T}^{\delta}\downarrow=\hat{\tau}^{\beta 2}+\Sigma\hat{\tau}'$. We are not interested in the compositions of the sums $\Sigma\tau$ and $\Sigma\tau'$, but $\Sigma\tau\neq\Sigma\tau'$. The IR $\tau^{\beta 1}$ and $\tau^{\beta 2}$ have identical matrices, but their basic sets are constructed according to (10) with the help of nonequivalent IR T^{α} and T^{δ}. We assume that the limitations $\hat{T}^{\alpha}\downarrow$ and $\hat{T}^{\delta}\downarrow$ are taken in the reduced form, and the matrices $\hat{\tau}^{\beta}$ occupy the upper left corners.

Obviously, the mixed matrix element

$$H_{12}(\mathbf{k}_1)=\langle\psi_1^{\beta 1}(\mathbf{k}_1),H\psi_1^{\beta 2}(\mathbf{k}_1)\rangle$$

of energy differs from zero for $\mathbf{k}_1\neq\mathbf{k}_{01}$. According to physical considerations, it must vanish at $\mathbf{k}_1=\mathbf{k}_{01}$. We shall prove that this is indeed the case if definition (10) is used. Taking into account expansions of the type (13), we obtain

$$H_{12}(\mathbf{k}_1)=\langle\psi_1^{\beta 1}(\mathbf{k}_{01}),H\psi_1^{\beta 2}(\mathbf{k}_{01})\rangle+\boldsymbol{\kappa}\cdot\mathbf{D}, \tag{15}$$

where $\mathbf{D}$ is the sum of the relevant matrix elements; $\mathbf{D}\neq 0$ in the general case. According to (10), $\psi_1^{\beta 1}(\mathbf{k}_{01})$ belongs to the first line of the IR T^{α} and $\psi_1^{\beta 2}(\mathbf{k}_{01})$ belongs to the first line of the IR T^{δ}. Since T^{α} and T^{δ} are nonequivalent, $H_{12}(\mathbf{k}_{01})=0$.

Remark. In (10) and other formulas, we use the first column of the matrix T^{α}, but any other column can also be used. The analysis is then complicated, but the results do not change. We can derive the relations ($T^{\alpha}=T$)

$$u_{in}(\mathbf{k}_1)=\sum_m T(g')w_{im}(h'), \quad g'=(\boldsymbol{\alpha}'/h'), \tag{16}$$

$$w_{im}(\mathbf{h}')=\sum{}' \exp\{i[(\mathbf{k}_{01}-h\mathbf{k}_{01})\cdot(\boldsymbol{\alpha}-\mathbf{r})]\} \times\hat{T}(h)_{im}gw(h'), \tag{17}$$

$$w(\mathbf{h}')=\exp(-i\mathbf{k}_{01}\cdot\mathbf{r})(g')^{-1}[u(\mathbf{k}_1)\exp i(\mathbf{k}_{01})\cdot\mathbf{r}]. \tag{18}$$

It can be seen from these relations that the periodic function $u_{in}(\mathbf{k}_1)$ obtained by using the nth column of the matrix T can be expressed in terms of periodic functions obtained with the help of other columns. In this case, however, we must take another arbitrary generating periodic function, namely, the function (18). In particular, if an element g' such that the sum (16) can be reduced to a single term (e.g., the one with the number m) exists, the transition from the nth to the mth column in (10) is equivalent just to another choice of an arbitrary generating function. Such an element exists for $\mathbf{k}_{01}=0$, but can be absent for a SP on the surface of the zone. Probably, practical calculations will necessitate the use of linear combinations of the functions u_{im} from different columns of the matrix T.

3. In this section, BV are linear combinations of mutually orthogonal localized functions. A transition from these vectors to the BV of induced representations is assumed to be unitary, and hence the BV form an orthogonal system (we are speaking of a Hermitian scalar product, viz., an integral over a unit cell). In this case, the energy spectrum is determined by the coefficients of invariant combinations (IC) of the corresponding local or symmetrized quantities (atomic displacements, magnetic moments, etc.).

Further, we consider not IR and their basic sets in general, but only a part of them. This limitation is due to the fact that we are dealing with a single system of equivalent positions, and only one IR Γ from a local group of positions. The problem concerning the relation between the BV of a IR from $i(\Gamma,\mathbf{k}_1)$ and the BV of a IR from $i(\Gamma,\mathbf{k}_{01})$ is solved just under these limitations.

TABLE II.

$\mathbf{k}_0$	T^8	T^9
$\mathbf{k}_1$	$\tau^3+\tau^5$	$\tau^2+\tau^5$

$\mathbf{k}_{10}$	τ^1	τ^2	τ^4
$\mathbf{k}_1$	τ^5	τ^5	$\tau^2+\tau^3$

Let l_Γ be the dimensionality of the IR Γ and m the number of equivalent positions in a unit cell. Then ml_Γ is the dimensionality of the small induced representation $i(\Gamma,\mathbf{k})$. This number is the same for all points of the Brillouin zone. This leads to the following

Theorem 1. All σml_Γ limiting BV which belonged to the induced representation $I(\Gamma,\mathbf{K}_\sigma)$ before the transition $\mathbf{k}_1\to\mathbf{k}_{01}$ and were associated with the vectors $\mathbf{k}_1,\ldots,\mathbf{k}_\sigma$ become linear combinations of ml_Γ limiting values of BV of the small induces representation $i(\Gamma,\mathbf{k}_{01})$ after the transition.

Indeed, first, ml_Γ BV of the induced representation $i(\Gamma,\mathbf{k}_1)$ were mutually orthogonal before the transition and remain the same after the transition. Second, the limiting BV mentioned in the theorem belong to the space of the small induced representation $i(\Gamma,\mathbf{k}_{01})$ whose dimensionality is ml_Γ.

Thus, if we construct the BV $\psi_i(\mathbf{k}_1),\ldots,\psi_i(\mathbf{k}_\sigma)$ of the representation $I(\Gamma,\mathbf{K}_\sigma)$ of the group $G(\mathbf{k}_{01})$ by the general method of induction from ml_Γ BV $\psi_i(\mathbf{k}_1)$ of the representation $i(\Gamma,\mathbf{k}_1)$ of the group $G(\mathbf{k}_1)$, and then proceed to the limit $\mathbf{k}\to\mathbf{k}_{01}$, only ml_Γ BV among $\psi_i(\mathbf{k}_{01}),\ldots,\psi_i(\mathbf{k}_{0\sigma})$ are linear independent. (It should be noted that, in contrast to Sec. 2, the transition is now not related to any assumptions concerning the continuity of the dependence on $\mathbf{k}$ and is simply reduced to the replacement of the vectors $\mathbf{k}_1,\ldots,\mathbf{k}_\sigma$ by the vectors $\mathbf{k}_{01},\ldots,\mathbf{k}_{0\sigma}$ in the corresponding sums over unit cells.)

It is expedient to introduce a new concept. We shall say that the nonequivalent IR $\tau^\beta(\mathbf{k}_1)$ and $\tau^\gamma(\mathbf{k}_1)$ from $i(\Gamma,\mathbf{k}_1)$ are in contact at the point $\mathbf{k}_{01}$ if $i(\Gamma,\mathbf{k}_{01})$ contains at least one IR $\tau^\alpha(\mathbf{k}_{01})$ which is compatible both with $\tau^\beta(\mathbf{k}_1)$ and $\tau^\gamma(\mathbf{k}_1)$. It should be emphasized that the solution of the problem of contact of two IR is determined by the chosen system of equivalent positions and IR Γ of a local group.

We illustrate the concept introduced above by the following examples. We consider the Fedorov system chosen earlier and the vectors $\mathbf{k}$ using Table I. We take a position (a) with the local group $G(a)=\bar{4}32=T_d$. The IR Γ are given in Table T192 in Refs. 2 and 3. According to Ref. 2, for $\Gamma=\Gamma5$ we have

$$i(\Gamma,\mathbf{k}_0)=T^8+T^9,\quad i(\Gamma,\mathbf{k}_1)=\tau^2+\tau^3+2\tau^5,$$

$$i(\Gamma,\mathbf{k}_{10})=\tau^1+\tau^2+\tau^4.$$

For the above-mentioned IR, we compose auxiliary compatibility tables (Table II) on the basis of Table I. It can be seen that the IR τ^3 and τ^5 as well as the IR τ^2 and τ^5 are in contact at $\mathbf{k}_0$, while the IR τ^2 and τ^3 are not in contact. On the contrary, τ^2 and τ^3 are in contact at $\mathbf{k}_{10}$, while neither τ^2 and τ^5 nor τ^3 and τ^5 are in contact at this point. (If we choose a different position or another IR, we obtain different results.)

The space of limiting BV of the induced representation $i(\Gamma,\mathbf{k}_1)$ can be split into mutually orthogonal spaces of the IR $\tau^\alpha(\mathbf{k}_{01})$. Let us suppose that the IR $\tau^\beta(\mathbf{k}_1)$ and $\tau^\gamma(\mathbf{k}_1)$ are not in contact at $\mathbf{k}_{01}$, i.e., $\tau^\beta(\mathbf{k}_1)$ is compatible with one set S_β of the IR $\tau^\alpha(\mathbf{k}_{01})$ from $i(\Gamma,\mathbf{k}_{01})$, and $\tau^\gamma(\mathbf{k}_1)$ with another set S_γ, the sets S_β and S_γ containing no identical IR $\tau^\alpha(\mathbf{k}_{01})$. The BV of the representation $t^\gamma(\mathbf{K}_{0\sigma})$ are orthogonal to the basic sets of all IR in S_β. Consequently, they are orthogonal to all BV of the IR $\tau^\beta(\mathbf{k}_{01})$, i.e., to the BV of the representation $t^\beta(\mathbf{K}_{0\sigma})$. On the other hand, according to Theorem 1, the BV of the representation $t^\gamma(\mathbf{K}_{0\sigma})$ can be expressed linearly in terms of the limiting BV of the representation $i(\Gamma,\mathbf{k}_1)$. Thus, Theorem 1 is refined by

Theorem 2. The BV of the representation $t^\beta(\mathbf{K}_{0\sigma})$ are linear combinations of the limiting BV of the IR $\tau^\beta(\mathbf{k}_1)$, and probably of small IR from $i(\Gamma,\mathbf{k}_1)$ that are in contact with $\tau^\beta(\mathbf{k}_1)$.

Let us clarify this theorem by the following example. We proceed to the limit $\mathbf{k}_1\to\mathbf{k}_0$. Let us suppose that the small IR τ^2, τ^3, and τ^5 in Table II generate the complete IR $T^2(\mathbf{K})$, $T^3(\mathbf{K})$, and $T^5(\mathbf{K})$, respectively. According to Theorem 2, the limiting BV of the complete IR $T^3(\mathbf{K})$ are linear combinations of the limiting BV of the small IR τ^3 and τ^{51}. Similarly, the limiting BV of the complete IR $T^2(\mathbf{K})$ are linear combinations of the limiting BV of the small IR τ^2 and τ^{52}. We introduced for the IR τ^5 the second superscript: the basis of the IR τ^{51} leads to the basis of the IR T^8, while the basis of the IR τ^{52} leads to the basis of the IR T^9. We must find the difference between the basic sets of the IR τ^{51} and τ^{52}. We continue an analysis of our example. Let us suppose that $\mathbf{k}_1\to\mathbf{k}_{10}$. We again have two IR τ^{51} and τ^{52}. They have identical matrices, but different basic sets. (By the way, there are no grounds to assume that the basis of the IR τ^{51} near the point $\mathbf{k}_0$ coincides with the basis of the IR τ^{51} near the point $\mathbf{k}_{10}$.) On the whole, the data contained in Table II suggest the following question: can the basic sets of two IR τ^5 under the transition $\mathbf{k}_1\to\mathbf{k}_0$ be chosen so that the space of the complete IR T^8 contains the limiting BV of only the IR τ^{51}, and the space of the IR T^9 only the IR τ^{52}? A similar question also arises under the transition $\mathbf{k}_1\to\mathbf{k}_{10}$. The affirmative answer to this question is given in

Theorem 3. If the limitation $\hat{\tau}^\alpha\downarrow(\mathbf{k}_{01})$ imposed from the group $H(\mathbf{k}_{01})$ on the subgroup $H(\mathbf{k}_1)$ is equal to

$$\hat{\tau}^{\beta 1}(\mathbf{k}_1)+\ldots+\hat{\tau}^{\beta m}(\mathbf{k}_1),$$

we can chose the basis of the small induced representation $i(\Gamma,\mathbf{k}_1)$ so that the limiting BV of the representation

$$t^{\beta 1}(\mathbf{K}_\sigma)+\ldots+t^{\beta m}(\mathbf{K}_\sigma)$$

of the group $G(\mathbf{k}_{01})$ form the basis of the small IR $\tau^\alpha(\mathbf{k}_{01})$.

We omit the proof since it is quite cumbersome. The choice of BV mentioned in the theorem is not complicated in specific cases. It is expedient to clarify the meaning of the theorem by considering a few examples.

According to Table II, we have $\hat{T}^8\downarrow(\mathbf{K}_0)=\hat{\tau}(\mathbf{k}_1)+\hat{\tau}^{51}(\mathbf{k}_1)$. The star $\mathbf{K}$ with the vector $\mathbf{k}_1$ has in all six rays: $(0,0,\pm\mathbf{k}_1)$, $(0,\pm\mathbf{k}_1,0)$, $(\pm\mathbf{k}_1,0,0)$. In the passage to the limit $\mathbf{k}_1\to 0$, all these six vectors are transformed into a single vector $\mathbf{k}_0=0$. The IR $t(\mathbf{K}_\sigma)$ in this case coincide with complete IR $T(\mathbf{K})$ so that the second sum mentioned in the theorem is equal to $T^3(\mathbf{K})+T^{51}(\mathbf{K})$. The latter representation is 18-dimensional. According to the theorem, its basis is transformed under the transition $\mathbf{k}_1\to 0$ into the three-dimensional basis of the IR $T^8(\mathbf{K}_0)$ (naturally, if the basis of the representation $\tau^3(\mathbf{k}_1)+\tau^{51}(\mathbf{k}_1)$ is chosen appropriately). Since three BV of the small representation $\tau^3(\mathbf{k}_1)+\tau^{51}(\mathbf{k}_1)$ are orthogonal prior to the limiting transition and after it, we can take the limiting values of the BV of the representation $\tau^3(\mathbf{k}_1)+\tau^{51}(\mathbf{k}_1)$ as the basis of the IR $T^8(\mathbf{K}_0)$. All eighteen limiting BV of the representation $T^3(\mathbf{K})+T^{51}(\mathbf{K})$ are linear combinations of the three limiting BV of the representation $\tau^3(\mathbf{k}_1)+\tau^{51}(\mathbf{k}_1)$ (as stated in Theorem 3). Similar arguments can be applied to the sum $\tau^2(\mathbf{k}_1)+\tau^{52}(\mathbf{k}_1)$. According to Theorem 3, the four-dimensional space of two IR $\tau^5(\mathbf{k}_1)$ can be divided into the spaces of the IR $\tau^{51}(\mathbf{k}_1)$ and $\tau^{52}(\mathbf{k}_1)$.

Point $\mathbf{k}_{10}$. In this case, we have, for example, $\hat{\tau}^1\downarrow(\mathbf{k}_{10})=\hat{\tau}^{51}(\mathbf{k}_1)$. As a result of the transition $\mathbf{k}_1\to\mathbf{k}_{10}$, the vectors $(0,0,\pm\mathbf{k}_1)$ become equivalent to the vector $\mathbf{k}_{10}$ so that $\mathbf{K}_\sigma=\{(0,0,\mathbf{k}_1),(0,0,-\mathbf{k}_1)\}$, $\mathbf{K}_{0\sigma}=\{\mathbf{k}_{10},\mathbf{k}_{10}-\mathbf{b}_3\}$. The role of the second sum mentioned in the theorem is played by the IR $t^{51}(\mathbf{K}_\sigma)$. (It can be regarded as the complete IR of the group $G(\mathbf{k}_1)+g_{25}G(\mathbf{k}_1)$, obtained from the small IR $\tau^{51}(\mathbf{k}_1)$ according to the general rules.) The IR $t^{51}(\mathbf{K}_\sigma)$ has a four-dimensional basis that is transformed into the two-dimensional basis of the small IR $\tau^1(\mathbf{k}_{10})$ upon the transition. In view of the one-to-one correspondence between small and complete IR, we can state that the 12-dimensional basis of the complete IR $T^{51}(\mathbf{K})$ is transformed as a result of the passage to the limit into a six-dimensional basis of the complete IR $T^1(\mathbf{K}_{10})$ ($\mathbf{K}_{10}$ is the star with the vector $\mathbf{k}_{10}$).

Theorem 3 in fact implies the same correspondence to a feasible physical pattern as that established in Sec. 2. However, it is difficult to obtain at the moment the proofs of some statements concerning the energy spectrum: the formula for the coefficients of invariant combination has not been derived, the properties of these coefficients have not been established, and so on.

If the basic sets of small IR at a nonsymmetric point are chosen so that they are transformed as a result of passage to the limit $\mathbf{k}_1\to\mathbf{k}_{01}$ directly into the BV of an IR at a SP in accordance with a correct physical pattern (we mean the one-to-one correspondence between IR and energy levels), such basic sets will be referred to as concordant. The statements made in Ref. 1 are valid only for concordant basic sets. Theorem 3 indicates that concordance of basic sets is possible in principle in the case of induced representations, but does not describe the method for attaining it. The method is similar to that described in Sec. 2 and will be formulated in our subsequent publication devoted to an analysis of the magnetic energy spectrum. The concordance of basic sets was apparently carried out for the first time in Ref. 4 for vibrational spectra. However, Ref. 4 does not contain a general algorithm and substantiation and disregards the emergence of a linear dependence at SP. The case of Bloch functions is not considered either.

[1] L. P. Bouckaert, R. Smoluchowski, and E. Wigner, Phys. Rev. **50**, 58 (1936).
[2] O. V. Kovalev, *Representations of the Crystallographic Space Groups*, Gordon and Breach Science Publ. (1993).
[3] O. V. Kovalev, *Irreducible Representations of the Space Groups*, Gordon & Breach, NY, 1965.
[4] O. V. Kovalev, Fiz. Nizk. Temp. **10**, 83 (1984) [Sov. J. Low Temp. Phys. **10**, 43 (1984)].

Translated by R. S. Wadhwa

LOW-DIMENSIONAL AND DISORDERED SYSTEMS

Current–voltage characteristic of a two-dimensional Corbino disk under the QHE conditions of quantum Hall effect

V. B. Shikin

*Institute of Solid-State Physics, Russian Academy of Sciences, 142432 Chernogolovka, Russia**

Yu. V. Shikina

Institute of Technological Problems in Microelectronics and Ultrapure Materials, Russian Academy of Sciences, 142432 Chernogolovka, Russia

(Submitted May 21, 1998; revised September 14, 1998)
Fiz. Nizk. Temp. **25**, 186–194 (February 1999)

A theory of current–voltage characteristic (IVC) is proposed for a gated Corbino disk with a $2D$ spinless electron system and magnetic filling factors close to an integral value. The described results systematically include the features of the electrochemical potential of the $2D$ electron system in a magnetic field, which are responsible for sharp magnetocapacitance ''dips'' for integral values of the magnetic filling factor. The theory is used for qualitative interpretation of the observed weakly nonlinear peculiarities of IVC as well as for prediction of local details in the distribution of electron density and electric potential in a current-carrying Corbino disc. Corresponding measurements can be made, for instance, by using the linear electrooptical effect. [S1063-777X(99)00902-0]

The measurements of conductance of a two-dimensional Corbino disk in a magnetic field normal to its surface give the most complete information on the diagonal component of the conductivity of the $2D$ system under investigation in a magnetic field. Naturally the expression for conductance must be exact to the maximum possible extent for extracting correctly the required conductance from the experimental data. We are speaking, among other things, of the effects of spatial inhomogeneity in the electron density distribution, which inevitably appear in a Corbino disk carrying transport current and strongly affect its conducting properties, especially under the conditions of the quantum Hall effect (QHE). In this paper, we consider the influence of the above-mentioned effects of spatial dispersion on the features of the current–voltage characteristic (IVC) and other parameters of the Corbino disk being measured. In addition to IVC, they also include the local distribution of electric potential along a radial direction of the disk, which is accessible for measurements based on the linear electrooptical effect.

It should be noted that nonlinear phenomena in the quantum Hall effect have been studied by many authors (in addition to the original communication,[1] see, for example Refs. 2–10). Usually, nonlinearities developing in drift fields eV much higher than the cyclotron energy $\hbar\omega_c$ are considered. They include overheating instability,[1,5] Zener effect,[2] injection of hot electrons from contact regions,[9] and so on. Among various reasons behind IVC nonlinearity, weakly nonlinear phenomena developing even at the stage when $eV<\hbar\omega_c$ take place. These effects involve the loss of spatial homogeneity in a $2D$ electron system under the action of transport current. An analysis of these effects started in an interesting publication by Shashkin *et al.*[8] is a problem of primary importance in the theory of IVC since strong nonlinearities inevitably develop against the background of weak nonlinearities.

The premises for studying of the loss of spatial homogeneity in a $2D$ electron system with transport current are well known. The current can flow only in the presence of a gradient of the electrochemical potential μ:

$$j_i = e^{-1}\sigma_{ii}\partial\mu/\partial x_i, \tag{1}$$

where σ_{ii} is the diagonal component of conductivity. The presence of the gradient $\partial\mu/\partial xi$ in $3D$ systems leads to the deformation of the electron density $\partial\rho$ since

$$\partial\rho \propto \partial^2\mu/\partial x_i^2. \tag{1a}$$

In two-dimensional systems, however, the charge is controlled by the derivatives of electric potential of the order lower than in (1a). For this reason, a uniform driving field can be sustained in a $2D$ system only by deforming the electron density. This considerably complicates the kinetics of $2D$ electron systems in a number of important cases. For example, the conditions for the emergence of the QHE, which are extremely sensitive to the uniformity of electron density, are blurred since the integral value of the filling factor required for this effect is observed only in some local regions of the $2D$ system. As a result, the QHE is manifested not in individual ''points'' of the magnetic field or cutoff voltage, but in an entire range of their values.

The paper has two parts. In the first part, the system of equations and approximations used for describing inhomogeneity effects in a magnetized $2D$ system with transport current is presented. A special discussion of these equations is required in order to modify some definitions usually appearing in the IVC theory for $2D$ systems under the conditions of the QHE. The second part contains the solution of the proposed equations under the conditions of weak nonlinearity of the problem, when a driving electric field causes perturbations in the $2D$ system, which are smaller than or comparable with the cyclotron energy. The paper is concluded with the discussion of the observed consequences of the proposed theory.

SYSTEM OF DEFINITIONS

Let us consider a screened Corbino disk with an inner and outer radii r_0 and r_1 in a magnetic field normal to its surface and sustaining the $2D$ electron system in a state close to the unit magnetic filling factor. A driving voltage V is applied to the banks of the Corbino disk. The presence of V leads to the emergence of a current in the system. The relation between the total current J and the electrochemical potential μ has the form

$$J/2\pi r = e^{-1}\sigma_{rr} d\mu/dr \tag{2}$$

(it should be noted that in Ref. 8 and subsequently in Ref. 11 the current J was defined as

$$J/2\pi r = \sigma_{rr} d\varphi(r)/dr, \tag{2a}$$

where $\varphi(r)$ is the electric potential of the problem; the difference between expressions (2) and (2a) is quite serious if the diffusion component of current is not smaller than the field component; it will be proved below that the current on the Hall plateau is just of this type).

As the current increases, the value of σ_{rr} ceases to be a constant in the theory. Under the conditions of the QHE, it is natural to take into account possible nonlinearities by using, for example, the well-known expression for σ_{rr}:[7,8,11,12]

$$\sigma_{rr} = \sigma_0 \mathrm{e}^{-\Delta/T} \cosh(\delta\mu/T), \tag{3}$$

where the Fermi energy (electrochemical potential) $\delta\mu$ is measured from the midpoint between the Landau levels, Δ is the activation energy for zero value of $\delta\mu$, and T the temperature. Approximation (3) has a meaning in the presence of changes in the value of $\delta\mu(r)$ in a $2D$ system and in the absence of changes in the behavior of the electric potential $\varphi(r)$. For the sake of definiteness, formula (3) will be referred to as the μ-representation in subsequent analysis.

The final result obtained by Iordanskii and Muzykantskii[12] [formula (21)] for the average diagonal conductivity in the presence of a random and quite smooth perturbing potential differs slightly from (3):

$$\sigma_{xx} = \frac{e^2}{\hbar} \exp\left[\frac{(\mu - V_c)}{T}\right] \int \frac{w(E)\exp(-E/T)dE}{T}. \tag{3a}$$

Here V_c is the percolation level, $w(E)$ the probability of passage through a typical saddle point, expressed in terms of characteristics of random potential, and μ the electrochemical potential.

It can be easily seen that the conductance definitions (3) and (3a) are qualitatively identical if we assume that

$$\exp(-\Delta/T) \to \exp(-V_c/T), \quad \varepsilon_F \to \mu,$$

$$\sigma_0 \to \frac{e^2}{\hbar} \int \frac{w(E)\exp(-E/T)dE}{T},$$

and take into account the symmetrization of the expression for conductance relative to electron and hole excitations, which is contained in the definition (3) of conductance.

It should also be noted that we do not calculate here the homogeneous component of conductance, i.e., the constant σ_0 in definition (3). It is only important that this quantity be finite. An example of the complete solution of the problem on conductance for a smooth random potential is given in Ref. 12.

Along with (3), we also introduce the modified phenomenological definition of conductance:

$$\sigma_{rr} = \sigma_0 \mathrm{e}^{-\Delta/T} \cosh[(\mu - e\varphi - \hbar\omega_c)/T]. \tag{4}$$

This expression takes into account the spatial dependence $\mu(x)$ as well as a possible coordinate dependence $\varphi(x)$. The explicit form of (4) presumes that the value of magnetic filling factor is close to unity.

The system of equations (2), (3) or (4) should be supplemented with the boundary conditions

$$\delta\mu(r_0)/\hbar\omega_c = \delta\mu_0, \quad \delta\mu(r_1)/\hbar\omega_c = \delta\mu_0 + v,$$

$$v = eV/\hbar\omega_c, \tag{5}$$

where all the energy characteristics are normalized to cyclotron energy.

In addition to Eqs. (2)–(5), we must have a definition of the electrochemical potential $\delta\mu(r)$. For an ideal spinless electron system with a filling factor close to unity, we have

$$\delta\mu(r) = \mu(r) - \hbar\omega_c = -\hbar\omega_c/2 + e\varphi(r) + \zeta(r), \tag{6}$$

$$\zeta(r) = -T \ln S(\nu), \quad \nu < 2, \tag{6a}$$

$$S(H,\nu) = (1/2)(1/\nu - 1) + \sqrt{(1/4)(1/\nu - 1)^2 + \varepsilon(2/\nu - 1)},$$

$$\nu(r) = \pi l_H^2 n(r), \quad n(r) = n_s + \delta n(r),$$

$$\varepsilon = \exp\left(-\frac{\hbar\omega_c}{T}\right) \ll 1. \tag{6b}$$

Here $n(r)$ is the local value of electron density, n_s its average value for zero current, l_H the magnetic length, and ω_c the cyclotron frequency.

In the ''dirty'' limiting case, when $T \ll \Gamma$, where Γ is the dispersion of the density of states at the Landau level, only the relation between ν and μ (and not the opposite relation as in (6)) has a relatively simple form:

$$\nu = \phi(\delta\mu_1/\Gamma\sqrt{2}) + \phi(\delta\mu_2/\Gamma\sqrt{2}) + 1, \tag{7}$$

$$\delta\mu_1=\mu-\hbar\omega_c/2-e\varphi, \quad \delta\mu_2=\mu-3\hbar\omega_c/2-e\varphi,$$

where $\phi(x)$ is the error function, $\phi(-x)=-\phi(x)$.

Using relation (6), we can write formula (4) as follows:

$$\sigma_{rr}=\sigma_0 e^{-\Delta/T}\cosh\left[\frac{-\hbar\omega_c/2+\zeta(r)}{T}\right]. \tag{7a}$$

This expression allows us to speak of (4) as of a ζ-representation of conductance. For $\nu=1$, i.e., in the region with an integral value of filling factor, the argument of hyperbolic cosine on the right-hand side of (7a) vanishes, and hence the conductance assumes the minimum value.

To make the system (2)–(7) complete, we must find the relation between the electric potential and local density of the $2D$ system. The required relation is of electrostatic origin and requires in the general case the simultaneous determination of the charge density along the $2D$ system and the screening electrode. In this region, it is possible to refine the existing definition quantitatively. However, claiming further to only quantitative analysis, we adhere, following Shashkin *et al.*, to the popular capacitor approximation in which the smallness of the distance $2d$ between the $2D$ system and the shutter is regarded as smaller than r_1-r_0:

$$2d\ll r_1-r_0. \tag{8}$$

In this case, we have

$$\varphi(r)\simeq 2ed[\nu(r)-\nu_0]/\kappa l_H^2, \tag{9}$$

where $\nu(r)$ is the local value of the filling factor, ν_0 its magnitude in the absence of current, and $\varkappa$ the dielectric constant.

Thus, the complete system of equations for determining the values of μ, φ, and ν includes formulas (2), (3), (5), (6) or (7) and (9). Alternatively, we are speaking of joint solution of Eqs. (2), (4), (5), (6) or (7) and (9). The final aim of the theory is the determination of the relation between J and V and the obtaining of the local distribution of electric potential of the Corbino disk, viz., the quantity accessible for measurements using the linear electrooptical effect.[13]

The main difference between our definitions and existing algorithms of calculating IVC for a Corbino disk under the conditions of the QHE from Refs. 8 and 11 is that we use (2) instead of (2a) and consider an alternative to (3) and (4). We are not aware of any general considerations testifying in favor of (3) or (4) without a preliminary analysis of the properties of these systems of equations.

ANALYSIS OF THE SYSTEM OF EQUATIONS

1. Let us consider a normal ohmic situation for the Corbino disk under investigation. We are speaking above all of Eq. (2) with a spatially homogeneous conductance $\sigma_{rr}=\text{const}$. In this case, we can write

$$\mu(r)=\mu_0+\frac{eJ}{\pi\sigma_{rr}}\ln\left(\frac{r}{r_0}\right), \quad r_0\leqslant r\leqslant r_1. \tag{10}$$

The current J is connected with the potential difference V across the metallic banks through the relation $\mu(r_1)-\mu(r_0)=eV$, $\mu(r_1)\equiv\mu_1$, so that

$$\frac{J}{2\pi\sigma_{rr}}\ln\left(\frac{r_1}{r_0}\right)=V. \tag{11}$$

Consequently, expression (10) can be written in the form independent of σ_{rr}:

$$\delta\mu_0\equiv\mu(r)-\mu_0=eV\ln\left(\frac{r}{r_0}\right)\Big/\ln\left(\frac{r_1}{r_0}\right). \tag{12}$$

Using the definition of $\mu(r)$ for a normal $2D$ system (the $2D$ system with a nonintegral filling factor in the given case), i.e.,

$$\delta\mu(r)=e\varphi(r)+\pi\hbar^2[n(r)-n_0]/m_* \tag{13}$$

and the relation (9) between φ and $n(r)$, we can easily write the following equation for $\varphi(r)$ by using (9), (12), and (13):

$$\delta\mu(r)=e\varphi(r)(1+a_B^*/d), \tag{14}$$

where a_B^* is the effective Bohr radius.

Thus, The IVC in the ohmic limit is defined by formula (11), and the electric potential distribution is proportional to $\delta\mu$ in accordance with (14), i.e., increases almost linearly from one bank of the Corbino disk to the other in accordance with (10) and (12). It can also be easily seen that as long as $a_B^*\ll d$, the definitions of current (2) and (2a) lead to approximately the same results both for the IVC and for the electric potential distribution along the Corbino disk. In other words, the diffusion component of electrochemical potential μ (13) under normal conditions is insignificant as compared to the electric component.

2. Let us now suppose that the filling factor is close to unity. As long as $\sigma_{rr}=\text{const}$, i.e., in the region $eV<T$ or $eV<\Gamma$ (the reasons behind these limitations will be considered below), expression (12) for $\mu(r)$ and (11) for IVC are valid. However, according to (6) or (7), the main contribution to the derivative $d\mu/dr$ comes from the diffusion component of electrochemical potential. For this reason, the version (6), for example, together with (12) leads to the following definition or the perturbation of the electron density $\delta\nu$ on the Hall plateau:

$$eV\ln\left(\frac{r}{r_0}\right)\Big/\ln\left(\frac{r_1}{r_0}\right)=-T\ln S(1+\delta\nu)/\ln S(1),$$
$$\delta\nu\ll 1, \quad eV<T, T>\Gamma, \tag{15}$$

The inequality $T>\Gamma$ allows us to combine the assumptions concerning the ideality of a $2D$ system and the finiteness of conductance.

The smallness of perturbation (15) of the electron density on the Hall plateau under the action of external effects is a typical general property of magnetized $2D$ systems. Such properties lead to the formation of well-known ''incompressible'' bands in equilibrium inhomogeneous $2D$ electron systems in the presence of local points with an integral filling factor on the electron density profile (see Refs. 14–16). The same properties of a $2D$ system on the Hall plateau are responsible for the well-known features of magnetocapacitance of such systems.[17]

The behavior of $\delta\nu$ for ''dirty'' $2D$ systems is determined by formulas (7) and (12). We are speaking of

qualitatively the same density perturbation scales as in (15) if the role of temperature is played by the parameter Γ.

Thus, Ohm's law on the Hall plateau is similar to (11), but the current J is mainly of diffusion origin, and the electric potential φ along the Corbino disk remains virtually at zero point. In other words, the situation justifying the application of the μ- representation for an analysis of the IVC on the Hall plateau takes place. This statement is also valid for the region $T<eV<\hbar\omega_c$ (this will be used below). A considerable difference between (2) and (2a) in favor of (2) is also obvious.

3. $T<eV<\hbar\omega_c$. In the μ-representation, the general problem on the IVC for a Corbino disk splits into two parts. At first, we can determine the behavior of $\mu(r)$ with the help of relations (2), (3) and (5). Then we can easily find $\delta\nu(r)$ and $\varphi(r)$ by using (6) or (7) as well as (9).

On the basis of (2), (3), and (5), we can write

$$\delta\mu(x)=t\,\mathrm{Arcsinh}\left[\sinh\left(\frac{\delta\mu_0}{t}\right)\left(1-\frac{\ln x}{\ln q}\right)+\sinh\left(\frac{\delta\mu_0+v}{t}\right)\left(\frac{\ln x}{\ln q}\right)\right],$$

$$q=r_1/r_0,\quad x=r/r_0, \tag{16}$$

$$\delta\mu_0=\mu_0-1=-1/2-t\ln S(\nu_0),\quad \delta\mu_0(\nu_0=1)=0,$$

$$t=T/\hbar\omega_c,\quad 1\leqslant x\leqslant q. \tag{16a}$$

The definition (16a) of $\delta\mu_0$ through the filling factor ν_0 is chosen for convenience. The value of ν and the combination $t\ln S(\nu_0)$ are given by formulas (6), and the expression (16a) for $\delta\mu_0$ is valid if we are dealing with phenomena in the vicinity of the Landau ground level, i.e., for $\nu<2$. The integral filling of the level with $\nu=1$ makes $\delta\mu_0$ equal to zero.

The relation between the current J and voltage V has the form

$$j/t=\left[\sinh\frac{\delta\mu_0+v}{t}-\sinh\frac{\delta\mu_0}{t}\right],\quad j=\frac{eJe^{+\Delta/T}\ln q}{2\pi\sigma_0\hbar\omega_c}. \tag{17}$$

Naturally the general formulas (16) and (17) for small V ($eV<T<1$) are transformed into the ohmic formulas (11) and (12).

It follows from expression (16) that the distribution of $\delta\mu$ along the direction of current changes noticeably with increasing v as compared to the logarithmic nonlinearity which is usually observed in the ohmic region [see formula (12)]. Here, the degree of nonlinearity is determined by the ratio eV/T, i.e., can be quite high even in the region $eV<\hbar\omega_c$. For example, Figs. 1a, 1b and 1c show the results obtained for $\delta\mu(x)$ for various initial values $\delta\mu_0$, the reaction of $\delta\mu(x)$ to the change in v for a fixed t, as well as the distribution of $\delta\mu(x)$ for given $\delta\mu_0, v$ and different values of t.

Obviously, if we ''start'' from the unit filling factor, the gradient of $\delta\mu$ has the maximum value at the origin (curve *1*). As the value of ν_0 decreases, the system first approaches the region with the unit filling factor and only then increases the gradient of $\delta\mu$ (curves *2–4*).

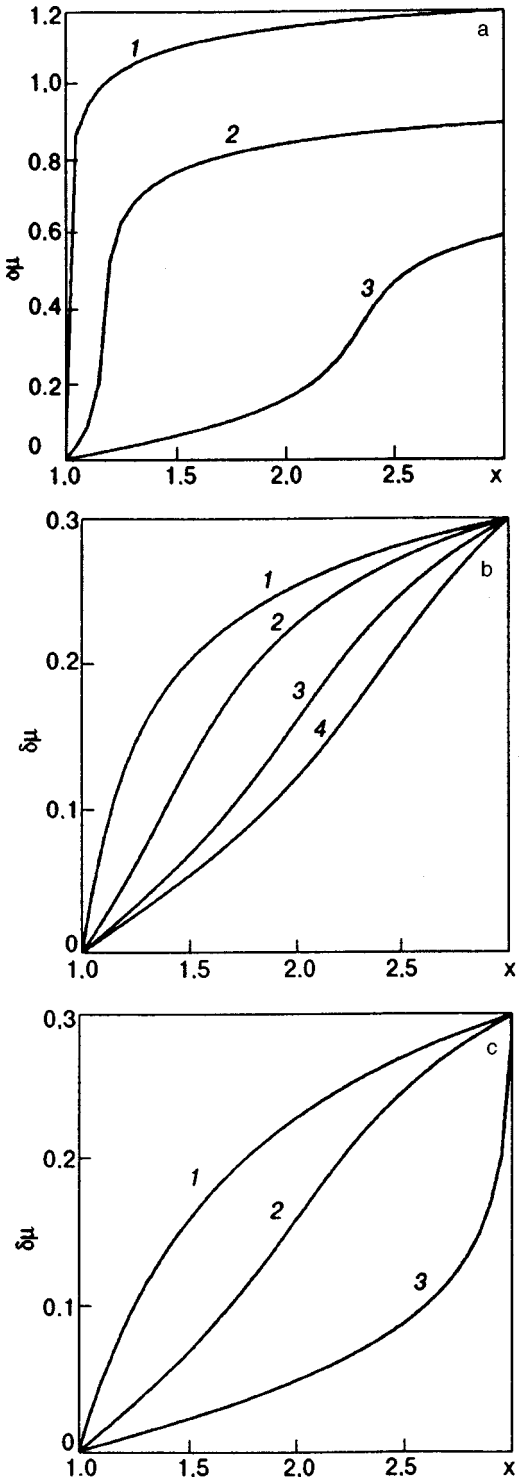

FIG. 1. Dependences $\delta\mu(x)$ (16) for fixed $\nu_0=0.8$, $t=0.1$, $q=3$ for different values of v: 0.6 (curve *1*), 0.8 (curve *2*), and 1.2 (curve *3*) (a); for fixed $v=0.3$, $t=0.1$, $q=3$ for different values of ν_0: 1.0 (curve *1*), 0.98 (curve *2*), 0.96 (curve *3*), and 0.94 (curve *4*) (b), for fixed $v=0.3$, $\nu_0=0.96$, and $q=3$ for different values of t: 0.2 (curve *1*), 0.1 (curve *2*), and 0.05 (curve *3*) (c).

Using formulas (16), we can find the dependence $\nu(x)$, and hence $\varphi(x)$ also, with the help of (6), (9), and (16). The relevant data for $\mu(x)$ and $\nu(x)$ are shown in Figs. 2a and 2b. The value of φ can then be estimated with the help of (9) or

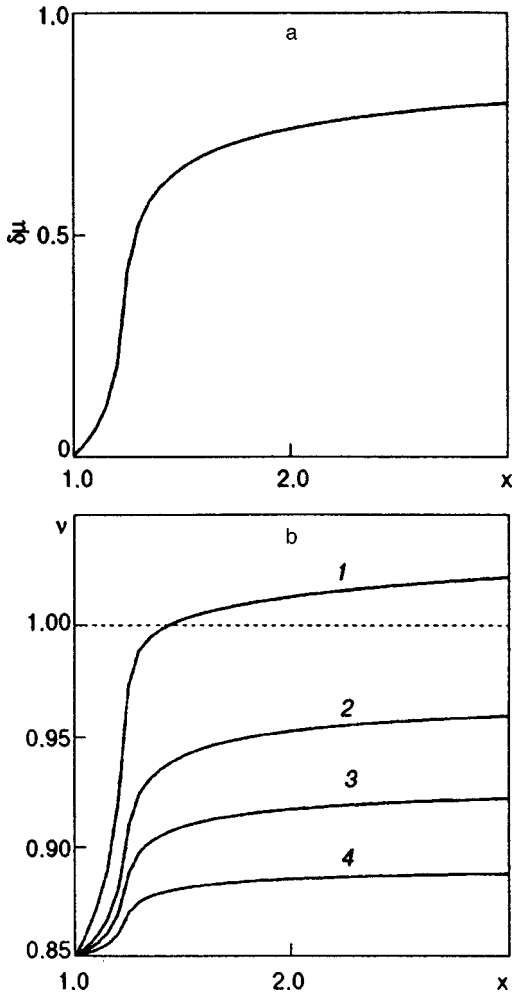

FIG. 2. Examples of behavior of $\delta\mu(x)$ from (16) and corresponding values of $\nu(x)$ from (6), (9), and (16) for the μ-model of conductance: $\delta\mu(x)$ from (16) for $\delta\mu_0=0.85$, $t=0.1$, $\upsilon=0.8\,(a)$, $\nu(x)$ from (6), (9), and (16) for $\delta\mu(x)$ from (16) and Fig. 2a; curves *1–4* correspond to different values of d: 1 (curve *1*), 3 (curve *2*), 5 (curve *3*) and 10 (curve *4*).

$$\psi(x)=e\varphi(x)/\hbar\omega_c\simeq 2d_*(\nu-\nu_0),\quad d_*=d/a_B^*. \tag{18}$$

A comparison of the quantities $\delta\mu\sim 1$ (see Fig. 2a), $\delta\nu\sim 0.1$ (see Fig. 2b), and $\psi\sim 0.1$ [see formula (18) for $d_*\geqslant 1$] readily shows that

$$\delta\mu\gg\psi, \tag{18a}$$

i.e., the conditions for the existence of the μ-representation (3) are fulfilled indeed. Such a situation is conserved up to $\upsilon\leqslant 1$.

4. In the region $\upsilon>1$, the electric potential is not small any longer. As a result, we have to deal with ζ from (4) and not with the μ-representation of conductance from (3). A formal consequence of these changes is the impossibility of uncoupling the system of equations in μ, φ, and ν into separate blocks [as was done for calculating $\delta\mu$ in (16)]. We shall solve this system below by using successive iterations starting from the ohmic limit (10)–(12) for $\delta\mu_0$ and the corresponding distribution $\nu_0(x)$ following from Eqs. (6) and (6a) with the left-hand side from (12). A formal basis for such a method of solution of the problem is the analogy with the problem of integral channels under nonhomogeneous equilibrium conditions. Chklovskii *et al.*[14,15] proved that the ''shelves'' in the electron density distribution can be calculated by solving first the problem on the density distribution in a magnetic field, and then the parameters of integral ''shelves'' in the magnetic can be calculated as a consequence of perturbation in the zeroth approximation. In our case, the role of the zeroth approximation leading to the loss of spatial homogeneity of the electron system is played by the solution of the problem (10)–(12). Then the definition of electrochemical potential (6) and (6a) responsible for the emergence of flattenings in the electron density distribution comes into play. The examples of the behavior of $\nu_0(x)$ in the framework of this program are presented in Figs. 3a and 3b. Among other things, the formation of the integral channel in the middle of the Corbino disk and the dependence of its characteristics on various extrinsic parameters can be seen clearly.

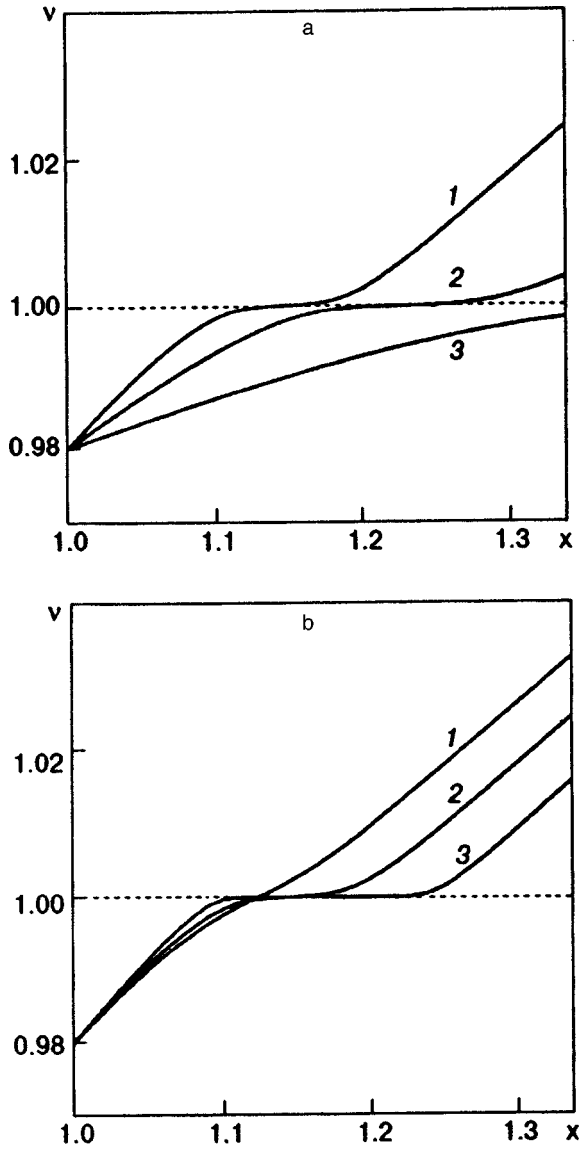

FIG. 3. Dependence of the filling factor ν on x for $\upsilon=1.5$, $d_*=10$, $\nu_0=0.98$ and different values of t: 0.075 (curve *1*), 0.05 (curve *2*), and 0.025 (curve *3*) (a); for $d_*=10$, $t_*=0.05$, $\nu_0=0.98$ and different values of υ: 1.5 (curve *1*), 1.0 (curve *2*), and 0.5 (curve *3*) (b).

It is convenient to present the data on the next iteration in the form of the ratio of the first approximation to the zeroth approximation for the same values of the total current j. For example, the nonlinear deviation

$$\delta v = v(j)/v_0(j) \tag{19}$$

from Ohm's law (11) can be written in the form

$$\delta v = \frac{1}{\ln q}\int_1^q \frac{dx\cosh[-1/2t-\ln S(\nu_0)]}{x\cosh[-1/2t-\ln S(\nu_0(x))]},$$

$$q = r_1/r_0, \tag{20}$$

$$v\frac{\ln x}{\ln q} = 2d_*[\nu_0(x)-\nu_0]-t\ln\frac{S(\nu_0(x))}{S(\nu_0)}. \tag{20a}$$

Here $\nu_0(x)$ is the electron density distribution in the zeroth approximation following from equation (20a). Such representations are presented schematically in Figs. 3a and 3b.

The final results for δv from (20) are shown in Figs. 4a and 4b. It should be noted that the results presented in Fig. 4 indicate the roughness of approximation (20) since the iteration possesses the required property (relation (20) slightly deviates from unity) only in the vicinity of $\nu_0 = 1$. The main reason behind this roughness is the actual rearrangement of fields in the disk as a result of formation of the integral channel. In this respect, the steady-state problem differs from the equilibrium problem in which the formation of a channel perturbs the problem only in the vicinity of the channel.

DISCUSSION OF RESULTS

Let us sum up the obtained results. We studied the linear region and weakly nonlinear effects in the IVC structure for a $2D$ electron Corbino disk with a magnetic field normal to its surface under the conditions corresponding to the emergence of QHE.

In the linear (ohmic) mode, the statement concerning the diffusive nature of the passing current is most remarkable. The electrostatic potential does not participate in sustaining the current, and this prediction can be verified directly with the help of the linear electrooptical effect.[13]

The initial premise for the evolution of weak nonlinearities of IVC is the loss of spatial homogeneity in the $2D$ system carrying current even if this system was perfectly homogeneous in equilibrium. Anomalous evolution of current nonuniformities under the conditions of QHE against the background of a linear or logarithmic increase in electron density, which are always observed in any $2D$ system with current, occurs through two channels. One of them is typical of $2D$ systems with a filling factor close to an integer. We are speaking of the tendency of a $2D$ system to oppose external perturbations leading to a change in the integral filling factor. This circumstance also takes place in equilibrium problems, being the main reason behind anomalies in magnetocapacitance of $2D$ systems and creating ''incompressible'' strips in nonhomogeneous systems. The presence of current modifies the parameters of such strips or leads to conditions required for their formation. This process can easily be simulated under the assumption that Ohm's law (2) is valid for uniform conductance. In this case, the electron

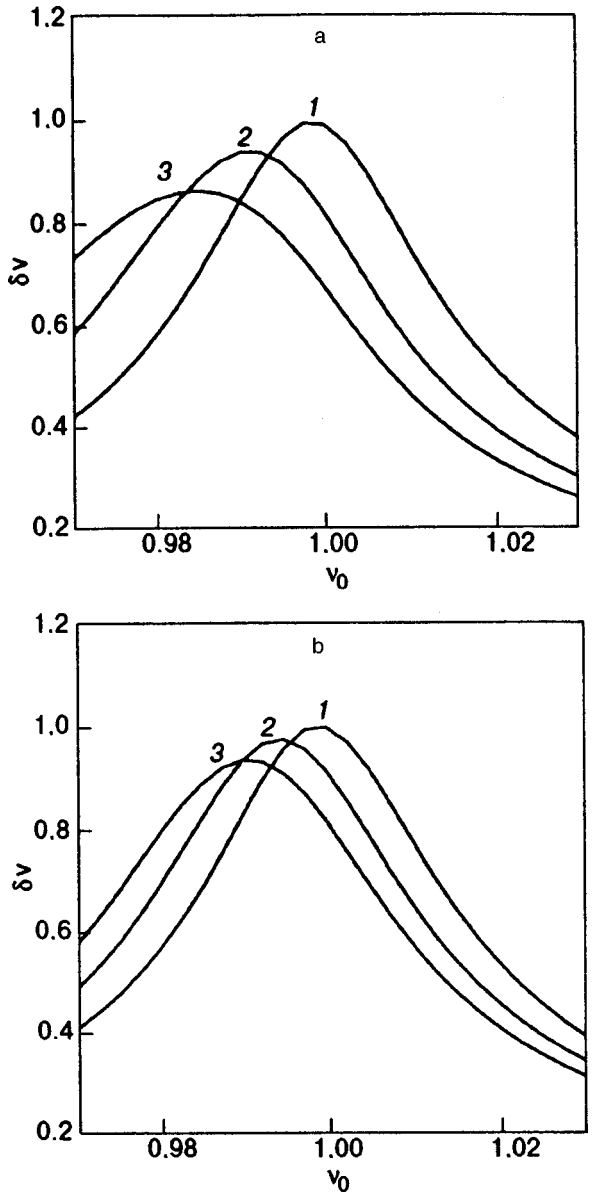

FIG. 4. Dependence of δv on ν_0 from (20) for $t = 0.1$ and different values of v: 0.05 (curve *1*), 0.3 (curve *2*), and 0.5 (curve *3*) for $d_* = 5$ (a) and 10 (b).

density distribution in a Corbino disk with current displays clearly manifested ''shelves'' with a geometry determined by extrinsic parameters (see Figs. 3a and 3b).

As the value of v increases, the other channel, viz., nonlinear sensitivity of conductance to μ or ζ on Hall's plateaus discovered for the first time in Refs. 7 and 8 comes into ''play.'' In actual practice, however, both nonlinearity channels are interconnected. The form of this relation are different in different intervals of voltage V. The corresponding features of IVC and electric potential distribution are given by formulas (15)–(19). We shall mention some of them. First, relation (17) between the parameters v and $\delta\mu_0$ for a fixed j has a peak which loses its symmetry relative to the point $\delta\mu_0 = 0$ with increasing j. The shift Δv relative to its position corresponding to small currents is given by the formula

$$\Delta v = v_{\max}/2, \tag{21}$$

where, according to (17), the maximum value $v_{\max}$ is a nonlinear function of the current j (the second nonlinear effect):

$$v_{\max} = 2t \ \ \mathrm{Arcsinh}(j/2). \tag{22}$$

Both effects are accessible to experimental verification.

Considering the available experimental data on nonlinear properties of IVC on the Hall plateau, we note above all that the experiments were mainly made on samples with rectangular geometry (see Refs. 1–6, 9, and 10), in which the breakdown of QHE is of the jump type. As regards the Corbino geometry, we are aware only of more or less systematic results[8] obtained under the conditions $v \gg 1$ as well as those from Ref. 18 (again with $v \gg 1$) related indirectly to the problem under consideration. According to these results, Corbino samples demonstrate IVC nonlinearity of the type (22). Besides, the effect (21) is also observed on the scale determined by this formula. However, we cannot state that the results or our calculations are similar quantitatively to the data presented in Ref. 8 since the range $v \gg 1$ used in Ref. 8 was not investigated by us in actual practice.

This research was partly financed in the framework of the program ''Physics of Solid Nanostructures,'' Grant No. 97-1059, and supported by the Russian Foundation of Fundamental Research, Grant No. 98 02 16 640.

*E-mail: shikin@issp.ac.ru

[1] G. Ebert, K. von Klitzing, K. Ploog, and G. Weimann, J. Phys. C **16**, 5441 (1983).
[2] M. E. Cage, R. F. Dziuba, B. F. Field *et al.*, Phys. Rev. Lett. **51**, 1374 (1983).
[3] O. Heinonen, P. Taylor, and S. Girvin, Phys. Rev. B **30**, 3016 (1984).
[4] P. Streda and K. von Klitzing, J. Phys. C **17**, 483 (1984).
[5] S. Komiyama, T. Takkumasu, S. Hiamizu, and S. Sasa, Solid State Commun. **54**, 479 (1985).
[6] Ch. Cimon, B. B. Goldberg, F. Fang *et al.*, Phys. Rev. B **33**, 1190 (1986).
[7] M. G. Gavrilov and I. V. Kukushkin, Pis'ma Zh. Éksp. Teor. Fiz. **43**, 79 (1986) [JETP Lett. **43**, 103 (1986)].
[8] A. A. Shashkin, V. T. Dolgopolov, and S. I. Dorozhkin, Zh. Éksp. Teor. Fiz. **91**, 1897 (1986) [Sov. Phys. JETP **64**, 1124 (1986)].
[9] S. Kawaji, K. Hirakawa, and M. Nagata, Physica B **184**, 17 (1993).
[10] N. Q. Balaban, U. Meirav, H. Shtrikman, and Y. Levinson, Phys. Rev. B **26**, 3648 (1983).
[11] M. I. Dyakonov and F. G. Pikus, Solid State Commun. **83**, 413 (1992).
[12] S. I. Iordanskii and B. A. Muzykantskii, Zh. Éksp. Teor. Fiz. **103**, 2116 (1993) [JETP **76**, 1055 (1993)].
[13] W. Dietsche, K. von Klitzing, and K. Ploog, Surf. Sci. **361**, 289 (1996).
[14] D. B. Chklovskii, B. I. Shklovskii, and L. I. Glazman, Phys. Rev. B **46**, 4026 (1992).
[15] D. B. Chklovskii, K. F. Matveev, and B. I. Shklovskii, Phys. Rev. B **47**, 12605 (1993).
[16] D. B. Chklovskii and P. Lee, Phys. Rev. B **48**, 18050 (1993).
[17] V. B. Shikin and S. S. Nazin, Fiz. Nizk. Temp. **20**, 658 (1994) [Low Temp. Phys. **20**, 515 (1994)].
[18] V. T. Dolgopolov, A. A. Shashkin, N. V. Zhitenev *et al.*, Phys. Rev. B **46**, 12560 (1992).

Translated by R. S. Wadhwa

QUANTUM EFFECTS IN SEMICONDUCTORS AND DIELECTRICS

Surface magnetic-plasma waves at the ferrodielectric–semiconductor boundary

V. L. Fal'ko, S. I. Khankina, and V. M. Yakovenko

*Institute of Radiophysics and Electronics, National Academy of Sciences of the Ukraine, 310085 Kharkov, Ukraine**

(Submitted September 11, 1998)
Fiz. Nizk. Temp. **25**, 195–200 (February 1999)

The electromagnetic properties of the ferrodielectric–conducting medium system are investigated in a constant magnetic field at low temperatures. It is shown that new vibrational branches, viz. pseudosurface waves characterized by collisionless damping, emerge in a strong magnetic field at sufficiently high concentrations of charge carriers. The mechanism of collisionless (radiative) damping is connected with the existence of additional electromagnetic fields propagating into the bulk of the conducting medium. The range of such waves is determined, and the functional dependences of their frequency and damping on the magnitude and direction of the external magnetic field are derived. © *1999 American Institute of Physics.* [S1063-777X(99)01002-6]

1. It is well known that oscillations of various types including magnetic polaritons, magnetostatic oscillations, and coupled waves can exist on the surface of magnets.[1–3] The propagation of these waves is determined by the properties of a magnet as well as the medium in contact with it.

The dependence of frequency and damping of surface waves on the properties of magnetic medium (permeability, the presence of conduction electrons, gyroanisotropy, etc.) has been studied extensively. These effects were analyzed in the review by Kaganov *et al.*[3] in which the electromagnetic properties of a magnet in contact with vacuum are investigated. It is shown that the dispersion in the spectrum of surface oscillations is determined by different physical mechanisms: the frequency- and spatial dispersion of permeability and permittivity tensor components and delay effects in the magnet. The inclusion of delay leads not only to the dependence of frequency on the wave vector, but also to attenuation of a nonmagnetic origin. It depends on the wave vector and the dissipative component of permittivity.

The influence of electromagnetic properties of the medium bordering a magnet on surface magnetic oscillations has been studied less extensively. It should be noted that surface waves at the magnetically active plasma–vacuum interface in radio frequency region exhibit a number of interesting peculiarities.[4] For this reason, an analysis of the properties of electromagnetic waves at the ferrite–magnetically active plasma interface is undoubtedly of primary importance. Such a composition leads to the formation of new branches of oscillations as a result of interaction between fields and conduction electrons. For instance, coupled surface helicon–spin waves emerge in the ferrite–superconductor structure in a strong magnetic field.[5] The coupling parameter for these waves was found to be of the order of unity, leading to a considerable change in the frequency and damping of oscillations.

In this communication, the interaction of surface magnetic oscillations with eigen electromagnetic oscillations of the conducting medium is investigated in a ferrodielectric–semiconductor system at low temperatures in the frequency range in which surface helicons do not exist. In a strong magnetic field, this interaction leads to a change in the frequency of magnetic surface waves if delay effects in the superconductor are significant. It was found that the frequency dispersion of magnetic oscillations in this case can be stronger than the dispersion associated with delay effects in the magnet. Moreover, attenuation of collisionless type is observed when surface waves propagate at an angle $\theta \neq \pi/2$ to the direction of a constant magnetic field. This is due to the existence in the magnetically active plasma of the semiconductor of partial electromagnetic waves removing the energy of the field from the boundary. The dispersion and damping are determined by macroscopic parameters of the magnet, the magnitude and direction of the magnetic field, and the charge carrier concentration in the semiconductor.

2. Let a ferromagnetic dielectric occupy the half-space $y>0$ (medium ''1'') and a semiconductor fill the region $y<0$ (medium ''2''). The external constant magnetic field $\mathbf{H}_0$ and the magnetic moment $\mathbf{M}$ are directed along the z-axis.

The electromagnetic properties of the ferromagnetic dielectric are described by the equations of magnetostatics and equations of motion of magnetic moment. Assuming that the dependence of all the variables on coordinates and time is proportional to $\exp[i(\mathbf{k}\cdot\mathbf{r}-\omega t)]$, we can find from these equations the relation between the wave vector $\mathbf{k}$ and frequency ω:

$$\mu_{ij}(\omega)k_i k_j = 0. \tag{1}$$

If the constant magnetic field $\mathbf{H}_0$ is directed along the anisotropy axis, the permeability tensor components $\mu_{ij}(\omega)$ in the absence of spatial dispersion have the form

$$\mu_{xx}=\mu_{yy}=\mu=1+\frac{\omega_g\omega_M}{\omega_g^2-\omega^2};$$

$$\mu_{xy}=-\mu_{yx}=\frac{i\omega\omega_M}{\omega_g^2-\omega^2};\quad \mu_{zz}=1;$$

$$\mu_{xz}=\mu_{zx}=\mu_{yz}=\mu_{zy}=0;$$

$$\omega_g=g(H_0+\beta M);\quad \omega_M=4\pi gM, \tag{2}$$

where g is the magnetomechanical ratio and β the anisotropy constant. It follows from (1) that

$$k_y^2=-k_x^2-k_z^2/\mu; \tag{3}$$

$\mathrm{Im}\,k_y>0$ being the emission condition for $y\to 0$. Henceforth, we assume that $k_x^2\gg k_z^2/\mu$, i.e., the wave propagates at an angle to the magnetic field. The components of the varying magnetic field in the wave (3) are connected through the relation

$$H_x=\frac{k_x}{k_y}H_y;\quad H_z=\frac{k_z}{k_y}H_y. \tag{4}$$

Electromagnetic fields in a conducting medium can be described by Maxwell's equations and the equations of motion for conduction electrons. The wave vectors of transverse waves can be found from the relation

$$\varepsilon_{xx}(k_x^2+k_y^2)^2+\left[(\varepsilon_{xx}+\varepsilon_{zz})\left(k_z^2-\frac{\omega^2}{c^2}\varepsilon_{xx}\right)-\frac{\omega^2}{c^2}\varepsilon_{xy}^2\right]$$
$$+\left(k_z^2-\frac{\omega^2}{c^2}\varepsilon_{xx}\right)^2\varepsilon_{zz}+\frac{\omega^4}{c^4}\varepsilon_{xy}^2\varepsilon_{zz}=0, \tag{5}$$

where the permittivity tensor components $\varepsilon_{ik}(\omega)$ in a one-component plasma in a strong magnetic field ($\omega_H\gg\omega,\nu$) are defined as

$$\varepsilon_{xx}=\varepsilon_{yy}=\varepsilon_0+\frac{\omega_0^2(\omega+i\nu)}{\omega\omega_H^2},$$

$$\varepsilon_{xy}=-\varepsilon_{yx}=\frac{i\omega_0^2}{\omega\omega_H},\quad \varepsilon_{zz}=\varepsilon_0-\frac{\omega_0^2}{\omega(\omega+i\nu)}. \tag{6}$$

Here ε_0 is the dielectric constant of the semiconductor lattice, and $\omega_H=eH_0/mc$; $\omega_0^2=4\pi e^2n_0/m$; e,m,n_0,ν are the charge, effective mass, equilibrium concentration, and effective frequency of collisions of charge carriers, respectively. We introduce the angle θ between the magnetic field direction (z-axis) and the projection of the wave vector on the xz plane ($k_x=k\sin\theta$, $k_z=k\cos\theta$).

The dispersion equation for surface magnetic waves can be derived from the boundary conditions for fields at the interface $y=0$ between the media. Such conditions are the continuity of the normal component of the magnetic induction vector and the continuity of the tangential components of the varying magnetic field:

$$H_y^{(2)}=B_y^{(1)}=\mu H_y^{(1)}+\mu_{yx}H_x^{(1)}\big|_{y=0},$$

$$H_x^{(1)}=H_x^{(2)}\big|_{y=0},\quad H_z^{(1)}=H_z^{(2)}\big|_{y=0}. \tag{7}$$

3. Let us first analyze the peculiarities of a magnetic wave in the simple case when the H-wave propagates at right angles to the vector $\mathbf{H}_0$ and $\mathbf{M}$ ($\theta=\pi/2$). The depth of penetration of this wave into the semiconductor is determined by the quantity $l=|k^2-(\omega^2/c^2)\varepsilon_{zz}|^{-1/2}$, and the energy–momentum relation has the form

$$\mathrm{sgn}\,k_x\omega+\omega_g+\frac{\omega_M}{2}=-\frac{\omega_0^2(\omega-i\nu)}{2c^2\omega^2\omega_M}\frac{1}{k^2}$$
$$\times(\mathrm{sgn}\,k_x\omega+\omega_g+\omega_M)^2. \tag{8}$$

The solution of this equation exists only for $k_x<0$. In the region of small values of wave numbers k ($k^2\ll\omega_0^2\omega/c^2|\omega+i\nu|$), the frequency of a surface magnetic wave is given by

$$\omega=\omega_1\equiv\omega_g+\omega_M. \tag{9}$$

Delay effects in the conducting medium lead to frequency dependence of the wave vector $\mathbf{k}$ (to dispersion $\delta\omega$) and damping $\gamma=-\mathrm{Im}\,\omega$:

$$\delta\omega(k)=\frac{\omega_Mkc}{\omega_0}\mathrm{Re}\left(1+i\frac{\nu}{\omega_1}\right)^{1/2},$$

$$\gamma=\frac{\omega_Mkc}{\omega_0}\mathrm{Im}\left(1+i\frac{\nu}{\omega_1}\right)^{1/2}. \tag{10}$$

For large values of k ($k^2\gg\omega_0^2\omega/c^2|\omega+i\nu|$), a wave with Damon–Eshbach frequency[2] propagates along the interface:

$$\omega=\omega_2\equiv\omega_g+\frac{\omega_M}{2}. \tag{11}$$

Its dispersion $\delta\omega$ and damping γ are given by

$$\delta\omega=\frac{\omega_M}{8}\frac{\omega_0^2}{k^2c^2}, \tag{12}$$

$$\gamma=\frac{\omega_M}{8}\frac{\omega_0^2\nu}{k^2c^2\omega_2}. \tag{13}$$

It should be noted that a surface wave with frequency (11) emerges in the structure ferromagnet–vacuum[3] for wave numbers $k\gg\omega_2/c$, and its dispersion caused by delay effects in the ferromagnet is $\Delta\omega_2=-\omega_M\omega_2^2(1+\varepsilon)/8k^2c^2$ (ε is the permittivity of the ferromagnet). In the structure under investigation, the wave (11)–(13) propagates for $k\gg\omega_0/c\gg\omega_2/c$. It can easily be verified that the change in its frequency (12) is much larger than $|\Delta\omega_2|$.

In the above geometry, attenuation is determined by the dissipative component of the permittivity of the semiconductor.

4. Let us analyze waves propagating along the boundary between the media at an arbitrary angle to the vector $\mathbf{H}_0$ ($\theta\neq\pi/2$). We consider the frequency range in which the following conditions hold:

$$\omega\ll\omega_H,\quad \omega_0/\sqrt{\varepsilon_0}, \tag{14}$$

i.e.,

$$|\varepsilon_{zz}|\gg|\varepsilon_{xy}|\gg|\varepsilon_{xx}|$$

and

$$k_z^2 \gg (\omega^2/c^2)\varepsilon_{xx}. \tag{15}$$

Then it follows from Eq. (5) that two waves (extraordinary and ordinary) existing in the conducting medium satisfy respectively the following conditions:

$$k_{y1}^2 = -(k_x^2+k_z^2) - \frac{\omega^4}{c^4 k_z^2}\varepsilon_{xy}^2, \quad \operatorname{Im} k_{y1} < 0, \tag{16}$$

$$k_{y2}^2 = -k_z^2 \frac{\varepsilon_{zz}}{\varepsilon_{xx}}, \quad \operatorname{Im} k_{y2} < 0. \tag{17}$$

Since $|k_{y2}| \gg k_x$, the characteristics of propagation of these waves differ strongly, and the components of their fields are connected through the relations

$$H_{x1} = -\frac{k_x k_{y1} + (\omega^2/c^2)\varepsilon_{yx}}{k_x^2+k_z^2} H_{y1},$$

$$H_{z1} = \frac{k_x(\omega^2/c^2)\varepsilon_{yx} - k_{y1}k_z^2}{k_z(k_x^2+k_z^2)} H_{y1},$$

$$E_z \approx 0, \quad E_{x1} = \frac{\omega}{k_z c} H_{y1},$$

$$E_{y1} = \frac{\omega}{k_z c} \frac{[k_x k_{y1} + (\omega^2/c^2)\varepsilon_{yx}]}{k_x^2+k_z^2} H_{y1}; \tag{18}$$

for the extraordinary wave and

$$H_{x2} = -\frac{k_{y2}}{k_x} H_{y2}, \quad H_{z2} = -\frac{\varepsilon_{xy}}{\varepsilon_{xx}} H_{y2}, \quad E_{y2} = \frac{k_{y2}}{k_x} E_{x2},$$

$$E_{x2} = \frac{k_z c}{\omega \varepsilon_{xx}} H_{y2}, \quad E_z = \frac{k_z^2}{k_x \varepsilon_{xx}} \frac{c}{\omega} H_{y2}. \tag{19}$$

for the ordinary wave.

Let us analyze different types of semiconductors with an isotropic energy–momentum relation for charge carriers. In some of them, the displacement current is smaller than the conduction current, and the following condition holds:

$$|\varepsilon_{zz}\varepsilon_{xx}| \approx |\varepsilon_{xy}^2|; \quad \varepsilon_0 \ll \frac{\omega_0^2|\omega + i\nu|}{\omega_H^2 \omega}. \tag{20}$$

(It should be noted that this condition rules out the propagation of a surface helicon.[4,5])

Semiconductors of the second type are characterized by a relatively low electron concentration, and the main contribution to the component ε_{xx} comes from displacement current. In other words, the following inequalities hold:

$$\frac{\omega_0^2}{\omega|\omega + i\nu|} \gg \varepsilon_0 \gg \frac{\omega_0^2|\omega + i\nu|}{\omega_H^2 \omega}. \tag{21}$$

In semiconductors with a high charge carrier concentration, we have $k_{y2} = k_z \omega_H(\omega - i\nu)/(\omega^2+\nu^2)$. The simultaneous fulfillment of the conditions $k_{y2}^2 \gg k_x^2$ and (3) indicates that in this case the wave propagates in the interval of angles whose magnitude is determined by the constant magnetic field H_0:

$$\frac{1}{\mu} \ll \tan^2\theta \ll \frac{\omega_H^2}{\omega^2}. \tag{22}$$

The dispersion relation for these waves has the form

$$\frac{\omega_g + \omega_M + (\operatorname{sgn}\sin\theta)\omega}{\omega_g + (\operatorname{sgn}\sin\theta)\omega} = -\frac{1}{|\sin\theta|\cos\theta}\left\{ i\frac{\omega_0^2\omega}{k^2c^2\omega_H} \pm \left[\cos^2\theta + \frac{2\omega_0^2\omega(\omega + i\nu)}{k^2c^2\omega_H^2}\sin\theta(i\cos\theta - \sin\theta) - \frac{\omega_0^4\omega^2}{k^4c^4\omega_H^2}\right]^{1/2}\right\}. \tag{23}$$

Let us consider the limiting cases:

$$|\cos\theta| \gg \frac{\omega_0^2\omega}{k^2c^2\omega_H}, \quad \frac{\omega_0|\omega(\omega + i\nu)|^{1/2}}{kc\omega_H}, \tag{24}$$

$$\frac{\omega_0|\omega(\omega + i\nu)|^{1/2}}{kc\omega_H} \ll |\cos\theta| \ll \frac{\omega_0^2\omega}{k^2c^2\omega_H}. \tag{25}$$

When inequalities (24) are satisfied, we can easily obtain from Eq. (23) the frequency of the surface wave propagating only in the range of angles $-\pi/2 < \theta < 0$, i.e., only in the negative of the x-axis (nonreciprocity effect):

$$\omega(\theta) = \omega_g + \omega_M \frac{|\sin\theta|}{1+|\sin\theta|}. \tag{26}$$

The delay effects in the semiconductor lead to the dispersion of frequency (26) and to damping of the form

$$\delta\omega = \omega_M \frac{\omega_0^2\omega^2(\theta)|\sin\theta|^3}{k^2c^2\omega_H^2\cos^2\theta(1+|\sin\theta|)^2}, \tag{27}$$

$$\gamma = \omega_M \frac{\omega_0^2\omega(\theta)|\sin\theta|}{k^2c^2\omega_H\cos\theta(1+|\sin\theta|)^2}. \tag{28}$$

In contrast to the Damon–Eshbach wave (11)–(13), damping (28) is of the collisionless type. The mechanism of its emergence is connected with the following factors. One of partial waves in the semiconductor, viz., the wave with the component k_{y2}, is a bulk wave in the high-frequency range ($\omega \gg \nu$) under the conditions (20). (The other partial wave is a surface wave for which $k_{y1} = -ik|\sin\theta|$.) The fields whose amplitudes decrease exponentially on both sides of the boundary plane between the media are transformed at the boundary into the field of a wave propagating to the bulk of the semiconductor and removing a part of energy.

When inequality (25) is satisfied, the partial wave with component k_{y1} defined as

$$k_{y1} = -\frac{\omega\omega_0^2}{\omega_H kc^2\cos\theta}\left(1 + i\frac{\omega\nu}{\omega_H^2}\right), \tag{29}$$

is also a bulk wave propagating in the conducting medium for arbitrary relations between the frequencies ω and ν.

In this case, the frequency of the surface wave is given by

$$\omega=(\omega_g+\omega_M)(1-\omega_M/\omega_H), \tag{30}$$

and its dispersion and collisionless damping are defined as

$$\delta\omega=-\frac{k^4c^4\omega_H^2\omega_M}{4\omega_0^4\omega_1^2}\cot^2\theta, \tag{31}$$

$$\gamma=\frac{k^2c^2\omega_H\omega_M}{2\omega_0^2\omega_1}\cot\theta, \tag{32}$$

where the frequency ω_1 is defined in (9).

Conditions (24) and (25) imply that if the charge carrier concentration in the semiconductor is such tat $\omega_0/kc<1$, a surface wave of only one type (26)–(28) is formed. For a high concentration, when $\omega_0/kc>1$, but the inequality $\omega_0^2\omega/k^2c^2\omega_H<1$ is observed, both types of waves (26)–(28) and (30)–(32) exist. These waves can be observed by varying the angle θ. Finally, when $1<\omega_0^2\omega/k^2c^2\omega_H$ only the wave (30)–(32) propagates.

For a low concentration (see (21)), surface waves exist at the magnet–semiconductor interface in the range of angles defined by the inequalities

$$\frac{1}{\mu}\ll\tan^2\theta\ll\frac{\omega_0^2}{\omega|\omega+i\nu|\varepsilon_0}. \tag{33}$$

In contrast to (22), the upper boundary of the angular interval (33) is determined by the conduction electron concentration and does not depend on the external magnetic field.

Expression (17) for k_{y2}, which has the form

$$k_{y2}^2=k_z^2\frac{\omega_0^2(\omega-i\nu)}{\varepsilon_0\omega(\omega^2+\nu^2)} \tag{34}$$

under conditions (21), does not depend on the magnetic field either. For $\omega\gg\nu$, it follows from (34) that the ordinary wave is a bulk wave.

As before, surface waves propagate only in the negative direction of the x-axis. Since their dispersion equation is quite cumbersome, we shall give analytic expressions for frequency, dispersion, and damping only in the limiting cases:

$$|\cos\theta|\gg\frac{\omega_0^2\omega}{k^2c^2\omega_H},\quad \frac{\omega}{kc}\sqrt{\varepsilon_0}, \tag{35}$$

$$\frac{\omega}{kc}\sqrt{\varepsilon_0}\ll|\cos\theta|\ll\frac{\omega_0^2\omega}{k^2c^2\omega_H}. \tag{36}$$

If inequalities (35) are satisfied, the surface magnetic wave with frequency (26) is characterized by the following values of $\delta\omega$ and γ:

$$\delta\omega=\frac{\omega_M\omega_0^2\omega(\theta)}{4k^2c^2\omega_H}\frac{1}{\cos^2\theta}, \tag{37}$$

$$\gamma=\frac{\omega_M\omega_0^3\omega(\theta)}{4k^2c^2\omega_H^2\sqrt{\varepsilon_0}}\frac{|\sin\theta|}{\cos^3\theta}. \tag{38}$$

In the case (36), the dispersion and damping for a wave of frequency ω_1 (9) are given by

$$\delta\omega=-\frac{\omega_M\omega_Hk^2c^2}{\omega_1\omega_0^2}\cos^2\theta, \tag{39}$$

$$\gamma=\frac{\omega_M\omega_Hk^2c^2}{\omega_1\omega_0^2}\frac{\cos^3\theta}{|\sin\theta|}. \tag{40}$$

It should be noted that the dependences of the frequency dispersion and collisionless damping on the value of a constant magnetic field are determined by the angular range in which surface waves with frequencies (9) and (26) propagate. In semiconductors of the first type (20), the functions $\delta\omega(H_0)$ and $\gamma(H_0)$ change in the angular range (24) as $(\text{const}+H_0)^2/H_0^2$ and $(\text{const}+H_0)/H_0$ respectively, i.e., their values decrease with increasing H_0, tending to a constant value. In the angular interval (25), the values of $\delta\omega(H_0)$ and $\gamma(H_0)$ increase with the magnetic field, tending to saturation according to the laws $\delta\omega(H_0)\sim H_0^2/(\text{const}+H_0)^2$ and $\gamma(H_0)\sim H_0/(\text{const}+H_0)$.

In semiconductors of the second type (21), $\delta\omega(H_0)\sim(\text{const}+H_0)/H_0$, $\gamma(H_0)\sim(\text{const}+H_0)/H_0^2$ if inequalities (35) are satisfied, and frequency dispersion and damping for values of angles (36) exhibit identical dependences on the magnetic field: $H_0/(\text{const}+H_0)$.

The properties of the semiconductor ((20) and (21)) also affect considerably the form of angular dependences $\delta\omega(\theta)$ and $\gamma(\theta)$. The effects described above can be observed experimentally by varying the direction or magnitude of the constant magnetic field $\mathbf{H}_0$.

*E-mail: yakovenko@ire.kharkov.ua

[1] M. A. Gintsburg, Zh. Éksp. Teor. Fiz. **34**, 1635 (1958) [Sov. Phys. JETP **7**, 1123 (1958)].
[2] I. R. Eshbach and R. W. Damon, Phys. Rev. **118**, 1208 (1960).
[3] M. I. Kaganov, N. B. Pustyl'nik, and T. I. Shalaeva, Usp. Fiz. Nauk **167**, 191 (1997) [*sic*].
[4] N. N. Beletskiĭ, A. A. Bulgakov, S. I. Khankina, and V. M. Yakovenko, *Plasma Instabilities and Nonlinear Phenomena in Semiconductors* [in Russian], Naukova Dumka, Kiev (1984).
[5] I. N. Oleĭnik and V. M. Yakovenko, Ukr. Fiz. Zh. **26**, 19 (1981).

Translated by R. S. Wadhwa

BRIEF COMMUNICATIONS

Acoustic magnetic resonance in absorption and dispersion of surface elastic waves in multilayers

V. I. Okulov and V. V. Ustinov

*Institute of Metal Physics, Ural Branch of the Russian Academy of Sciences, 620219 Ekaterinburg, Russia**

E. A. Pamyatnykh and V. V. Slovikovskaya

Ural State University, 620083 Ekaterinburg, Russia

(Submitted September 14, 1998)
Fiz. Nizk. Temp. **25**, 201–203 (February 1999)

It is shown that magnetic resonances related to excitation of oscillations of the layer magnetization can appear in the spectrum and absorption of the Love acoustic surface waves propagating in a multilayered film with a Fe/Cr type magnetic ordering on a massive substrate. The magnetoelastic resonant contribution to the elastic shear modulus of the film is calculated and the relation between the resonant frequencies and the frequencies of electromagnetically excited uniform ferromagnetic resonance is established. © *1999 American Institute of Physics.* [S1063-777X(99)01102-0]

The nature of magnetic ordering and giant magnetoresistance in multilayers of the Fe/Cr type has been studied till now by using a set of experimental methods providing vast information concerning the magnetic and atomic structure of such films.[1,2] Although this information makes it possible in principle to explain the main features of the observed regularities, it is insufficient, however, for an unambiguous and consistent description of the physical nature of magnetic ordering itself and the mechanisms of giant magnetic resistance on atomic level.

One of the ways for solving related problems is to extend the scope of phenomena whose analysis in magnetic multilayers makes it possible to determine qualitatively new microscopic parameters of such films. In our earlier publication,[3] we proved that the application of acoustic methods (including the study of frequencies and damping of surface elastic waves in the system comprising a film and a massive crystalline substrate) is promising in this respect. The frequencies of surface waves exhibit the dependence of elastic moduli of the film on the magnetization and magnetic field strength, which provides information on the nature of ordering, while the mechanisms of giant magnetoresistance are manifested in damping.

Along with nonresonant field dependences considered in Ref. 3, the parameters of surface elastic waves can also exhibit magnetic resonance. Such a resonance was observed, for example, in Rayleigh waves propagating in a system consisting in a nickel film of thickness 200 Å on a piezoelectric substrate.[4] In this communication, we describe the results of the theory describing manifestations of magnetic resonance in absorption and dispersion of surface elastic waves for the Love waves propagating in a multilayer–substrate system.

Let us consider the actual situation, when the length of a surface wave is larger than the film thickness. In this case, the expression for the phase velocity s of a Love wave can be written in the form

$$s = v_0 - \frac{1}{2} k^2 L_f^2 \left(\frac{\rho_f}{\rho_0} - \frac{\lambda_f}{\lambda_0} \right)^2 v_0, \tag{1}$$

where k is the wave vector, v_0, ρ_0, and λ_0 are the velocity of sound, density, and elastic modulus of the substrate, and L_f, ρ_f, and λ_f the thickness, density, and elastic modulus of the film. The magnetic resonance can be manifested in the contribution emerging in the elastic modulus λ_f of the magnetic film due to the interaction of elastic vibrations with magnetization oscillations.

In order to calculate this contribution, we consider ultrasonic vibrations in an individual magnetic layer occupying the region $0<z<L$. We assume that the elastic displacement vector and equilibrium magnetization are parallel to the x-axis. Expanding the displacement amplitude $u(z)$ and the nonequilibrium magnetization component $m(z)$ into Fourier series

$$u(z) = \frac{2}{L} \sum_{N=0}^{\infty} \left(1 - \frac{1}{2} \delta_{N0} \right) u_N \cos q_N z,$$

$$m(z) = \frac{2}{L} \sum_{N=0}^{\infty} m_N \sin q_N z, \quad q_N = \frac{\pi N}{L}$$

and presuming the isotropy in the boundary plane, we obtain the following equation for u_N:

$$-\omega^2 \rho_f u_N = -q_N^2 \lambda u_N + h_{me} q_N m_{zN} + (-1)^N F(L) - F(0), \tag{2}$$

where ω is the frequency, λ the elastic modulus of the crystal lattice, h_{me} the magnetoelastic interaction parameter, and $F(L)$ and $F(0)$ are the values of elastic stress at the boundaries $z=L$ and $z=0$.

Solving Eq. (2), we find the amplitudes of displacements $u(0)$ and $u(L)$ at the boundaries, and then use the relation

$$u(L)-u(0)=\frac{L}{\lambda_f}\frac{1}{2}[F(L)+F(0)] \tag{3}$$

(which is valid for a thin layer whose thickness is smaller than the wavelength) to obtain the elastic modulus λ_f in the form $\lambda_f=\lambda+\lambda_{me}$, where λ_{me} is the contribution from magnetoelastic interaction. Assuming that the multilayered film consists of identical fragments, we can apply relation (3) to our film, replacing the thickness L of an individual fragment by the thickness L_f of the entire film. Peculiarities of a multilayered system are manifested in this case in the type of magnetic ordering.

In the case when the recurring fragment consists of two layers with elastic moduli λ_1 and λ_2, the value of λ_f is determined by the formula $\lambda_f^{-1}=\lambda_1^{-1}+\lambda_2^{-1}$. For a Fe/Cr film, one of the contributions comes from the iron layers, the difference in the directions of equilibrium magnetizations of the layers being manifested in that this contribution depends on the relative orientation of magnetizations of adjacent layers.

The value of m_{zN} can be expressed in terms of the displacement amplitude u_N from the equation for magnetization with appropriate boundary conditions. The general expression has the form

$$m_{zN}=h_{me}q_N^2\sum_{N'}\alpha_{NN'}u_{N'}. \tag{4}$$

The dependence of the coefficient $\alpha_{NN'}$ on the wave vectors q_N and $q_{N'}$ is due to nonuniform exchange interaction, and the integral form of relation (4) reflects the emergence of magnetization at the film boundaries due to elastic vibrations. If the contribution of the boundary values can be neglected (rigid fixation of spins in the boundary layers), formula (4) assumes the form

$$m_{zN}=h_{me}q_N^2\chi_N^{zz}u_N, \tag{5}$$

where χ_N^{zz} is the magnetic susceptibility component due to the varying magnetic field at the boundary $z=0$. In this approximation, we can obtain the following simple expression for λ_{me}:

$$\lambda_{me}=h_{me}^2\frac{4}{L^2}\sum_{N=1}^{\infty}\frac{1}{q_N}[(-1)^N-1]\chi_N^{zz}. \tag{6}$$

This formula describes the resonant dependence of the velocity of the surface wave on the frequency and strength of the magnetic field. If magnetic oscillations of a layer are reduced to oscillations of average magnetization (for instance, in the case of parallel orientation of magnetizations in all the layers), the corresponding formula for χ_N^{zz} derived from the well-known equations for magnetization[5] has the form

$$\chi_N^{zz}=-\frac{1}{q_N}\frac{\Omega_0(\Omega_f+\eta q_N^2)}{(\omega+i\Gamma)^2-(\Omega_f+\eta q_N^2)(\Omega_f+\eta q_N^2+4\pi\Omega_0)}, \tag{7}$$

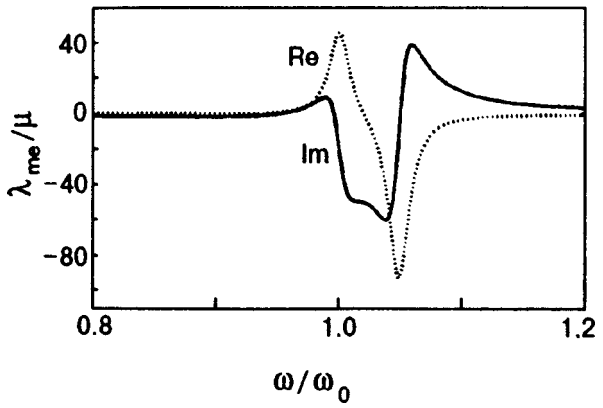

FIG. 1. Acoustic magnetic resonance as a function of the frequency of elastic modulus of the film with a strong effect of exchange interaction on the line shape; $\mu=h_{me}^2m^2\Omega\Omega_0/\omega_0^2$, m is the film magnetization normalized to the saturation magnetization.

where $\Omega_0=\gamma M_0$, γ is the magnetomechanical ratio, M_0 the equilibrium magnetization, Ω_f the frequency of uniform resonance in zero demagnetizing field, η the exchange interaction parameter, and Γ the damping factor. Formula (6) combined with (7) describes acoustic magnetic resonance broadened by the exchange interaction as well as spin-wave resonances under definite conditions. If the exchange interaction is insignificant ($\eta\ll\Omega_fL^2$), we have

$$\lambda_{me}=h_{me}^2\frac{\Omega_0\Omega_f}{(\omega+i\Gamma)^2-\Omega_f(\Omega_f+4\pi\Omega_0)} \tag{8}$$

and elastic moduli reflect the uniform magnetic resonance.

For multilayers of the Fe/Cr type, the susceptibility χ_N^{zz} should be referred to the recurring fragment including adjacent ferromagnetic layers with different directions of magnetization in the general case (antiparallel or noncollinear ordering). Resonant frequencies for such systems were calculated by Bebenin *et al.*[6] Using the results of these calculations, we can obtain an expression of the type (8) in the chosen geometry for uniform resonance, in which the resonant frequency $\sqrt{\Omega_f(\Omega_f+4\pi\Omega_0)}$ is replaced by another frequency taking into account the difference in the orientations of magnetizations of adjacent layers.

The effect of exchange interaction on acoustic magnetic resonance is illustrated in Fig. 1 showing the frequency dependence of the quantity λ_{me} under the conditions when exchange interaction distorts the curve corresponding to uniform resonance and leads to the emergence of a new resonant singularity.

According to the above arguments, the parameters of surface elastic waves can acquire resonances associated wit the excitation of natural magnetic oscillations in multilayers. The position and shape of the curves describing such resonances and their dependence on the magnetic field strength are determined by the type of magnetic ordering and other fundamental properties of films, which can therefore be analyzed on the basis of observation of surface acoustic waves.

This research was supported by the Russian Fund for Fundamental Research (Grant No. 98-02-17517) and INTAS (Grant No. 05-31).

*E-mail: elph@ifm.e-burg.su

[1] R. E. Camley and R. L. Stamps, J. Phys.: Condens. Matter **5**, 3727 (1993).
[2] P. M. Levy, Solid State Phys. **47**, 367 (1994).
[3] I. S. Masharova, V. I. Okulov, E. A. Pamyatnykh *et al.*, Pis'ma Zh. Tekh. Fiz. **22**, 53 (1996) [Tech. Phys. Lett. **22**, 52 (1996)].
[4] M. Levy and H. Yoshida, J. Magn. Magn. Mater. **35**, 139 (1983).
[5] A. G. Gurevich and G. A. Melkov, *Magnetic Oscillations and Waves* [in Russian], Nauka, Moscow (1994).
[6] N. G. Bebenin, A. V. Kobelev, A. P. Tankeyev, and V. V. Ustinov, J. Magn. Magn. Mater. **165**, 468 (1997).

Translated by R. S. Wadhwa

BIBLIOGRAPHY

Magnetic Domains. The Analysis of Magnetic Microstructures

A. N. Bogdanov
Fiz. Nizk. Temp. **25**, 204–205 (February 1999)

[S1063-777X(99)01202-5]

A. Hubert and R. Schäfer, **Magnetic Domains. The Analysis of Magnetic Microstructures**, Springer-Verlag, Berlin, Heidelberg, New York (1998), 720 pp., 400 figs., ISBN 3-540-64108-4

An overwhelming majority of magnetic materials used in science and engineering exist in the polydomain state. Hence the physical properties of magnetic domains and their evolution in external magnetic fields determine most of the functional characteristics of devices containing magnetic components. Decades of intensive studies have yielded numerous methods for observing and analyzing magnetic domains and a large body of experimental results, as well as different theoretical methods which were developed for describing the polydomain states. Recent advances in the field of nanotechnology have led to the production of basically new magnetic materials, which has further stimulated fundamental and applied research of magnetic domains. This is mainly due to the fact that at the current level of miniaturization of magnetoelectronic instruments, the behavior of individual domains affects significantly the functioning of such devices.

In spite of the large number of monographs and reviews devoted to individual aspects of the physics of magnetic domains, the present book is the first attempt in the world literature to present this comprehensive branch of magnetism in a single volume. The book is authored by Prof. Alex Hubert, a leading authority in the field of magnetic materials science, and his pupil Dr. R. Schäfer, a specialist in magneto-optical research. It should be recalled that Hubert's monograph entitled ''*Theorie der Domänenwände in Geordneten Medien*'' (Theory of Domain Walls in Ordered Media) (Springer-Verlag, Berlin, 1974), which was also translated into Russian in 1977 by Mir Publishers, Moscow, continues to be one of the most veritable publications on the basic principles of the physics of domain walls in condensed media.

The authors of the project realized it at the expense of enormous efforts and time. The book was written over a very long time (beginning in 1984). During this period, the authors gathered, analyzed and systematized a very large number of publications devoted to the experimental, theoretical and applied aspects of the investigations of domain structure.

The monograph has an elegant and carefully planned structure. The historical review presented in Chapter 1 is followed by a detailed description of the methods of observing magnetic domains, as well as their comparative characteristics (Chap. 2). The third chapter deals with the theory of domain structures. Numerous theoretical results obtained by using various approximations and covering different aspects of the domain theory are presented using a unified approach. Modern methods of numerical micromagnetism are described in detail for the first time, and several new theoretical results obtained especially for inclusion in this book are presented. Chapter 4 is devoted to an analysis of various physical parameters of magnetic materials and to a detailed description of the methods used to determine the magnetic constants to a detailed description of the methods used to determine the magnetic constants required for characterizing domain structures. In Chapter 5, which deals with an analysis of various polydomain states, the authors have gone further than providing just a classification and presentation of the material. On the basis of the results presented in previous chapters, they consider in detail the physical mechanisms leading to the formation of the main types of the observed domain textures. Using numerous examples, they have shown how a domain structure is formed depending on the symmetry of a magnet, crystallographic and induced anisotropy, shape of the sample as well as various other characteristics. In the last, sixth chapter, the authors study the effect of domains on the magnetic properties of basic types of magnets and discuss the role of polydomain states and their evolution in the functioning of various devices based on magnetic materials. Current problems of micromagnetism are discussed and the ways to solve them indicated.

A large number of superbly drawn figures and charts greatly facilitate the understanding of the material. Most of the illustrations of the domain structures are original and have been prepared specially for this edition. The exhaustive list of the cited literature at the end of the book will also be appreciated greatly by many specialists. For the first time, a decent classification has been provided for publications in the field of magnetic domains research, starting from the very first papers and terminating with the results of latest investigations.

This monograph by A. Hubert and R. Schäfer, in which a vast body of tangible material on the physics of magnetic domains has been gathered and presented systematically, imparts a finishing touch and inherent logic to this vital branch of magnetism. The wide range of the material, the profundity

of the analysis and the encyclopedic coverage of the topics make this book a unique example of monographic presentation in scientific literature. It should be of considerable interest not only for specialists in the field of magnetic research, but also for physicists from other fields.

Further information about the book and its authors can be obtained on the Internet (http://www6.ww.uni-erlangen.de/hubert/magnetic-domains.html).

Translated by R. S. Wadhwa

The role of pair correlations in the formation of the ground state and the elementary excitation spectrum in a superfluid Bose liquid (A Review)

E. A. Pashitskii

*Institute of Physics, National Academy of Sciences of the Ukraine, 252650 Kiev, Ukraine**
(Submitted August 10, 1998; revised October 7, 1998)
Fiz. Nizk. Temp. **25**, 115–140 (February 1999)

The paradoxes and disparities in the contemporary microscopic theory of superfluid helium (He–II) are discussed along with possible ways of resolving them by taking pair correlations of ^{4}He atoms into consideration. It is shown that most paradoxes are associated with the commonly accepted initial assumption concerning the dominating role of single-particle Bose condensate (SPBC) in the quantum microstructure of the superfluid component ρ_s. The existence of intensive SPBC leads to a strong hybridization of the elementary excitation branches and to a common dispersion law for all boson branches, which is identified with the quasiparticle spectrum $E(\mathbf{p})$ observed experimentally from slow neutron scattering in liquid helium. However, the stability of this spectrum during a transition through the λ-point and the large value of the gap in the vicinity of the ''rotonic'' minimum contradict both the Landau theoretical criterion of superfluidity and the small value of experimentally measured critical velocity. At the same time, a strong interaction between particles in the Bose liquid ^{4}He strongly suppresses the SPBC which amounts to less than 1% of all ^{4}He atoms and hence cannot be the main constituent of the superfluid component, unlike the case of a weakly nonideal Bose gas. Moreover, for a quite strong attraction between particles in a certain region of the momentum space, bound pairs of bosons can be formed in the superfluid Bose liquid, and a coherent pair condensate (CPC) analogous to the Cooper pair condensate in superconductors may appear. Such a strong CPC may completely suppress the weak SPBC. In this case, the one-particle spectrum $\varepsilon(\mathbf{p})$ of elementary excitations does not hybridize with the collective (two-particle) spectrum and does not appear in the structure of the dynamic form factor $S(\mathbf{p},\varepsilon)$, i.e., does not coincide with the spectrum measured from neutron scattering. The dispersion of one-particle spectrum is defined by the momentum dependence of the pair order parameter $\tilde{\Psi}(\mathbf{p})$ and may have a minimum or a point of inflection at $\mathbf{p}\neq 0$. This peculiarity in the one-particle spectrum of a Bose liquid with CPC but without SPBC vanishes together with $\tilde{\Psi}(\mathbf{p})$ at the temperature $T_c = T_\lambda$ of the phase transition from the superfluid to the normal state (unlike the rotonic minimum in the collective spectrum), while the corresponding critical velocity $v_c = \min[\varepsilon(\mathbf{p})/p]$ vanishes at the λ-point in accordance with the Landau criterion and the experimental data. The assumption that the strong ''Cooper-like'' CPC is responsible for the quantum structure of the superfluid component ρ_s is confirmed indirectly by the successful application of the Justrow approximation (based on strong pair correlations) for describing the properties of liquid ^{4}He and quantum liquid mixtures ^{3}He–^{4}He on one hand, and by an anomalously large effective mass of ^{3}He impurity atoms in ^{4}He, which is approximately equal to total mass of ^{3}He and ^{4}He atoms, thus pointing to the existence of helium atoms in superfluid liquid He–II. The value of the superfluid velocity circulation quantum in the Onsager–Feynman vortices in a Bose liquid with CPC but without SPBC is discussed as well as the critical velocities of superfluid ^{4}He in ultrathin films and channels in which the creation and motion of quantum vortices are ruled out, and the quasiparticle spectrum undergoes dimensional quantization. [S1063-777X(99)00102-4]

1. INTRODUCTION

The elementary excitation spectrum in superfluid helium (He–II) with a linear (phonon) dispersion relation $E(\mathbf{p})\sim p$ for small values of the momentum ($\mathbf{p}\to 0$) and with the ''rotonic'' minimum at $\mathbf{p}\neq 0$ was predicted by Landau[1] on the basis of the superfluidity criterion derived by him for Bose- and Fermi-type quantum liquids.

Such a form of the spectrum subsequently received a brilliant confirmation in experiments[2] on inelastic scattering of slow neutrons in liquid helium. Feynman[3] attributed the existence of the ''rotonic'' minimum in the quasiparticle spectrum $E(\mathbf{p})$ to the structure of the dynamic form factor $S(\mathbf{p},\varepsilon)$ of the Bose liquid ^{4}He, while Brueckner and Sawada[4,5] showed that such a minimum can be obtained in Bogoliubov's microscopic theory[6] of superfluidity for a weakly nonideal Bose gas if the pseudopotential of the

''rigid spheres'' model is used for describing the interaction between particles.

The advances made later in the phenomenological (two-fluid hydrodynamics) and microscopic (Green's functions method) theories of superfluidity[7,8] subdued some of the paradoxes associated with the hydrodynamics of the superfluid liquid as well as with the shape of the quasiparticle spectrum. Let us consider these paradoxes in detail.

Paradox 1. In view of a weak temperature dependence of the *quasiparticle spectrum* $E(\mathbf{p})$, the value of the ''rotonic'' gap $\Delta_r = 8.65$ K at the minimum of $E(\mathbf{p})$ dependence for $p_r = 1.9$ Å^{-1} remains practically unchanged right up to the λ-point ($T_\lambda = 2.17$ K). This contradicts the very meaning of *Landau's superfluidity criterion*.[1] At the same time, the superfluidity criterion is satisfied for the spectrum of quasiparticles in the electron Fermi liquid in superconductors[9] for the superconducting phase below the transition temperature T_c, when the spectrum contains a finite energy gap Δ. This criterion is not satisfied in the normal state at $T > T_c$, when there is no gap in the spectrum.

Paradox 2. The value of the critical velocity

$$v_c = \min[E(\mathbf{p})/p] \approx \Delta_r / p_r \approx 60 \text{ m/s}, \tag{1}$$

calculated according to the superfluidity criterion[1] for the quasiparticle spectrum $E(\mathbf{p})$ observed from neutron scattering in liquid ^{4}He, is two orders of magnitude higher than the experimentally measured value of the maximum velocity $v_c^{\exp}$ of superfluid flow in He–II. The velocity $v_c^{\exp}$ increases many times in ultrathin capillaries and wetting films of superfluid helium, but still remains much lower than the critical velocity (1) corresponding to the rotonic gap and, unlike the latter, vanishes at the λ-point.[10] This contradiction is usually attributed to the generation of *Onsager–Feynman quantum vortices* or vortex loops (see Ref. 10) in superfluid helium moving at a low velocity. This results in the emergence of a finite viscosity owing to the force of friction between normal cores of vortex tubes and the walls (solid surfaces). Such a point of view is in accord with the experimentally observed increase in the critical velocity upon a decrease in the thickness of superfluid helium films[10] since this is accompanied by an increase in the coupling force between vortices and walls per unit vortex length.

However, such an explanation is inapplicable to ultrathin capillaries (''supergaps'') in which the generation of quantum vertices with a superfluid velocity $v_s(r) = \kappa/r$ decreasing slowly with increasing distance from the axis is ruled out (here $\kappa = h/m_4$ is the velocity circulation quantum, h the Planck's constant, and m_4 is the mass of a ^{4}He atom). This situation is analogous to that of the *critical currents in type II superconductors*[11]: the critical current j_c in bulk superconductors is determined by forces of ''pinning'' of normal cores of *Abrikosov quantum vortices* at crystal lattice defects, while in thin superconducting filaments (wires) whose thickness is smaller than the London penetration depth $\lambda_L \approx 3000-5000$ Å of the magnetic field and which ''cannot accommodate'' vortices of diameter $d \approx 2\lambda_L$, the value of j_c is determined by the maximum ''depairing current'' for which the flow velocity of conduction electrons exceeds the limiting critical velocity $v_c \approx \Delta/p_F$ determined by the band gap in the spectrum of quasiparticles in the superconducting state ($T < T_c$) and sufficiently large for the rupture of Cooper pairs (p_F is the Fermi momentum).

Paradox 3. Unlike the case in a Bose gas, the *single-particle Bose condensate* (SPBC) in a superfluid Bose liquid must be depleted in particles even at $T = 0$ due to a strong interaction between bosons. Analysis of the experimental data on neutron scattering[12] shows that, superfluid ^{4}He in the Bose condensate state at low temperatures (with zero values of energy ε and momentum $\mathbf{p}$) contains no more than 1% of all ^{4}He atoms, while classical measurements of viscosity in He–II show[13] that the *density of the superfluid component* ρ_s at $T < 1$ K is almost *equal to the total density* **of liquid helium**. This means that in spite of the generally accepted view, superfluidity in the Bose liquid ^{4}He cannot be attributed to the *conventional Bose–Einstein condensation only*, and the microscopic structure of the superfluid component ρ_s must be of a more complex quantum nature in the form of a many-particle *coherent effective condensate* (CEC).[14–17] Among other things, it cannot be ruled out that the *coherent pair condensate* (CPC), which consists of bound boson pairs[18] and is analogous to the Cooper pair condensate in superconductors,[9] is the main superfluid component in He–II.

Paradox 4. It was shown by Brueckner and Sawada[4,5] (see also Refs. 19 and 20) that quite realistic potentials of interaction between particles can lead to a good agreement between the Bogoliubov spectrum of quasiparticles in a weakly nonideal Bose gas[6]:

$$E_B(\mathbf{p}) = \sqrt{\mathbf{p}^2 u_B^2(\mathbf{p}) + (\mathbf{p}^2/2m)^2};$$
$$u_B(\mathbf{p}) = \sqrt{nV(\mathbf{p})/m}, \tag{2}$$

[$V(\mathbf{p})$ is the Fourier component of the potential of pair interaction between the bosons], and the spectrum of elementary excitations in liquid ^{4}He observed from neutron scattering experiments,[2] in spite of the fact that SPBC is strongly suppressed (or is completely absent) in a Bose liquid while a Bose gas contains an overwhelming majority of particles $n_0 \approx n$ in the SPBC state (n is the total number of particles per unit volume).

This review is devoted to a discussion of these paradoxes and the possible ways of resolving them, in particular, by taking into account the *pair correlations* between ^{4}He atoms and the formation of *bound pairs of helium atoms*.

2. MICROSCOPIC STRUCTURE OF THE SUPERFLUID COMPONENT IN He–II (PRELIMINARY REMARKS)

The quantum-mechanical structure of the superfluid component in liquid ^{4}He below the λ-point (He–II) remains the main problem in the construction of a consistent microscopic theory of superfluidity of Bose liquids (including exotic liquids like the biexciton,[21,22] bipolaron,[23] and pion[24] liquids).

The microscopic base of the superfluid state in a weakly nonideal Bose gas is an intense SPBC[6] with a nonzero mean value of the field operator $\langle \hat{\psi}_0 \rangle = n_0^{1/2}$. It is usually assumed that SPBC is also preserved in a quantum Bose liquid, and

the eigenenergy can be presented in the form of a power expansion in $n_0^{1/2}$,[25,26] i.e., as a sequence of Feynman diagrams with increasing number of external condensate lines. However, if the SPBC is highly ''depleted'' in a Bose liquid with a strong interaction between particles (see Ref. 12) so that $n_0 \ll n$, we can confine the analysis to the lowest-order terms in the power expansion in $n_0^{1/2}$ (see Ref. 18).

On the other hand, the formation of *bound pairs of bosons* (^{4}He atoms) or a strong CPC[18] is possible on account of a quite strong effective attraction prevailing over a wide range of the momentum space even for a dominating (but rapidly decreasing with increasing separation between particles) repulsion in the real space.[4,5]

The possibility of the existence of such a ''Cooper-type'' CPC in superfluid ^{4}He was discussed by many authors.[27–33] However, the coexistence of SPBC and CPC results in a large number of contradictions between the theory and the experiment, as also within the theory itself.

First, the formation of CPC must apparently lead, in analogy with the *Bardeen–Cooper–Schrieffer (BCS) theory of superconductivity*,[9] to the emergence of a finite *gap* $\Delta_0 \neq 0$ for $\mathbf{p}=0$ in the one-particle branch of the elementary excitation spectrum.[27–33] This must result in heat capacity anomalies[32] which, however, were not observed experimentally in He–II.

Second, the existence of SPBC must lead to a strong *hybridization of one-particle and collective spectral branches*, i.e., to a coincidence of the poles of one- and two-particle Green's functions of bosons, as well as all Green's functions involving a larger number of particles[8] (we consider here excitations with zero helicity). However, since the collective (hydrodynamic) branch has an acoustic dispersion relation $E(\mathbf{p}) \approx pc$ in the limit $\mathbf{p} \to 0$ (c is the velocity of sound in liquid ^{4}He), the existence of a gap $\Delta_0 \neq 0$ in a one-particle spectrum is ruled out for $\mathbf{p}=0$.

Third, it was shown by us earlier[18] that the coexistence of a highly depleted SPBC and a strong CPC results in the *instability* of the one-particle acoustic spectrum if the phase of the ''pair'' order parameter $\Psi(\mathbf{p})$ coincides with the phase of the SPBC ''wave function.'' If, however, the phase of $\Psi(\mathbf{p})$ is shifted by π relative to the SPBC phase, the ground state of the system is unstable to spontaneous creation of boson pairs with a negative energy.

According to our earlier work,[18] a stable Bose liquid state does not contain any SPBC ($n_0=0$), and the superfluidity is determined by the strong CPC under the condition that interaction between particles ensures the existence of a nontrivial (nonzero) solution of the homogeneous integral equation for the *complex pair order parameter* $\Psi(\mathbf{p}) = |\Psi(\mathbf{p})| \exp^{i\theta}$ with an arbitrary (degenerate) macroscopic phase θ. The superfluid component is a pair CEC which contains the CPC of bound (''Cooper'') boson pairs and ''higher-order'' many-particle condensates with an even number of unbound particles, since the coexistence of several bound condensates in a one-component Bose liquid is forbidden due to the same gauge invariance of the initial Hamiltonian.

It should be noted that several peculiarities of the superfluid Bose liquid without SPBC were studied earlier by Kondratenko[15] who showed that the emergence of a gap Δ_0 for $\mathbf{p}=0$ in the one-particle branch of the spectrum $\varepsilon(\mathbf{p})$ is due to the violation of the *Hugenholtz–Pines theorem*,[26] while the *Goldstone branch* with an acoustic dispersion relation for $\mathbf{p} \to 0$ *(hydrodynamic sound)* is the pole of a two-particle Green's function. However, the author of Ref. 15 did not take into account the dynamic factor responsible for the vanishing of SPBC, which involves[18] a quite strong *attraction* over a wide range of momenta $\mathbf{p} \neq 0$, that is nearly capable of forming a bound state of two bosons and leads to the emergence of a CPC.

Hybridization of excitations is restricted in a Bose liquid with CPC but without SPBC[18,34]: hybridization occurs only between those branches of the spectrum which correspond to excitations differing by two particles, i.e., the one-particle branch hybridizes with all excitations having an odd number of particles, while the two-particle branch hybridizes with all collective excitations with an even number of particles. Consequently, the one-particle spectrum $\varepsilon(\mathbf{p})$ is omitted from the *dynamic form factor*:

$$S(\mathbf{p},\varepsilon) = -\frac{1}{\pi} \operatorname{Im} \chi(\mathbf{p},\varepsilon), \tag{3}$$

where $\chi(\mathbf{p},\varepsilon)$ is the susceptibility of the Bose system, carrying information about the collective (including two-particle) excitations. Hence, in contrast to the two-particle spectrum, the spectrum $\varepsilon(\mathbf{p})$ cannot be measured in experiments on slow neutron scattering.

It follows from here that the model of a superfluid Bose liquid ^{4}He with a ''pair'' base of the superfluid component in the form of CPC and higher-order even condensates (with no SPBC and higher-order odd condensates) considered in Ref. 18 can be helpful in resolving the paradoxes formulated in the Introduction owing to the restriction on the hybridization of excitations with different parities and the separation of roles of one-particle and collective branches in the quasiparticle spectrum. In other words, it can be assumed that the $E(\mathbf{p})$ spectrum observed in neutron scattering experiments,[2] which is a collective spectrum and is determined by the dynamic form factor (3), has nothing to do with the supefluidity criterion. However, the one-particle spectrum $\varepsilon(\mathbf{p})$, which does not make any contribution to the dynamic form factor and is therefore not observed in neutron experiments, is determined for $\mathbf{p} \neq 0$ by the momentum dependence of the interaction $V(\mathbf{p})$ and can have a minimum at the point corresponding to the peak of the modulus $|\tilde{\Psi}(\mathbf{p})|$ of the ''pair'' order parameter. As the critical temperature $T_c = T_\lambda$ of phase transition from the superfluid to normal state (λ-point) is approached, the order parameter $\tilde{\Psi}(\mathbf{p})$ determining the minimum of the ratio $\varepsilon(\mathbf{p})/p$, and hence the critical velocity v_c, become equal to zero in accord with the experimental results[10] and Landau's superfluidity criterion.[1] This resolves **Paradox 1**.

Assuming that the ''gap'' Δ_1 at the minimum of $\varepsilon(\mathbf{p})$ and at $T \to 0$ is much smaller than the ''rotonic'' gap Δ_r in the collective spectrum $E(\mathbf{p})$ of elementary excitations (observed from neutron scattering experiments), the reason be-

hind the small value of the critical velocity v_c in superfluid ^{4}He becomes obvious and, **Paradox 2** is resolved.

The absence of SPBC in a Bose liquid with a strong CPC (see Ref. 18) also resolves **Paradox 3** automatically.

As regards **Paradox 4**, it is connected with the (coincidental) assumption that both Bogoliubov spectrum (2) and the form factor (3) are defined by the nonmonotonic momentum-dependent pair interaction $V(\mathbf{p})$ between particles (see below).

Note that the absence of hybridization between one-particle and collective branches of the spectrum in a Bose liquid with CPC but without SPBC solves the problem of the coexistence of a gap $\Delta_0 \neq 0$ for $\mathbf{p}=0$ in the former branch for an acoustic type of latter branch. However, it was mentioned recently by us[35] that the *existence of a gap* Δ_0 *in the one-particle spectrum* $\varepsilon(\mathbf{p})$ *of a Bose liquid with a ''pair'' CEC is not at all a must*. Hence for $\Delta_0=0$ the one-particle spectrum is of the acoustic type $\varepsilon(\mathbf{p}) \approx pu$ (for $\mathbf{p}\to 0$) with a phase velocity $u=\sqrt{\Psi(0)/m^*}$ which tends to zero as $T \to T_\lambda$ when $\Psi(0)\to 0$. The $\varepsilon(\mathbf{p})$ spectrum then becomes parabolic and does not satisfy Landau's supefluidity criterion in the normal phase (for $T>T_\lambda$).

The acoustic nature of the one-particle gapless spectrum in the long-wave limit ($\Delta_0=0$ for $\mathbf{p}=0$) in the superfluid state ($T<T_\lambda$) is in accord with the Hugenholtz–Pines theorem[26] as well as with the Reatto–Chester power asymptotic form[36,37] for the pair correlation function $\langle \hat{\psi}(\mathbf{r})\hat{\psi}(\mathbf{r})\rangle \sim |\mathbf{r}-\mathbf{r}'|^{-2}$ for $|\mathbf{r}-\mathbf{r}'|\to\infty$, and does not lead to additional singularities in the heat capacity (cf. Ref. 32).

On the other hand, the important role of pair correlations between ^{4}He atoms in the superfluid Bose liquid He–II is indicated by the successful application of the Justrow–Feenberg approximation[38–46] for describing the ground and excited states of liquid ^{4}He as well as quantum liquid mixtures ^{3}He–^{4}He.[47]

It was reported earlier by us[35] that the experimentally observed[48–51] anomalously large effective mass m_3^* of ^{3}He impurity atoms in ^{4}He, which is close to the total mass of ^{3}He and ^{4}He atoms: $m_3^* \gtrsim (m_3+m_4)$, may serve as an empirical confirmation for the existence of bound pairs of helium atoms in He–II. This may point towards the formation of a bound state of ^{3}He–^{4}He atomic pairs. However, since the potentials of interaction between ^{3}He and ^{4}He atoms are identical and the energy of zero-point vibrations in the bound state for the ^{3}He–^{4}He pair is higher than for the ^{4}He–^{4}He pair, the formation of pairs of ^{4}He atoms in He–II becomes easier than the formation of ^{3}He–^{4}He pairs, the more so when boson–boson correlations facilitating attraction are taken into consideration.

All these questions are studied in detail in this review on the basis of the *Bogoliubov's canonical transformations method* (Sec. 3) and the *Green's functions method* (Sec. 4).

3. BOGOLIUBOV'S CANONICAL TRANSFORMATIONS METHOD FOR NONIDEAL BOSE SYSTEMS

3.1. A weakly nonideal Bose gas with a strong SPBC

The first rigorous microscopic theory of superfluidity was constructed more than 50 years ago by Bogoliubov[6] for a nearly ideal (or weakly nonideal) Bose gas. The main advantage of this theory was that it did not use the standard methods of the perturbation theory employing the series expansion in the weak interaction constant. A correct choice of the ground state at $T=0$, when an overwhelming number of bosons are at the lowest quantum level with zero energy and zero momentum, i.e., in the SPBC state (in view of the Bose gas being weakly nonideal), helps in a radical simplification of the initial Hamiltonian of the system with pair interaction $V(\mathbf{q})$ which is a function of the transferred momentum $\mathbf{q}=\mathbf{p}-\mathbf{p}'$:

$$H=\sum_{\mathbf{p}} \frac{\mathbf{p}^2}{2m} b_{\mathbf{p}}^+ b_{\mathbf{p}} + \frac{1}{2}\sum_{\mathbf{p},\mathbf{p}',\mathbf{q}} V(\mathbf{q}) b_{\mathbf{p}}^+ b_{\mathbf{p}+\mathbf{q}}^+ b_{\mathbf{p}'} b_{\mathbf{p}'-\mathbf{q}}, \quad (4)$$

where m is the particle mass, while $b_{\mathbf{p}}^+$ and $b_{\mathbf{p}}$ are the creation and annihilation operators for a boson with momentum $\mathbf{p}$ in the secondary quantization representation (for simplicity, the boson spin is put equal to zero). Indeed, assuming that the number n_0 of particles in SPBC is macroscopically large and approaches the total number n of particles per unit volume, we can disregard the noncommutativeness of the Bose operators b_0^+ and b_0 except for terms of the order of $1/n_0 \sim 1/n \ll 1$, which can be replaced by c-numbers $\sqrt{n_0}$ (the accuracy of this approximation is much higher than that of any experiment).

Consequently, isolating terms in the Hamiltonian (4) with zero momentum and considering that the number of excitations with $\mathbf{p}\neq 0$ over the condensate is small $n' = \Sigma_{\mathbf{p}\neq 0} b_{\mathbf{p}}^+ b_{\mathbf{p}} \ll n_0$, we obtain, taking into account the momentum conservation law, the following expression for a fixed number of particles ($n=\text{const}$) accurate to within small terms of the order of n'/n_0:

$$H_B=\frac{1}{2}n^2 V(0)+\sum_{\mathbf{p}\neq 0}\left[\frac{\mathbf{p}^2}{2m}+nV(\mathbf{p})\right] b_{\mathbf{p}}^+ b_{\mathbf{p}} + \frac{n}{2}\sum_{\mathbf{p}\neq 0} V(\mathbf{p}) \times [b_{\mathbf{p}}^+ b_{-\mathbf{p}}^+ + b_{\mathbf{p}} b_{-\mathbf{p}}]. \quad (5)$$

This simplified quadratic Hamiltonian can be subjected to strict diagonalization with the help of Bogoliubov's linear canonical transformations[6] to new creation $\beta_{\mathbf{p}}^+$ and annihilation $\beta_{\mathbf{p}}$ operators for noninteracting quasiparticles:

$$b_{\mathbf{p}}^+ = \lambda_{\mathbf{p}} \beta_{\mathbf{p}}^+ + \mu_{\mathbf{p}} \beta_{-\mathbf{p}}; \quad b_{\mathbf{p}} = \lambda_{\mathbf{p}} \beta_{\mathbf{p}} + \mu_{\mathbf{p}} \beta_{-\mathbf{p}}^+. \quad (6)$$

For simplicity, the coefficients $\lambda_{\mathbf{p}}$ and $\mu_{\mathbf{p}}$ are assumed to be real and even in $\mathbf{p}$ and satisfy the normalization condition $\lambda_{\mathbf{p}}^2 - \mu_{\mathbf{p}}^2 = 1$ so that the operators $\beta_{\mathbf{p}}^+$ and $\beta_{\mathbf{p}}$ satisfy the same commutation relations as the original operators $b_{\mathbf{p}}^+$ and $b_{\mathbf{p}}$.

Substituting (6) into (5) and taking into account the ideal nature of a gas of quasiparticles as well as the normalization condition, we obtain an expression for the coefficients $\lambda_{\mathbf{p}}$ and $\mu_{\mathbf{p}}$ and finally arrive at the following expression for the renormalized spectrum of quasiparticles [see also Eq. (2)]:

$$E_B(\mathbf{p})=\left\{\frac{\mathbf{p}^2}{2m}\left[\frac{\mathbf{p}^2}{2m}+2nV(\mathbf{p})\right]\right\}^{1/2}. \quad (7)$$

It follows hence that for $\mathbf{p}\to 0$, the spectrum (7) is an acoustic spectrum $E_B(p) \approx |\mathbf{p}| u_B(0)$, where $u_B(0)$

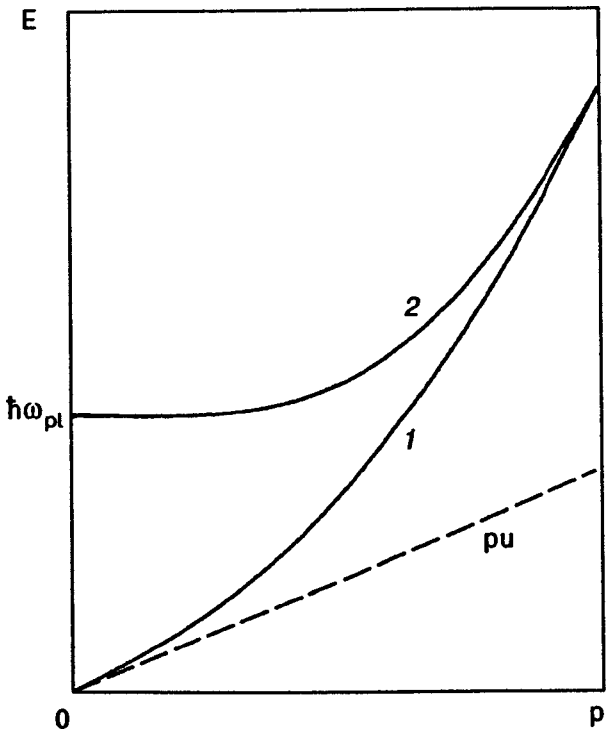

FIG. 1. Bogoliubov spectrum of quasiparticles in a weakly nonideal Bose gas of point-like neutral (curve *1*) and charged particles (curve *2*).

$=\sqrt{nV(0)/m}$ which is stable only when repulsion between particles dominates at large distances when $V(0)>0$.

The basic methodical drawback in the original version of Bogoliubov's theory[6] is not the omission of quadratic terms $\sim(n'/n_0)^2$, but the assumption on the model of a Bose gas consisting of point particles with an interaction potential $V(\mathbf{r})=V_0\delta(\mathbf{r})$, where $\delta(\mathbf{r})$ is the three-dimensional δ-function, so that the Fourier component $V(\mathbf{p})=V_0$ $=$const. In this case, formula (7) describes the superlinear dispersion relation (see curve *1* in Fig. 1) which satisfies Landau's superfluidity criterion,[1] but is unstable to the decomposition of any elementary excitation into two other excitations (the energy and momentum are conserved).

3.1.1. High-density Charged Bose-gas. It was observed soon after by Foldy[52] that for a *Bose gas of charged particles* with Coulomb repulsion $V_c(\mathbf{r})=e^2/r$ and a Fourier component $V_c(\mathbf{p})=4\pi e^2/\mathbf{p}^2$, the Bogoliubov spectrum (7) has a finite energy gap for $\mathbf{p}=0$ (curve *2* in Fig. 1):

$$E_B(\mathbf{p})=\sqrt{\hbar^2\omega_{\rm pl}^2+(\mathbf{p}^2/2m)^2}, \tag{8}$$

where $\omega_{\rm pl}=\sqrt{4\pi e^2 n/m}$ is the plasma frequency of bosons, and $\hbar=h/2\pi$. In the first place, such a spectrum is stable to decay processes. In addition, it also satisfies Landau's superfluidity criterion[1] owing to a finite value of the critical velocity:

$$v_c\equiv\min[E_B(p)/p]=2\sqrt{\hbar\omega_{\rm pl}/m}. \tag{9}$$

As a matter of fact, this circumstance later served as the basis for discussing the possibility of the *bipolar superconductivity mechanism*[23,53] in ionic (polar) crystals with a strong electron–phonon interaction following from the superfluidity of a charged Bose gas of *bipolarons*.[54]

Note that the condition

$$\left\langle\sum_{\mathbf{p}\neq 0} b_{\mathbf{p}}^{+}b_{\mathbf{p}}\right\rangle\ll n,$$

for a weakly nonideal gas, which must be satisfied for the application of Bogoliubov's theory,[6] is reduced to the inequality $n_B^{1/3}a_B^*\gg 1$, where $a_B^*=\varepsilon_0\hbar^2/4e^2m_B^*$ is the Bohr radius with effective mass m_B^* and charge $2e$ in a polar crystal with permittivity $\varepsilon_0\gg 1$. As in the case of a charged Fermi gas,[55] this condition corresponds to the high-density approximation, but it can be satisfied in ionic (ferroelectric) crystals with an anomalously large value of $\varepsilon_0\gtrsim 10^3$ even for a relatively low concentration of particles $n_B\gtrsim 10^{21}\,\mathrm{cm}^{-3}$ if $m_B^*\lesssim 10m_0$ (where m_0 is the free electron mass). The critical temperature T_c of transition to superconducting (superfluid) state, which coincides in the present case with the Bose condensation temperature[55]

$$T_B=3.31\frac{\hbar^2 n_B^{2/3}}{k_B m_B^*}, \tag{10}$$

where k_B is the Boltzmann constant, may attain quite high values $T_c=T_B\gtrsim 200\,\mathrm{K}$ which exceed the highest values of T_c for cuprate-based metaloxide *high-temperature superconductors*[57] discovered by Bednorz and Müller.[56 1)] However, there are no sound (theoretical or experimental) reasons to believe that the bipolaron mechanism of *high-temperature superconductivity* (HTSC) is realized in these compounds.

3.1.2. Neutral Bose-gas with finite-size particles. Unlike Bogoliubov[6] and Foldy,[52] Brueckner and Sawada[4,5] considered the model of a Bose gas consisting of finite-size neutral particles in the shape of rigid spheres of diameter a, so that the pair interaction potential corresponds to infinite repulsion at distances $r\leqslant a$ and is equal to zero for $r>a$. In this case, the Fourier component of the effective interaction, taking into account the quantum (wave) properties of particles and their mutual diffraction, assumes the form[5] ($\hbar=1$)

$$V(p)=V_0\frac{\sin pa}{pa}\equiv V_0 j_0(pa), \tag{11}$$

where $j_0(x)$ is the zeroth-order spherical Bessel function and V_0 the positive constant of long-range repulsion (for $p=0$) ensuring the stability of the system to spontaneous compression (collapse). However, it follows from (11) that, for quite large transferred momenta (in particular, for $\pi/a<p<2\pi/a$), the sign of the interaction $V(p)$ is reversed, which corresponds to effective attraction of diffraction quantum origin (Fig. 2a). Substitution of the potential (11) into the Bogoliubov spectrum (7) leads to a nonmonotonic dispersion relation with a minimum at $p\approx 3\pi/2a$ (Fig. 2b), which is qualitatively in accord with the spectrum of elementary excitations in liquid ^{4}He with a ''rotonic'' minimum, observed in neutron scattering experiments.[2]

In the model of ''semitransparent'' spheres[19] with a finite repulsion $V_1>0$ in the region $r\leqslant a$, taking into account additionally the weak (Van der Waals) attraction $V_2<0$ in a

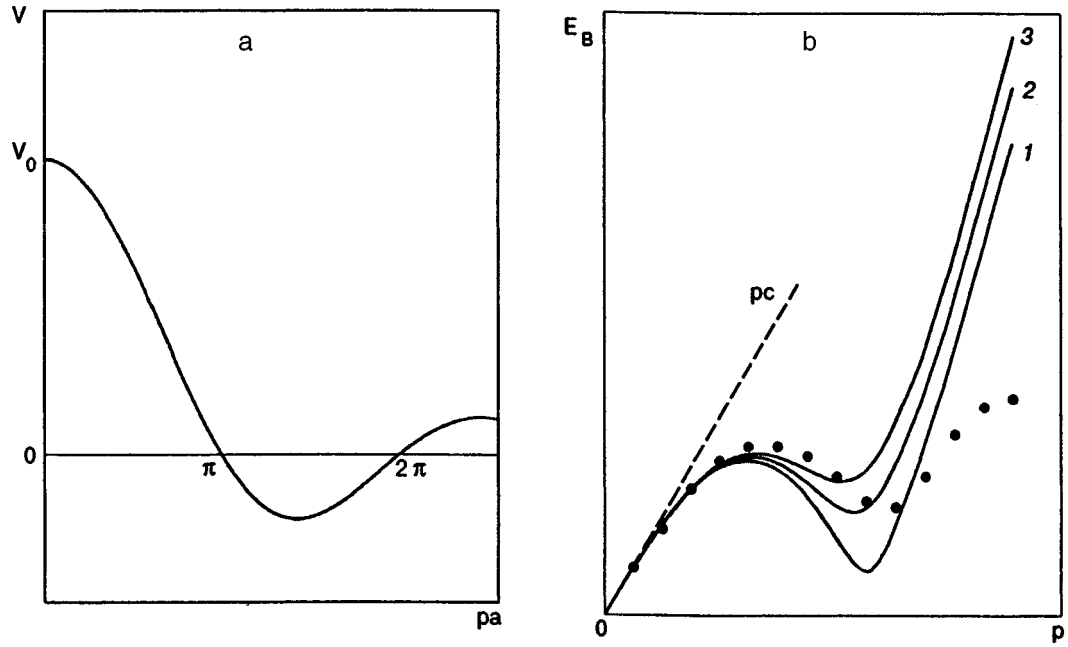

FIG. 2. Pseudopotential of the pair interaction between Bose particles in the model of ''rigid spheres'' (a) and the Bogoliubov spectrum in the ''rigid spheres'' model for $u=c$ and for different values of the dimensionless parameter $\beta_0=4nma^2V_0/\hbar^2$: 80 (curve *1*), 64 (curve *2*), and 53 (curve *3*). Dark circles show the experimental spectrum of quasiparticles in ^{4}He (b).

certain interval $a<r<b$, the Fourier component of pair interaction potential can be represented in the following form (Fig. 3a):

$$V(p)=V_1 j_1(pa)/pa-|V_2|j_1(pb)/pb, \tag{12}$$

where $V_1 \gg |V_2|$, and $j_1(x)=-3(x\cos x-\sin x)/x^3$ is a first-order spherical Bessel function. By choosing the parameters appropriately, we can use the potential (12) to attain a close coincidence between the theoretical spectrum (7) and the experimentally observed spectrum (Fig. 3b) of quasiparticles in ^{4}He. However, it is obvious that such a coincidence is accidental to a large extent and does not correspond to the real situation since Bogoliubov's theory[6] is not applicable for describing the properties of a Bose liquid with a strongly ''depleted'' SPBC ($n_0 \ll n$). Moreover, it was mentioned in Sec. 2 that the structure of the collective spectral branch, which was reconstructed from the dynamic neutron scattering form

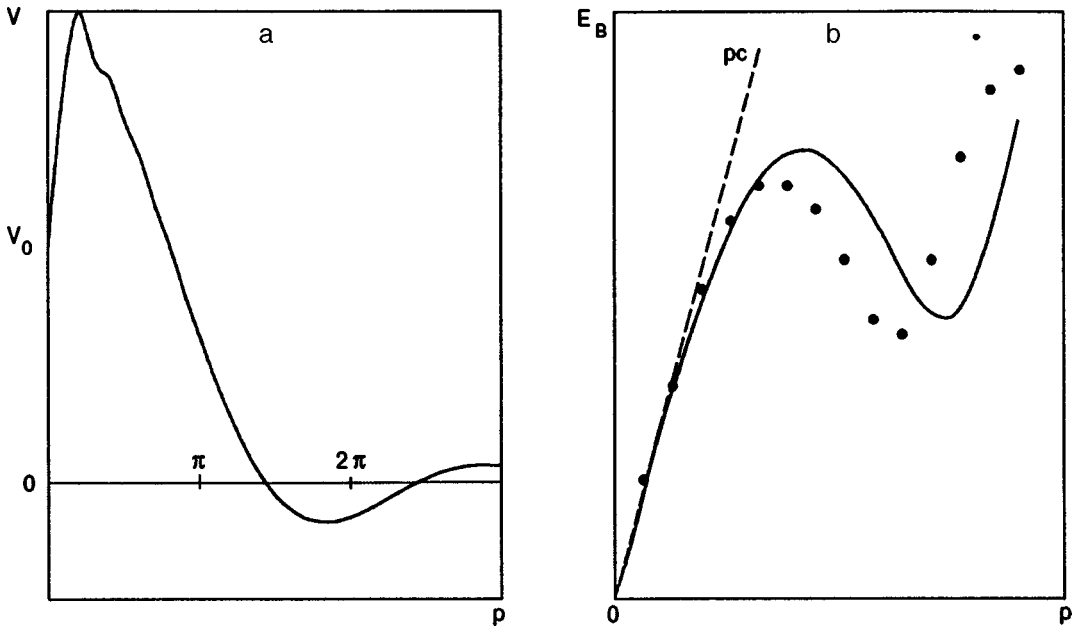

FIG. 3. Pseudopotential of the pair interaction between Bose particles in the model of ''semitransparent spheres'' with attraction in the region $a<r<b$ for parameters $|V_2|/V_1=0.5$, $a/b=0.1$ and $V_0=V_1-|V_2|$ (a) and the Bogoliubov spectrum in the ''semitransparent spheres'' model with attraction for the above values of parameters for $u=c$ and $\beta_0=667$. Dark circles show the experimental spectrum of quasiparticles in ^{4}He (b).

factor, has no direct relation with the criterion of superfluidity ^{4}He. This calls for a more consistent analysis of nonideal Bose systems.

3.2. Nonideal Bose systems with a fixed number of particles (Foldy–Brueckner method)

In the Bogoliubov approximation,[6] all particles of a weakly nonideal Bose gas, which are not in a SPBC with density $n_0 \approx n$, combine to form a condensate of free Boson pairs. One can endeavor to improve this approximation, in the Hamiltonian (4) retaining (at least partially) in the Hamiltonian (4) higher-order terms in the small parameter n'/n_0, which describes a condensate of bound Cooper pairs of bosons with opposite momenta, as was done in Refs. 27–33.

We shall solve this problem by using the technique developed by us in Ref. 20, in which the Hamiltonian (5) contains terms quadratic in $b_{\mathbf{p}}^+$ and $b_{\mathbf{p}}$ as well as fourth-order terms (second-order in n'/n_0) which can be presented in the mean-field approximation as combinations of nonzero normal $\langle b_{\mathbf{p}}^+ b_{\mathbf{p}}\rangle$ and anomalous $\langle b_{\mathbf{p}}^+ b_{-\mathbf{p}}^+\rangle$ and $\langle b_{\mathbf{p}} b_{-\mathbf{p}}\rangle$ means. Consequently, Bogoliubov's, renormalized quadratic Hamiltonian (5) with a conserved total number of particles assumes the form

$$\tilde{H}_B = \frac{1}{2} n_0^2 V(0) + \sum_{\mathbf{p}} \left[\frac{\mathbf{p}^2}{2m} + \Phi(\mathbf{p}) \right] b_{\mathbf{p}}^+ b_{\mathbf{p}} + \frac{1}{2} \sum_{\mathbf{p}} [n_0 V(\mathbf{p}) - \Psi(\mathbf{p})](b_{\mathbf{p}}^+ b_{-\mathbf{p}}^+ + b_{\mathbf{p}} b_{-\mathbf{p}}), \quad (13)$$

where

$$\Phi(\mathbf{p}) = n_0 V(\mathbf{p}) + \varphi(\mathbf{p}) - \varphi(0) + \Psi(0); \quad (14)$$

$$\varphi(\mathbf{p}) = \sum_{\mathbf{p}'} V(\mathbf{p}-\mathbf{p}') \langle b_{\mathbf{p}'}^+ b_{\mathbf{p}'}\rangle; \quad (15)$$

$$\Psi(\mathbf{p}) = -\sum_{\mathbf{p}'} V(\mathbf{p}-\mathbf{p}') \langle b_{\mathbf{p}'} b_{-\mathbf{p}'}\rangle. \quad (16)$$

Applying the canonical transformation (6) to Eq. (13) and considering that new noninteracting quasiparticles have anomalous means $\langle \beta_{\mathbf{p}}^+ \beta_{-\mathbf{p}}^+\rangle = \langle \beta_{\mathbf{p}} \beta_{-\mathbf{p}}\rangle = 0$, we can reduce the Hamiltonian (13) to the form

$$\tilde{H}_B = \tilde{E}_0 + \sum_{\mathbf{p}} [\varepsilon_0(\mathbf{p})(\lambda_{\mathbf{p}}^2 + \mu_{\mathbf{p}}^2) + 2\lambda_{\mathbf{p}}\mu_{\mathbf{p}}\eta(\mathbf{p})]\beta_{\mathbf{p}}^+ \beta_{\mathbf{p}} + \sum_{\mathbf{p}} \left[\varepsilon_0(\mathbf{p})\lambda_{\mathbf{p}}\mu_{\mathbf{p}} + \frac{1}{2}(\lambda_{\mathbf{p}}^2 + \mu_{\mathbf{p}}^2)\eta(\mathbf{p}) \right](\beta_{\mathbf{p}}^+ \beta_{-\mathbf{p}}^+ + \beta_{\mathbf{p}}\beta_{-\mathbf{p}}), \quad (17)$$

where

$$\varepsilon_0(\mathbf{p}) = \frac{\mathbf{p}^2}{2m} + \Phi(\mathbf{p}); \quad \eta(\mathbf{p}) = n_0 V(\mathbf{p}) - \Psi(\mathbf{p}); \quad (18)$$

$$\tilde{E}_0 = \frac{1}{2} n_0^2 V(0) - \sum_{\mathbf{p}} [\varepsilon_0(\mathbf{p})\mu_{\mathbf{p}}^2 + \lambda_{\mathbf{p}}\mu_{\mathbf{p}}\eta(\mathbf{p})]. \quad (19)$$

The condition of vanishing of the interaction between quasiparticles in (17) leads to the expression

$$\lambda_{\mathbf{p}} = \frac{\eta(\mathbf{p})}{\sqrt{\eta^2(\mathbf{p}) - [\tilde{E}(\mathbf{p}) - \varepsilon_0(\mathbf{p})]^2}}; \quad \mu_{\mathbf{p}} = \frac{\tilde{E}(\mathbf{p}) - \varepsilon_0(\mathbf{p})}{\sqrt{\eta^2(\mathbf{p}) - [\tilde{E}(\mathbf{p}) - \varepsilon_0(\mathbf{p})]^2}}, \quad (20)$$

where $\tilde{E}(\mathbf{p})$ is the renormalized quasiparticle spectrum:

$$\tilde{E}(\mathbf{p}) = \sqrt{\varepsilon_0^2(\mathbf{p}) - \eta^2(\mathbf{p})}. \quad (21)$$

In this case, Eq. (16) for the pair ''order parameter'' $\Psi(\mathbf{p})$ can be represented in the following form if we take Eqs. (20) into consideration:

$$\Psi(\mathbf{p}) = \sum_{\mathbf{p}'} V(\mathbf{p}-\mathbf{p}') \frac{\eta(\mathbf{p}')[\tilde{E}(\mathbf{p}') - \varepsilon_0(\mathbf{p}')]}{[\tilde{E}(\mathbf{p}') - \varepsilon_0(\mathbf{p}')]^2 - \eta^2(\mathbf{p}')} \times [1 + 2\langle \beta_{\mathbf{p}'}^+ \beta_{\mathbf{p}'}\rangle], \quad (22)$$

where $\langle \beta_{\mathbf{p}}^+ \beta_{\mathbf{p}}\rangle = [e^{\tilde{E}(\mathbf{p})/T} - 1]^{-1}$ is the Bose–Einstein distribution function for quasiparticles at $T \neq 0 (k_B = 1)$.

Taking Eqs. (18) into account, we can easily show that the quasiparticle spectrum (21) has the following form for $\mathbf{p} \to 0$:

$$\tilde{E}(\mathbf{p}) \cong \sqrt{\mathbf{p}^2 \tilde{u}^2(0) + \Delta_0^2}, \quad (23)$$

where

$$\tilde{u}(0) = \sqrt{\Phi(0)/m}; \quad \Delta_0 = 2\sqrt{n_0 V(0)\Psi(0)}. \quad (24)$$

It follows hence, that for the simultaneous existence of SPBC and CPC ($n_0 \neq 0$ and $\Psi(0) \neq 0$), the one-particle spectrum of elementary excitations has a finite gap $\Delta_0 \neq 0$ for $\mathbf{p} = 0$ (cf. Refs. 27–33). This is in contrast with the generally accepted concepts about a strong hybridization of one-particle and collective (two-particle) branches and the acoustic nature of the spectrum for $\mathbf{p} \to 0$ in neutral Bose systems.[8,26]

According to Eqs. (23) and (24), the acoustic dispersion relation is obeyed in this case for $\mathbf{p} \to 0$ only if the macroscopically filled SPBC is completely absent, i.e., only for $n_0 = 0$ when $\Delta_0 = 0$, $\eta(\mathbf{p}) = \Psi(\mathbf{p})$, and $\Phi(0) \equiv \Psi(0)$, so that $\tilde{E}(\mathbf{p}) \approx p\tilde{u}(0)$. In this case, the integral equation (22) is reduced to the form

$$\Psi(\mathbf{p}) = -\sum_{\mathbf{p}'} V(\mathbf{p}-\mathbf{p}') \times \frac{\Psi(\mathbf{p}')[\tilde{E}(\mathbf{p}') - \varepsilon_0(\mathbf{p}')]}{[\tilde{E}(\mathbf{p}') - \varepsilon_0(\mathbf{p}')]^2 - \Psi^2(\mathbf{p}')} \coth \frac{\tilde{E}(\mathbf{p}')}{2T}, \quad (25)$$

while the phase velocity $\tilde{u}(0) = \sqrt{\Psi(0)/m}$ is real only for $\Psi(0) > 0$, i.e., for a certain type of two-particle interaction $V(\mathbf{p}-\mathbf{p}')$ which must have a quite extended attraction region (see Figs. 2a and 3a).

However, the above approximate approach to the description of the superconducting state of a nonideal Bose system with a constant number of particles $n = \text{const}$, which is often called the *Foldy–Brueckner method*, is not strictly

consistent from the theoretical point of view, and is analogous in a certain sense to the initial simplified versions of the BCS model[9] or to the method of Bogoliubov's canonical uv-transformations[58] in the theory of superconductivity. In the next section, we shall describe a more consistent approach (the *Hugenholtz–Pines* method) based on the *Green's functions method*[8] with a fixed value of the chemical potential $\mu = \text{const}$ of a Bose system.

4. APPLICATION OF THE GREEN'S FUNCTION METHOD FOR DESCRIBING A SUPERFLUID BOSE LIQUID WITH A STRONG BOSE PAIR CONDENSATE

4.1. Dyson–Belyaev equations and Hugenholtz–Pines method for a Bose liquid with a "depleted" SPBC

In order to describe the properties of a superfluid Bose liquid by using the method of Green's function,[8] Dyson–Belyaev equations[25] are commonly used for expressing the one-particle normal G_{11} and anomalous G_{12} Green's functions in terms of the corresponding eigenenergy components Σ_{11} and Σ_{12}:

$$G_{11}(p)=[G_0^{-1}(-p)-\Sigma_{11}(-p)]/Z(p);$$
$$G_{12}(p)=\Sigma_{12}(p)/Z(p), \tag{26}$$

where

$$Z(p)=[G_0^{-1}(-p)-\Sigma_{11}(-p)][G_0^{-1}(p)-\Sigma_{11}(p)] - |\Sigma_{12}(p)|^2; \tag{27}$$

$$G_0^{-1}(\pm p)=\left[\pm\varepsilon-\frac{\mathbf{p}^2}{2m}+\mu-i\delta\right];$$
$$p=(\mathbf{p},\varepsilon); \quad \delta\to+0; \tag{28}$$

μ is the chemical potential of quasiparticles satisfying the Hugenholtz–Pines relation[26]

$$\mu=\Sigma_{11}(0)-\Sigma_{12}(0). \tag{29}$$

Instead of conventional formulation of the perturbation theory,[8,25] we shall henceforth use the field theory[14,16] renormalized in the range of small momenta, where the initial variables ψ are replaced by "adequate" variables $\tilde{\psi}=\tilde{\psi}_L+\tilde{\psi}_{\rm sh}$ which are combinations of the long-wave "hydrodynamic" variables $\tilde{\psi}_L$ and short-wave "field" variables $\tilde{\psi}_{\rm sh}$. In this theory, the "infrared anomaly of anharmonism"[14,16] leading to a nonanalytic form of the eigenenergy component $\Sigma_{ik}(p)$ for $p\to0$ and to the equality $\Sigma_{12}(0)=0$ is eliminated. In terms of the renormalized variables, we have $\tilde{\Sigma}_{12}(0)\neq0$, so that the same formulas as in the original field theory[8] remain valid for the quasiparticle spectrum $\varepsilon(\mathbf{p})$:

$$\varepsilon(\mathbf{p}\to0)\approx c|\mathbf{p}|; \quad c=[\tilde{\Sigma}_{12}(0)/m^*]^{1/2}, \tag{30}$$

where

$$\frac{1}{m^*}=\frac{2}{B}\left[\frac{1}{2m}+\frac{\partial\tilde{\Sigma}_{11}(0)}{\partial|\mathbf{p}|^2}-\frac{\partial\tilde{\Sigma}_{12}(0)}{\partial|\mathbf{p}|^2}\right], \tag{31}$$

$$B=\left[1-\frac{\partial\tilde{\Sigma}_{11}(0)}{\partial\varepsilon}\right]^2-\tilde{\Sigma}_{11}(0)\frac{\partial^2\tilde{\Sigma}_{11}(0)}{\partial\varepsilon^2} + \frac{1}{2}\frac{\partial^2}{\partial\varepsilon^2}[\tilde{\Sigma}_{12}(0)]^2. \tag{32}$$

In the general case, the spectrum of elementary excitations with zero helicity is defined by the poles of $G_{ik}(p)$, i.e., by zeros of the function $Z(p)$:

$$\varepsilon(\mathbf{p})=\left\{\left[\frac{\mathbf{p}^2}{2m}+\tilde{\Sigma}_{11}^{s}(\mathbf{p})-\mu\right]^2-|\tilde{\Sigma}_{12}(\mathbf{p})|^2\right\}^{1/2}+\tilde{\Sigma}_{11}^{a}(\mathbf{p}), \tag{33}$$

where

$$\tilde{\Sigma}_{11}^{s,a}(\mathbf{p})=\frac{1}{2}[\tilde{\Sigma}_{11}(\mathbf{p},\varepsilon(\mathbf{p}))\pm\tilde{\Sigma}_{11}(-\mathbf{p},-\varepsilon(\mathbf{p}))]. \tag{34}$$

The main difficulty in the theory of Bose systems with an intense SPBC is encountered in the computation of the eigenenergy $\tilde{\Sigma}_{ik}(p)$ written in the form of an infinite sequence of Feynman diagrams with an increasing number of external condensate lines,[25] which corresponds to a power expansion in $n_0^{1/2}$.

However, it was proved for the first time in Ref. 18 that the problem can be simplified considerably in the case of a Bose liquid with a strong interaction between particles, and hence with a strongly suppressed SPBC, when the inequality

$$n_0\ll n'=\left\langle\sum_{\mathbf{p}\neq0}b_{\mathbf{p}}^{+}b_{\mathbf{p}}\right\rangle\approx n, \tag{35}$$

directly opposite to the condition of weak nonideality of a Bose gas in the Bogoliubov theory[6] ($n'\ll n_0\approx n$) holds. In this case, we can confine (to a fairly high degree of accuracy) our analysis of equations for $\tilde{\Sigma}_{11}$ and $\tilde{\Sigma}_{12}$ to only the first term in the expansion in $n_0^{1/2}$, which contains only two condensate lines, and neglect higher-order terms in $n_0^{1/2}$.

The corresponding "truncated" system of equations for $\tilde{\Sigma}_{ik}(p)$ has the form[18]

$$\tilde{\Sigma}_{11}(p)=n_0\Lambda(p)\tilde{V}(p)+n'V(0)+\tilde{\varphi}(p); \tag{36}$$

$$\tilde{\Sigma}_{12}(p)=n_0\Lambda(p)\tilde{V}(p)+\tilde{\Psi}(p), \tag{37}$$

where

$$\tilde{\varphi}(p)=i\int\frac{d^4p'}{(2\pi)^4}G_{11}(p')\tilde{V}(p-p')\Gamma(p,p'); \tag{38}$$

$$\tilde{\Psi}(p)=i\int\frac{d^4p'}{(2\pi)^4}G_{12}(p')\tilde{V}(p-p')\Gamma(p,p'); \tag{39}$$

$$\tilde{V}(p)=V(p)[1-V(p)\Pi(p)]^{-1};$$
$$\Lambda(p)=\Gamma(p,0)=\Gamma(0,p); \tag{40}$$

$$\Pi(p)=i\int\frac{d^4p'}{(2\pi)^4}[G_{11}(p')G_{11}(p'-p) + G_{12}(p')G_{12}(p'-p)]\Gamma(p,p'). \tag{41}$$

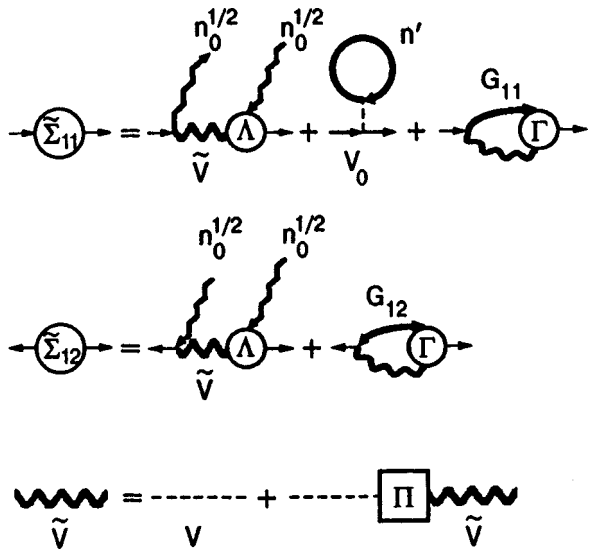

FIG. 4. Diagrammatic representation of the Dyson–Belyaev equations for $\tilde{\Sigma}_{11}$ and $\tilde{\Sigma}_{12}$ for a Bose liquid with a ''depleted'' SPBC in the lowest approximation in the number of condensate lines (taking into account n_0-th order terms) and Dyson's equation for renormalized (''screened'') pair interaction $\tilde{V}$ between bosons.

Here $\Gamma(p,p')$ is the vertex (tripolar) component of the interaction, which describes many-particle effects, $\Pi(p)$ the polarization operator for bosons, $\tilde{V}(p)$ the renormalized (''screened'') Fourier component of the pair interaction potential, and the function $\tilde{\Psi}(p)$ plays the role of a *pair order parameter of the superfluid component* in the boson system. Figure 4 shows equations for $\tilde{\Sigma}_{11}$, $\tilde{\Sigma}_{12}$, and $\tilde{V}$ in the graphic form.

If we disregard the poles of the vortex $\Gamma(p,p')$ and the delay effects in the ''screened'' interaction $\tilde{V}(p)$, i.e., neglect the contribution of two-particle and collective excitations,[2] the integration with respect to frequencies in (38) and (39) can be reduced to the calculation of residues at the poles of one-particle Green's functions $G_{11}(p)$ and $G_{12}(p)$. As a result, the integral equations (38) and (39) combined with (26)–(28), (36), and (37) assume the form (see Ref. 18)

$$\tilde{\Psi}(\mathbf{p}) = -\int \frac{d^3p'}{(2\pi)^3}\Gamma(\mathbf{p},\mathbf{p}')\tilde{V}(\mathbf{p}-\mathbf{p}') \times \frac{n_0\Lambda(\mathbf{p}')\tilde{V}(\mathbf{p}')+\tilde{\Psi}(\mathbf{p}')}{2\varepsilon(\mathbf{p}')}, \tag{42}$$

$$\tilde{\varphi}(\mathbf{p}) = \frac{1}{2}\int \frac{d^3p'}{(2\pi)^3}\Gamma(\mathbf{p},\mathbf{p}')\tilde{V}(\mathbf{p}-\mathbf{p}')\left[\frac{A_0(\mathbf{p}')}{\varepsilon(\mathbf{p}')}-1\right], \tag{43}$$

where

$$A_0(\mathbf{p}) = n_0\Lambda(\mathbf{p})\tilde{V}(\mathbf{p}) + n'V(0) + \tilde{\varphi}(\mathbf{p}) + \frac{\mathbf{p}^2}{2m} - \mu. \tag{44}$$

In this case, the total number of particles is defined by the relation

$$n = n_0 + i\int \frac{d^4p}{(2\pi)^4}G_{11}(p) = n_0 + \frac{1}{2}\int \frac{d^3p}{(2\pi)^3}\left[\frac{A_0(\mathbf{p})}{\varepsilon(\mathbf{p})}-1\right], \tag{45}$$

and relation (29) together with (36) and (37) can be reduced to the form

$$\mu = n'V(0) + \tilde{\varphi}(0) - \tilde{\Psi}(0). \tag{46}$$

However, the coexistence of a weak SPBC and a strong CPC can lead to instability of the ground state of a Bose system (see below).

4.2. Instability of the state of a Bose system with a weak SPBC and a strong CPC

Let us first consider the integral equation (42) for $\mathbf{p}=0$:

$$\tilde{\Psi}(0) = -\int \frac{d^3p}{(2\pi)^3}\frac{n_0[\Lambda(\mathbf{p})\tilde{V}(\mathbf{p})]^2 + \Lambda(\mathbf{p})\tilde{V}(\mathbf{p})\tilde{\Psi}(\mathbf{p})}{2\varepsilon(\mathbf{p})}. \tag{47}$$

It can easily be seen that the first term on the right-hand side of (47), which is proportional to n_0 and independent of $\tilde{\Psi}(\mathbf{p})$, is negative for any sign of $\Lambda(\mathbf{p})$ and $\tilde{V}(\mathbf{p})$. Consequently, if we assume that the minus sign of this inhomogeneous term describing the contribution of SPBC determines in the whole the sign (phase) of the parameter $\tilde{\Psi}(\mathbf{p})$,[3] the state of a Bose system with a weak (''depleted'') SPBC and with a strong CPC can be unstable since, according to Eq. (37),

$$\tilde{\Sigma}_{12}(0) = n_0\Lambda(0)\tilde{V}(0) + \tilde{\Psi}(0) < 0,$$

$$\text{i.e.,}\quad c^2 = \frac{\tilde{\Sigma}_{12}(0)}{m^*} < 0, \tag{48}$$

for $\tilde{\Psi}(0)<0$ and for a small value of n_0 in spite of the condition $\Lambda(0)\tilde{V}(0)>0$ required for ensuring macroscopic stability of the system to spontaneous compression (collapse). In other words, as it was proved for the first time in Ref. 18, the coincidence of the phase $\tilde{\Psi}(\mathbf{p})$ with the phase induced by zero SPBC leads to an *instability of the phonon spectrum of the Bose system* for $n_0 < |\tilde{\Psi}(0)|/\Lambda(0)\tilde{V}(0)$.

It should be noted that, if we neglect the term $\sim n_0$, Eq. (42) assumes a form similar to the equation for the Fourier component of the wave function of a pair of particles in vacuum, i.e.,

$$\Psi_0(\mathbf{p}) = \int \frac{d^3p'}{(2\pi)^3}V(\mathbf{p}-\mathbf{p}')\frac{\Psi_0(\mathbf{p}')}{\omega_0 - 2\varepsilon(\mathbf{p}) + i\delta} \tag{49}$$

with the zero binding energy $\omega_0 \equiv \Omega - \mathbf{P}^2/4m = 0$ where Ω and $\mathbf{P}$ are the total energy and momentum. This analogy shows that a strong CPC is formed only when the *effective potential* $\Gamma(\mathbf{p},\mathbf{p}')\tilde{V}(\mathbf{p}-\mathbf{p}')$ corresponds to the *attraction in a considerable part of the momentum space* essential to the integral with respect to $\mathbf{p}'$ in (42). Such an attraction ($\Gamma\tilde{V}<0$) must be almost sufficient for maintaining the *bound*

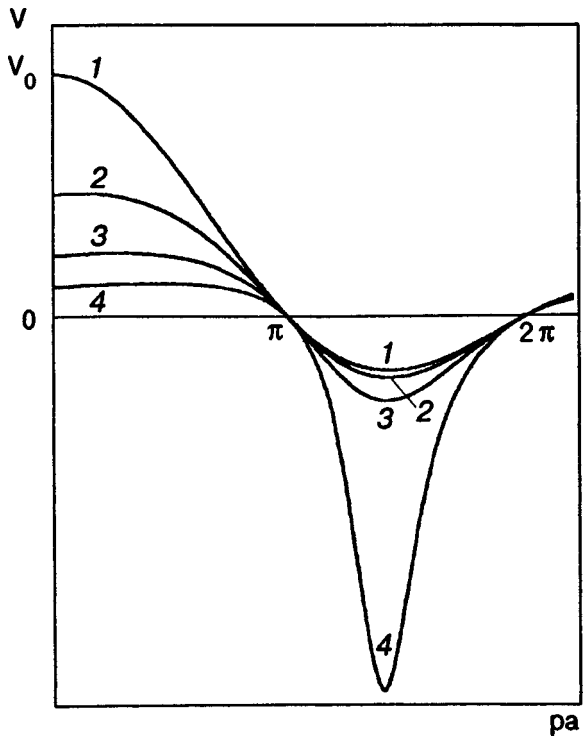

FIG. 5. Dependence of the static ''screened'' potential $\tilde{V}$ on p for the ''rigid spheres'' model in the random-phase approximation for the polarization operator $\Pi(p,0)$ for different values of the dimensionless parameter $\alpha = mV(0)/(\pi a)$: 0 (curve *1*), 1 (curve *2*), 3 (curve *3*), and 7 (curve *4*).

state of a pair of quasiparticles with the kinetic energy $2\varepsilon(\mathbf{p})$, i.e., for the existence of a nontrivial solution ($\tilde{\Psi} \neq 0$) of Eq. (42) for $n_0 \to 0$.

It should be noted in this connection that the static effective potential $\tilde{V}(\mathbf{p})$ can differ considerably from the initial potential $V(\mathbf{p})$ describing the interaction between particles. In particular, since the static polarization operator $\Pi(\mathbf{p},0)$ is negative for any $\mathbf{p}$, the *repulsion is suppressed* in the ''screened'' potential $\tilde{V}(\mathbf{p}) = V(\mathbf{p})[1 - V(\mathbf{p})\Pi(\mathbf{p},0)]^{-1}$ in the range of momenta where $V(\mathbf{p}) > 0$ (for example, for $p < \pi/a$ in the ''rigid spheres'' model), while *attraction is enhanced* in the region where $V(\mathbf{p}) < 0$ (for potential (11), this region corresponds to $\pi/a < p < 2\pi/a$). This circumstance was taken into account in Ref. 35 in which $\Pi(\mathbf{p},0)$ was replaced for simplicity by its long-wave limit $\Pi_0 = -m/\pi a$ for $\mathbf{p} \to 0$. The inclusion of the momentum dependence in the random-phase approximation (RPA) leads to the following expression:

$$\Pi(\mathbf{p},0) = -\frac{m}{2\pi}\left[1 - \frac{a\beta(\mathbf{p})}{2\pi}\operatorname{arctg}\frac{2\pi}{a\beta(\mathbf{p})}\right];$$
$$\beta(\mathbf{p}) = \sqrt{\mathbf{p}^2/4 - 2m\mu}. \tag{50}$$

The corresponding effective potential $\tilde{V}(\mathbf{p})$ for $\mu = 0$ is shown in Fig. 5 for different values of the dimensionless parameter $\alpha = mV(0)/\pi a$. It can be seen that the integral contribution from the region of enhanced attraction for quite large values of α can exceed the contribution from suppressed repulsion in Eq. (42) or (47) for $n_0 = 0$ even in the ''rigid spheres'' model with an infinitely strong repulsion for $r \leqslant a$. The inclusion of the *Van der Waals forces of attraction* in more realistic models of interaction between ^{4}He atoms (like the *Lennard–Jones potential*) must lead to even stronger enhancement of effective attraction, which is sufficient for the formation of a strong CPC in He–II or, probably, bound pairs of ^{4}He atoms (see below).

According to (47), the formation of a CPC is hampered by the negative inhomogeneous term proportional to n_0 and associated with the SPBC, which, in addition, leads to instability of the phonon spectrum if the CPC phase coincides with the SPBC phase (see above). At the same time, the nonlinear inhomogeneous integral equation (42) has in principle a solution for $\tilde{\Psi}(\mathbf{p}) > 0$ also in the case when the phase of a strong CPC differs from the SPBC phase by π. Then the phonon spectrum seems to be stable since $\tilde{\Sigma}_{12}(0) > 0$ and $c^2 > 0$. In this case, however, the stability of the state of a Bose system with a CPC in antiphase with the SPBC for the one-particle branch ($c^2 > 0$) is violated in the channel of two-particle excitations. Indeed, it was proved in Ref. 18 that the signs of the first and second terms in (42) are opposite ($\tilde{\Psi}(\mathbf{p}) > 0, \tilde{V}(\mathbf{p}) < 0$) in the integration domain ($\pi/a < p < 2\pi/a$) in which a CPC can be formed. For this reason, Eq. (42) can formally be written in the form similar to (49):

$$\tilde{\Psi}(\mathbf{p}) = \int \frac{d^3p'}{(2\pi)^3}\Gamma(\mathbf{p},\mathbf{p}')\tilde{V}(\mathbf{p}-\mathbf{p}')\frac{\tilde{\Psi}(\mathbf{p}')}{\tilde{\omega}_0(\mathbf{p}') - 2\varepsilon(\mathbf{p}')}, \tag{51}$$

but with a *negative binding energy* $\tilde{\omega}_0 < 0$. This corresponds to an *unstable state with spontaneous generation of pairs* associated with the ''rotation'' of the CPC phase through π till it coincides with the SPBC phase, i.e., the sign reversal in $\tilde{\Psi}(\mathbf{p})$, which is advantageous from the energy point of view. Indeed, it can easily be seen that the negative ''pairing energy''

$$\Delta E = \frac{i}{2}\int \frac{d^4p}{(2\pi)^4}\tilde{\Sigma}_{12}(p)G_{21}(p)$$
$$= -\frac{1}{2}\int \frac{d^3p}{(2\pi)^3}\frac{[n_0\Lambda(\mathbf{p})\tilde{V}(\mathbf{p}) + \tilde{\Psi}(\mathbf{p})]^2}{2\varepsilon(\mathbf{p})}, \tag{52}$$

appearing in the interaction Hamiltonian averaged over the ground state, i.e.,

$$\langle H_{\text{int}}\rangle = \frac{i}{2}\int \frac{d^4p}{(2\pi)^4}[\tilde{\Sigma}_{11}(p)G_{11}(p) + \tilde{\Sigma}_{12}(p)G_{21}(p)]$$
$$+ \frac{\mu n_0}{2}, \tag{53}$$

has the maximum absolute value when the signs of $\tilde{\Psi}(\mathbf{p})$ and $\Lambda(\mathbf{p})\tilde{V}(\mathbf{p})$ coincide in the momentum range that is most important for (42) and (52) and in which $\Lambda(\mathbf{p})\tilde{V}(\mathbf{p}) < 0$. In other words, the *ground state energy* E_0 *has the minimum value when the phases of CPC and SPBC coincide*. However, the phonon spectrum instability ($c^2 < 0$) appears again for $\tilde{\Psi}(\mathbf{p}) < 0$ in the case of small values of $n_0 \ll n$.

Thus, the instability appearing in the Bose system with an intense CPC and a weak SPBC is preserved for any sign of $\tilde{\Psi}(\mathbf{p})$: it appears in the one-particle spectrum for $\tilde{\Psi}(\mathbf{p})<0$ when the CPC and SPBC phases coincide and in the two-particle spectrum for $\tilde{\Psi}(\mathbf{p})>0$. A possible *way to eliminate the instability of the ground state is the complete suppression of SPBC with preserved CPC* (naturally, if a nontrivial (nonzero) solution of Eq. (42) exists for $n_0=0$).

The assumption concerning the absence of a macroscopically filled SPBC in superfluid ^{4}He does not contradict the experimental results[12] and allows us to explain the complete vanishing of the normal component in He–II at $T\to 0$,[13] i.e., the equality of the density of the superfluid component to the total density of ^{4}He, in spite of the strong ''depletion'' of the SPBC due to the interaction between particles in the Bose liquid. In this case, the *superfluid component ρ_s is determined* not by strong CPC as in a weakly nonideal Bose gas,[6] but *by the ''Cooper'' CPC and higher many-particle condensates containing even numbers of free particles*.[18]

4.3. One-particle spectrum of a Bose system with CPC and without SPBC and the superfluidity criterion

In the absence of SPBC ($n_0=0$), all field diagrams with condensate lines disappear in the expansions of $\tilde{\Sigma}_{ik}(p)$ in $n_0^{1/2}$,[25] and Eqs. (36) and (37) for $n'=n$ are transformed into the identities[18]

$$\tilde{\Sigma}_{11}(p)\equiv nV(0)+\tilde{\varphi}(p);\quad \tilde{\Sigma}_{12}(p)\equiv\tilde{\Psi}(p). \tag{54}$$

In this case, Eqs. (42)–(45) at $T=0$ assume the form

$$\tilde{\Psi}(\mathbf{p})=-\int\frac{d^3p'}{(2\pi)^3}\Gamma(\mathbf{p},\mathbf{p}')\tilde{V}(\mathbf{p}-\mathbf{p}')\frac{\tilde{\Psi}(\mathbf{p}')}{2\varepsilon(\mathbf{p}')}; \tag{55}$$

$$\tilde{\varphi}(\mathbf{p})=\frac{1}{2}\int\frac{d^3p'}{(2\pi)^3}\Gamma(\mathbf{p},\mathbf{p}')\tilde{V}(\mathbf{p}-\mathbf{p}')\left[\frac{A(\mathbf{p}')}{\varepsilon(\mathbf{p}')}-1\right]; \tag{56}$$

$$\varepsilon(\mathbf{p})=\sqrt{A^2(\mathbf{p})-|\tilde{\Psi}(\mathbf{p})|^2}, \tag{57}$$

where

$$A(\mathbf{p})=\frac{\mathbf{p}^2}{2m}-\mu+nV(0)+\tilde{\varphi}(\mathbf{p});$$
$$n=\frac{1}{2}\int\frac{d^3p}{(2\pi)^3}\left[\frac{A(\mathbf{p})}{\varepsilon(\mathbf{p})}-1\right]. \tag{58}$$

It can be seen that Eq. (55) for the ''pair'' order parameter $\tilde{\Psi}(\mathbf{p})$ for $n_0=0$ becomes homogeneous. This means that the *CPC phase is independent and arbitrary* and characterizes the *degeneracy of the ground state of the Bose liquid* (in analogy with the degeneracy of the ground state of superconductors[9]).

Accordingly, the *two-particle spectral branch $E(\mathbf{p})$* which is determined by the poles of the two-particle Green's function and contains in the structure of the dynamic form factor $S(\mathbf{p},\varepsilon)$ is the *Goldstone mode* corresponding to *hydrodynamic sound*.[15] At the same time, the one-particle branch $\varepsilon(\mathbf{p})$ may in principle have a finite gap $\Delta_0\neq 0$ for $\mathbf{p}=0$ since we cannot rightfully assume that relation (29) based on the expansion of $\tilde{\Sigma}_{ik}(p)$ into a power series in $n_0^{1/2}$ for a fixed phase of the parameters $\tilde{\Sigma}_{11}(p)$ and $\tilde{\Sigma}_{12}(p)$ still holds in our case (for an arbitrary phase $\tilde{\Psi}$) (see Ref. 18).

Moreover, according to Refs. 18 and 29, a decrease in the gap Δ_0 upon an increase in the number density n of particles (or external pressure P) in a Bose system with a ''gap-type'' one-particle spectrum $\varepsilon(\mathbf{p})$ leads to the loss of stability of the system for a certain finite value of $\Delta_0\neq 0$. In other words, the vanishing and emergence of SPBC is accompanied by a jump in n_0 and Δ_0. This means that a *transition from a state with SPBC* ($n_0\neq 0$) and with an acoustic spectrum $E(\mathbf{p})\approx pc$ of elementary excitations for $\mathbf{p}\to 0$ *to a state with CPC but without SPBC* ($n_0=0$) and with a reconstructed gap-type one-particle spectrum ($\Delta_0\neq 0$) upon a change in n or P is a *first-order phase transition*.

Finally, we must take into account the fact that the gap spectrum $\varepsilon(\mathbf{p})=\sqrt{\Delta_0^2+\mathbf{p}^2\tilde{u}^2}$ for small values of $\mathbf{p}$ lies above the collective acoustic spectrum $E(\mathbf{p})\approx pc$ so that we cannot disregard the contribution from the poles $\Gamma(\mathbf{p},\mathbf{p}')$ and $\tilde{V}(\mathbf{p}-\mathbf{p}')$ while calculating the integrals with respect to frequencies in (38) and (39), and Eqs. (42) and (43) are insufficient for describing the superfluid state of the Bose liquid.

In this connection, let us consider an alternative possibility of the existence of an *acoustic one-particle spectrum* $\varepsilon(\mathbf{p})\sim p$ for $\mathbf{p}\to 0$ in a superfluid Bose liquid with CPC but without SPBC, which was discussed in Refs. 20 and 35. Such a possibility is realized under the assumption that the *Hugenholtz–Pines theorem*[26] is valid as before [see Eqs. (29) and (46) for $n'\equiv n$]. For arbitrary values of $\mathbf{p}$, the one-particle spectrum (57) taking (58) into account assumes the form

$$\varepsilon(\mathbf{p})=\left\{\left[\frac{\mathbf{p}^2}{2m}+\tilde{\varphi}(\mathbf{p})-\tilde{\varphi}(0)+\tilde{\Psi}(0)\right]^2-\left|\tilde{\Psi}(\mathbf{p})\right|^2\right\}^{1/2}. \tag{59}$$

For $\mathbf{p}\to 0$, this equation leads to

$$\varepsilon(\mathbf{p}\to 0)\approx|\mathbf{p}|\tilde{u};\quad \tilde{u}^2=\tilde{\Psi}(0)/m^*, \tag{60}$$

where

$$\frac{1}{m^*}=\left\{\frac{1}{m}+2\left[\frac{\partial\tilde{\varphi}(\mathbf{p})}{\partial|\mathbf{p}|^2}-\frac{\partial\tilde{\Psi}(\mathbf{p})}{\partial|\mathbf{p}|^2}\right]_{\mathbf{p}=0}\right\}. \tag{61}$$

It should be emphasized that the velocity $\tilde{u}$ is not equal to the velocity c of hydrodynamic sound, and $\tilde{u}^2>0$ for $\tilde{\Psi}(0)>0$. For large values of momentum, Eq. (59) becomes quadratic in $\mathbf{p}$, and hence must have a minimum (or point of inflection) in the region of intermediate values of $\mathbf{p}\neq 0$ in order to ensure the stability to quasiparticle decays. Indeed, it follows from the integral equation (55) with the difference kernel $\tilde{V}(\mathbf{p}-\mathbf{p}')$ that the *modulus of $\tilde{\Psi}(\mathbf{p})$ may have a maximum at the point of a negative minimum of the renormalized (''screened'') pair interaction potential $\tilde{V}(\mathbf{p})$* (see Fig. 5) if the main contribution to the integral with respect to $\mathbf{p}'$ comes from the region of small values of $|\mathbf{p}'|\ll p_{\min}$. This means that, according to (59), the *one-particle spectrum $\varepsilon(\mathbf{p})$ may have a local minimum* near the point $p=p_{\min}$ (Fig. 6). Con-

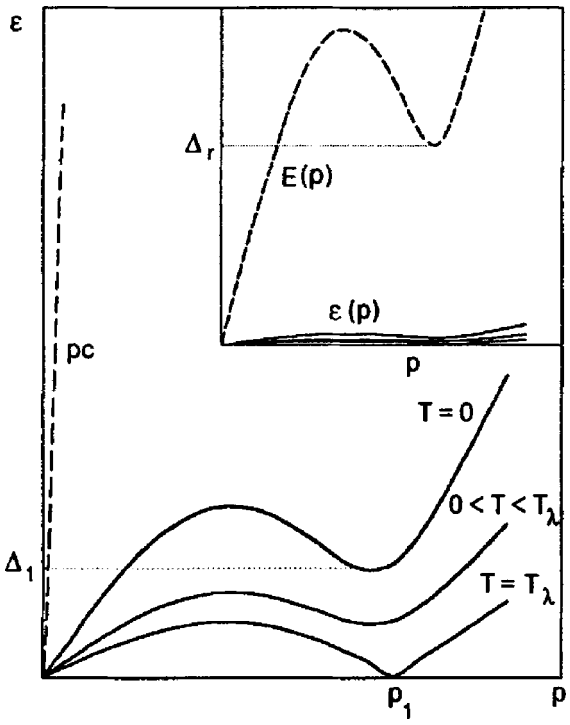

FIG. 6. Predicted form of the gapless one-particle spectrum $\varepsilon(p)$ for bosons in the superfluid Bose liquid with CPC but without SPBC at different temperatures. The dashed curve shows the experimental spectrum of elementary excitations $E(p)$ in ^{4}He for the ratio $\Delta_r/\Delta_1=30$, which corresponds to the maximum critical velocity $v_{cm}=2$ m/s at $T=0$.

sequently, there exists a nonzero value of $v_c=\min[\varepsilon(\mathbf{p})/p]\neq 0$ for $p\approx p_{\min}$, i.e., spectrum (59) satisfies the Landau superfluidity criterion.[1]

On the other hand, the one-particle spectrum (59) for $\tilde{\Psi}(\mathbf{p})\to 0$ degenerates into a quadratic dependence $\varepsilon(\mathbf{p})\sim\mathbf{p}^2$ for small $\mathbf{p}$ and does not satisfy the superfluidity criterion any longer since in this case $\min[\varepsilon(\mathbf{p})/p]=0$ for $p=0$. For this reason, the superfluid Bose liquid with vanishing CPC in the absence of SPBC ($n_0=0$) must be transformed to the normal state in spite of the fact that the ''rotonic'' minimum is preserved in the collective spectrum $E(\mathbf{p})$ (i.e., $E(\mathbf{p})$ formally satisfies the superfluidity criterion). It will be proved below that CPC can vanish upon heating.

4.4. Phase transitions in a Bose liquid with strong CPC

At finite temperatures ($T\neq 0$), the system of equations (42)–(45) taking into account (46) for a Bose liquid with a ''depleted'' SPBC and a strong CPC has the form[18]

$$\tilde{\Psi}_T(\mathbf{p})=-\int\frac{d^3p'}{(2\pi)^3}\Gamma(\mathbf{p},\mathbf{p}')\tilde{V}(\mathbf{p}-\mathbf{p}')\times\frac{n_0\Lambda(\mathbf{p}')\tilde{V}(\mathbf{p}')+\tilde{\Psi}_T(\mathbf{p}')}{2\varepsilon_T(\mathbf{p}')}\coth\frac{\varepsilon_T(\mathbf{p}')}{2T};\quad(62)$$

$$\tilde{\varphi}_T(\mathbf{p})=\frac{1}{2}\int\frac{d^3p'}{(2\pi)^3}\Gamma(\mathbf{p},\mathbf{p}')\tilde{V}(\mathbf{p},\mathbf{p}')\times\left[\frac{A_T(\mathbf{p}')}{\varepsilon_T(\mathbf{p}')}\coth\frac{\varepsilon_T(\mathbf{p}')}{2T}-1\right];\quad(63)$$

$$n=n_0(T)+\frac{1}{2}\int\frac{d^3p}{(2\pi)^3}\left[\frac{A_T(\mathbf{p})}{\varepsilon_T(\mathbf{p})}\coth\frac{\varepsilon_T(\mathbf{p})}{2T}-1\right],\quad(64)$$

where

$$A_T(\mathbf{p})=n_0\Lambda(\mathbf{p})\tilde{V}(\mathbf{p})+\frac{\mathbf{p}^2}{2m}+\tilde{\varphi}_T(\mathbf{p})-\tilde{\varphi}_T(0)+\tilde{\Psi}_T(0),\quad(65)$$

$\varepsilon_T(\mathbf{p})$ is defined by expression (33), and $\tilde{\varphi}$ and $\tilde{\Psi}$ in Eqs. (36) and (37) are replaced by $\tilde{\varphi}_T$ and $\tilde{\Psi}_T$.

We first assume that the SPBC density at $T=0$ is small ($n_0\ll n$), but $n_0>|\tilde{\Psi}(0)|/\Lambda(0)\tilde{V}(0)$ so that $\tilde{\Sigma}_{12}(0)>0$ and $c^2>0$ (see (48)). However, as the temperature increases, thermal ''depletion'' of SPBC must take place, i.e., the value of $n_0(T)$ decreases upon heating and becomes smaller than $|\tilde{\Psi}_T(0)|/\Lambda(0)\tilde{V}(0)$ above a certain value T_0. In this case, the one-particle phonon spectrum becomes unstable (since $\tilde{\Sigma}_{12}(0)<0$ and $c^2<0$), and the Bose system is abruptly transformed into a state with a CPC but without SPBC ($n_0=0$), i.e., a *first-order transition in temperature occurs at the point* $T=T_0$.[4)] If, however, the inequality $n_0<|\tilde{\Psi}(0)|/\Lambda(0)\tilde{V}(0)$ holds even at $T=0$ due to strong interaction between particles, such a transition does not take place (since the SPBC is initially suppressed), and the superfluid component of the Bose liquid is determined initially by a ''Cooper-type'' CPC and higher even condensates that form a pair CEC in aggregate.[18] In this case, Eqs. (62) and (64) for any $T\geqslant 0$ have the form ($n_0=0$)

$$\tilde{\Psi}_T(\mathbf{p})=-\int\frac{d^3p'}{(2\pi)^3}\Gamma(\mathbf{p},\mathbf{p}')\tilde{V}(\mathbf{p}-\mathbf{p}')\times\frac{\tilde{\Psi}_T(\mathbf{p}')}{2\varepsilon_T(\mathbf{p}')}\coth\frac{\varepsilon_T(\mathbf{p}')}{2T};\quad(66)$$

$$n=\frac{1}{2}\int\frac{d^3p}{(2\pi)^3}\left[\frac{A_T(\mathbf{p})}{\varepsilon_T(\mathbf{p})}\coth\frac{\varepsilon_T(\mathbf{p})}{2T}-1\right],\quad(67)$$

where $\varepsilon_T(\mathbf{p})$ is defined by formula (59) in which $\tilde{\varphi}(\mathbf{p})$ and $\tilde{\Psi}(\mathbf{p})$ are replaced by $\tilde{\varphi}_T(\mathbf{p})$ and $\tilde{\Psi}_T(\mathbf{p})$ so that $\varepsilon_T(\mathbf{p})\approx p\sqrt{\tilde{\Psi}_T(0)/m^*}$ for $\mathbf{p}\to 0$.

It was noted above that a nontrivial (nonzero) solution of the homogeneous integral equation (55) at $T=0$, and hence of Eq. (66) at $T>0$ for the pair order parameter $\tilde{\Psi}_T(\mathbf{p})$, is possible only if the main contribution to the integral with respect to $\mathbf{p}'$ comes from the region of a strong effective attraction between particles ($\Gamma\tilde{V}<0$). With increasing T, such an attraction must be enhanced due to an increase in the thermal factor $\coth\varepsilon_T(\mathbf{p}')/2T$ in the integrand of (66), i.e., the parameter $\tilde{\Psi}_T(\mathbf{p})$ should apparently increase with T.

On the other hand, for a boson concentration n which remains unchanged or decreases upon an increase in T, the first term in (67) may remain constant or decrease upon an increase in the ''thermal component'' $\sim\coth\varepsilon_T(\mathbf{p})/2T$ only if the coefficient $A_T(\mathbf{p})$ decreases accordingly, i.e., if $\tilde{\Psi}_T(0)$ in (65) decreases quite rapidly upon an increase in T. According to Eq. (66), for $\mathbf{p}=0$ we have

$$\tilde{\Psi}_T(0) = -\int_0^\infty \frac{p^2 dp}{2\pi^2}\Lambda(\mathbf{p})\tilde{V}(\mathbf{p})\frac{\tilde{\Psi}_T(\mathbf{p})}{2\varepsilon_T(\mathbf{p})}\coth\frac{\varepsilon_T(\mathbf{p})}{2T}, \tag{68}$$

and the value of $\tilde{\Psi}_T(0)$ must indeed decrease with heating as a result of the competition between opposite contributions from two regions in the momentum space, i.e., the region of small $p<\pi/a$, in which repulsion prevails $\tilde{V}(\mathbf{p})>0$, and the region $\pi/a<p<2\pi/a$ of intermediate values of momentum, in which effective attraction between bosons $\tilde{V}(\mathbf{p})<0$ is observed (see Fig. 5). If the contribution from the second integration domain (corresponding to attraction) prevails at $T=0$, we have $\tilde{\Psi}_T(0)>0$. But as the value of T becomes higher, the contribution from the first region (repulsion) increases due to the increase in the width and height of the peak of the ''thermal'' function $(1/\varepsilon_T(\mathbf{p}))\coth\varepsilon_T(\mathbf{p})/2T \sim T/\mathbf{p}^2$ for $\mathbf{p}\to 0$ so that the value of $\tilde{\Psi}_T(0)$ decreases and tends to zero at a certain ''critical'' temperature T_c^* at which the negative and positive integral contributions to the right-hand side of (68) have equal absolute values.

However, for $\tilde{\Psi}_T(0)\to 0$ the one-particle spectrum $\varepsilon_T(\mathbf{p})$ degenerates into a parabolic spectrum for small $\mathbf{p}$ (see above):

$$\varepsilon_T(\mathbf{p}) \approx \frac{\mathbf{p}^2}{2m_0^*}; \quad \frac{1}{m_0^*} = \frac{1}{m} + \frac{\partial\tilde{\varphi}_T(\mathbf{p})}{\partial|\mathbf{p}|^2}\bigg|_{\mathbf{p}=0}. \tag{69}$$

As a result, the ''thermal'' function $[1/\varepsilon_T(\mathbf{p})] \times\coth(\varepsilon_T(\mathbf{p})/2T)\sim T/\mathbf{p}^4$ for $\mathbf{p}\to 0$, which leads to the divergence of the integral on the right-hand side of (68) at the lower limit (for $\mathbf{p}=0$) and to an infinitely large negative contribution due to repulsion $\Lambda(0)\tilde{V}(0)>0$. It follows hence that a nontrivial solution of Eq. (66) at $T\neq 0$ can exist only when $\tilde{\Psi}_T(0)>0$ and $\varepsilon_T(\mathbf{p})\sim p$ for $p\to 0$ due to prevailing attraction. This means that a *transition from the superfluid state in which* $\tilde{\Psi}_T(\mathbf{p})\neq 0$ and $v_c=\min[\varepsilon_T(\mathbf{p})/p]\neq 0$ to the normal state in which $\tilde{\Psi}_T(\mathbf{p})=0$ and $v_c=0$ is accompanied by a jump in the value of $\tilde{\Psi}_T(0)$ from a certain finite (minimum) value to zero, and hence is a *first-order phase transition*.[5)] The temperature $T_c<T_c^*$ corresponding to this transition can be put in correspondence with the temperature at which the minimum of the ratio $\varepsilon_T(\mathbf{p})/p$, and hence the critical velocity v_c of superfluidity, vanish (see Fig. 6), i.e., T_c corresponds to the λ-point in ^{4}He.

The situation with disappearing superfluidity in a Bose liquid above $T_c=T_\lambda$ is similar to the mechanism of superconductivity vanishing in an electron Fermi liquid of metals,[9] in which the superconducting order parameter Ψ_S, the energy gap Δ in the quasiparticle spectrum at the Fermi level, and the critical velocity $v_c=\Delta/p_F$ determining the maximum critical depairing current vanish simultaneously at $T=T_c$. However, a transition from the *superconducting to the normal state in superconductors* in zero magnetic field is known to be a *second-order phase transition*.[9,11] Such a transition is accompanied by a finite jump in the heat capacity $C_v(T)$ and can be described to a high degree of accuracy by the *Landau theory of phase transitions* in the self-consistent field approximation (*Ginzburg–Landau equation*). This is due to a strong (on the atomic scale) correlation length (or coherence length ξ_0) in traditional superconductors, and accordingly due to an anomalously small value of the dimensionless Ginzburg number $\mathrm{Gi}\lesssim 10^{-12}$,[59] which characterizes the relatively large width of the fluctuation region near T_c (in high-T_c superconductors with an anomalously small value of ξ_0, the number $\mathrm{Gi}\lesssim 10^{-3}-10^{-2}$).[60]

On the contrary, in *liquid* ^{4}He the number $\mathrm{Gi}\sim 1$ so that *critical fluctuations* with frequencies $\omega_q\sim q^{3/2}$ play a decisive role[59] in this case near the temperature T_λ of transition from the superfluid (He–II) to the normal (He–I) state, and the *Landau theory of the self-consistent field is inapplicable*. This explains, among other things, the *logarithmic divergence of the heat capacity* $C_v(T)$ of liquid helium at the λ-point,[7,61] but the *transition at* $T=T_\lambda$ *remains a second-order phase transition*.

Generally speaking, this is in contradiction with the conclusion [which follows from Eq. (66)] about a *first-order phase transition* at $T=T_c$ with a finite jump in the ''pair'' order parameter $\tilde{\Psi}_T(0)$, but with a smooth vanishing of the critical velocity $v_c(T)=\min[\varepsilon_T(p)/p]$ for $T\to T_c$ (according to the results of measurements of v_c for He–II in ultrathin channels near the λ-point).[10] It should be borne in mind, however, that the integral equation (66) for $\tilde{\Psi}_T(p)$ essentially corresponds to the mean (self-consistent) field approximation and hence cannot be applied in the vicinity of the critical temperature in view of fluctuation effects for $\mathrm{Gi}\sim 1$. In this case, the *order parameter* $\tilde{\Psi}_T(0)$ *is suppressed by large-scale critical fluctuations* below T_c (and, conversely, is initiated above T_c) in a fairly wide temperature range $\Delta T=|T_c-T|\lesssim T_c$.

For this reason, the acoustic part of the one-particle spectrum $\varepsilon_T(\mathbf{p})\approx p\tilde{u}_T$ with $\tilde{u}_T=\sqrt{\tilde{\Psi}_T(0)/m^*}$ near T_c must be strongly blurred due to fluctuations in $\tilde{\Psi}_T(0)$, i.e., *long-wave excitations must attenuate rapidly* with time, and hence cannot make a noticeable contribution to the kinetic and thermodynamic properties of liquid ^{4}He. In the region of large momenta $\mathbf{p}$, the role of fluctuations is not so important, and the conclusion following from (66) and concerning the existence of the minimum value of $\varepsilon_T(\mathbf{p})/p$ that can vanish at $T=T_c$ (i.e., at the λ-point) remains in force (see Fig. 6).

Moreover, it was noted above (see footnote 5) that a phase transition from the superconducting to the normal state in finite-size systems (thin channels, films, or capillaries) may remain a second-order phase transition even in the self-consistent field approximation since the divergence of the integral in (68) is absent at the lower limit for a quadratic spectrum $\varepsilon(\mathbf{p})\sim\mathbf{p}^2$, and the point T_c^* can be lower on the temperature scale than the phase-transition point $T_c=T_\lambda$ in the case of a strong attraction (in the range of $p>\pi/a$).

4.5. Structure of boson pairs in CPC

It was noted in Sec. 3 that over-the-condensate excitations in a weakly nonideal Bose gas with a strong SPBC are combined into free (unbound) boson pairs with antiparallel

momenta. The wave function of such a gas in the first order of the Bogoliubov–Zubarev perturbation theory[62] has the form

$$|\Phi_B\rangle=\exp\left\{-\frac{1}{4V}\sum_{\mathbf{p}\neq 0}U_B(\mathbf{p})\hat{n}_{\mathbf{p}}\hat{n}_{-\mathbf{p}}\right\}|0\rangle, \tag{70}$$

where

$$U_B(\mathbf{p})=\frac{1}{n}\left[\frac{2m}{\mathbf{p}^2}E_B(\mathbf{p})-1\right];\quad \hat{n}_{\mathbf{p}}=b_{\mathbf{p}}^{+}b_{\mathbf{p}}; \tag{71}$$

V is the system volume, and $E_B(\mathbf{p})$ the Bogoliubov spectrum (2). For small $\mathbf{p}$ for which $E_B(\mathbf{p})\approx pu_B(0)$, we obtain from (71)

$$U_B(\mathbf{p})\approx\frac{2mu_B(0)}{n|\mathbf{p}|};\quad u_B(0)=\sqrt{nV(0)/m}, \tag{72}$$

so that the long-wave asymptotic form of the potential $U_B(\mathbf{r})$ for $\mathbf{r}\to\infty$ has the form

$$U_B(\mathbf{r})\approx\frac{mu_B(0)}{2\pi n\mathbf{r}^2}. \tag{73}$$

Let us prove that a similar asymptotic form is also typical of strongly bound (''local'') boson pairs. The wave function of the condensate of N independent boson pairs with zero total momentum in the configuration space and in the representation of secondary quantization has respectively the form[18]

$$\Phi=C\sum_{(P)}\prod_{j=1}^{2N-1}f(\mathbf{r}_j-\mathbf{r}_{j+1});\quad |\Phi\rangle=\frac{(\hat{O}^{+})^N}{(N!)^{1/2}}|0\rangle, \tag{74}$$

where C is the normalization factor, and the sum $\Sigma_{(P)}$ is the sum over all transpositions of the arguments of the function f, while $\hat{O}^{+}$ is the pair creation operator:

$$\hat{O}^{+}=\int{}'\frac{d\mathbf{r}\,d\mathbf{r}'}{(v_0V)^{1/2}}f^{*}(\mathbf{r}-\mathbf{r}')\hat{\psi}^{+}(\mathbf{r})\hat{\psi}^{+}(\mathbf{r}')$$

$$=\frac{1}{(v_0V)^{1/2}}\sum_{\mathbf{p}}{}'f(\mathbf{p})b_{\mathbf{p}}^{+}b_{-\mathbf{p}}^{+}. \tag{75}$$

The prime on the symbols of integral and sum indicates here that the integration or summation domains are bounded by the half-space in order to avoid taking into account the same state twice, and the correlation volume v_0 is defined by the relations

$$\int{}'d\mathbf{r}\,d\mathbf{r}'|f(\mathbf{r}-\mathbf{r}')|^2=v_0V;$$

$$\int d\mathbf{r}|f(\mathbf{r})|^2=v_0\equiv\frac{4}{3}\pi r_0^3. \tag{76}$$

In analogy with the well-known relations for the Bose condensate of ''elementary'' bosons, i.e.,

$$\langle\hat{\psi}(\mathbf{r})\rangle=\frac{1}{V^{1/2}}\sum_{n}f_n(\mathbf{r})\langle\hat{b}_n\rangle;\quad \langle\hat{b}_n\rangle=N^{1/2}\delta_{n0}, \tag{77}$$

where $\hat{b}_n$ is the annihilation operator and $f_n(\mathbf{r})$ the wave function of a particle in the nth quantum state, we can present, in accordance with (75) and (76), anomalous average values for the condensate of N bound boson pairs in the configuration and momentum spaces in the form[18]

$$\langle\hat{\psi}(\mathbf{r})\hat{\psi}(\mathbf{r}')\rangle=\left(\frac{n}{v_0}\right)^{1/2}f(\mathbf{r}-\mathbf{r}');\quad \langle b_{\mathbf{p}}b_{-\mathbf{p}}\rangle=\left(\frac{n}{v_0}\right)^{1/2}f(\mathbf{p}), \tag{78}$$

where $n\equiv N/V$. It should be emphasized that the possibility of considering the pair operators $\hat{O}^{+}$ and $\hat{O}$ as boson operators is, strictly speaking, substantiated only in the case when the size of pairs is smaller than the average distance between them ($r_0\ll n^{-1/3}$), and the wave functions of pairs do not overlap.

In the case of *overlapping pairs*, the wave function of the condensate taking into account correlations between particles belonging to different pairs can be chosen in the form of the *Jastrow function*[38]

$$\Phi_J=\prod_{i<j}f(|\mathbf{r}_i-\mathbf{r}_j|)=\exp\left\{-\frac{1}{2}\sum_{i<j}U(|\mathbf{r}_i-\mathbf{r}_j|)\right\}, \tag{79}$$

where $U(\mathbf{r})$ is the potential energy of pair interactions between particles.

For a Bose system with SPBC, the wave function $f(\mathbf{r}-\mathbf{r}')$ in (79) correctly describes strong pair correlations at short distances and is determined by the form of the interaction $U(\mathbf{r}-\mathbf{r}')$. At the same time, Φ_J at large distance corresponds to the asymptotic form following from the general postulates of quantum hydrodynamics,[7] and hence $f(\mathbf{r}-\mathbf{r}')$ for $|\mathbf{r}-\mathbf{r}'|\to\infty$ becomes universal and varies according to a power (quadratic) law.[36,37] Indeed, the *ground state in hydrodynamics is a vacuum of independent acoustic vibrations* (phonon harmonic oscillators) with frequencies $\omega=pc$, whose wave function is given by

$$|\Phi_{\mathrm{ph}}\rangle=\exp\left\{-\frac{1}{4N}\sum_{|\mathbf{p}|<Q}\frac{2mc}{|\mathbf{p}|}n_{\mathbf{p}}n_{-\mathbf{p}}\right\}|0\rangle, \tag{80}$$

where

$$n_{\mathbf{p}}=\sum_{j=1}^{N}e^{i\mathbf{p}\mathbf{r}_j};\quad n(\mathbf{r})=\sum_j\delta(\mathbf{r}-\mathbf{r}_j')=\frac{1}{V}\sum_{\mathbf{p}}n_{\mathbf{p}}e^{i\mathbf{p}\cdot\mathbf{r}}. \tag{81}$$

Expression (80) can be written in the form of the Jastrow function (79):

$$\Phi_{\mathrm{ph}}=\exp\left\{-\frac{1}{2}\sum_{i<j}U_{\mathrm{ph}}(\mathbf{r}_i-\mathbf{r}_j)\right\}$$

$$=\exp\left\{-\frac{1}{4V}\sum_{\mathbf{p}}U_{\mathrm{ph}}(\mathbf{p})n_{\mathbf{p}}n_{-\mathbf{p}}\right\}, \tag{82}$$

where

$$U_{\mathrm{ph}}(\mathbf{p})=\frac{2mc}{n|\mathbf{p}|};$$

$$U_{\mathrm{ph}}(\mathbf{r})=\frac{1}{V}\sum_{\mathbf{p}}U_{\mathrm{ph}}(\mathbf{p})e^{i\mathbf{p}\cdot\mathbf{r}}=\frac{mc}{2\pi n\mathbf{r}^2}. \tag{83}$$

Thus, we obtain the Reatto–Chester quadratic asymptotic form[36] for the wave function $f(\mathbf{r})$ of pairs for $\mathbf{r}\to\infty$:

$$f(\mathbf{r}\to\infty)\approx f_{\rm ph}(\mathbf{r})=\exp\left\{-\frac{1}{2}U_{\rm ph}(\mathbf{r})\right\}$$
$$\approx 1-\frac{U_{\rm ph}(\mathbf{r})}{2}=1-\frac{mc}{4\pi n\mathbf{r}^2}. \qquad (84)$$

It should be noted that the wave function (70) of a weakly nonideal Bose gas also has the form of the Jastrow function (79).

According to (84), the Fourier component of the wave function of a pair is given by

$$f_{\rm ph}(\mathbf{p})\approx -\frac{1}{2}U_{\rm ph}(\mathbf{p})=-\frac{mc}{n|\mathbf{p}|}, \qquad (85)$$

in analogy with the case of unbound ''Bogoliubov's'' pairs with an infinitely large radius [see Eq. (72)].

On the other hand, taking into account relations (81), we obtain the following asymptotic form for the anomalous mean:

$$\langle b_{\mathbf{p}}b_{-\mathbf{p}}\rangle\approx -\left(\frac{n}{v_0}\right)^{1/2}\frac{mc}{n|\mathbf{p}|}. \qquad (86)$$

In a Bose liquid with CPC but without SPBC, the one-particle spectrum $\varepsilon(\mathbf{p})$ with the gap $\Delta_0\neq 0$ for $\mathbf{p}=0$ corresponds to a Hamiltonian of the Bogoliubov type (see Sec. 3), from which we can obtain the following expression for the anomalous mean in the ground state (see Ref. 18):

$$\langle b_{\mathbf{p}}b_{-\mathbf{p}}\rangle\approx -\frac{\tilde{\Psi}(\mathbf{p})}{(\Delta_0^2+\mathbf{p}^2\tilde{u}^2)^{1/2}}. \qquad (87)$$

Taking into account the universal nature of relation (78), we obtain the asymptotic form of the (correlation) wave function for $\mathbf{p}\to 0$:

$$f(\mathbf{p})\sim\langle b_{\mathbf{p}}b_{-\mathbf{p}}\rangle\approx -\frac{2\Delta_0\tilde{\Psi}(0)}{\tilde{u}^2(\kappa_0^2+\mathbf{p}^2)};\quad \kappa_0^2=\frac{2\Delta_0^2}{\tilde{u}^2}. \qquad (88)$$

This expression leads to the following relation for the spatial component $f(\mathbf{r})$ for $\mathbf{r}\to\infty$[18]:

$$|f(\mathbf{r})-1|\sim\frac{\Delta_0\tilde{\Psi}(0)}{2\pi\tilde{u}^2 r}\,e^{-\kappa_0 r}. \qquad (89)$$

In other words, the power asymptotic form of the pair correlation function (86) in the presence of a gap ($\Delta_0\neq 0$) in the one-particle spectrum is transformed to an exponential dependence.

On the other hand, a comparison of (86) and (87) shows that *in the absence of a gap* ($\Delta_0=0$) the conventional Reatto–Chester power asymptotic form[36,37] is recovered in a Bose liquid having a CPC but no SPBC and the spectrum $\varepsilon(\mathbf{p})\approx p\tilde{u}$ for $\mathbf{p}\to 0$:

$$\langle b_{\mathbf{p}}b_{-\mathbf{p}}\rangle\approx -\tilde{\Psi}(0)/\tilde{u}|\mathbf{p}|;\quad |f(\mathbf{r})-1|\sim\tilde{\Psi}(0)/4\pi\tilde{u}\mathbf{r}^2. \qquad (90)$$

Thus, the emergence of bound pairs in CPC and the vanishing of SPBC do not necessarily lead to a change in the asymptotic form of the pair correlation function. The superfluid state having a CPC but no SPBC and characterized by an acoustic one-particle spectrum [$\varepsilon(\mathbf{p})\sim p$] has the regular hydrodynamic asymptotic form of pair correlations ($\sim r^{-2}$), satisfies the Hugenholtz–Pines theorem,[26] and has a ''pair'' structure of the CEC which contains only ''even'' condensates (bound boson pairs existing only in CPC). Indeed, the existence of an ''odd'' (e.g., three-particle) condensate $\langle\hat{\psi}\hat{\psi}\hat{\psi}\rangle\neq 0$ would have led to the emergence of a SPBC owing to the interaction with the CPC. Bosons in higher ''even'' condensates do not form bound many-particle states since different types of bound coherent systems (phases) cannot co-exist in a one-component Bose liquid (in contrast to mixtures of different Bose- and Fermi liquids).

4.6. Role of pair correlations in Bose liquid ^{4}He in mixtures of quantum liquids ^{3}He–^{4}He

4.6.1. Experimental evidence of the existence of bound pairs of helium atoms in superfluid ^{4}He. The important role of pair correlations between bosons (^{4}He atoms) in the superfluid state of a quantum Bose liquid is indirectly confirmed by the successful application of the Jastrow approximation[38] for the wave function of the ground state in the description of properties of He–II.[39,40] On the other hand, the theoretical results obtained in Refs. 15 and 18 lead to the quite justified assumption that the structure of the superfluid component in liquid ^{4}He below the λ-point is determined by the pair CEC containing a strong CPC with the bound states of boson pairs as well as higher-order even condensates and absolutely no SPBC or higher-order odd condensates.

It was noted in Ref. 35 that the anomalously high value of the effective mass m_3^* of ^{3}He impurity atoms in superfluid ^{4}He can serve as a direct experimental evidence of the existence of bound pairs of helium atoms in He–II. This ''hydrodynamic'' effective mass is close to the total mass of ^{3}He and ^{4}He atoms and is even slightly larger than the latter quantity[47–49]:

$$m_3^*\gtrsim(m_3+m_4)=\frac{7}{3}m_3\simeq 2.33m_3. \qquad (91)$$

If we assume on the basis of this effect that bound states of ^{3}He and ^{4}He atoms are indeed formed in a dilute ^{3}He–^{4}He solution, we immediately arrive at a conclusion concerning the existence of bound pairs of ^{4}He atoms also. Indeed, the initial potential $V(r)$ of interaction between ^{3}He and ^{4}He atoms is the same as for the interaction between pairs of ^{4}He atoms,[5] while the energy of zero-point vibrations in the bound state in the former case is higher than in the latter case in view of the smaller value of the reduced mass ($4m_3/7$ for a ^{3}He–^{4}He pair and $2m_3/3=m_4/2$ for a ^{4}He–^{4}He pair). In addition, exchange correlations between bosons facilitate additional attraction. Consequently, the existence of bound pairs of ^{3}He and ^{4}He atoms must indicate the existence of ^{4}He–^{4}He bound pairs.

It should be noted that subsequent measurements[50,51] of the effective mass of bound pairs of ^{3}He atoms in ^{4}He proved that the values of $m_3^*\gtrsim 2.33m_3$ are observed only for a large applied pressure ($P\gtrsim 5$ atm), while the value of m_3^* under zero pressure does not exceed $2.1m_3$.[51] It should be borne in mind, however, that pairs of bosons (^{4}He atoms) under nor-

mal conditions in a CPC are rather ''Cooper-type'' (strongly overlapping) than ''local'' (strongly bound) pairs.[18] The concept of a ''bound pair'' of ^{3}He–^{4}He or ^{4}He–^{4}He atoms should not be treated literally; such a state should be regarded as the result of strong pair and many-particle correlation.

4.6.2. Justrow–Feenberg method for describing ^{3}He–^{4}He *mixtures.* The important role of pair and many-particle correlations is confirmed by the results obtained in Refs. 42–46, where the *Justrow–Feenberg variational method*[38,41] was used for describing the physical properties of mixtures of quantum Bose- and Fermi ^{4}He and ^{3}He liquids. The essence of this method lies in an optimal choice of the trial wave function of the ground state of a system in the form of the following ''ansatz'' [41,63,64]:

$$\Psi_0(\{\mathbf{r}_i^{(\alpha)}\})=\Phi_0(\{\mathbf{r}_i^{(3)}\})\exp\left[\frac{1}{2}U(\{\mathbf{r}_i^{(\alpha)}\})\right], \tag{92}$$

where Φ_0 is the Slater determinant describing the fermion subsystem of ^{3}He, and U is the potential of interaction between ^{3}He atoms ($\alpha=3$) and ^{4}He atoms ($\alpha=4$), which takes into account both pair and triple correlations and is chosen in the form

$$U(\{\mathbf{r}_i^{(\alpha)}\})=\frac{1}{2!}\sum_{\alpha,\beta}\sum_{i,j}^{N_\alpha,N_\beta}u^{(\alpha\beta)}(\mathbf{r}_i,\mathbf{r}_j)+\frac{1}{3!}\sum_{\alpha,\beta,\gamma}\sum_{i,j,k}^{N_\alpha,N_\beta,N_\gamma}u^{(\alpha\beta\gamma)}(\mathbf{r}_i,\mathbf{r}_j,\mathbf{r}_k). \tag{93}$$

Then the variational principle proposed by Campbell and Feenberg[42,43] is used, which involves the minimization of ground-state energy

$$E_0=\langle\Psi_0|\hat{H}|\Psi_0\rangle/\langle\Psi_0|\Psi_0\rangle$$

in $u^{(\alpha\beta)}$ and $u^{(\alpha\beta\gamma)}$ for optimizing the interaction parameters.

In a recent publication by Krotscheck *et al.*,[65] this method was applied for analyzing the dynamics of solitary ^{3}He impurity atoms in liquid ^{4}He as well as the properties of solutions of ^{3}He in ^{4}He, taking into account Fermi-liquid effects in the system of ^{3}He atoms. The dependences of the effective mass m_3^* of ^{3}He atoms on their concentration is the solution and external pressure P obtained in Ref. 65 are in good agreement with the experimental data.[50,51] A considerable increase in m_3^* under pressure up to $m_3^*\simeq 2.9m_3$ at $P\simeq 20$ atm and 10% concentration of ^{3}He indicates not only the possibility of formation of bound states of ^{3}He and ^{4}He atoms, but also the existence of strong collective (many-particle) effects in the interaction of ^{3}He atoms with ^{4}He atoms and with one another. Bulaevskii *et al.*[65] calculated the hydrodynamic mass of a solitary ^{3}He atom in ^{4}He and the Fermi-liquid corrections to m_3^* in ^{3}He–^{4}He mixtures as well as the attenuation (drag) in the motion of ^{3}He quasiparticles in ^{4}He, the magnetic susceptibility of the ^{3}He subsystem, and the phase shift in the scattering matrix in ^{3}He–^{4}He mixtures. The calculation of the latter quantity made it possible to obtain the critical temperature of the phase transition of the ^{3}He Fermi liquid from the normal to the superfluid state for the s-wave (singlet) and the p-wave (triplet) Cooper pairing of ^{3}He atoms in a ^{3}He–^{4}He mixture at ultralow (millikelvin) temperatures as a function on the density of ^{4}He (i.e., the applied pressure).

4.6.3. Quantization of velocity circulation in a superfluid Bose liquid with CPC but without SPBC. Let us consider the type of quantization of the superfluid velocity $v_s(r)=\kappa/r$ in Onsager–Feynman quantum vortices and the value of the circulation quantum κ in a Bose liquid with CPC but without SPBC. It was noted above that the superfluid component in this case is determined by a pair CEC comprising CPC with bound (''Cooper'') pairs of bosons and high-order even condensates with unbound quadruples $\langle\hat{\psi}\hat{\psi}\hat{\psi}\hat{\psi}\rangle$, sextuples $\langle\hat{\psi}\hat{\psi}\hat{\psi}\hat{\psi}\hat{\psi}\hat{\psi}\rangle$, etc. of particles since different types of bound subsystems (condensates) cannot exist simultaneously in a one-component Bose liquid.[6)] Indeed, the *exchange of particles between diffrent condensates (vacuums) is forbidden by energy considerations* since they correspond to local energy minima and are separated by potential barriers. For this reason, these condensates should correspond to different phases like in *systems with spontaneously broken symmetries*.

Since *bound boson pairs* of a ''Cooper-type'' CPC *are ''fundamental'' quasiparticles in a pair CEC*, we can expect that an *effective circulation quantum* $\kappa^*=h/m^*$ *is half the ordinary quantum* $\kappa=h/m_4$ (see Ref. 18) because the effective mass of a pair is $m^*=2m_4$. Experimental observations of half-integral circulation quanta $h/2m_4$ in superfluid ^{4}He could be a direct confirmation of the existence of bound pairs of ^{4}He atoms.

Such a situation is similar to that with a *doubled charge* $2e$ *of Cooper pairs in superconductors*[9] and a *half-integral magnetic flux quantum* $\varphi_0=hc/2e$ in Abrikosov vortices[11] (as compared to the integral flux quantum $\varphi=hc/e$ piercing the Landau minimum quantum orbit of a normal electron in a strong magnetic field).

Jumps of the total circulation of the superfluid and normal components in He–II by an integral number of quanta $\kappa_4=h/m_4$ were detected in most of experiments.[66–68] However, the half-integral value of the velocity circulation quantum in superfluid ^{4}He cannot be ruled out completely as yet in view of not very rich statistics of observations and the possibility of creation of pairs of vortices with the same direction of rotational velocity and with conserved total momentum of the system.

4.6.4. Problem of critical velocities in ultrathin films and capillaries. Concluding the section, let us consider again the magnitude of the critical velocity in a superfluid ^{4}He flow, which is almost two orders of magnitude smaller than the ''rotonic'' critical velocity $v_{cr}=\Delta_r/p_r\approx 60$ m/s calculated in accordance with the dispersion relation of the experimentally observed (from neutron scattering) spectrum of elementary excitations in He–II.[2]

According to experimental data,[69,70] the critical velocity v_c of the superfluid component ρ_s in wide channels is virtually independent of temperature and is connected with the channel width d through the relation $v_c\sim d^{-1/4}$ over a very broad range 8×10^{-7} cm$<d<1$ cm. The value of v_c in narrower channels decreases rapidly to zero with d and becomes

a function of T starting from $d \approx 3 \times 10^{-5}$ cm.[71–73] This temperature dependence $v_c(T)$ is especially significant near the λ-point at which v_c vanishes. It was emphasized by Putterman[10] that neither the value of the critical velocity, nor the mechanism of its variation in ultrathin films and capillaries has been explained unambiguously so far, while the anomalously small value of v_c in macroscopic He–II flows is generally attributed to the creation of Onsager–Feynman quantum vortices[74] or closed vortex loops.[75]

Proceeding from an analogy with the dynamics of Abrikosov vortices in type–II superconductors in magnetic fields,[11] let us analyze the empirical regularities in the behavior of the critical velocity v_c in superfluid ^{4}He. For example, we can attribute the increase in v_c upon a decrease in the channel width d to an increase in coupling (frictional) forces between the normal cores of vortex filaments and the walls of the channel per unit vortex length, which are similar to ''pinning'' forces exerted on Abrikosov vortices at interfaces and surfaces of the crystals. When superfluidity is limited by the effects of creation and dissipative flow of quantum vortices (in analogy with the resistive state of superconductors under the conditions of low-temperature dynamic depinning of Abrikosov vortices), the critical velocity should not depend on T.

On the other hand, the creation and flow of quantum vortices (and the more so, vortex loops) in ultrathin films and capillaries whose thickness (diameter) is comparable to the size of a normal vortex core are ruled out so that the critical velocity of a superfluid Bose liquid with CPC but without SPBC must be determined by the maximum possible ''depairing'' velocity v_{cm} at which boson pairs are ruptured, and CPC is destroyed. This situation is similar to that in thin superconducting threads (filaments) with a thickness smaller than the London penetration depth λ_L of a magnetic field (or the coherence length ξ_0), which cannot accommodate Abrikosov vortices, and whose critical current density $j_c = env_c$ attains its limiting value for which Cooper pairs are ruptured.

According to the results obtained in Refs. 71 and 72, the maximum critical velocity in ultrathin wetting He–II films with a thickness of a few atomic layers increases upon cooling, attaining the value $v_{c\,\max} \approx 2$ m/s at $T \approx 1.5$ K. If we assume that this velocity is equal to the critical depairing velocity v_{cm}, the radius R_c of the normal vortex core, which is determined from the condition of equality of the superfluid velocity $v_s(r) = \kappa^*/r$ to the critical value v_{cm}, is $R_c \approx 40$ Å for $\kappa^* = h/2m_4$, which coincides with half the minimum film thickness ($d_{\min} \approx 80$ Å), up to which the value of v_c increases with decreasing d.[10] For $d < d_{\min}$, quantum vortices are fixed rigidly between the solid wall and the film surface and are actually two-dimensional (planar).

The critical ''depairing'' velocity $v_{cm} \approx 2$ m/s should be also attained in ultrathin capillaries of diameter $d \lesssim 2R_c \approx 80$ Å, in which even a normal vortex core ''cannot be accommodated.''

Since $v_{cm} \ll v_{\rm cr}$, the superfluidity criterion for He–II (see above) must be determined by peculiarities of the one-particle spectrum $\varepsilon(\mathbf{p})$ of quasiparticles which was not observed in neutron-diffraction experiments and which differs considerably from the collective spectrum $E(\mathbf{p})$ as well as from the kinetic energy $\mathbf{p}^2/2m_4$ of free ^{4}He atoms (see Fig. 6).

As regards the decrease of v_c with d starting from the minimum thickness $d \approx 80$ Å and the vanishing of v_c in ultrathin films having a thickness smaller than five atomic layers,[71,72] this effect can be associated with size quantization of the transverse momentum $p_\perp$ of quasiparticles for which the de Broglie wavelength $\lambda_D = h/p_\perp$ is comparable with the film thickness d. Since v_c is determined by quasiparticles in the vicinity of the minimum value of the ratio $\varepsilon_T(\mathbf{p})/p$, and the position of this minimum is displaced towards smaller momenta upon an increase in T due to a decrease in $\tilde{\Psi}_T(0)$ and $\tilde{u}_T$, the quantization condition $\lambda_D \sim d$ at higher T must be observed for thicker films, which is in qualitative agreement with the experimental data.[71,72]

In the ultraquantum limit ($\lambda_D \gg d$), the quasiparticle spectrum becomes two-dimensional for a film and one-dimensional for a capillary. It is well known,[76] however, that the long-range order in $2D$- and $1D$-systems, which corresponds to the superfluid (superconducting) state of Bose- and Fermi liquids, is ruled out at $T \neq 0$ in view of long-wave density fluctuations, so that $\tilde{\Psi}_T(0) = 0$ and $v_c = 0$.

5. CONCLUSION

The analysis of experimental and theoretical publications indicates that investigations of the unique phenomenon of superfluidity of liquid helium, which was discovered 60 years ago by Kapitza[77] and observed independently by Allen and Misener,[78] are far from being completed. A number of discrepancies between the theoretical and experimental results include, for example, the 1.5–2 orders of magnitude difference between the theoretical value of critical velocity $v_{\rm cr} \approx 60$ m/s calculated on the basis of the Landau superfluidity criterion[1] from the value of the gap Δ_r near the rotonic minimum in the elementary excitation spectrum reconstructed from the scattering of slow neutrons[2,79,80] on the one hand and the experimentally measured values of v_c[69–73] on the other hand as well as the discrepancy between the theoretical density of the Bose–Einstein condensate, which is identified with the density ρ_s of the superfluid component in He–II, and the experimentally measured (from the scattering of fast neutrons[81]) fraction of ^{4}He atoms (1–3%) in the state with zero momentum at $T \approx 1$ K.

The former discrepancy can be partially removed if we take into account the processes of creation of quantum vortices and vortex loops in a superfluid He–II flow,[74,75] but cannot be eliminated for the flow of the superfluid component in ultrathin films and capillaries[10] in which the creation and flow of vortices is impossible. An attempt to eliminate the second discrepancy by introducing an effective condensate[16,17] containing higher-order many-particle condensates along with the one-particle condensate did not lead to a significant improvement in the understanding of the quantum microstructure of the superfluid component in He–II.

At the same time, the assumption put forth in Refs. 15 and 18 concerning the absence of a SPBC in superfluid ^{4}He

does not contradict the experimental results[12,81] and makes it possible to resolve **Paradox 3** (see Introduction) and to formulate a qualitatively new approach to the description of the superfluid state in a Bose liquid on the bases of the concept of ''paired'' effective condensate comprising a coherent condensate of bound ''Cooper'' pairs of bosons (see, for example, Ref. 84) and higher-order even condensates of free particles. It was proved in Ref. 18 that a strong CPC is formed in the case of a strong effective attraction between bosons in a broad momentum range $\mathbf{p}\neq 0$ and leads to the suppression of a weak SPBC ''depleted'' due to the interaction between particles in the quantum Bose liquid. The superfluid state with CPC but without SPBC is characterized by a number of singularities, including the absence of hybridization between the one-particle and two-particle (collective) branches in the elementary excitation spectrum. This allows us to eliminate the discrepancy between the experimentally observed form of the quasiparticle spectrum in ^{4}He and the Landau superfluidity criterion (**Paradoxes 1 and 2** formulated in Introduction).

However, the assumption concerning the existence of an energy gap $\Delta_0\neq 0$ for $\mathbf{p}=0$ in the one-particle spectrum $\varepsilon(\mathbf{p})$[15,18] (see also Refs. 27–33) leads, in analogy with a gap in the spectrum of superconductors,[9,11] to new paradoxes: the violation of the Hugenholtz–Pines theorem[26] for chemical potential, the replacement of the power (hydrodynamic) asymptotic form of a pair correlation function[36,37] by the exponential asymptotic form, and to the emergence of singularities on the temperature dependence of heat capacity,[32] which were not observed in experiments. The rejection of the gap nature of the one-particle spectrum proposed in Ref. 35 resolves these paradoxes (for example, reestablishes the validity of the Hugenholtz–Pines theorem[26] and the Reatto–Chester power asymptotic form[36]). In this case, $\varepsilon(\mathbf{p})\approx p\tilde{u}$ for $\mathbf{p}\to 0$, where the velocity $\tilde{u}$ does not coincide with the velocity c of hydrodynamic sound in liquid helium ($\tilde{u}\ll c$) and is determined by the pair order parameter $\tilde{\Psi}(\mathbf{p})$ for $\mathbf{p}=0$: $\tilde{u}=\sqrt{\tilde{\Psi}(0)/m^*}$ In the region of large momenta, the spectrum $\varepsilon(\mathbf{p})$ may have a minimum (or inflection point) and determines the critical velocity $v_c=\min[\varepsilon(\mathbf{p})/p]\approx\Delta_1/p_1$ which can be put in correspondence with the maximum critical velocity $v_{cm}\approx 2$ m/s of superfluid ^{4}He in ultrathin films and capillaries.[71,72]

The hypothesis on the pair structure of the superfluid component ρ_s in He–II with an intense ''Cooper-type'' CPC is confirmed by the important role of pair correlations which can be described to a fairly high degree of accuracy by the Justrow–Feenberg method[38–46] both for the ^{4}He Bose liquid and for ^{3}He–^{4}He mixtures of quantum liquids. The experimentally measured anomalously large effective mass of ^{3}He impurity atoms in liquid ^{4}He,[47–51] whose value is close to the total mass (m_3+m_4) of ^{3}He and ^{4}He atoms, can serve as an empirical confirmation of the formation of bound pairs of helium atoms in He–II. It indicates the bound state of ^{3}He and ^{4}He atoms, and hence ^{3}He–^{4}He pairs.[35] This hypothesis, however, requires a more rigorous theoretical substantiation on the basis of numerical calculations of the pair order parameter $\tilde{\Psi}_T(\mathbf{p})$ and the one-particle spectrum $\varepsilon_T(\mathbf{p})$ at different T by using realistic potentials of interaction between ^{4}He atoms, as well as a more detailed experimental verification, including precision measurements of the velocity circulation quantum in the superfluid component of He–II and the maximum critical velocity v_c in ultrathin channels.

The author is pleased to place on record his deep gratitude to Yu. A. Nepomnyashchii for opening up many new aspects in the theory of superfluidity during a brief but highly fruitful co-operation. Thanks are also due to I. P. Fomin for his active participation in the discussion of the problems considered in this review and also for drawing the authors attention to the remarkable closeness of the effective masses of ^{3}He impurity atoms in ^{4}He to the total mass of ^{3}He and ^{4}He atoms indicating the possibility of formation of bound pairs of helium atoms in the superfluid Bose liquid He–II.

*E-mail: pashitsk@iop.kiev.ua

1) In this case, $\omega_{\rm pl}^*=(16\pi e^2 n_B/\varepsilon_0 m_B^*)^{1/2}\gtrsim 3.6\times 10^{13}\ {\rm s}^{-1}$ and $v_c=2\sqrt{\hbar\omega_{\rm pl}^*/m_B^*}\gtrsim 4\times 10^6$ cm/s, so that the critical current density $j_c=2en_Bv_c\gtrsim 10^8$ A/cm^2.

2) Such an approximation is justified if the one-particle excitation branch is much lower than the collective excitation branch (see below).

3) The negative sign of $\tilde{\Psi}(\mathbf{p})$ is also confirmed by the effective interaction when $\tilde{V}(\mathbf{p})<0$ in a certain region $\mathbf{p}\neq 0$.

4) A similar first-order phase transition was considered by Iordanskii[82] and Chernikova[83] for a rarefied Bose gas with attraction at large distances.

5) For a strong attraction, this may be a first-order phase transition close to second, with a small value of the jump $\tilde{\Psi}_T(0)$ at $T=T_c$. A second-order phase transition can occur in a spatially limited region with a finite minimum value of the momentum $p_{\min}\neq 0$ if $T_c^*\leqslant T_c$.

6) It should be noted that CPC can be a small fraction of CEC even at $T\to 0$ in contrast to superconductors in which all electrons (fermions) are bound into Cooper pairs at $T=0$.

[1] L. D. Landau, Zh. Éksp. Teor. Fiz. **11**, 592 (1941); *ibid.* **17**, 91 (1947).
[2] D. G. Henshaw and A. D. B. Woods, Phys. Rev. **121**, 1266 (1961).
[3] R. Feynman, Phys. Rev. **94**, 262 (1954).
[4] K. A. Brueckner and K. Sawada, Phys. Rev. **106**, 1117 (1957); *ibid.*, , 1128 (1957).
[5] K. Brueckner, *Theory of Nuclear Structure*, London (1964).
[6] N. N. Bogoliubov, Izv. Akad. Nauk SSSR, Ser. Fiz. **11**, 77 (1947); J. Phys. **9**, 23 (1947).
[7] I. M. Khalatnikov, *Theory of Superfluidity* [in Russian], Fizmatgiz, Moscow (1971).
[8] A. A. Abrikosov, L. P. Gor'kov, and I. E. Dzyaloshinskii, *Methods of Quantum Field Theory in Statistical Physics*, Prentice Hall, Englewood Cliffs, NJ (1963).
[9] J. Schrieffer, *Theory of Superconductivity*, Benjamin, NY, 1964.
[10] C. Putterman, *Superfluid Hydrodynamics*, North-Holland, Amsterdam (1974).
[11] P. De Gennnes, *Superconductivity of Metals and Alloys*, New York (1966).
[12] H. W. Jackson, Phys. Rev. A **10**, 278 (1974).
[13] E. A. Andronikashvili, Zh. Éksp. Teor. Fiz. **16**, 780 (1946).
[14] A. A. Nepomnyashchii and Yu. A. Nepomnyashchii, Pis'ma Zh. Éksp. Teor. Fiz. **21**, 3 (1975) [JETP Lett. **21**, 1 (1975)].
[15] P. S. Kondratenko, Teor. Mekh. Fiz. **22**, 278 (1975).
[16] Yu. A. Nepomnyashchii and A. A. Nepomnyashchii, Zh. Éksp. Teor. Fiz. **75**, 976 (1978) [Sov. Phys. JETP **48**, 493 (1978)].
[17] Yu. A. Nepomnyashchii, Zh. Éksp. Teor. Fiz. **85**, 1244 (1983) [Sov. Phys. JETP **58**, 722 (1983)]; *ibid.* **89**, 511 (1985) [*ibid.* **62**, 289 (1985)].
[18] Yu. A. Nepomnyashchii and E. A. Pashitskii, Zh. Éksp. Teor. Fiz. **98**, 178 (1990) [Sov. Phys. JETP **71**, 98 (1990)].
[19] E. A. Pashitskii, Ukr. Fiz. Zh. **18**, 1435 (1973).
[20] E. A. Pashitskii, *Fundamentals of the Theory of Superconductivity* [in Russian], Vysshaya Shkola, Kiev (1985).

[21] C. Mavroyanis, Phys. Rev. A **10**, 1741 (1974).
[22] A. N. Bobrysheva and S. A. Moskalenko, Ukr. Fiz. Zh. **25**, 3282 (1975).
[23] V. L. Vinetskii and E. A. Pashitskii, Ukr. Fiz. Zh. **20**, 338 (1975); Fiz. Tverd. Tela (Leningrad) **25**, 1744 (1983) [Sov. Phys. Solid State **25**, 1005 (1983)].
[24] A. B. Migdal, *Fermions and Bosons in Strong Fields* [in Russian], Nauka, Moscow (1978).
[25] S. T. Belyaev, Zh. Éksp. Teor. Fiz. **34**, 417 433 (1958) [Sov. Phys. JETP **7**, 289, 299 (1958)].
[26] N. M. Hugenholtz and D. Pines, Phys. Rev. **116**, 489 (1959).
[27] T. G. Valatin and D. Butler, Nuovo Cimento **10**, 37 (1958).
[28] M. Girardean and R. Arnowitt, Phys. Rev. **113**, 755 (1959).
[29] A. Coniglio and M. Marinero, Nuovo Cim. **48**, 248 (1967).
[30] W. A. B. Evans and Y. Imry, Nuovo Cim. **63**, 155 (1969).
[31] A. Coniglio and F. Mancini, Nuovo Cim. **63**, 227 (1969).
[32] R. Hasting and T. W. Halley, Phys. Rev. B **12**, 267 (1975).
[33] S. I. Shevchenko, Fiz. Nizk. Temp. **11**, 339 (1985) [Sov. J. Low Temp. Phys. **11**, 191 (1985)].
[34] Yu. A. Nepomnyashchii, Pis'ma Zh. Éksp. Teor. Fiz. **15**, 211 (1972) [JETP Lett. **15**, 146 (1972)].
[35] S. I. Vil'chinskii, E. A. Pashitskii, and P. I. Fomin, Fiz. Nizk. Temp. **23**, 1267 (1997) [Low Temp. Phys. **23**, 951 (1997)].
[36] L. Reatto and C. V. Chester, Phys. Rev. **155**, 88 (1967).
[37] R. A. Ferrell, N. Meyard, and H. Schmidt, Ann. Phys. **47**, 565 (1968).
[38] R. Justrow, Phys. Rev. **98**, 1479 (1955).
[39] M. L. Ristig, P. Hecking, P. M. Lam, and T. W. Clark, Phys. Lett. A **63**, 94 (1977).
[40] M. L. Ristig, Phys. Rev. B **18**, 1207 (1978).
[41] E. Feenberg, *Theory of Quantum Liquids*, Academic Press, New York (1969).
[42] C. E. Campbell and E. Feenberg, Phys. Rev. **188**, 396 (1969).
[43] C. E. Campbell, Phys. Lett. A **44**, 471 (1973).
[44] E. Krotscheck, Phys. Rev. B **33**, 3158 (1986).
[45] E. Krotscheck and M. Saarela, Phys. Rep. **232**, 1 (1993).
[46] M. Saarela and E. Krotscheck, J. Low Temp. Phys. **90**, 415 (1993).
[47] B. N. Esel'son, V. N. Grigor'ev, V. G. Ivanov *et al.*, *Mixtures of* ^{3}He–^{4}He *Quantum Liquids* [in Russian], Nauka, Moscow (1973).
[48] A. C. Anderson, W. R. Roach, R. E. Sarwinskii, and P. C. Wheatly, Phys. Rev. Lett. **16**, 263 (1968).
[49] V. I. Sobolev and B. N. Esel'son, Zh. Éksp. Teor. Fiz. **60**, 240 (1971) [Sov. Phys. JETP **33**, 132 (1971)].
[50] C. Yorozu, H. Fukuyama, and H. Ishimoto, Phys. Rev. B **48**, 9660 (1993).
[51] R. Simons and R. M. Mueller, Czech. J. Phys. **46**, 201 (1996).
[52] L. L. Foldy, Phys. Rev. **83**, 397 (1951); *ibid.* **124**, 649 (1961).
[53] A. Alexandrov and J. Ranninger, Phys. Rev. B **24**, 1164 (1982).
[54] V. L. Vinetskii, Zh. Éksp. Teor. Fiz. **40**, 1459 (1961) [Sov. Phys. JETP **13**, 1023 (1961)].
[55] L. D. Landau and E. M. Lifshitz, *Statistical Physics*, Pergamon Press, Oxford, 1980.
[56] J. G. Bednorz and K. A. Müller, Z. Phys. B **64**, 189 (1986).
[57] N. M. Plakida, *High-temperature Superconductivity* [in Russian], Nauka, Moscow (1996).
[58] N. N. Bogoliubov, V. V. Tolmachev, and D. V. Shirkov, *New Method in the Theory of Superconductivity*, Consultants Bureau, NY, 1959.
[59] A. Z. Patashinskii and V. L. Pokrovskii, *Fluctuation Theory of Phase Transitions* Pergamon Press, Oxford, 1979.
[60] L. N. Bulaevskii, V. L. Ginzburg, and A. A. Sobyanin, Zh. Éksp. Teor. Fiz. **94**, 355 (1988) [Sov. Phys. JETP **67**, 1499 (1988)].
[61] J. Wilks, *The Properties of Liquid and Solid Helium*, Clarendon Press, Oxford (1967).
[62] N. N. Bogoliubov and D. I. Zubarev, Zh. Éksp. Teor. Fiz. **28**, 129 (1955) [Sov. Phys. JETP **1**, 83 (1955)].
[63] C. E. Campbell, *Progress in Liquid Physics* (ed. by C. A. Croxton), Wiley, London (1977).
[64] M. Saarela, *Resent Progress in Many Body Theories* (ed. by Y. Asishai), Plenum, New York (1990).
[65] E. Krotscheck, J. Paaso, M. Saareda *et al.*, *Proc. INTAS Workshop*, Lviv, Ukraine (1998).
[66] W. F. Vinen, Proc. Roy. Soc. **F260**, 218 (1961).
[67] G. W. Rayfield and F. Reif, Phys. Rev. Lett. **11**, 305 (1963).
[68] S. C. Whitmore and W. Zimmermann, Phys. Rev. **166**, 181 (1968).
[69] W. M. Van Alphen, J. F. Olijhoek, R. de Bruyn Ouboter, and K. W. Taconis, Physica **32**, 1901 (1966).
[70] R. de Bruyn Ouboter, K. W. Taconis, and W. M. Van Alphen, *Progress in Low Temperature Physics* (ed. by C. J. Gorter), Vol. 5, North-Holland, Amsterdam (1967).
[71] D. F. Brewe and K. Mendelssohn, Proc. R. Soc. London, Ser. A **260**, 1 (1961).
[72] K. Fokkens, K. W. Taconis, and R. de Bruyn Ouboter, Physica **32**, 2129 (1966).
[73] W. E. Keller and E. F. Hammel, Physics **2**, 221 (1966).
[74] P. W. Anderson, Rev. Mod. Phys. **38**, 298 (1966).
[75] F. Reif and L. Meyer, Phys. Rev. Lett. **5**, 1 (1960); Phys. Rev. **119**, 1164 (1960).
[76] P. C. Hohenberg, Phys. Rev. **158**, 383 (1967).
[77] P. L. Kapitza, Nature (London) **141**, 74 (1938).
[78] J. F. Allen and A. D. Misener, Nature (London) **141**, 75 (1938).
[79] J. L. Yarnell, G. P. Arnold, P. J. Bendt, and E. C. Kerr, Phys. Rev. **113**, 1379 (1959).
[80] A. D. B. Woods and R. A. Cowly, Rep. Prog. Phys. **36**, 1135 (1973).
[81] H. A. Mook, R. Sherm, and M. K. Wilkinson, Phys. Rev. A **6**, 2268 (1972).
[82] S. V. Iordanskii, Zh. Éksp. Teor. Phys. **47**, 167 (1964) [Sov. Phys. JETP **20**, 112 (1964)].
[83] D. M. Chernikova, Zh. Éksp. Teor. Phys. **57**, 2125 (1969) [Sov. Phys. JETP **30**, 1154 (1969)].
[84] B. D. Josephson, Phys. Lett. **21**, 608 (1966).

Translated by R. S. Wadhwa